ABSTRACT

Title of dissertation: DATA DRIVEN APPROACHES TO IDENTIFY DETERMINANTS OF HEART DISEASES AND CANCER RESISTANCE

Avinash Das Sahu, Doctor of Philosophy, 2016

Dissertation directed by: Professor Sridhar Hannenhalli
Department of Computer Science

Cancer and cardio-vascular diseases are the leading causes of death world-wide. Caused by systemic genetic and molecular disruptions in cells, these disorders are the manifestation of profound disturbance of normal cellular homeostasis. People suffering or at high risk for these disorders need early diagnosis and personalized therapeutic intervention. Successful implementation of such clinical measures can significantly improve global health. However, development of effective therapies is hindered by the challenges in identifying genetic and molecular determinants of the onset of diseases; and in cases where therapies already exist, the main challenge is to identify molecular determinants that drive resistance to the therapies. Due to the progress in sequencing technologies, the access to a large genome-wide biological data is now extended far beyond few experimental labs to the global research community. The unprecedented availability of the data has revolutionized the capabilities of computational researchers, enabling them to collaboratively address the long standing problems from many different perspectives. Likewise, this thesis

tackles the two main public health related challenges using data driven approaches.

Numerous association studies have been proposed to identify genomic variants that determine disease. However, their clinical utility remains limited due to their inability to distinguish causal variants from associated variants. In the presented thesis, we first propose a simple scheme that improves association studies in supervised fashion and has shown its applicability in identifying genomic regulatory variants associated with hypertension. Next, we propose a coupled Bayesian regression approach – eQTeL, which leverages epigenetic data to estimate regulatory and gene interaction potential, and identifies combinations of regulatory genomic variants that explain the gene expression variance. On human heart data, eQTeL not only explains a significantly greater proportion of expression variance in samples, but also predicts gene expression more accurately than other methods. We demonstrate that eQTeL accurately detects causal regulatory SNPs by simulation, particularly those with small effect sizes. Using various functional data, we show that SNPs detected by eQTeL are enriched for allele-specific protein binding and histone modifications, which potentially disrupt binding of core cardiac transcription factors and are spatially proximal to their target. eQTeL SNPs capture a substantial proportion of genetic determinants of expression variance and we estimate that 58% of these SNPs are putatively causal.

The challenge of identifying molecular determinants of cancer resistance so far could only be dealt with labor intensive and costly experimental studies, and in case of experimental drugs such studies are infeasible. Here we take a fundamentally different data driven approach to understand the evolving landscape of emerging re-

sistance. We introduce a novel class of genetic interactions termed synthetic rescues (SR) in cancer, which denotes a functional interaction between two genes where a change in the activity of one vulnerable gene (which may be a target of a cancer drug) is lethal, but subsequently altered activity of its partner rescuer gene restores cell viability. Next we describe a comprehensive computational framework –termed INCISOR– for identifying SR underlying cancer resistance. Applying INCISOR to mine The Cancer Genome Atlas (TCGA), a large collection of cancer patient data, we identified the first pan-cancer SR networks, composed of interactions common to many cancer types. We experimentally test and validate a subset of these interactions involving the master regulator gene mTOR. We find that rescuer genes become increasingly activated as breast cancer progresses, testifying to pervasive ongoing rescue processes. We show that SRs can be utilized to successfully predict patients' survival and response to the majority of current cancer drugs, and importantly, for predicting the emergence of drug resistance from the initial tumor biopsy. Our analysis suggests a potential new strategy for enhancing the effectiveness of existing cancer therapies by targeting their rescuer genes to counteract resistance.

The thesis provides statistical frameworks that can harness ever increasing high throughput genomic data to address challenges in determining the molecular underpinnings of hypertension, cardiovascular disease and cancer resistance. We discover novel molecular mechanistic insights that will advance the progress in early disease prevention and personalized therapeutics. Our analyses sheds light on the fundamental biological understanding of gene regulation and interaction, and opens up exciting avenues of translational applications in risk prediction and therapeutics.

DATA DRIVEN APPROACHES TO IDENTIFY DETERMINANTS OF HEART DISEASES & CANCER RESISTANCE

by

Avinash Das Sahu

Dissertation submitted to the Faculty of the Graduate School of the
University of Maryland, College Park in partial fulfillment
of the requirements for the degree of
Doctor of Philosophy
2016

Advisory Committee:
Professor Sridhar Hannenhalli, Chair/Advisor
Professor Eytan Ruppin, Co-Advisor
Professor Laura Elnitski
Professor Hector Corrada Bravo
Professor Michael Cummings

Contents

List of Figures

List of Abbreviations

DNA Deoxyribonucleic acid	
SNP	Single Nucleotide Polymorphism
RNA	Ribonucleic acid
mRNA	Messenger RNA
GWAS	Genome wide association studies
eQTL	expression quantitive trait loci
SCNA	Somatic copy number variance
H3K4me3	H3 at lysine 4
ChIP-seq	chromatin immunoprecipitation sequencing
ChIP-seq	chromatin immunoprecipitation sequencing
RNA-seq	RNA sequencing
DHS	DNase I hypersensitive sites
FPKM	Fragments Per Kilobase of transcript per Million
RPKM	Reads Per Kilobase of transcript per Million
SVM	Support vector machine
bp	base pair
kbps/kb	kilo base pairs
eSNP	eQTL-SNP
LD	Linkage Disequilibrium
OMIM	Online Mendelian Inheritance in Man

Chapter 1: Introduction

1.1 How does a cell function?

All living organisms, from bacteria to human, are made of cells. Cells are basic structural, functional and biological building block of living organisms [3]. Bacteria, perhaps the simplest organism that exists today, is a self contained single cell. Humans, on the other hand, are multicellular and comprise of around 10 trillion cells.

All cells in a unicellular or a multicellular organism contain an outer cellular membrane that encapsulates liquid cytoplasm. Around 70% of cytoplasm is water, rest comprises proteins and number of other small molecules (amino acids, glucose etc.). DNA is a molecule that carries genetic hereditary information [3]. It holds all the instructions for life of an organism in genes, which are stretches of DNA and most of them encode protein molecules. In simple organisms, referred to as prokaryotes, DNA resides in the cytoplasm. Whereas in more complex organisms, called eukaryotes, a special nuclear membrane protects the DNA and separates it from the cytoplasm [4].

Proteins carry out all essential processes necessary to maintain life, including

development, maintenance functions and reproduction [5]. There are many different kinds of proteins including enzymes, antibodies (related to immune system), regulatory proteins, contractile proteins (related to muscle function), structural proteins and transport proteins [6]. The enzymes catalyze more than 5,000 bio-chemical reactions and convert substrates to products inside the cells. Almost all metabolic reactions need enzymes, which thus are essential for life [7]. What metabolic processes occurs in a cell depends on the set of enzymes present in the cell [7]. The case of lactose intolerance illustrates the importance of enzymes. People with lactose intolerance cannot produce lactase enzymes. Lactase breaks down lactose into monomers glucose and galactose, completing the first step in lactose digestion, therefore people who suffer from the lactose intolerance cannot digest milk that contains lactose. This condition can be mitigated by taking lactase pill prior to drinking milk [3, 8].

1.2 How does a cell produce proteins?

The answer to the question lies in a **central dogma** of molecular biology [9], which explains how genetic information flows in an organism. DNA, mRNA and proteins are major players in the central dogma [10]. The end product of this process involves manufacturing of proteins by genes, which constitutes of following two steps:

- **Transcription**: is a process by which information in DNA is transferred to a messenger RNAs (mRNA). Specific proteins, RNA polymerase and tran-

scription factors, form a core of the transcription machinery and facilitate the transcription [3]. Using a DNA-encoded gene as a template, DNA-polymerase copies the gene to its corresponding mRNA.

In eukaryotic cells transcription process generates first primary transcript mRNA (pre-mRNA) [5,11], which is then processed to mature mRNA (Fig 1.1).The processing involves attaching a poly-A tail and a $5'$ cap to pre-mRNA. This is followed by splicing, which gives the final product - the mature mRNA molecule [12].

- **Translation**: is a process transfers information from mRNAs to corresponding proteins [3]. During translation, a protein complex called ribosome reads the mRNA according to genetic code [10], where each mRNA triplet codon encodes for an amino acid (Fig 1.1) [10]. Thus, mRNA is used as a template to assemble a chain of amino acids that form the final protein product. In eukaryotic cells, transcription occurs in the nucleus while translation occurs in cytoplasm, therefore mRNA are transported out of nucleus (to the cytoplasm)(Fig 1.1).

In many organisms, the translated protein can be further modified by various enzymes. This process, referred as post-translation modification, is not covered in the central dogma.

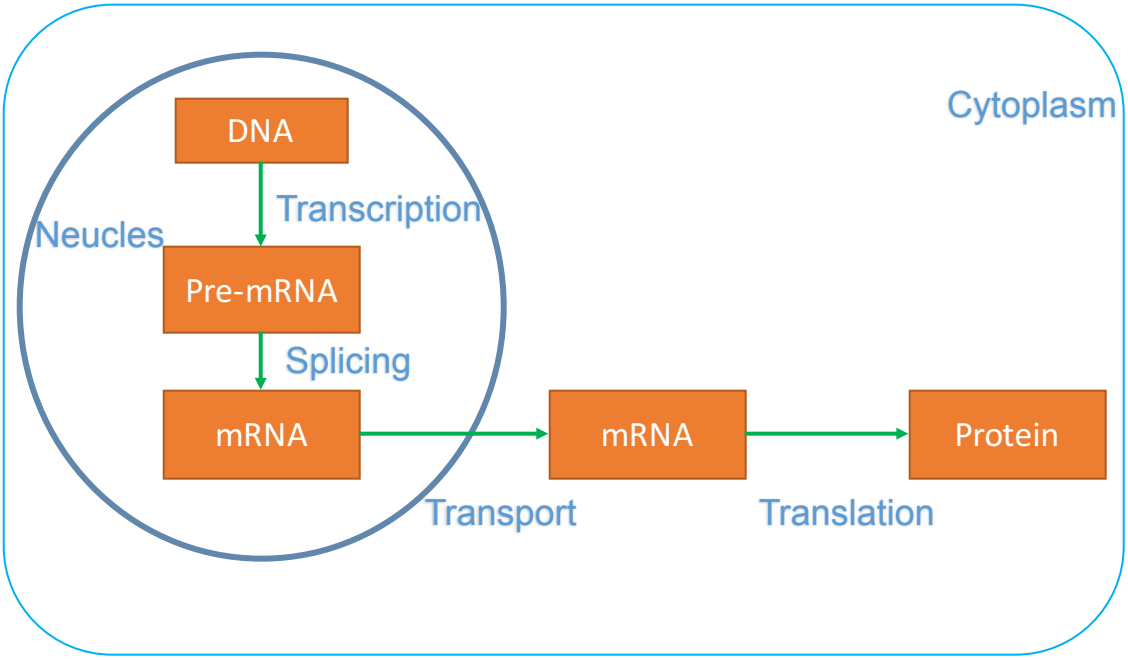

Figure 1.1: Central dogma of molecular biology.

1.3 How can same DNA give rise to drastically different cells?

All cells in a human body are created by cell-divisions and DNA replications from a single fertilized cell; thus all cells in an individual share identical DNA (with exceptions of B cells) [13]. If DNA contains all genetic information, how do the differences in tissues and cell types arise in a multicellular organism? How does the same genetic information translate into morphologically and phenotypically distinct cells (Fig 1.2).

The underlying mechanism involved in generation of different morphologies and functions of cell types is called differentiation [13]. It is mechanism by which a less specialized stem cell produces more specialized differentiated cells. Each

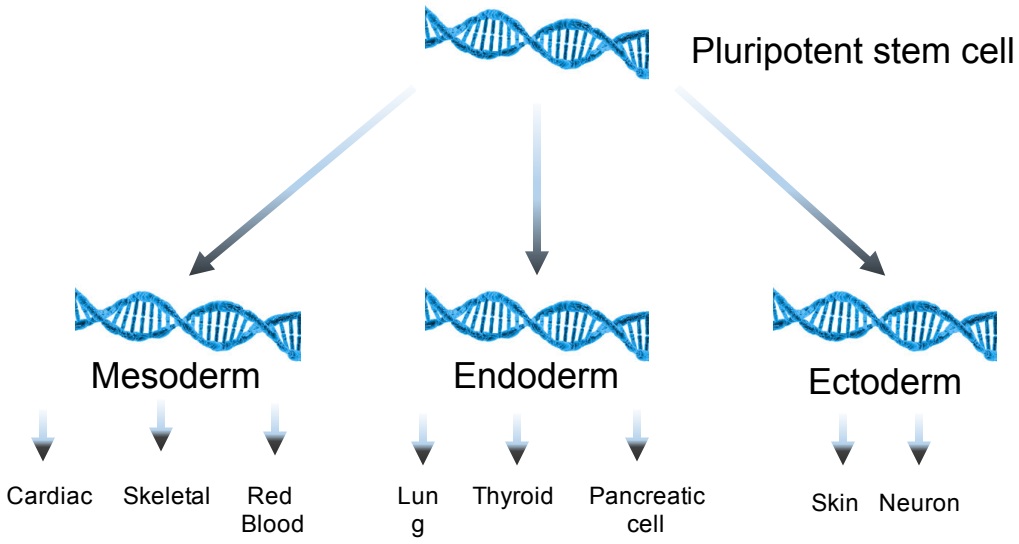

Figure 1.2: In multicellular organism different cell and tissue types share same DNA

cell type expresses a unique subset of genes which is specific to the cell type [13]. Conversely, set of the genes expressed in a cell determines its identity (including its morphology and functions) [14]. For example, the set of genes that is expressed in stem cells is different from those in cardiac muscle cells or in neurons, that's the reason all of the cell types look and act differently. Thus, at the molecular level differentiation is a mechanism by which a daughter cell acquires the capability to express different set of genes than the parent cell. The signal of differentiation comes from diverse factors such as external environment, signals from neighboring cells, etc. [13]. Cancer cells also activate set of genes that are different from any normal cell, thus acting differently from any normal cell [15].

1.4 How do eukaryotes regulate genes in a cell-type specific manner?

In eukaryotes, a promoter Fig 1.3 is a genomic region that is necessary to initiate transcription of a specific downstream gene. They are generally located a few base pairs upstream of the transcription initiation site (TSS) of its target gene [16]. Each transcription factor (TF), protein that helps in transcription of genes, contains a specific DNA binding domain that recognizes a 6-10 base-pair motif of DNA. A promoter contains a specific set of motifs, also called transcription factor binding sites (TFBS), which allow specific set of TFs to bind and modulate expression of its target gene [16].

For a gene to be transcribed, its promoter region must be accessible (or open) to TFs [17], so that a pre-initiation complex can be formed. Once TFs are bound to the promoter, RNA polymerase binds to the promoter forming a transcription initiation complex. This initiates the transcription of the gene.

In eukaryotic cells, the transcriptional regulation depends upon chromatin, which is a complex of DNA and proteins called histones [18]. The DNA in the default state is tightly wrapped around histones in the nucleus, a state referred as closed chromatin. TFs and RNA polymerase cannot bind to promoters in a such state because they are inaccessible. Genes in such a state are inactive [18].

A set of chemical modifications to the histones can change the local accessibility of DNA for TF binding and therefore can modulate gene expression [17,18]. For

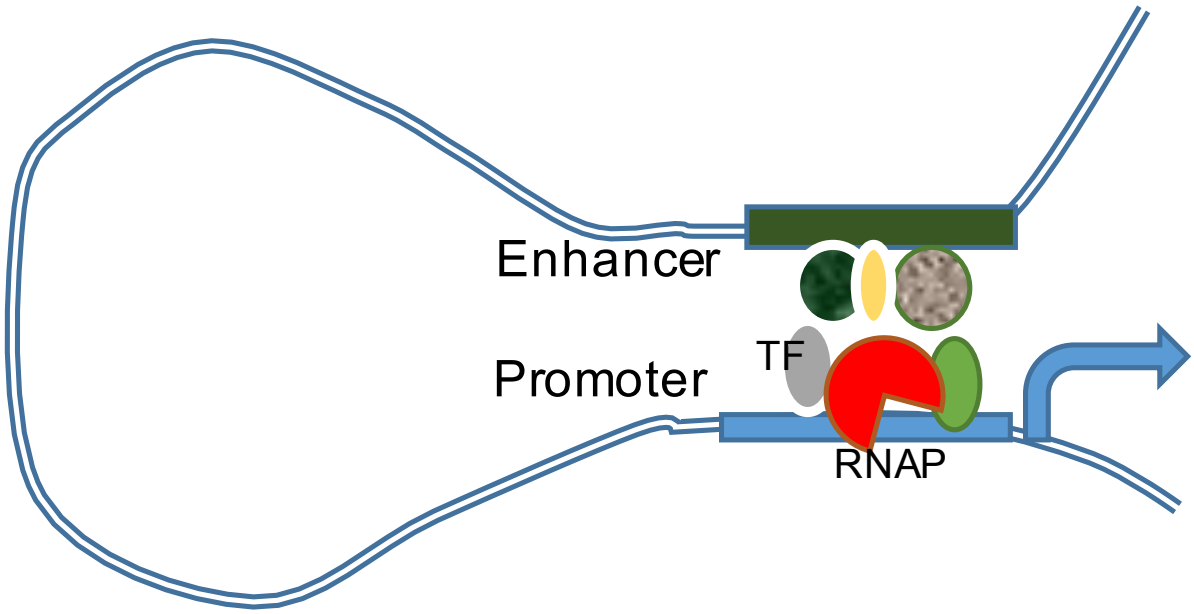

Figure 1.3: Regulatory elements in a cell: Promoter and enhancer in DNA. The few hundreds to a thousand base pairs region immediately upstream of a gene that mediates the assembly of the pre-initiation complex and initiate gene transcription is referred to as the promoter. An enhancer, on the other hand, is a distal regulatory element that interacts with a promoter by forming a loop.

example, a histone modification H3K4me3 at promoter of a gene can make promoter accessible to TFs and RNA polymerase, thus activating the gene. There are other types of histone modifications (for eg. H3K27me3) that repress the gene. DNA methylation is another modification to DNA that silences gene expression. Histone modifications and DNA methylation are also known to be inherited during the cell division and therefore are collectively called epigenetics [3]. Epigenetics, in summary, decides how transcription machinery reads the genetic instruction from DNA in a cell. It is also widely known that undesirable epigenetic changes cause many human disease [19, 20].

For transcription, a promoter needs to be unwound from histones so that TFs can bind [17]. Many TFs are activators, while others are repressor of genes. The

TFs not only bind to promoter but it can also bind a distal regulator of gene called enhancer (Fig 1.3). Like a promoter, an enhancer is a genomic region that can be bound by TFs to activate transcription of its distal target gene by interacting with the gene promoter [17]. To activate its target gene an enhancer physically interacts with the gene-promoter by forming a chromatin loop as shown in Fig 1.3. Enhancers are located up to 1Mbp away from TSS. Enhancers are also activated or inactivated by epigenetic factors like histone modifications and DNA methylation [21]. Some histone modifications are known to be specific to enhancers.

1.5 Biological processes performed by genes

Genes are involved in variety of biological processes in a cell. One of the way biological processes can be broadly categorized into [3]:

- Cellular metabolism: These are the set of biochemical reactions needed to maintain life and allow to the cells function properly. In a case of environmental changes, metabolism helps in cellular response to maintain the cell growth. Metabolism is perhaps the most studied cellular process, since it is often altered in diseases [7].

- Genetic information processing: It involves processes associated with the central dogma of molecuar biology (see section 1.2, i.e DNA replication, translation, transcription and DNA repair [22]).

- Cellular process: It involves process related to cell cycle, e.g. cell growth and

cell death. It also includes cell membrane function [22].

- Organismal systems: This involves organ specific functions such as associated with immune system, endocrine system, cardio-vascualar system, nervous system etc [3].

Many genes are multi-functional and may be active in multiple functional processes. The aforementioned categories are also not strictly disjoint. Because each cell type expresses specific set of genes, set of the active biological processes in a given cell type is unique to it.

1.6 Disruption of biological processes causes diseases

Each of biological process activated in a cell type is necessary for its normal functioning , and their disruption interferes with normal functioning of the cells. A severe malfunction manifests into a disease. Disruptions in biological processes are often mediated by gene expression changes. Various genetic and environmental factors can affect gene expression patterns in a cell [23].

1.6.1 Mutation

Any alteration to DNA sequence or genetic element is called mutation. Mutations may occur due to errors in DNA replication during cell divisions. It may also be a result of segmental insertion or duplication caused by mobile genetic el-

ements [24, 25]. Mutations at single nucleotide level that accumulate over time in a population, and are present at appreciable degree within the population (for eg. $> 5\%$), is referred to as single nucleotide polymorphism (SNP).

1.6.2 Coding mutation

Mutations that occur in genes are called coding mutations. Coding mutations can be of different kinds. A mutation in a gene may have no effect, alter the gene product, or hamper partially or completely the normal gene function. Most coding mutations that change amino acid of the resultant protein (called non-synonymous mutations) are harmful to the organism. For example 70% of non-synonymous mutations are estimated to be harmful in *Drosophila* [26]. The rest of the mutations are neutral. Only a few coding mutations are known to be beneficial to the organisms.

1.6.3 Non-coding mutation

Mutations can also occur in non-coding regions (called non-coding mutations) of the genome. Most mutations in human DNA are known to be neutral i.e they do not have any discernible effect on phenotype of the organism. However, many non-coding mutation in regulatory elements, such as enhancers and promoters, can also be deleterious. These mutations although do not change any protein product of genes, can severely affect regulatory network within cells. A mutation in a gene promoter can destroy the TFBS of an essential regulatory TF necessary for its transcription. It will prevent the TF from binding to the promoter, ultimately causing

down-regulation of the gene. Therefore, a non-coding mutation in a promoter can disrupt gene regulation and can have severe phenotypic consequences. For instance, SDHD is a metabolic gene and mutations in its promoter are known to cause down-regulation. The mutation in SDHD promoter mutations are associated with gastric cancer and paraganglioma [27, 28].

A mutation in a gene promoter can also affect the gene. A somatic mutation – mutation that is not inherited, i.e, it does not appear in germ-line cells but in somatic cell – in promoter of TERT gene over-activates the gene. The occurrence of somatic mutations are associated with oncogenesis, particularly in melonomas, bladder and hepatocellular cancer [29].

A mutation in an distal regulatory element can also affect expression of its target gene, and therefore can contribute to a disease. The disruption of enhancers by mutations has been linked to both Mendelian and complex disease traits. In human, sonic hedgehog (SHH) gene is controlled by an enhancer that is almost a megabase away from it. Further, mutations in the enhancer is shown to result in pre-axial polydactyly in families [30].

It must be noted that, the impact of non-coding mutations on phenotype may vary from that of coding mutations, even if the both mutations disrupt same gene. Mutations in enhancers or promoters only affect expression levels of their target genes, whereas those in coding regions may alter protein product, stability or folding [31]. Generally, coding mutations are more detrimental than those of non-coding mutations. Most enhancers are tissue specific, they are active and regulate genes in few tissues. Consequentially, a mutation in a tissue specific enhancer will

manifest into a phenotypic disorder only in specific tissues. In contrast, mutations in promoters will affect expression more globally. For example TBX5 is a gene involved in heart and forelimb development. Smemo et al. demonstrated that a mutation in heart specific enhancer of TBX5 affects heart development and not forelimb development [32]. Localization of phenotypic effect is another distinction between the coding and non-coding mutations.

1.7 Heritable mutation disorder

Heritable mutations, mutation which are either inherited from parents, or occur in germ-line, cause two class of genetic disorders:

1. Monogenic disorders (Mendelian disorder): They are disorders that manifest due to disruption of a single gene. For example sickle cell anemia is caused by mutation in haemoglobin gene [33].

2. Polygenic disorders (Complex disorder): They are disorders that are caused by mutation in multiple genes. For example cardiovascular diseases, diabetes and hypertension are caused by mutation in multiple genes.

Online Mendelian Inheritance in Man (OMIM) have cataloged around 4,000 diseases which are believed to be caused by alterations in a single gene. Mendelian disorder are not common and are generally very rare disorder. Since monogenic disorders manifest due mutation in single gene, it relatively not hard to predict the disease onset. They are inherited in families, so tracking the genes that cause the

disease through families is relatively easy. Complex disorders also occur in families, but the inheritance rules are much more complex. We have poor understanding these rules of why some family members develop them while others remain healthy [34].

In past decade, association studies are extensively used to identify genetic and molecular determinants associated with a disease (or phenotype). These studies were aimed at identifying genomic variants that are associated with phenotypic traits in the population, specifically at detecting association either between SNPs and common diseases such as cardiovascular diseases, cancer risk, hypertension, diabetes etc, or between SNP and gene expression [35]. There are two types of association studies :

1.7.1 Expression quantitative trail loci (eQTL)

The primary goal of Expression quantitative trait loci (eQTLs) is to identify genetic variations that determine the expression variation among individuals in a population and ultimately uncover underlying regulatory network by which an individual variation leads to expression changes [36].

eQTL studies are conducted using gene-expression and genotype of multiple individuals. A SNP is deemed associated with a gene if the gene expression is significantly different in people with one particular allele compared to other.

1.7.2 Genome wide association studies (GWAS)

The ultimate aim of Genome wide association studies (GWAS) is to determine genetic risk of an individual to develop a disease and to reveal biological mechanism that underlies the genetic disease, so that it can be harnessed for prevention and therapeutics [37].

GWAS are conducted similarly to eQTL, however it requires genotype and disease information (phenotype) of each individual in a population. If people with a particular SNP allele have much higher occurrence of disease compared to others, the SNP is called to be associated. GWAS represents a powerful tool for understanding molecular underpinnings and genetic makeup of complex polygenic diseases [38–40]. These studies have revealed thousand of risk loci associated with such disorders and have provided valuable molecular insights into their regulatory architecture [41, 42].

1.7.3 Limitation of association studies

In the past decade, numerous association studies were conducted, and yet at the same time, they have been heavily criticized. The criticisms include association studies cannot explain enough genetic and phenotypic variation in the population. However, the major disappointment with the association studies is due to perception that results they produce are neither biologically relevant nor have any therapeutic utility [35]. The major limitations [43] and challenges of the association studies are:

- **Associated variants in non-coding region**: Less than 5% of associated SNPs fall in coding region of genome (both synonymous and non-synonymous).

Rest of the associated SNPs fall in non-coding region [44]. Therefore they are not immediately informative. Further they are hard to validate experimentally.

- **Linkage disequilibrium**: It is defined as non-random association of alleles between different loci. When two alleles occur together significantly more often than expected by random chance, they are called to be in linkage disequilibrium. Linkage disequilibrium are caused due to variety of factors such as selection, recombination rate, mutation rate, genetic drift, population structure, mating system and genetic linkage [45].

  In the human genome, each SNP loci are in linkage disequilibrium with hundreds of other SNPs. All SNPs which are in a strong linkage disequilibrium with a causal variant of a phenotype will also show strong association. Therefore association does not necessarily imply causality of the factor. Further, most of the association studies use genotyping and the original causal SNP may not be in the genotyped chip [44].

- **Missing heritability**. Only a portion of phenotypic variance is determined by genetics (called heritability). Further, as any association studies consider a subset of all possible genetic factors in the analyses, there is upper bound on how much of heritability, called as narrow sense heritability [38], can be explained by association studies. This can be estimated by twin studies. However, phenotypic variance explained by most of GWAS are much smaller than the estimated narrow sense heritability [38] (difference referred to as missing heritability).

- **Rare variants (and not common variants) may be causal** : Missing heritability in GWAS points to the fact that rare rather than common variants may be causal, which are generally missed by SNP array technologies [44]. Further, in order to achieve enough statistical power much larger sample size will be required to detect associations [38].

- **Reproducibility**. Many GWAS are conducted on single population and are not generalizable across studies or populations, suggesting that many of the associations are false positive and have no biological relevance. [46].

1.7.4 How to improve association studies?

In recent years, multiple association studies have shown strong and consistent association of thousand of genomic variants with various diseases. However, their interpretation of the molecular mechanisms remain challenging. Characterization of missense and nonsense coding mutations offers a solution for coding variants. Given the abundance of non-coding functions and current state of incomplete annotation of transcriptional regulators and their poor understanding, the challenge of interpretation is far more formidable for non-coding variants [47–50].

Several recent efforts were geared to provide a comprehensive map of regulatory annotations. For example, the Encyclopedia of DNA Elements (ENCODE) [51] project has released comprehensive map of epigenetic data for many primary cell lines. Epigenome road-map project [52] has taken initiative to deliver these annotation in primary cells and cultured cells. The explosion of epigenetic data has made it

possible to detect cell-type-specific regulatory regions [43,47–50], which can be used to distinguish regulatory SNPs from non-regulatory SNPs in LD blocks. Further it will help us to interpret non-coding associated variants, which constitute majority of reported GWAS variants. Finally, the data will help to solve the problem of limited statistical power to detect associations of rare variants (refer to chapter 3 for details).

1.8 Somatic mutation disorder

Although certain germ-line mutations are known to be associated with risk of cancer onset, only around 5-10% [53] of cancer incidences are known to be hereditary. Cancer is mainly caused by genetic alterations that occur in cells within the life span of an individual, i.e somatic mutations.

1.8.1 Hallmarks of cancer

Genetic diseases, such as Cardio-vascular diseases or hypertension, are result of a systematic break down of the normal functioning of cells, where regulatory networks and cellular processes are severely compromised. In contrast, cancer is a unique genetic disorder where transcription machinery and cellular processes are hijacked to allow cancer to proliferate continuously.

In cancer, existing cellular processes and regulatory networks are reprogrammed in systematic manner to tailor the need of malignant cancer cells. In the remodeling of normal cells to cancerous cells, a tumor undergoes a series of genetic and tran-

scriptome alterations, each conferring specific proliferative advantage, which leads to gradual conversion of normal cells to cancer cells. Proliferation and homeostasis of normal cell are governed and limited by check points embedded in a robust regulatory circuit. Systematic reprogramming in cancer cells allow them to bypass these checkpoints. Hanahan et. al. suggested six essential alterations in cells that dictate the oncogensis [54, 55]:

- **Self sufficiency of growth signal**: Normal cells require specific growth signal (GS) from extracellular signaling molecules to proliferate. Tumor cells, in contrast, show a greatly reduced dependence on the external growth stimulation. Many oncogenes mimic growth signals in tumors and evade the external GS dependence. For instance glioblastomas and sarcomas produce growth factors PDGF and TGFα. Alternatively, cancer can alter the downstream pathways of GF signaling by permanently activating the pathways that respond to the GFs.

- **Insensitivity to growth-inhibitory (antigrowth) signals**: Multiple antigrowth signals operate in cells, blocking the uncontrolled proliferation of normal tissue, predominately acting through trans-membrane signaling receptors and intracellular signaling pathways. They either force a cell out of the proliferation in a quiescent state (G0) or permanently switch off the proliferation potential of a cell.

  Cancer evades these antigrowth factor signals to keep proliferating uncontrollably. Much of the insensitivity is achieved by disruption of pRB pathway

responsible for blocking cell transit through G1 into S phase. Tumor suppressor genes that primarily control the antigrowth signal, are highly disrupted in cancer so that cell divisions are not prevented in cancer [56].

- **Evasion of programmed cell death (apoptosis)**: Rate of tumor expansion depends upon proliferation rate and rate of cell death. Programmed cell death, known as apoptosis, is a major mechanism by which uncontrolled growth is tackled in the normal cells. The acquired resistance to the apoptosis is a hallmark of all cancer types [54]

  Cancer acquires the apoptosis resistance through a variety of strategies. Most commonly through mutation in p53, a tumor suppressor gene that regulates apoptosis. The P53 functional inactivation is observed in more than half of the tumors [57]. In addition antiapoptic signals are over-expressed in tumors such as over-expression of AKT/PKB pathway mitigates apoptosis and are over-expressed in many melonomas. Cancer cells may also alter the capability to detect DNA damage or abnormalities, thus avoiding the apoptosis.

- **Limitless replicative potential**: Three acquired capabilities – independence of the growth signals, insensitivity to antigrowth signals, and resistance to apoptosis – do not suffice in supporting uncontrolled tumor growth and tumorogenesis due to an intrinsic limit on a number of cell divisions allowed. Once cells have achieved a certain number of doubling they stop dividing, a concept termed as senescence. This program is independent of cell signaling. In order for cells to grow in malignant tumor, they must evade this program

too.

Telomeres located at the ends of chromosomes are the counting devise, which shorten with every cell divisions. The progressive shortening causes cells to eventually lose their capability to divide further. Telomere maintenance is evident in all types of tumors. In most tumors, their maintenance is mediated by telomerase up-regulation, the enzyme responsible for maintaining telemore length in stem cells [58].

- **Sustained angiogenesis**: Nutrients and oxygen are supplied by blood to each cell and are necessary for maintenance and survival. The formation of new blood vessels is referred to as angiogenesis. The expanding tumor needs additional routes for blood supply. Cancer hijacks the angiogenesis to ensure adequate oxygenation. This is achieved by disruption of the production of factors that regulate blood vessel formation.

- **Tissue invasion and metastasis**: Advanced stages of tumors eventually acquire capability to invade adjacent tissue and metastasize to distant sites. Most of cancer types do not lead to patient's death unless they metastasize. In fact 90% of cancer deaths are due to metastasis [59].

1.8.2 Cancer therapies

The main aim of an anti-cancer therapy is to selectively kill cancer cells, without affecting the normal cells. Current cancer therapies in one way or another target one of the hallmarks of cancer. For example kinase inhibitor like Gleevec (iman-

tinib msylate) selectively kills chronic myeloid leukemia (CML) and gastrointestinal stromal tumors (GIST) cells. CML is driven by over-activation of growth factor ABL kinase through a mutation of kinase fusion protein BCR-ABL. Whereas GIST is caused by over-activation of PDGFR (platelet derived growth factor receptor). Gleevec effectively inhibits the activity of all of these growth factor kinases. The therapy shows remarkable initial response in the patient's where the kinases are over-active by selectively eliminating tumor cells and in many cases tumors disappear within few regimens of the therapy. Similarly, in lung cancer, epidermal growth factor receptor (EGFR) inhibitors have great response in tumors with activating mutation in EGFR gene. In lung cancer, clinical responses to epidermal growth factor receptor (EGFR) inhibitors are associated with point mutations in the EGFR kinase domain. Nearly 25% of breast cancer patients have over-expressed ERBB2 (HER2) gene, which drives tumor cell growth. Targeting the oncogene has been shown to be effective treatment in HER2 positive breast cancer patients [60].

1.8.3 Cancer resistance and molecular reprogramming

Advances in biomarker discovery approaches have led to significant improvements in targeted cancer therapies in the past decade. However, the success of most of the therapies are short-lived due to emergence of resistance to drugs and eventual relapse of cancer. The mechanisms of drug resistance share many features such as activation of drug efflux, alterations in the drug target, and downstream adaptive responses [61]. A key driving force underlining in the emergence of cancer resis-

tance to specific drug treatments involves changes in the activity of a gene that can buffer the inactivation of the specific drug targets. For instance Lapatinib show impressive initial response in HER2 positive breast cancer patient by inhibiting HER2 (ERBB2) gene. However, resistance to the therapy eventually emerges in patients. Lapatinib resistance is known to be caused either by over-expression of ERBB3 gene that replaces the downstream function of ERBB2, or by over-expression of other kinases that compensates for the ERBB2 inhibition by over-activating downstream target of ERBB2 gene directly [60]. Interaction between genes are likely to be major determinant of cellular reprogramming that leads to resistance.

1.8.4 Genetic interactions in cancer

In order to better understand the mechanism of drug resistance and long term effectiveness of cancer therapies, we need to understand landscape of genetic interaction in cancer. There are a few well-known and extensively studied types of gene interactions (GIs). First and foremost are Synthetic lethal interactions (SL), which describe the relationship between two genes whose individual inactivation results in a viable phenotype while their combined inactivation is lethal to the cell [62–70]. SLs have long been considered a potential basis for developing selective anticancer drugs [71–73]. Such drugs are aimed at inhibiting the SL partner of a gene that is inactivated by genomic alterations in the particular cancer, thus potentially leading to more selective cancer treatments that primary kill the cancer cells with few cytotoxic effects on healthy cells. Another important class of GIs are synthetic dosage

lethal (SDL) interactions, where the under-activity of one gene together with the over-activity of another gene is lethal but not each event individually [74]. In a manner similar to SLs, SDL interactions also provide a powerful alternative for targeting cancer cells, and are potentially promising for targeting tumors with activated oncogenes, many of which are known to be difficult to target directly. Instead, targeting the oncogenes SDL partner may selectively kill cancer cells [75].

Fueled by Next Generation Sequencing technologies, TCGA (The cancer genome atlas) have provided genetic, molecular and clinical annotations of thousands of tumor samples for 27 different tumor types [76]. Capitalizing on TCGA, Jerby et. al. proposed a direct data-driven approach, termed DAISY [71], for identifying candidate SL and SDL-interactions via the analysis of the omics data directly from a large collection of patient tumor samples. Mapping the first genome-wide pan-cancer SL-network, they showed SL can successfully predict both gene essentiality and drug response as well as patient survival [71].

1.9 Computation challenges

With advances in high throughput sequencing, the emphasis have shifted towards analyzing the data using big data approaches. Beside posing a computational challenge due to size of data, the rapid accumulation of large data poses challenge to integrate informations from diverse dataset to extract inferences about the adaption, diversity and complexity of biological system. The main computational issues in the problem covered in this thesis i.e, identifying molecular underpinning of dis-

eases onset and drug resistance are :

1. Substantial amount of noise in the biological data

2. Integrating the information flow to account for the biological mechanism

3. Over-fitting in modeling

4. Confounding factors

Bayesian approaches are ideally suited for the problems, which need to extract information from complex data, especially where there exists uncertainty in the data due to noise. The source of noise may include experimental error or noise, as well as noise due to intrinsic random variations. In Bayesian approaches it is imperative to specify a "prior" distribution before the data is observed. Assigning priors implies all sources of variance and uncertainty are now treated in the unified and consistent manner. This forces us not only to integrate our assumptions and constraints in the model but also integrate our prior knowledge (for eg. mechanism) about the biological system, which is a philosophically appealing feature of the Bayesian paradigm [77, 78]. This also provides relatively richer information about the model parameters. Further, this makes inference robust to outliers and lack of data [77].

The information flow within a cell are essentially hierarchal. Information in DNA are transcribed to mRNAs [3]. Transcriptional regulators modulate also the mRNA, which in turn are modulated by different epigenetic factors. Epigenetic factors themselves are dependent on DNA and environment. Many of the biological

problems therefore can be improved in a fundamental manner by modeling the information hierarchies. Emphasis, therefore, has now shifted to data driven bottom-up approaches, integrating the different hierarchies of the information flow to parameterize bottom-up mechanistic models of biological processes. Bayesian methods offer a systematic approach to propagate uncertainty across different levels of modeling to make inferences. Not surprisingly, Bayesian methods are now a day extensively used in genetics, bioinformatics and system biology.

When a model fits the training data, but does not generalize to unseen data is called Over-fitting. It occurs in a statistical model when it tries to describe the random variation with in the data instead of the underlying relationship. The main consequence of the over-fitting is that it exaggerates performance of the model and also will have poor performance in unseen (test) data. The over-fitting is usually caused by over-parameterization and lack of the regularization. Cross-validation is the most popular technique to estimate level of the over-fitting and reduce it from the modeling [79].

The most attractive feature of the Bayesian paradigm is "integrating out" all irrelevant variables, which inherently leads to implementation of Ockhams Razor [78, 80, 81]. Bayesian frameworks in that case automatically prefer a simple model provided that it is sufficient to explain the observed data. This concept enables to set regularization parameters and select models without the need for any additional validation [77].

Confounding factors are the variables that are correlated with both dependent and independent variables. Due to confounding factors inferences from the model

are often biased and in many instances completely wrong. For example when determining what gene causes a disease, co-expression between genes is a confounding factor. It is one of the most challenging issue in computational modeling, which cannot be automatically corrected but needs explicit correction by including them in modeling. The presented thesis proposes multiple ways to account for confounding factors both in Bayesian and frequentist paradigms.

1.10 Significance

Recent advances in high throughput sequencing have made it possible to assay new arrays of genome-wide biological data. Methods that can capitalize on these to identify the molecular and genetic underpinnings of disease can significantly advance not only our understanding of biology but also clinical applications. In consonance, the thesis presents our computational efforts to bridge the diverse array of genome-wide biological data into statistical frameworks to make inferences about mechanistic understandings, molecular and genetic underpinning of cardiovascular diseases, hyper-tension and cancer. In the first part of the presented work, we demonstrate ways to improve association studies by integrating epigenetic and genetic interaction information to the association studies. In second part, we discover a new class of genetic interactions that underlies ongoing molecular reprogramming in cancer in order to overcome drug treatment and become resilient to external onslaughts like various drug treatments.

1.10.1 Cardio-vascular disease and hypertension

Genetic diseases such as Cardio-vascular diseases (CVD), hyper-tension, and cancer affect millions of people all over the world. Cardio-vascular diseases are the leading cause of the deaths in US. As per World health organization (WHO) overall 31% of all the deaths worldwide are due to Cardio-vascular diseases which includes coronary heart diseases and strokes [82]. More people die due to CVDs than any other cause. It accounts for nearly 17% of total the National health expenditures. Most of Cardio-vascular diseases can be prevented if people at high risk for CVD are diagnosed early and therapeutic interventions are personalized. Despite extensive research, genetic and molecular factors that lead to CVDs in humans remain elusive, undermining the efforts of the early detection and prevention. Further, it severely limits our ability to devise new CVD targeted therapies and interventions.

With advances in the next generation sequencing technologies in the past decade, genomic, epigenomic and molecular data obtained both from patients and healthy population are rapidly accumulating. Approaches that can systematically exploit the rapidly expanding data to identify determinants of CVD can significantly advance our efforts to detect risk of CVD, prevent and devise novel targeted therapeutic interventions. The presented thesis first describes our efforts to identify determinants of CVD followed by developing computational approaches that integrate a diverse array of high-throughput data pertaining to regulation and disease etiology.

1.10.2 Cancer

Cancer is also among the leading cause of death worldwide and in US. Around 15 million new cases of cancer and 8.2 million deaths were reported in 2012 [82]. Among all diseases National institute of health devotes highest amount of its budgetary allocation to the cancer research. It is expected that the number of cancer cases will increase by 70% in the next two decades. In the past decade multiple anti-cancer therapies have been introduced showing a promising initial response. However, the frequent emergence of resistance to therapies and eventual relapse remains most daunting challenge in fighting cancer. Molecular determinants of the resistance emergence that limit effectiveness of the current therapies remain elusive and a pressing challenge in cancer research.

Our computational efforts in cancer research were geared towards identification of molecular determinants and mechanisms that determine resistance and effectiveness of anti-cancer therapies. Indeed, recent studies published in many high-impact journals have aimed to address this challenge by measuring the molecular profiles (typically DNA or RNA sequencing) of tumors before and after a given drug treatment to characterize drug and tumor specific molecular signatures of emerging resistance (e.g., [83–86]]). Such studies – which are another example of causal inference – are quite labor intensive and costly, requiring the designated collection and assessment of pre- and post-treatment data for every specific treatment and cancer type in dedicated painstaking clinical studies. Moreover, importantly, such clinical studies are infeasible for estimating the potential of emerging resistance to

investigational drugs during their development. In the present work, we take a fundamentally different and novel approach to address resistance to therapy in cancer. We define a new class of genetic interactions termed synthetic rescues (SRs) (defined in Background) that provide fundamental insights into the molecular underpinnings by which cancers reprogram their molecular activity in response to specific drug treatments, to rescue themselves from the onslaught. The reprogramming can be mediated by cellular response (such as changes in regulatory network) to external onslaughts. Alternatively, such reprogramming can be explained by selection of tumor cells (within a heterogeneous tumor or rapid genetic and molecular alterations in a tumor) that confer selective advantage to the tumor to cope with the onslaughts.

1.11 Organization of Thesis

Part 1 consists of following two chapters:

In Chap. 2, we present a model to predict human heart enhancer using epigenomic data. We then show utility of the model by applying to hypertension data and showing improvement in identifying regulatory SNPs over traditional association studies. [47]

In Chap. 3, we introduce a coupled Bayesian regression approach – eQTeL [87], which leverages epigenetic data to estimate regulatory and gene interaction potential, and identifies combination of regulatory SNPs that explain the gene expression variance. We apply eQTeL to the human heart data and demonstrate its superior performance in identifying putative causal regulatory SNP over existing eQTL meth-

ods. The model unravels specific regulatory mediators that participate in interaction between regulatory SNPs and target genes.

In Part 2 or the thesis we introduce a novel class of gene interactions termed Synthetic Rescue (SR) that underlies extensive genetic reprogramming emerging with cancer progression. We also propose a data driven computation framework, termed INCISIOR, to identify SR in a genome-wide fashion [88]. Applying INCISOR to mine The Cancer Genome Atlas (TCGA) [76], a large collection of cancer patient data, we present the first genome-wide pan-cancer compendium of synthetic rescue (SR) interactions. In the rest of the chapter we (i) comprehensively characterize emergence and evolution of SR and (ii) demonstrate their role in the emergence of resistance to current cancer therapies and (iii) determine personalized effectiveness of the therapies. Finally, we provide therapeutic application emerging from the SR.

Chap. 5 concludes the thesis providing a discussion and a future perspective.

1.12 Contribution

The presented work was only possible due to immense support and guidance from numerous collaborators. The work shown in this thesis has been done by the author by collaborating with many others. The collaborator contributions for each chapter are shown below. Keywords used for collaborator names: S.H - Sridhar Hannenhalli, E.R - Eytan Ruppin, J.L - Joo Sang Lee, S.G - Silvio Gutkind, R.B - Ramiro Iglesias-Bartolome, R.A - Radhouane Aniba, Y.P.C - Yen-Pei Christy Chang, MM - Michael Morley, CSM - Christine S. Moravec, WT - W. H. Wil-

son Tang,H.H- Hakon Hakonarson, M.C- MAGNet Consortium, K.M- Kenneth B. Margulies, T.C - Thomas P. Cappola, S.J - Shane Jensen A.D - Avinash Das Sahu.

- *Chapter 2*: S.H conceived the project. A.D developed the model under supervision of S.H. S.H, A.D and R.A analyzed the data and performed the analyses. All authors wrote the manuscript.

- *Chapter 3*: S.H and A.D conceived the project. A.D developed the Bayesian method under supervision of S.H. A.D devised the inference algorithm with help from S.J. A.D and S.H analyzed the data and performed the analyses. M.M, C.M, W.T, H.H, K.M, T.C and other members of MAGNet Consortium generated the MAGNet data. S.H and A.D wrote the manuscript, with help from others.

- *Chapter 4*: A.D, J.L and E.R conceived the project. E.R supervised the project. A.D and J.L developed INCISIOR method under guidance of E.R and with help from S.H. E.R, A.D, J.L and S.H designed the analyses and experiments. A.D and J.L analyzed the data and performed the analyses. S.G and R.B conducted the shRNA experiments. E.R, J.L and A.D wrote the manuscript, with help from others.

Determinants of Cardio-vascular disease and hypertension

Chapter 2: EPIGENOMIC MODEL OF CARDIAC ENHANCERS WITH APPLICATION TO GENOME WIDE ASSOCIATION STUDIES

2.1 Overview

Eukaryotic transcription is intricately regulated at multiple levels including chromatin reorganization through epigenomic modifications and sequence specific binding of transcription factors (TF) to either proximal promoter or to distal enhancer/repressor regions of the gene [89, 90]. Enhancers can regulate their target genes from long distances, up to a megabase away and are especially important in regulating developmental and tissue-specific genes [91, 92]. Numerous genome wide association studies (GWAS) have revealed genomic loci associated with various human traits [93]. Going from association to causality is however a major challenge, because a vast majority of GWAS signals lie in non-coding regions, often far from any gene, and our understanding of functional consequences of non-coding mutations is incomplete. It is possible that many of these associations are mediated via regulatory regions [94]. By investigating putative polymorphic enhancers near GWAS signals, we might be able to identify the causal links between genetic variability

and disease, at least in some cases. Thus, both for our fundamental understanding of transcriptional regulation as well as for interpretation of genotype-phenotype relationships, a comprehensive knowledge of context-specific enhancers is critical.

Large scale identification of enhancers is challenging because they do not have sufficiently discriminating sequence properties (except for their tendency to harbor homotypic binding motifs [95]) and their location is not restricted relative to the location of the target gene. Moreover, enhancers are often tissue and cell-type specific and are detectable only under the appropriate conditions. Recent revolution in sequencing technologies have triggered several large scale profiling of epigenomic marks and analysis of these marks have revealed strong associations between enhancers and specific epigenomic marks (either positive or negative [96–98]). Using genome-wide profiling of several epigenomic marks, Ernst et al. segmented the genome into 51 segment classes, where each segment class is defined by a specific combination of epigenomic marks [96, 99]. They designated two of these segment classes as strong and weak enhancers. Apart from epigenomic marks, histone acetylase P300 is known to bind to tissue-specific enhancers, with high rate of experimental validation using mouse transgenic [98, 100]. However, it is argued that while P300 may mark tissue-specific enhancers, those enhancers are not necessarily active in a specific context [101]. This assertion is consistent with less than perfect validation rate of P300 bound regions as enhancers. Despite this, previous approaches to predict enhancers have used P300 bound regions as the gold standard to assess the methods prediction accuracy [102, 103].

Here we report an SVM trained specifically on 83 validated cardiac enhancers

using four epigenomic profiles marks (H3K4me1, H3K27me3, P300 and DNase hypersensitivity) in human heart tissue. Our model achieves a cross-validation classification accuracy of 84% and 92% on positive and negative sets respectively. It was encouraging that our model can distinguish validated enhancers from those that were bound by P300 but failed to exhibit enhancer activity in transgenic mouse. Next, starting with a comprehensive set of 229 SNPs associated with cardiac phenotypes in 36 GWAS studies, we identified putative enhancers harboring SNPs in linkage disequilibrium (LD) with the GWAS SNP. We found that our predicted enhancers are enriched for binding sites for all known core cardiac transcriptional regulators GATA, MEF2, STAT, NF-AT, Nkx, and FOX. Using a novel approach we show that the predicted enhancers are likely to regulate the nearby gene. Our predicted enhancers uniquely point to a few genes highly relevant to the heart disease. Moreover, these tendencies of having enriched cardiac transcriptional motifs and likelihood of regulating nearby genes are more favorable for the predicted enhancers compared with an approach that uses P300 binding as a marker of enhancer activity. Overall, we show that a SVM model trained exclusively on validated enhancers performs better than those that use P300 binding as gold standard and that GWAS studies can be better interpreted in light of predicted polymorphic enhancers.

2.2 Background

2.2.1 Expression quantitive trait loci

Expression quantitative trait loci (eQTLs) identifies genetic variations that determine the expression variation among individual in a population. And aim to ultimately uncover underlying regulatory network that drives gene expression. [36].

Jansen et. al. first proposed the concept of eQTL mapping in 2001 [104] and the first eQTL study was conducted on two yeast strains [105]. Since then, eQTL have attained tremendous amount of attention in understanding of regulatory variation and its consequence in humans and other species.

eQTL studies identifies genomic regions that effect the expression of on or more genes. These are inferred based on population studies. Individual in population vary at multiple loci from each other. In human, any two individual vary at rate of 1 in 1300, i.e on average any two individual have different sequence at around 4.6 million loci in genome called Single polymorphic nucleotide (SNP). Most of the variations in an individual are non-functional, i.e. they does not have any phenotypic consequences. In order to capture large variation in regulation a population with genetically different individual is required for conducting eQTL.

To conduct an eQTL study two types of data are required. First, DNA sequence information of the individuals in the population. This is usually accomplished by genotyping (such as SNP micro-array), if the sequence variant in the population is known. Alternatively, with advances in high throughput technology

it is now possible to sequence whole genome of individual such that all variants are collected. The whole genome sequencing approach is becoming more popular due to decrease in cost of the sequencing. Further, it ensures that rare variants or individual specific variants are accounted. Second type of data needed for eQTL studies are expression quantification of each gene in each of the individual. Micorarray and RNA sequencing are two popular technologies to quantify gene expression. To establish association between a genomic variant and a gene expression by frequentist appraoch, individuals are divided into groups according to the alleles for the variant. The variant is associated with the gene if the gene has significantly higher expression in one of the group compared to another. The test is conducted for for each variant and gene combinations.

Cis and trans effects

Expression of a target gene can be directly modulated by an eQTL in its regulators (such as in its enhancer and promoter). Alternatively, expression of a target gene can also be modulated indirectly by an eQTL of another gene B (such as transcription factor genes). The former type of eQTL lies in proximity of the target gene and hence referred as cis-eQTL. The later type can lie any where within genome and referred as trans-eQTL.

The successful eQTL will enable to understand of mechanism of gene regulation and how a mis-regulation manifest into a disease and ultimately to devise personalize treatment for patients. Amid advancement in next generation sequencing, recent eQTL have been conducted on larger and larger sample size to detect the rare SNP

association with gene regulation. However, two fundamental problems remains : (i) if the associations are causal (ii) if causal, then what is the mechanism by which a SNP regulate its target. In the third chapter of the thesis, we propose an alternative to eQTL to address both of the questions using a computation method by integrating information pertaining to regulations to eQTL.

2.2.2 Genome wide association studies

The ultimate aim of Genome wide association studies (GWAS) is to determine genetic risk of an individual to develop a disease and to underpin biological mechanism that underlies the genetic disease, so that it can be harnessed for prevention and therapeutics [37].

Analogous to eQTL, it involves DNA sequencing of large population of individual with and without disease, followed by finding association between Single nueclotide polymorphisms (SNPs) and the disease. The most popular frequentist approach to infer association is to calculate p-value of correlation for the null hypothesis (H_0) of no association, although many sophisticated approaches are proposed to overcome the shortcomings of the frequentist approach [**?**, 106, 107]. Factors such as population structure are known to be confounder in association studies. Such confounder factors are tackled by controlling for confounders in the sampled population. Alternatively, many recent studies take into account the confounding factors by explicitly modeling them in the association studies.

In one of the successful GWAS identified genetics disruption of CFH gene of

associated with age-related muscular destrophy (AMD). Not only they identified the association but also they determine precisely how the disruption manifest into AMD in an individual [108, 109].

Besides studying several genetic diseases, multiple GWAS studies are conducted to study various phenotypes. Many recent studies have identified genetic determinants that leads to variation in the drug response [110, 111]. For eg. Harper et. al. identified genetic variants associated with variation of warafin dosage response among humans [111]. The GWAS have been also studied to identify genetics variation associated with non-deleterious phenotype such as height etc [112].

2.2.3 Epigenetics and regulation

Sequencing of human genome laid the foundation to understand information stored in the genome. How this information is processed depends upon an additional layer of heritable biological information referred as *epigenetics* that have only just begun to be appreciated in past decade. The term *epigenetics*, which literally means *above or outside conventional genetics*, is now used to describe information stored in cell via chemical changes to cytosine and to the histones (proteins that regulates how the genome is packaged inside a cell) [18]. In a cell, how the genome will be finally read by the transcription machinery in the cells are maintained by these chemical modifications. They modulate the chromatin structure making available only part of the genome accessible to the machinery. Thus these modifications decide cellular fate and how same genome manifests into diverse array of biological state,

in particular different developmental stages and disease states [21, 113, 114].

Beside developmental processes, epigenetic modifications are known to be associated with two other processes (i) random changes and (ii) environmental changes. Our understanding how an external factors regulate the epigenetic modifications and in turn regulate the genome remains limited. However, it is clear now the epigenetic processes are key mediators that regulates the modification to DNA itself or protein associated with DNA [115]. The modifications are read and processed by specific protein and mediates appropriate biological effects.

2.2.4 Epigenetic Modifications

Epigenetics modification occurs in four broad categories: (i) DNA methylation, (ii) histone modification, (iii) DNA accessibility and (iv) Transcription factor binding. The CPG methylation occurs mostly at CpG dinucleotide and occur at lower frequency in at embryonic stages [116] and decreases significantly in somatic tissues [117]. Riggs et. al. first proposed DNA methylation could stabilize a particular gene expression pattern through mitotic cell division [118, 119]. Now DNA methylation is recognized to regulator of the stability of gene expression states, particularly in chromatin state silencing [120, 121].

Histone are protein that is essential of DNA packaging in the cells, DNA wrap around the histones to make primary cellular packaging. Histones undergoe around 100 different kind of post-translation modifications. The functionality of a histone modification depends upon two factors type of modification (acetylation, methy-

lation, phosphorylation, and ubiquitination) and position of modification in the histone tail. Most of the modifications are currently poorly understood. Modifications involving acetalyation are associated with DNA accessibility and transcription. Modifications involving methylation comes in different flavors – H3K4 and H4K36 are associated with transcribed chromatin, on the other hand H3K9, (H3K27), and H4K20 are associated with repression of gene transcription [18].

2.2.5 Epigenetic Inheritance

The epigenetic factors DNA methylation and histone modification are known to heritable which is not encoded in the DNA. DNA methylation patterns known to be propagated through cell division [21, 113]. In addition of DNA methylation, compelling evidence supports the heritability of specific histone modifications in multicellular organisms [122]. However, precise mechanism of histone modification inheritance remains still elusive. It must be noted that heritability of the epigenetic factor is much lower then DNA sequence, in other words during mitosis, accuracy with which DNA is replicated (from parent to daughter cell) is several order higher than epigenetic replication accuracy.

2.2.6 Support vector machines (SVM)

Support vector machines (SVMs) are supervised learning algorithms that among most popular machine learning metod to perform classification. Here we briefly revisit basic of SVM.

Given the labeled training data $\{\bar{x}_i, y_i\}, i = 1, ..., n$, where $y_i \in \{1, -1\}$ is label and $\bar{x}_i \in R^d$ are d dimensional features of training data i, the goal of support vector machine is to identify best hyperplane that separates positive and negative examples [123].

SVM assumes best hyperplane called "separating hyperplane", is a linear model of form $\bar{w} \cdot \bar{x} + b = 0$ (however, the separating plane is linear in transformed (dual) space and not in feature space [123]). Where, $\bar{w}$ is normal to the hyperplane. If d^+ (d) be the shortest distance from a hyperplane to the closest positive (negative) example, the separating plane have the properties that it maximizes the margin $d^+ + d^-$ Fig 2.1. Therefore, SVM simply searches for the hyperplane that maximizes the margin [123]. The maximization translates into quadratic programming formulation. As seen in the Fig 2.1, in training examples that lies closest to the separating plane, called as support vectors. They are defined as point in the training examples whose removal will change the solution of SVM.

2.3 Methods

More on SVM and grid search criteria

In SVM, vector in original feature space is projected onto a higher dimensional feature space using kernel function (usually non-linear). Because of this the data which in original space is not linearly separable, may become separable in transformed space, where the SVM tries to find a maximum margin hyperplane that separates the positive and negative set in the kernel space. SVM, employs a struc-

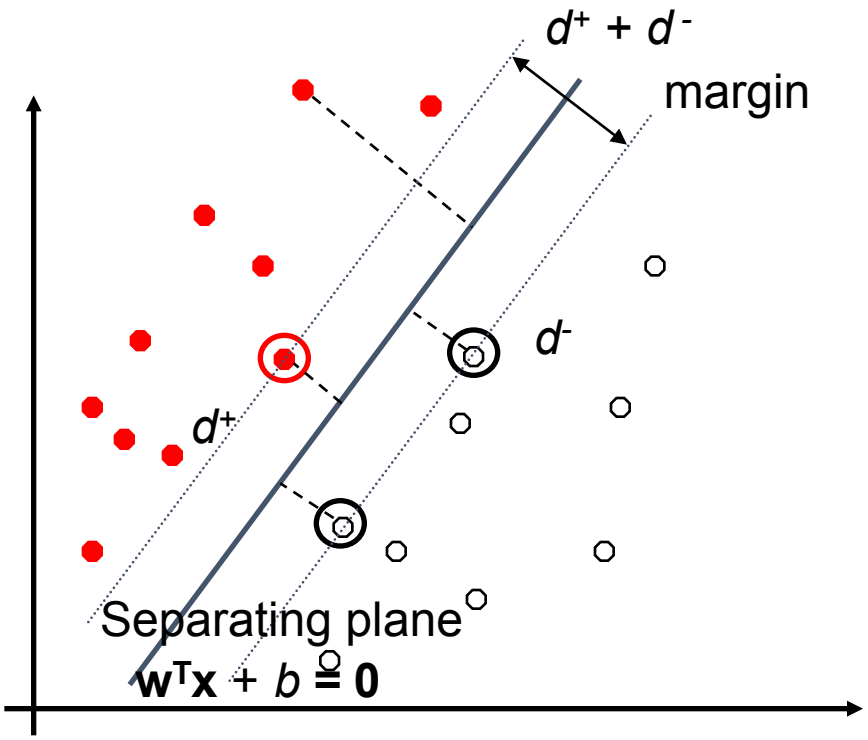

Figure 2.1: Support Vector Machine (SVM): SVM illustration for a linear separate case. Red (green) dot are positive (negative) examples. Support vectors are circled.

tural risk minimization (SRM) method [124, 125] to obtain the hyperplane, which tries to balance complexity of the model while minimizing the empirical risk. Therefore, relative to traditional methods based on empirical risk minimization, SVM is better suited to handle the problem of overfitting. SVM chooses a maximum margin hyperplane by identifying subset of training data (called support vectors), which would be closer to the optimal separating plane. Support vectors are cases which are most difficult to classify as positive or negative. Therefore to ensure good performance of SVM classifier, it is necessary to have a set of extreme examples (in both positive and negative example in the training set) that would qualify as support vectors.

Our positive training set included 330 (80% of 415) regions while the negative

training set included 1000 regions. We weighted the positive and negative examples to accommodate for the difference in sizes. An exhaustive search over the weight space was conducted to obtain best possible cross-validation result on a tuning set. The weight used for negative and positive set respectively was 1 and 1.2. Furthermore, we defined our criteria for grid search based on the observation that randomly sampled negative set may contain enhancer regions and therefore, it is not desirable to minimize false positive rate to extreme. In addition, we required that difference between two rates is below a fixed threshold. This is equivalent to maximizing the F-score, while keeping difference of true positive (TP) and true negative (TN) rate below a fixed threshold.

2.3.1 Correlating DNase Hypersensitivity and Gene Expression

To assess correlation of chromatin accessibility at a putative enhancer to expression level of a putative target gene, we extracted genome wide DHS as well as RNA-seq data from 15 cell types from a single study (GSE29692, GSE23316) representing a breadth of cell types HepG2, GM12878, A549, HeLa-S3, AG04450, BJ, NHLF, NHEK, HUVEC, h1-Hesc, HMEC, HSMM, K562, MCF-7, SK-N-SH_RA. For the enhancer region we extracted the DHS tag density in each of the 15 cell types using bigWigSummary tool. Correspondingly, for the putative target genes we obtained the gene expression (RPKM) in the same set of cell types. We then estimated the pearson correlation between DHS and gene expression as an indicator

of interaction between the enhancer and the gene.

2.4 Results

2.4.1 SVM model for cardiac enhancers

Data

Heart tissue was chosen for our analysis because of the availability of both relevant epigenetic data (H3K4me1, H3K27me3, P300 and DNase hypersensitivity) and validated human enhancers. We collected 83 experimentally heart enhancers validated in mouse transgenic from VISTA browse and split them into 1kb regions (step size 500 bps) to be used as positive training set. Negative set was constructed by mixing random samples of 1 Kb long regions from the genome and randomly selected promoters. H3K4me1, H3K4me3, H3K27me3, P300 and DNase-I epigenetic markers, which have previously been shown to be associated with tissue-specific enhancers, were collected for the heart tissue from the GEO database. For each epigenetic mark we calculated its average signal strength across every 1 Kb genomic region as feature vector of the region. In order to normalize the feature vectors of the positive and negative set to zero mean and unit variance, we randomly sampled 40,000 1 Kb regions across the genome to estimate mean and variance of feature vector.

Training

Epigenetic marks relevant to enhancers are relatively sparse in the genome. If the negative example in the training set only included random regions then SVM would choose subset of these inactive regions as its support vectors and would create a classifier hyperplane separating inactive regions from any epigenetically active region, resulting in high false positive rate. Therefore, in our negative set, in addition to random genomic regions, we added gene promoters as examples of epigenetically active non-enhancer regions. Figure 2.2 shows the effect of varying the proportion of promoters region in negative training set. In general, we found that a greater proportion of promoters in negative set improves positive set accuracy with relatively smaller decline in negative set accuracy, at least initially. This suggests that including a small fraction of promoters in the negative training set results in a better classification. Therefore, we constructed the negative training set by mixing 1000 random genomic regions and 250 randomly selected gene promoters.

Testing

We used 5-fold cross validation for positive set accuracy estimate. For negative test set we randomly sampled 1000 1kb genomic regions. On performing grid search (see Methods) to train the SVM model the average testing classification accuracy on positive set was 84.1% and on negative set was 92%. The roc curve for the model prediction is shown in Figure 2.3. The AUC of the model was 0.9231.

Despite some evidence to the contrary, a number of previous works have as-

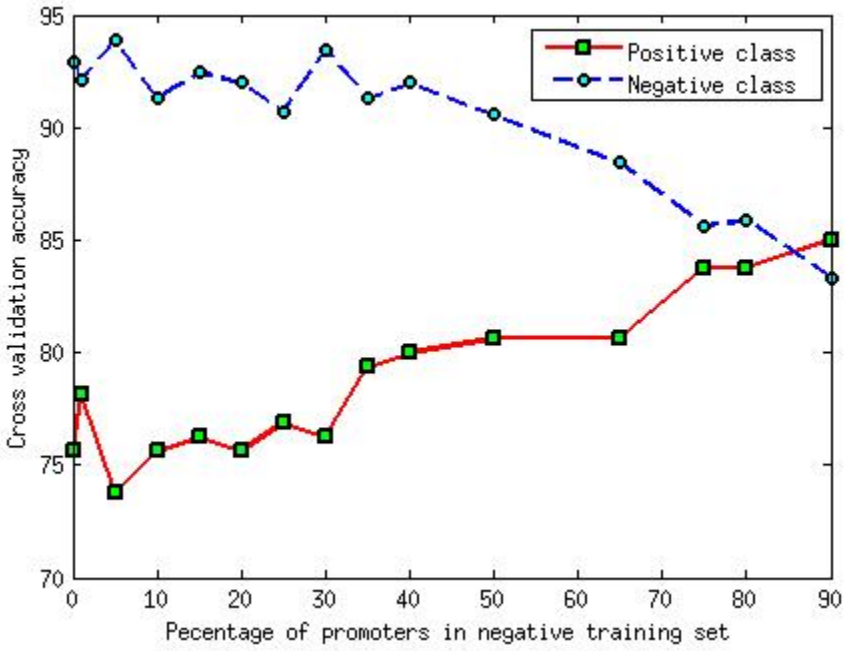

Figure 2.2: Effect of variation of proportion of promoter region on accuracy of model. Two fold cross validation is used for positive set. Negative set accuracy is calculated by running the trained model on large number of random 1 kb genomic regions not including those used for training.

sumed P300-bound regions to be active enhancers and used them as gold standards to train and evaluate enhancer prediction tools. Next, we tested whether our model trained on validated enhancer and oblivious of P300 binding can nevertheless distinguish active and inactive P300-bound regions. We tested our model with 12 P300 peaks in human heart which were found not to have enhancer activity [126]. Interestingly, the model classified 10(83%) of these cases as non-enhancers. Although based on a small set of examples, this suggests that our model can distinguish inactive P300-bound regions from active enhancers.

Narlikar et al. [127] proposed a model based on specific motifs as features for cardiac enhancer identification. To compare performance of our model with their's,

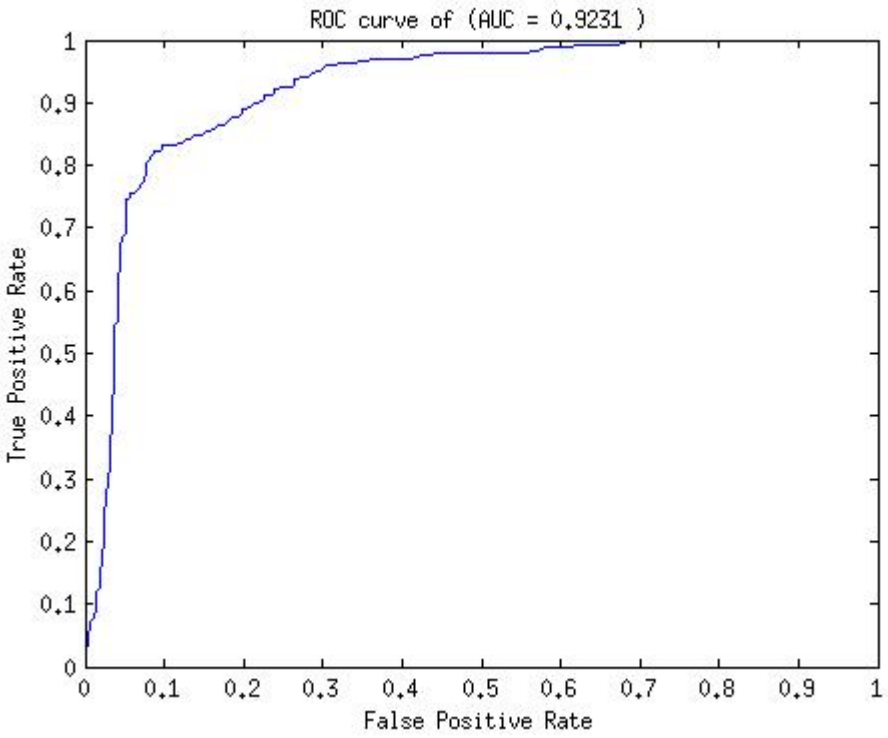

Figure 2.3: ROC curve of SVM model

83 validated enhancers were separated into 60 training and 23 testing instances. SVM was trained on the 60 instances. We extracted the 1Mb regions flanking each of the 23 test enhancers and predicted enhancer in those genomic regions using the trained SVM. We first checked how well P300 can retrieve the validated enhancers. We found that there are only 69 P300 peaks in adult human heart in the 23 genomic regions, out of which only one overlapped with a validated enhancer. In other words, P300 peaks are poor predictor of enhancer activity in this context.

Using our trained SVM model we scored each 1 Kb region in the test set. Cardiac enhancer predicted in Narlikar et al. [127] are typically much shorter. For fair comparison with Narlikar et al. [127] (1) we extended each of their enhancer to 1 Kb region flanking the reported location, and (2) used a threshold on the enhancer

score such that the predictions made by our SVM and the Motif based model cover almost the same number of enhancers (same basepair coverage as well due to extension) in the genomic test set. Among the 8522 enhancer regions predicted by the SVM, 21 of the 23 validated enhancers were included, while among 8551 enhancer regions predicted by Narlikar et al. [127] only 13 were covered. we repeated the above comparison between our method, P300 peaks and Narlikar et. al. 10 times with different sets of 60 training and 23 testing instances out of total 83 enhancers. Figure 2.4 shows the number of enhancer predicted by each method across different iterations.

Taken together, these results suggest that the SVM model trained on epigenomic data is more suitable for identifying cardiac enhancers than are P300 binding or motif based models.

2.4.2 Identification of cardiac enhancers near SNPs associated with cardiac phenotypes

Next, we hypothesized that the causal variants underlying GWAS signals might lie within an enhancer element and affect gene regulation. We tested this hypothesis on SNPs associated with a variety of cardiomyopathies. Starting with NHGRI's GWAS catalog [93], which includes 1332 studies revealing 6852 SNPs, we manually selected studies for cardiovascular disease traits. This yielded 229 SNPs from 36 studies. We then extended this seed SNPs set to include all other SNPs in Linkage Disequilibrium (LD) with a seed SNP using Broad Institutes SNAP

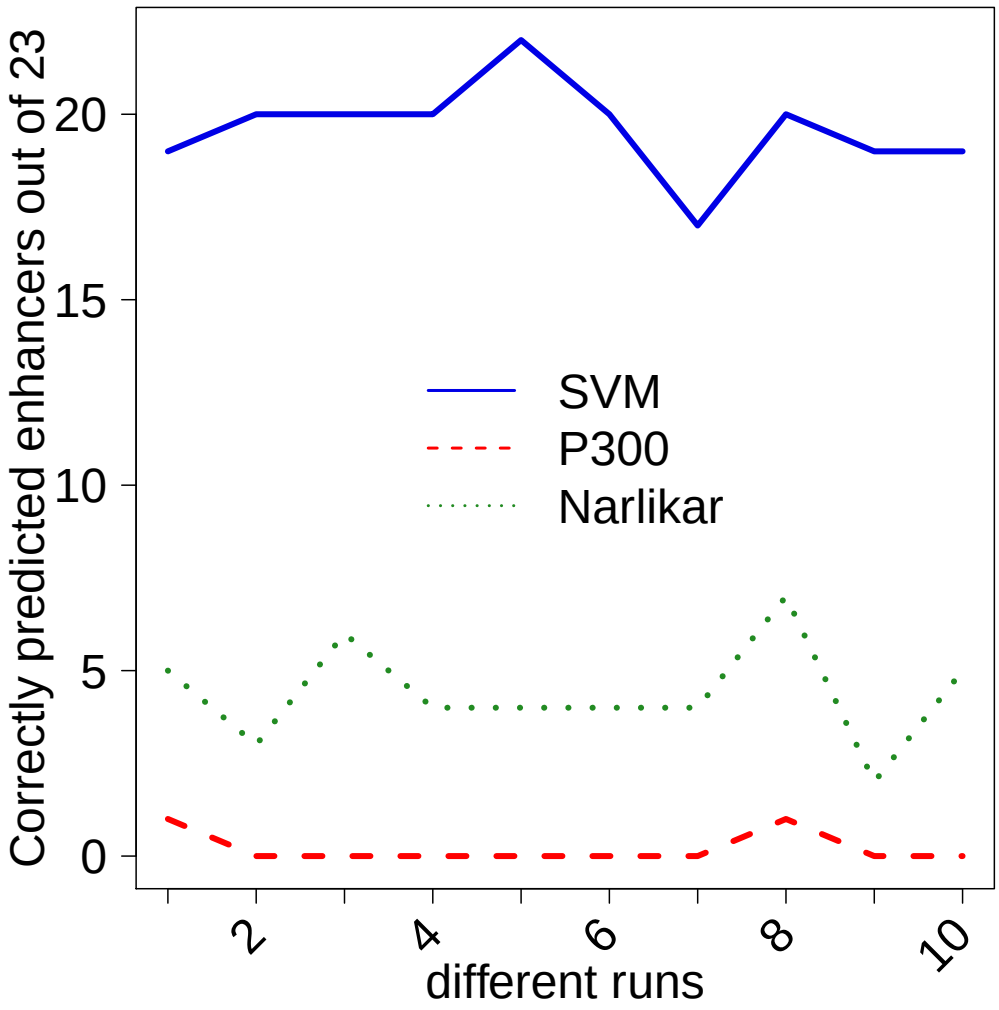

Figure 2.4: Number of enhancers (out of 23) predicted by SVM, P300 peaks and Narlikar et. al.

server [128]. We included all SNPs within 500kb from a seed SNP with $r^2 \geq 0.3$. The extended SNP were merged from the 1000 Genome Project and multiple HapMap releases (Consortium 2003; Consortium 2010). For each of the resulting 14233 SNPs, we scored 1kb flanking region using our SVM model to prioritize them as potential cardiac enhancers. Of all SNPs, the SVM scored 1054 as having enhancer probability ≥ 0.8. We found that distance of these enhancers from the corresponding GWAS SNP was significantly shorter than expected (Wilcoxon p-value = 3.9E-05).

2.4.3 Cardiac enhancers near cardiac GWAS SNPs are enriched for cardiac regulator motifs

Cardiac transcription is primarily regulated by members of GATA, MEF2, STAT, NF-AT, Nkx, and FOX families of TFs [129–132]. Next, we tested whether predicted enhancers near GWAS SNPs are enriched for known cardiac TF binding motifs. We first constructed three SNP sets: (1) eSNPs: comprised of the top 500 SNPs in LD with a GWAS SNP ranked by the SVM score, (2) pSNPs: the top 500 SNPs in the LD with a GWAS SNP ranked by mean P300 tag density (using bigwig summary tool from UCSC) in human heart, (3) gSNPs: The GWAS SNPs themselves. For each SNP we extracted the 1kb genomic flanking region resulting in three sets of sequences. For each sequence we determined the binding sites corresponding to 981 vertebrate motifs in TRANSFAC [133] whose motif match score (using our own tool [134]) was in the top 95th percentile of scores achievable by that motif. We then determined the enriched motifs in one set of sequences relative to the other using Fisher Exact Test. Because enhancers have distinctive compositions which can bias motif enrichment, we normalized the two sequence sets for their GC composition via random sampling prior to motif enrichment analysis. When comparing SVM SNPs to the GWAS SNPs, 50 motifs were enriched with p-value ≤ 0.05, 11 of which corresponded to multiple representatives of GATA, STAT, NF-AT, Nkx families. When we compared the P300 SNPs with GWAS SNPs, among the 34 enriched motifs with GATA, Nkx and STAT families were represented by 4 motifs. Importantly, when we compare SVM SNPs directly to the P300 SNPs,

GATA, FOX, MEF2 families of TF motifs were found to be enriched among the 32 enriched motifs. Figure 2.5 shows the top 50 motifs significantly enriched in SVM SNPs compared to GWAS SNPs or P300 SNPs. When we restrict the motif search to 20 bps flanking the SNP using same parameters, we still observe enrichment of NF-AT and STAT motifs in SVM SNPs relative to GWAS SNPs. However similar enrichment is also observed in P300 SNPs. It is possible that the SNP affect the formation of cis regulatory modules indirectly. Further investigation is required. In summary, all core cardiac TF families are enriched near eSNP loci, relative either to GWAS SNPs or to P300-bound regions. The overall conclusion was comparable when we used top 200 SVM scores and top 200 P300 score to be construct eSNP and pSNP sets. We note that because of small numbers, the p-values were modest and did not qualify a strict FDR threshold.

2.4.4 Cardiac enhancers near cardiac GWAS SNPs are likely to regulate the nearby genes

Next we tested whether the predicted enhancers are likely to regulate genes. While enhancers can in principle regulate non-neighboring genes, a majority of them do regulate nearby genes [135], therefore, we focused only on the gene promoter closest to the SNP. For a SNP locus and a gene promoter, we estimated the likelihood of SNP locus to regulate the gene as the correlation between the DNase-I hypersensitivity (DHS) at the locus and the expression of the genes across 15 cell types in which DHS and RNA-seq was performed in parallel (see Methods); this approach to

(a) SVM VS GWAS

(b) SVM VS P300

Figure 2.5: Significantly enriched motifs in SVM SNPs. The size of each TF label is proportionsal to its significance. For instance, the p-value for GATA1 in (a) is 0.001 and in (b) is 0.004. The largest p-value is 0.05.

link a putative enhancer to a target genes is similar to Ref. [99]. We constructed three comparison SNP sets. gSNP comprised of 229 GWAS SNPs. To construct eSNP set, we selected the SNP with highest SVM score in LD with each GWAS SNP as long as the SVM score was ≥ 0.8, resulting in 115 eSNP, all of which were intronic or intergenic. Similarly, to construct pSNP set, we selected the SNP with highest P300 mean tag density in LD with each GWAS SNP as long as the P300 tag density was ≥ 1, resulting in 58 pSNP. For each SNP we obtained the closest gene promoter. We then performed three pair-wise comparisons. For instance, when comparing eSNPs with gSNPs, we focused on genes that were closest to both an eSNP and a gSNP. Then we computed two DHS-expression correlations - between

eSNP locus and the gene and between gSNP and the same gene. Given all such pairs of correlations we tested whether eSNP-gene correlation was greater than the gSNP gene correlation using paired one-side Wilcoxon test. We found that eSNP loci were more likely than gSNP loci to regulate the closest gene (based on 124 genes, p-value = 0.03), eSNP loci were more likely than pSNP loci to regulate the closest gene (based on 50 genes, p-value = 0.01), and pSNP loci were not more likely than eSNP loci to regulate the closest gene (based on 23 genes, p-value = 0.87). We also checked whether the distance of eSNPs from the closest gene promoter was shorter than that for gSNP or pSNP and we did not observe a statistical difference. The results suggest that SVM predicted enhancers are more likely to regulate the nearby genes relative to both the original GWAS SNPs and P300 predicted enhancers.

2.4.5 Genes near cardiac enhancers are enriched for cardiac function

Next we tested whether the genes uniquely closest to the eSNPs provide greater insight into the cardiovascular disease phenotype, relative to genes uniquely closest either to gSNPs or the pSNPs. We used the same criteria as above to obtain the closest gene lists, but unlike the expression analysis above we retained only the unique genes in each list. Unfortunately, the uniqueness requirement greatly reduced the number of genes with 94 for gSNP, 17 for eSNPs and only 2 for pSNPs. We then used ToppGene [136] to compare enrichment of disease categories in the three gene lists. ToppGene uses three sources for disease ontology terms - GWAS, Comparative

Toxicogenomics Database, and OMIM. We excluded GWAS to avoid circularity. As expected, the pSNP gene list did not show any enrichment. At FDR ≤ 0.05 the genes near gSNP also did not show enrichment for any disease term. The 17 genes in the eSNP list include NOS3 and MYH7. NOS3 alone showed enrichment for 2 terms - "Hypertension, Pregnancy-Induced" and "Coronary Vasospasm". MYH7 alone was enriched for 5 distinct terms from OMIM database, all immediately related to myopathy or cardiomayopathy. The results are based on very limited dataset and one cannot draw general conclusion but they suggest that SVM can uniquely lead to genes directly relevant to the phenotype.

2.5 Conclusion

Here we present a SVM model for human cardiac enhancers based on four epigenomic marks H3K4me1, H3K27me3, DHS and P300, each of which have previously shown to be associated with enhancers in various cell types. While P300 is known to bind to tissue specific enhancers [100], and have been used as the gold standard for estimating accuracy of previous enhancer prediction approaches [102, 103, 127], many P300 bound regions fail to exhibit enhancer activity [100, 101]. Our SVM trained specifically on experimentally human cardiac enhancers validated in trangenic mouse, can not only predict other validated enhancers with high accuracy, it can also distinguish validated enhancers from the regions that were bound by P300 but failed to exhibit enhancer activity in transgenic mouse.

There are three prior approaches to predict enhancers. Narlikar et al. use

clusters of known cardiac TF motifs as predictor of cardiac enhancers [127]. Lee at al. train a SVM model based on genomic features based on cardiac P300 bound regions [102]. Another SVM model for CD4+ T-cell enhancers based on epigenomic features, again, using P300-bound regions as the gold standard was proposed in [103]. We have demonstrated the ability of our SVM model to distinguish between active and inactive P300 bound sites. Additionally, direct comparison of prediction accuracy on novel validated cardiac enhancers of our SVM model with that of P300 [102] and Narlikar et al. [127], explicitly shows that active enhancers have specific epigenomic properties not captured just by P300 binding or by clusters of putative binding sites. Genomic regions bound by P300 may not be active. Therefore, use of additional features add the tissue specific context to the model. Furthermore, kernel transformation of feature space used by SVM builds a non-linear classifiers. Thus it captures a greater variety of enhancers by recognizing a wider combination of epigenetic factors.

It has been previously suggested that a better knowledge of context-specific enhancers can help interpret GWAS signals [96]. However, this reasonable assertion has not been tested explicitly on a specific disease area. Here we use our enhancer prediction tool to interpret GWAS studies related to cardiovascular phenotypes. We found an enrichment of high scoring cardiac enhancers near cardiac GWAS SNPs. Analysis of these putative enhancers suggest that (1) they are enriched for known core cardiac transcription factor binding sites, (2) they are likely to regulate nearby genes, and (3) they can uniquely point to certain genes involved with cardiac function and heart disease.

Chapter 3: Bayesian integration of genetics and epigenetics detects causal regulatory SNPs underlying expression variability

3.1 Introduction

Numerous expression Quantitative Trait Loci (eQTL) studies have been performed to determine the cell-type-specific regulatory architecture of the human genome [1]. However, since single nucleotide polymorphisms (SNP) within a linkage disequilibrium (LD) region are statistically indistinguishable from each other, these studies essentially reveal LD blocks that are associated with a genes expression but do not reveal the potential causative regulatory SNPs, which limits the utility of these studies [43, 46, 47, 137, 138]. The recent explosion of epigenetic data has made it possible to detect cell-type-specific regulatory regions [43, 47–50], which can be used to distinguish regulatory SNPs from non-regulatory SNPs in LD blocks.

Recently, a few approaches have incorporated regulation specific epigenetic data into association studies [43, 47–51]. However, these methods have utilized the regulatory information either retrospectively or as an empirical prior to prioritize eQTL SNPs. Such approaches are prone to missing regulatory SNPs with small effects due to the severe multiple testing correction (or sparsity constraints) [1].

Furthermore, these approaches ignore interaction between the region harboring the SNP and the target gene, which is useful in identifying regulators specific to a gene. Multiple SNPs are known to regulate single genes [139], yet many current methods [49, 50, 139] limit the number of causal SNPs per gene to a single SNP. In this paper, we introduce a new method, expression Quantitative Trait enhancer Loci (eQTeL), which addresses these limitations. It identifies combination of regulatory SNPs – including SNPs with small effect sizes – that jointly determine expression variance.

eQTeL is a fully Bayesian approach (Fig. 3.1), which infers cis regulatory polymorphisms underlying gene expression variability by integrating: (i) genotype and gene-expression variance across individuals (ii) epigenetic data in appropriate cell types [51, 52] (iii) DNAse I hypersensitivity (DHS) variance of SNPs and promoters across cell types [17] (iv) expression variance of genes across multiple cell types (v) linkage disequilibrium blocks [140], and (vi) imputed haplotypes inferred from the 1000 Genomes Project [141]. Our approach addresses a number of key methodological challenges. First, it systematically integrates three characteristics of a causal regulatory eQTL, i.e, correlation with the target genes expression across individuals, the regulatory properties of the harboring region, and interaction with the target gene. Second, it can account for heterogeneity of regulatory regions in terms of different combinations of epigenetic marks. Third, to learn the regulatory model, eQTeL leverages regulatory polymorphisms that are not associated with gene expression in addition to expression-regulators. Fourth, it interrogates the LD structure to find the optimal combination of explanatory SNPs. Fifth, it implements a

hierarchical scheme to select a sparse set of SNPs, while simultaneously explaining a maximal fraction of gene expression variance. Finally, eQTeL is scalable to large datasets.

We statistically validated our method using human heart data as well as realistic simulated data and demonstrated that it can predict an individual's expression from the genotype more accurately compared to other methods. SNPs identified by our method include regulatory SNPs with small effect sizes. Further assessment of functional relevance of identified SNPs suggest that they tend to (i) overlap a high resolution DNAse footprint, (ii) have an allele-specific DNAse footprint, (iii) preferentially disrupt putative binding of core cardiac regulators, and (iv) be spatially proximal to their putative target gene. We also estimate that 58% of SNPs identified by eQTeL (which we call eeSNPs, Supplementary Data 1) are likely to be causal. Collectively, these results strongly suggest that eeSNPs have functional role.

3.2 Results

3.3 Quantitative Trait enhancer Loci (eQTeL) model

We first provide a broad overview of the eQTeL model and further details can be found in Methods. As illustrated in Fig. 3.1, eQTeL is composed of two Bayesian regression models, an expression model and a regulatory model, which are coupled through message passing. The expression model is a Bayesian variable selection model [142, 143] which explains the gene expression variance among samples as a

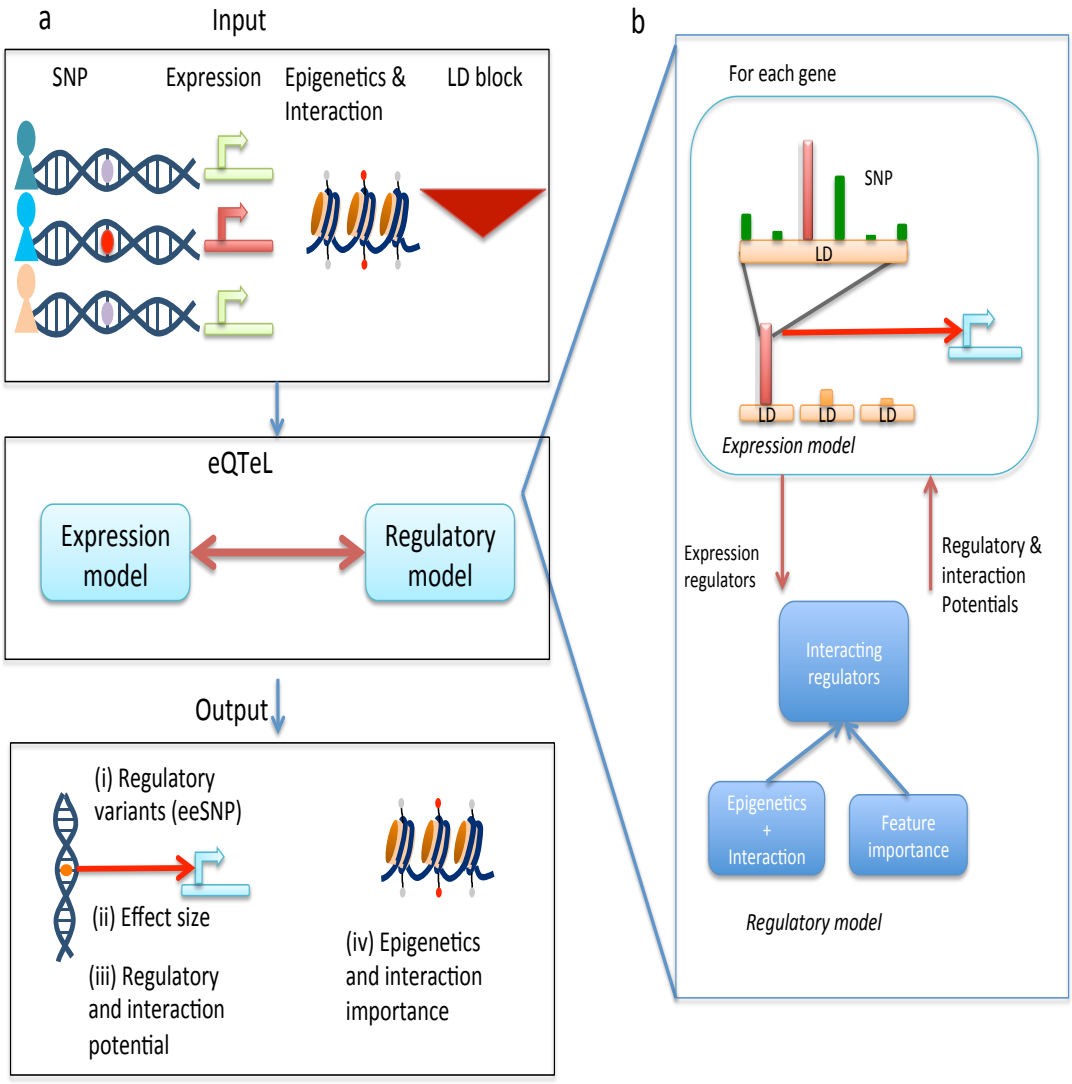

Figure 3.1: Overview of eQTeL model: (a) Input and output of eQTeL. eQTeL takes genotype and gene-expression across samples, epigenetic and interaction features for each SNP and LD block as input. It outputs regulatory SNPs and their target genes, their effect sizes and regulatory-interaction potentials, as well as estimated feature importance of each epigenetic and interaction feature. (b) eQTeL is composed of two coupled regression models (i) a Bayesian variable selection with informative priors models expression as a linear combination of SNPs. Given the regulatory and interaction priors, this hierarchical model first identifies LD blocks and then combinations of SNPs that explains expression variance and that also have high regulatory and interaction potentials. (ii) a Bayesian logistic regression specifies the regulatory and interaction potential as linear model of epigenetic and interaction features in semi-supervised manner. The logistic regression passes the regulatory and interaction potentials to the variable selection model, while the variable selection model passes expression-regulators to the logistic regression model.

linear function of SNP alleles. A distinct feature of the expression model is that it uses informative prior for each SNP, which depends on the SNPs regulatory [47] and interaction potential. The regulatory model, which is common for all genes, uses a Bayesian logistic regression [144] to estimate that informative prior as a probabilistic function of epigenetic and interaction features. Known expression regulators can be used to train the regulatory model, while an accurate model of regulatory and interaction potential can help to identify expression regulators. The expression model then passes current estimates of expression regulators to the regulatory model, which in passes current estimates of regulatory and interaction priors for each SNP back to the expression model. eQTeL starts with estimating expression regulators assuming equal priors for each SNP and then, using current estimates of expression-regulators, trains the regulatory-model. In turn, current estimates of regulatory and interaction potential are used as informative priors to re-estimate expression regulators. This iterative process continues until convergence. Thus, our eQTeL model gradually improves estimation accuracy by joint learning.

In our approach (see equations below and Methods for details), expression Y relates to candidate SNPs X via a standard normal linear model [142, 145, 146] with noise σ^2. However, for each SNP β, its effect size is non-zero only if its regulatory-interaction indicator γ is 1, which depends on a function $\phi'(\theta)$ of regulatory-interaction potential θ (Methods). The potential θ of a SNP is modeled as a combination of (i) features for regulatory potential and (ii) features for SNP-gene interaction P, via a logistic function. Vector α represents feature weights that are shared across all genes, thus we learn a single genome wide model of regulators. This choice

of modeling α obviates the need to explicitly scale genetic and epigenetic factors.

$$
\begin{aligned}
Y &\sim \mathcal{N}(\mathbf{X}_\gamma \cdot \boldsymbol{\beta}_\gamma, \sigma^2 I) \\
\gamma &\sim \mathcal{B}ern(\phi(\theta)) \quad \forall \text{SNPs} \\
\theta &\sim \mathcal{B}ern(\text{logistic}(\{\mathbf{E}, \mathbf{P}\} \cdot \boldsymbol{\alpha})) \quad \forall \text{SNPs}
\end{aligned}
$$

We use Markov chain Monte Carlo (MCMC) [147] to infer all model parameters jointly (Supplementary Note 1). At each iteration of the sampler, the decision whether a region is a regulator (i.e., $\theta = 1$) depends not only on correlation between corresponding SNP and gene, but also on the regulatory and interaction features, as well as the current estimates of feature weights. This leads to a semi-supervised [148, 149] clustering of SNPs into regulators and non-regulators (Supplementary Note 1). Our MCMC implementation explicitly uses LD [150] block information to judiciously choose combination of regulatory SNPs by sampling over the model space hierarchically [147] at the top level it explores combinations of LD blocks and at the lower level it explores the sparse set of SNPs within each LD block that optimally explain the expression-variance (Fig. 3.1, Methods, Supplementary Note 1, Appendix A Fig. 1). This approach results in a superior exploration of the model space relative to approaches that disregard the LD structure. eQTeL uses a Rao-Blackwell estimate of θ that improves the mixing rate (Appendix A Fig. 1) of the sampler and leads to robust competition between SNPs within a LD block (Fig. 3.1). Further, the overall sparsity constraint (equivalent to a multiple testing correction

in non-Bayesian approaches) of eQTeL is controlled by two factors: (i) the fraction of SNPs that are interacting-regulators and (ii) the fraction of interacting-regulators that are expression-regulators. This allows for a less conservative sparsity constraint and makes it possible to identify SNPs with small effect sizes which are typically missed by alternative approaches due to severe multiple testing correction. eQTeL assumes Normal priors on α. Finally, eQTeL implementation allows an option to select a subset of epigenetic factors important for estimating regulatory potential through Bayesian variable selection model.

3.4 eQTeL detects expression regulatory SNP in MAGNet

We applied eQTeL to genotype and gene expression data for 313 human hearts (procured by MAGNet consortium (www.med.upenn.edu/magnet/)) and compared to the performance of other eQTL methods (Supplementary Note 2 & 3). To determine regulatory and interaction potentials, we used 95 epigenetic and interaction features (Appendix A Fig. 2) for primary tissues and cell lines of heart from ENCODE and Roadmap Epigenome project [51, 52]. For expediency we selected 1880 genes with expression deemed to have a significant genetic component according to the univariate eQTL [139, 151].

Consistent with its ability to explain a greater expression variance, eQTeL also predicts expression of genes much more accurately compared to other methods (Fig.

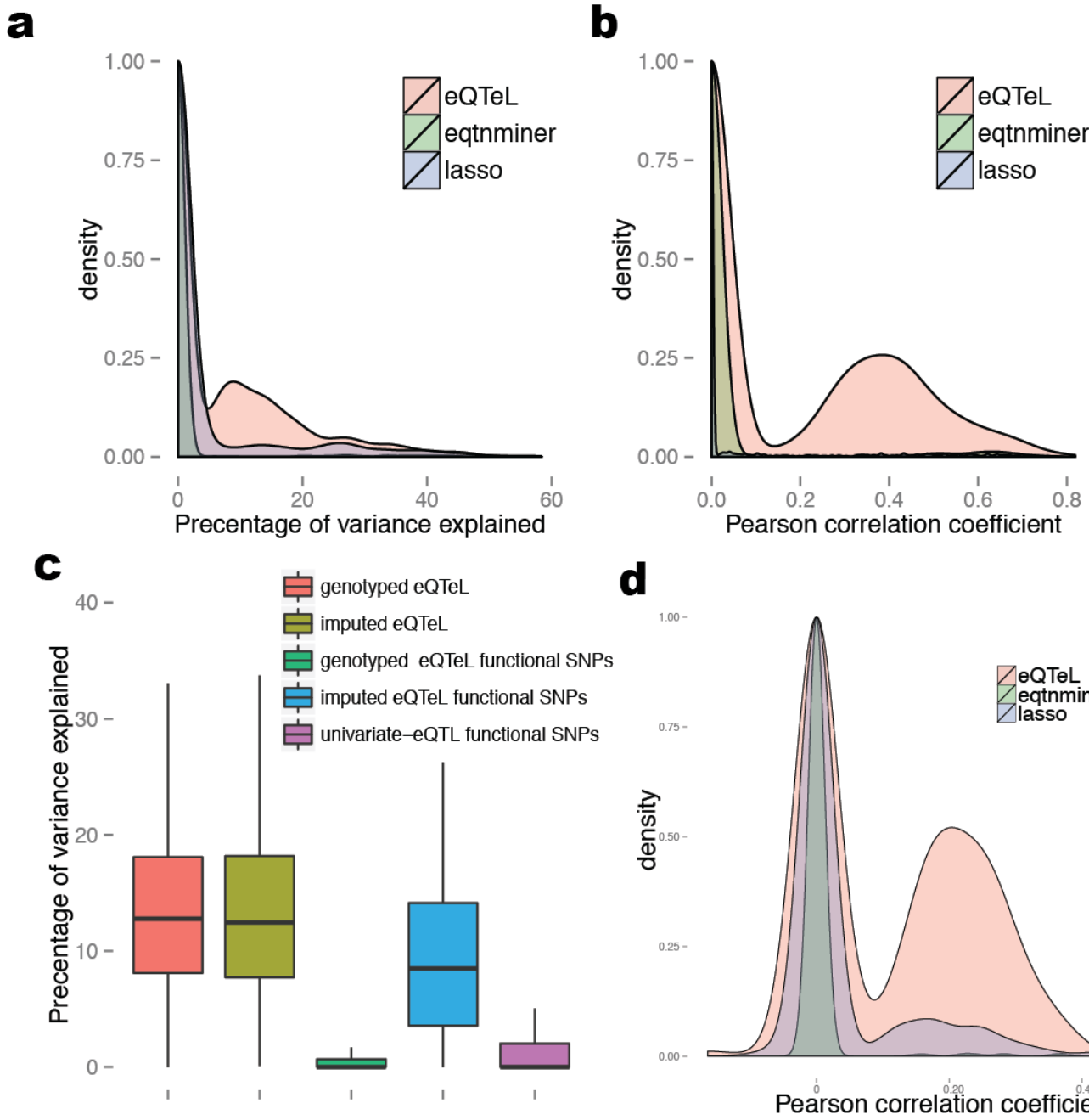

Figure 3.2: Comparative performance of different methods applied to human heart data (MAGNet). The analysis is based on 2428 SNPs identified by eQTeL for which posterior probability of selection > 0.5. To ensure the same total number of SNPs selected by eQTeL, eqtnminer and LASSO: for eqtnminer we sort SNPs based on posterior probability and for LASSO based on absolute estimated effect size and then selected top 2428 SNPs. (a) Explained expression variance based on three representative methods on human heart data. (b) Accuracy of predicted expression of three methods. (c) Explained expression variance for human heart data by potentially functional (approximated by overlap with a footprint) genotyped SNPs and imputed SNPs. (d) Cross-dataset generalization of MAGNet eeSNPs: Expression predictability in GTEx by eeSNPs identified in MAGNet.

3.2b). The mean (cross-validated) Pearson correlation coefficient between predicted and actual expression is 0.176 -+ 0.065 (in contrast with 0.025 for eqtnminer [49] and 0.088 for LASSO [152]). The bimodality of distribution of correlation coefficient implies that for a subset of genes, the expressions are highly predictable by eQTeL.

Because of its ability to discriminate among multiple SNPs based on regulatory and interaction potentials, eQTeL is expected to be much more advantageous on imputed data, which has a substantially greater number of linked SNPs. To confirm this, we imputed [153] around 6.5 million SNPs using the 1000 Genome Project data [141]. Note that each imputed SNP is derived from the reference SNPs using the linkage information, and cannot be any more associated (in a statistical sense) with the gene expression than the reference SNPs, and therefore are not expected to increase the explained variance (as evident from Fig. 3.2c). However, eQTeL with imputation is expected to improve detection of causal functional SNPs compared with the genotyped SNPs [51, 139]. Therefore, restricting our search to potentially functional SNPs, imputed SNPs should explain the expression better. Restricting our analysis only to SNPs mapped to a DNAse footprint (as a proxy for putative functional SNPs), the relative advantage of imputation with eQTeL becomes evident (Fig. 3.2c). Indeed, with imputed data, there is no significant improvement in detection of likely causal SNPs if standard eQTL approaches are used. Therefore it becomes imperative to use an integrative approach, such as eQTeL, in the presence of a large number of linked SNPs (Fig. 3.2c).

To validate eeSNPs in an independent cohort, we analyzed expression and genotype of 85 Left ventricle samples from GTEx [1] (Supplementary Note 2). We

note that compared to an exhaustive eQTL, eQTeL cannot identify novel associated loci, but instead is designed to identify putatively causal SNPs within an associated locus. We found that 18.9% of eGenes detected in MAGNet replicates in GTEx (Supplementary Data 2). To assess the relative generalizablity of eQTeL in independent cohort, using the eeSNPs identified by eQTeL in MAGNet, we estimated the explained variance in GTEx. We repeated this for other methods while controlling for the number of eeSNPs as well as other regularization procedures. While, as expected due to the differences in the datasets, the cross-cohort explained variance is lower than that within MAGNet (Fig. 3.2b versus 3.2d), relative to other methods, eQTeL exhibits substantially and significantly greater (in both cases Wilcoxon test p-value between eQTeL and other methods is $< 1.0e-16$) cross-dataset generalizability (Fig. 3.2d, Appendix A Fig. 3).

3.5 eQTeL detects causal SNPs in semi-synthetic data

To demonstrate that eQTeL can accurately identify putatively causal SNPs, we use a synthetic data evaluation (Fig. 3.3a) (for additional details refer to Methods). We used 174800 SNP probes along with their genotypes from 313 MAGNet samples that were within 1MB from transcription start of 200 genes (Methods). Since regulatory region may have no effect on genes included in our analyses and yet can contribute to learning the regulatory-model, eQTeL makes a distinction

between a regulator and a gene-specific expression-regulator. This distinction was made explicitly in our simulation by designating 1% of all SNPs as regulators (as an approximation of previous estimation in humans [154]). We then used a frequency distribution of expression regulators per gene inferred from MAGNet data to randomly choose gene specific expression-regulators for 200 genes. Using allele status of 313 samples for expression-regulators, we generated gene expression and added random noise such that expected explained variance from simulated data matched MAGNets explained variance (Fig. 3.2a). We generated the epigenetic features for each SNP using ENCODE epigenetic data and validated heart-enhancers from VISTA [47]. Thus our simulated data closely parallels the experimental data.

Next we applied eQTeL to the simulated data. The precision-recall plot (Fig. 3.3b) shows that eQTeL significantly outperforms other methods. In fact, the performance of full-eQTeL is close to the theoretically best eQTeL model that uses the original feature weights (see Methods). The previous integrative method eqtnminer [49, 50], the only other current method that uses epigenetic data in eQTL, shows only a modest increase in precision compared to methods that do not use epigenetic data.

The immediate effect of increase in precision of detecting expression regulators, especially for SNPs with high regulatory potential, is that eQTeL explains a significantly greater proportion of expression variability (Appendix A Fig. 4). There is also significant improvement in correlation between predicted expression and actual gene expression; mean correlation for eQTeL was 0.298 -+ 0.02 (compared to 0.18 for eqtnminer and 0.23 for LASSO regression, Appendix A Fig. 5). Note that

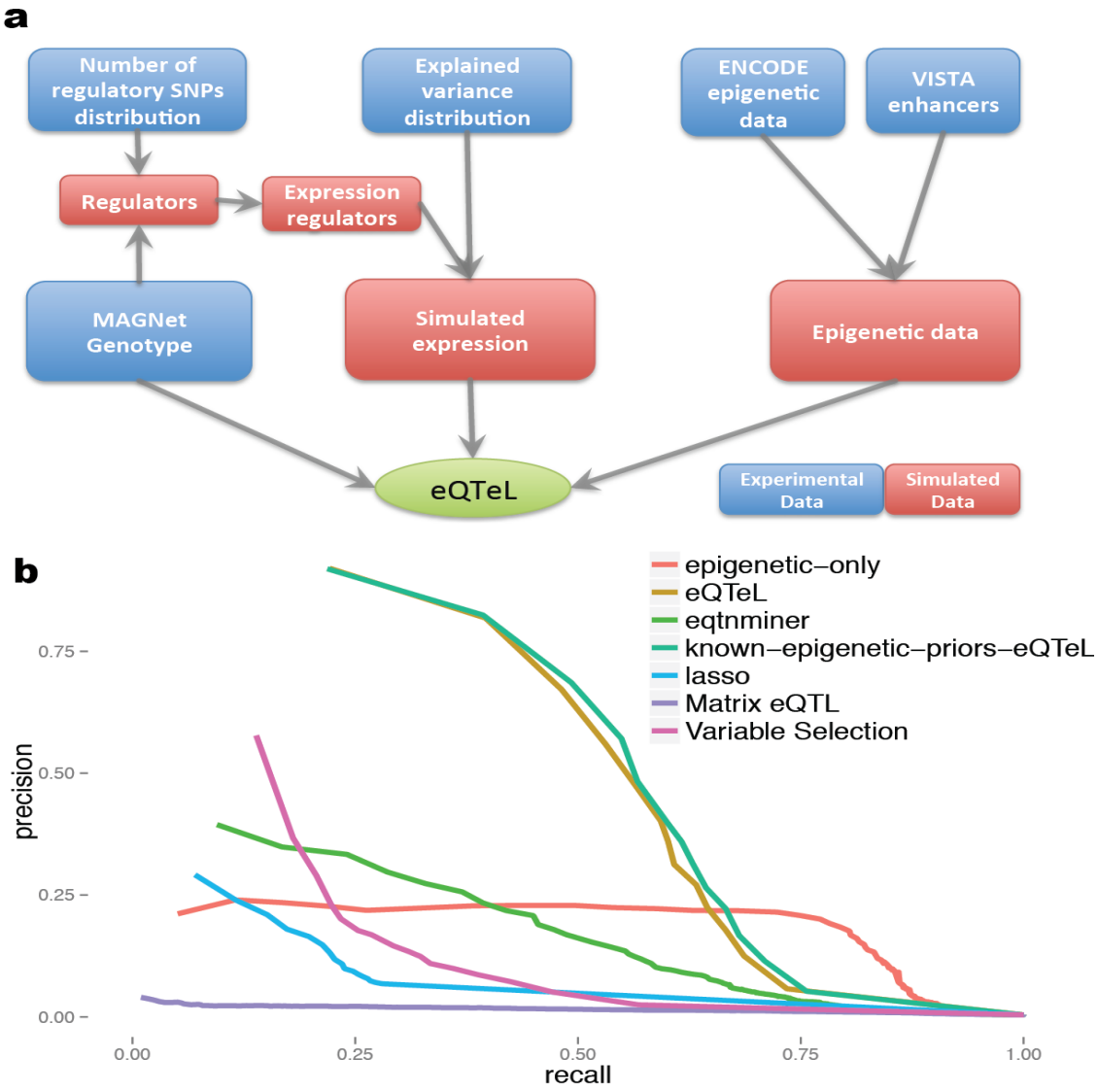

Figure 3.3: eQTeL identify causal SNP accurately in semi-simulated data. (a) Design of simulaton study: Simulation study uses (i) 174800 SNPs from MAGNet Genotype (874 SNPs per gene) data for 313 samples (ii) distribution of number of expression-regulators per gene from MAGNet data (iii) distribution of explained expression variance estimated from MAGNet data (iv) ENCODE epigenetic data for heart cell lines, and (v) distribution of epigenetic data for regulators VISTA heart enhancers. Expression regulators per gene were chosen amongst regulators (1% of MAGNet SNPs). Using allele status of expression regulators in 313 samples expression of 200 genes was generated such that explained variance distribution matches MAGNets explained variance. Epigenetic data for regulators were generated using the epigenetic distribution estimated from VISTA heart enhancers. (b) Comparative performance assessment on simulated data. Methods include (i) Matrix-eQTL (univariate-eQTL): univariate regression (Lappalainen et. al.), (ii) LASSO: L1 regularizer multivariate regression, (iii) variable selection: Bayesian variable selection, (iv) eqtnminer: Bayesian variable selection with empirical-priors (Gaffney et. al.), (v) epigenetic-only: epigenetic feature weights derived from verified enhancers and used to prioritize SNPs, (vi) eQTeL: proposed method, (vii) known-epigenetic-priors-eQTeL: eQTeL with fixed epigenetic priors as in epigenetic-only. Number of SNPs each methods were controlled.

for this analysis we controlled for the number of SNPs that were selected for each method, using the most explanatory respective SNPs for each method. Overall, eQTeL can accurately identify around 75% of putative causal SNPs (at 40% recall) reinforcing the fact that our method can identify substantial fraction of likely causal genetic determinants of transcriptomic variance.

3.6 eQTeL detects SNPs with small effect sizes

The statistical power to detect SNPs associated with expression variance (i.e., the probability of correctly rejecting the null hypothesis that the SNP is not associated with gene expression) depends on various factors such as sample size, noise to signal ratio, number of hypothesis tested (number of SNPs) and effect size of SNP. The effect size, in turn, depends on the allele frequency of SNP, thus low allele frequency limits statistical power to detect regulatory SNPs [1, 155]. Another advantage of eQTeL model is that it can detect SNPs with small effect sizes by distributing sparsity between: (a) sparsity in the number of regulators and, (b) sparsity in expression regulators among all regulators. eQTeL employs relatively relaxed sparsity constraints for SNPs that have high regulatory potential and therefore the model has higher statistical power to retrieve a greater fraction of SNPs with low minor allele frequency (small effect sizes) compared to eqtnminer (Fig. 3.4). Furthermore, eQTeLs statistical power to identify low minor allele frequency SNPs is greater among SNPs with high regulatory-interacting potential (labeled as eQTeL-high in Fig. 3.4). This trend of differential statistical power is also observed

in simulated data, where we know the exact effect size of regulatory SNPs (Appendix A Fig. 6).

eQTeL leverages LD information to judiciously choose combinations of SNPs (per gene) which explains a much greater proportion of expression variance (details in Supplementary Note 2). The power to detect SNPs with low allele frequency is the primary reason that eQTeL captures substantial proportion of causal genetic determinants underlying transcriptomic variance. However, it should be noted that SNPs with small effect sizes are only detected by eQTeL if they have a high regulatory potential.

eQTeLs performance gain is potentially due to two factors: (i) integration of epigenetic data, (ii) allowing multiple causal variants per gene [156]. We assessed relative contribution of the two factors. eQTeLs expression predictability by functional SNPs increases substantially when multiple SNPs per gene were allowed (Appendix A Fig. 3.7, Supplementary Note 2), supporting a contribution due to multiple explanatory SNPs. However, in the absence of epigenomic data, i.e., when using standard LASSO, we do not see a performance gain, and in general, the performance is substantially worse than the performance of eQTeL. This suggests that allowing multiple SNPs per gene is useful specifically when functional information is used.

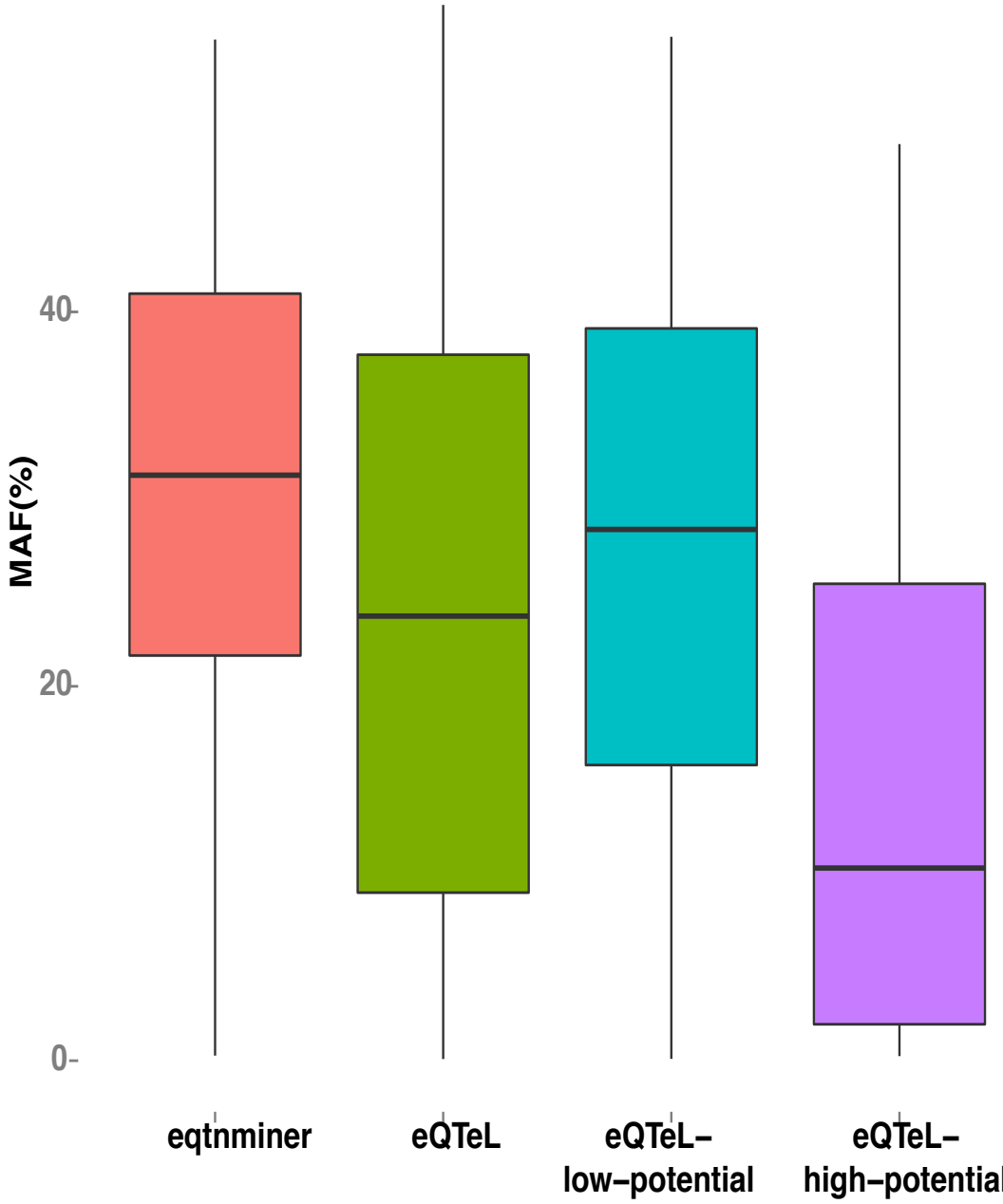

Figure 3.4: eQTeL increase statistical power to detect small-effect regulatory SNPs : eQTeL identify causal SNP accurately in semi-simulated data. Comparsion of effect-size of SNPs detected by eQTeL and eqtnminer. Number of SNPs for each method was controlled. eQTeL can detect SNPs with small effect size if the regulatory potential of SNP is high. eQTeL-high-potential are subset of eeSNPs with interacting-regulatory potential =1 and eQTeL-low-potential are subset with interacting-regulatory potential $<$ .1.

3.7 eeSNPs lie within protein-bound genomic regions

Putative causal regulatory SNPs are expected to be bound by regulatory proteins. Earlier studies have shown enrichment of regulatory elements near causal SNPs [48–50, 139]. Since eQTeL and eqtnminer use epigenetic data, which is known to be correlated [51] with protein binding, we expect to find enrichment of DNAse footprints near the identified regulatory SNPs. Using genome-wide high-resolution DNAse footprint data for 41 cell types [157], we obtained the fraction of eeSNPs (and control SNPs) overlapping with a footprint; Note that DNAse footprints were not used in eQTeL so they could be used for validation. 76.3 % of eeSNP have a footprint overlapping the eeSNP (Fig. 3.5), in contrast to 6.3% of in SNPs detected by eqtnminer that uses same epigenetic data as eQTeL. The performance of eqtnminer did not improve even if the best SNP per gene were chosen for this analysis. For SNPs chosen by LASSO, which does not use epigenetic data, only 5.95 % of SNPs have overlapping DNAse footprints. Only 2% of SNPs identified by Lirnet (for 200 genes) overlap with the DNAse footprints (Appendix A Fig. 3.8). Using top 8 epigenetic features estimated from eQTeL allowed to improve performance of eqtnminer, but could not bring it up to eeSNPs enrichment level (Appendix A Fig. 9 & Supplementary Note 4). Notably, the DNAse footprint enrichment is high in the four heart-related cell types. This result suggests that majority of SNPs identified by eQTeL coincide with regions of in vivo protein binding and are at least 12 fold

more likely to be functional than the next closest method.

3.8 eeSNPs exhibit binding and regulatory allele specificity

To ascertain the functional role of eeSNPs, we checked whether the change of a SNPs allele would affect their regulatory properties (such as protein binding, histone modifications etc.). For each cell line, we selected heterozygous SNPs by inspecting genotyped data or pooled reads from different histone modifications, DNAse-seq and CTCF. We first assessed allelic differences in footprint reads for human cardiac myocyte (HCM) (see Methods). As shown in Fig. 3.6, the eeSNPs that overlap a footprint show significantly greater (with odd-ratio of M = 3.005 and p-value < 3.83E-17) allele-specificity relative to SNPs identified by eqtnminer, consistent with eeSNP having a regulatory impact (allele-specifity comparison with LASSO is shown in Appendix A Fig. 10). For eeSNPs, we obtained 6.57-fold more reads mapping to the allele with more DNA-seq reads compared to the other allele (for eqtnminer, the average read difference was 1.8). We also found higher allele specificity for eeSNPs in other heart cell lines (Appendix A Fig. 11, HCF, SKMC) for DNASe-Seq reads. The trend of higher allelic specificity is also true in heart cell lines for histone modification H3K4me3, which is associated with active enhancers (Appendix A Fig. 12). Allele-specificity of eeSNPs suggests that they may underlie population variance in gene expression.

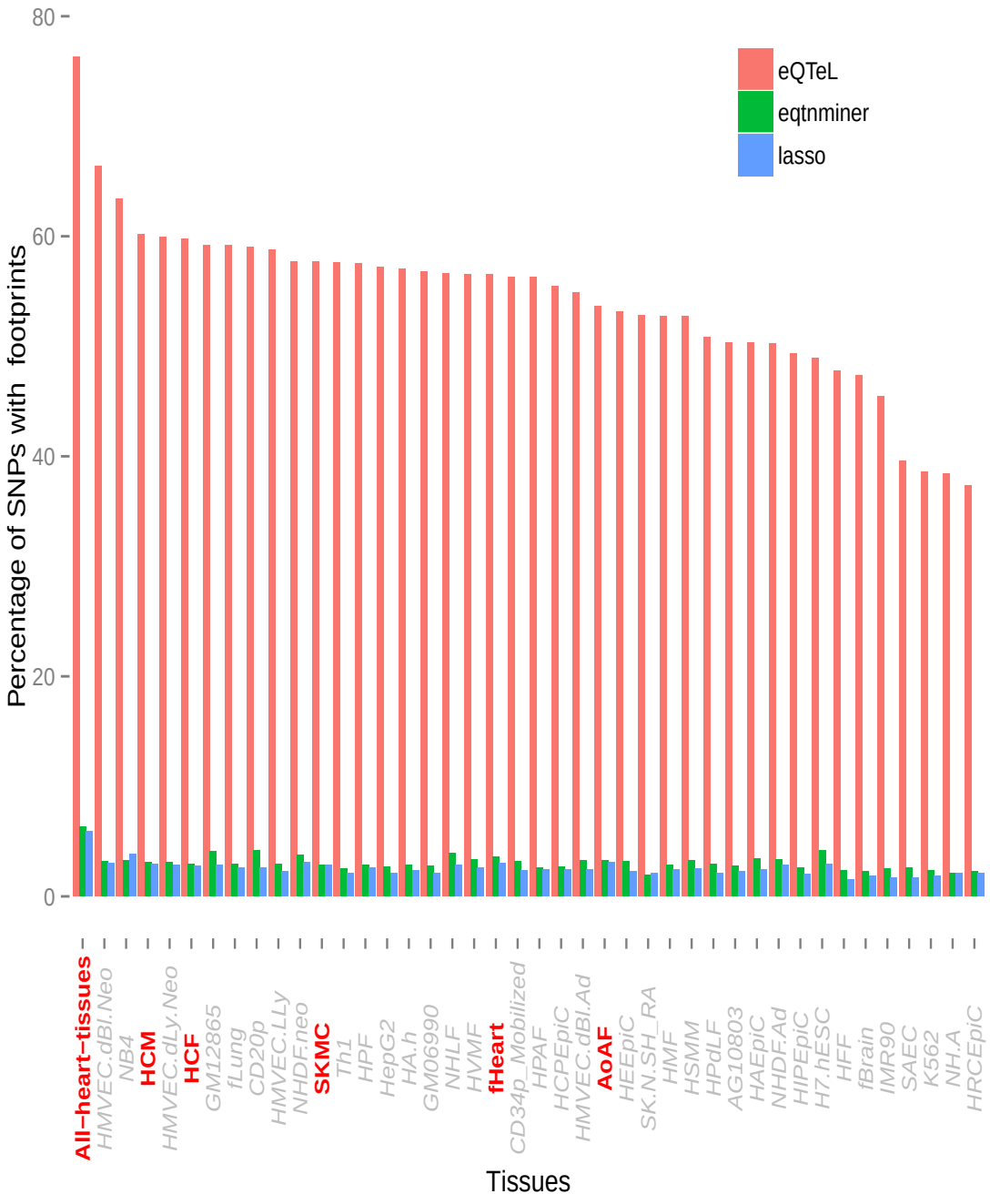

Figure 3.5: Large fraction of eeSNPs overlaps with DNAse footprint relative to other methods, particularly for heart-related tissues (highlighted in red). This analysis is based on 2428 SNPs identified by eQTeL for which posterior probability of selection > 0.5. For eqtnminer, we selected the best SNP reported for each gene. For LASSO we selected 2428 SNPs by sorting the effect sizes. We looked at the footprint in 42 cell lines from Neph et. al. overlapping the SNP within 25 bps the SNP loci by using bedtools for each method. The heart-related-tissues are highlighted in red in the figure. The left-most bar represents pooled data from all heart-related cell types. Note the relative enrichment of each method remains same even if we control for SNPs per gene in each method.

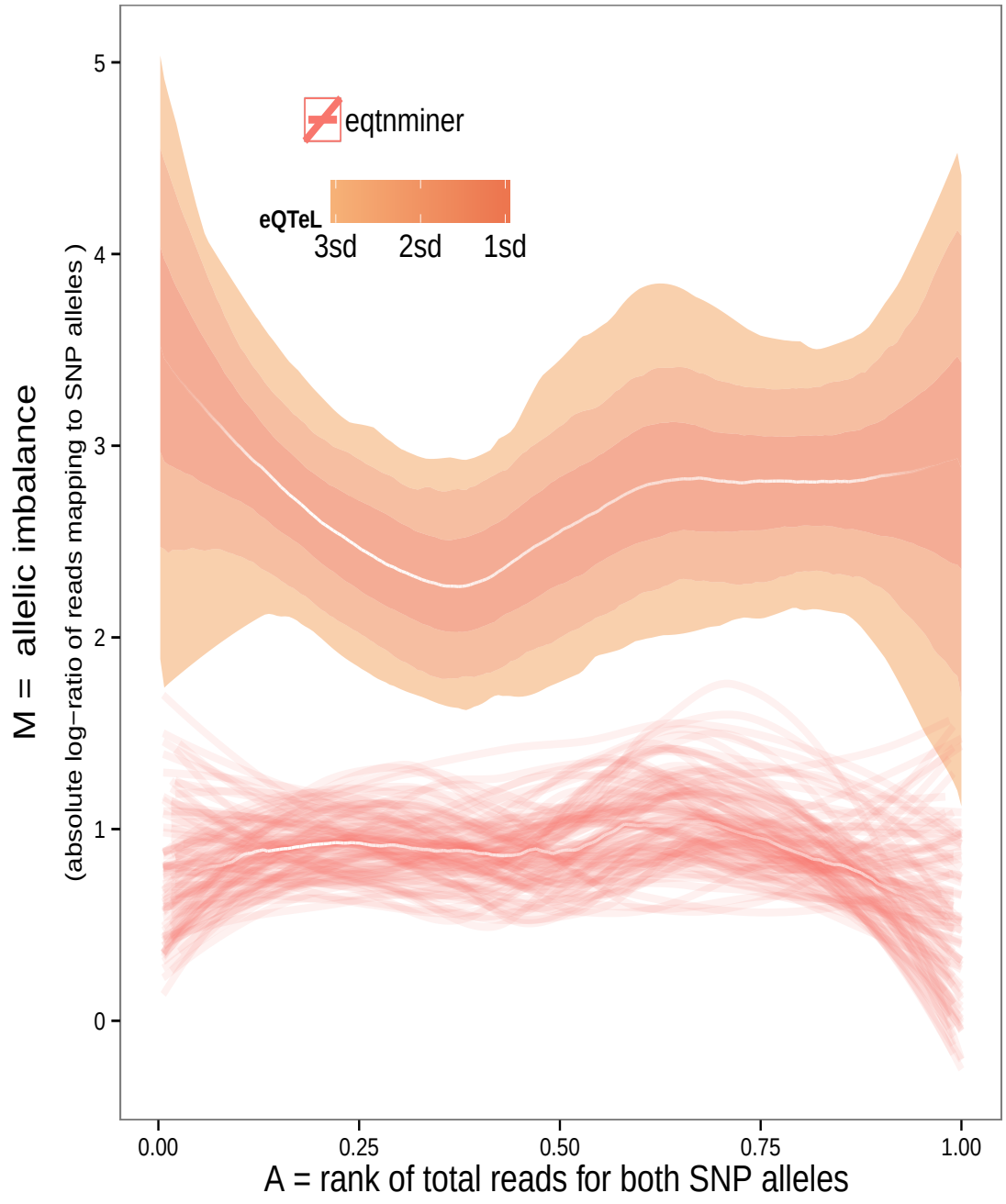

Figure 3.6: DNAse hypersensitivity at eeSNPs shows greater allele specificity in HCM: X axis: rank of DHS read counts, Y axis: absolute log-ratio of read counts mapping to the two alleles at a SNP. SNPs from different methods are selected similarly to Fig 5. The analysis was performed on a subset of SNPs that were heterozygous in the sample. The median *white* lines represent LOESS (local regression) for each method. Confidence intervals for each median line is estimated using bootstrapping and are represented either by thin lines representing the LOESS of each bootstrap or by colored shades representing confidence intervals in terms of standard deviation of bootstraps. Note the allele-specificity at SNPs detected by eQTeL and eqtnminer remains the same even if we control for number of SNPs per gene.

3.9 eeSNPs are spatially proximal to their target gene

The spatial proximity of eeSNP with its target promoter is a pre-requisite for cis-regulation. Spatial proximity has been experimentally determined using chromatin interaction analysis with paired-end tags (ChIA-PET) assays [158]. Identified SNPs that were closer than 100 bps from their target promoters were excluded. We quantified spatial proximity of each eeSNP and its target by the number of pair-end reads supporting the proximity, whereby one of the reads overlaps with the target promoter and other read overlaps with the eeSNP. Analysis of pooled ChIA-PET data from various cell types suggests that, relative to controls, eeSNPs are significantly more proximal to their target genes (Fig. 3.7). This implies that eeSNPs are more likely to be cis-regulators of their target genes.

3.10 eeSNPs disrupt motifs of cardiac transcription factors

A likely mechanism by which a regulatory SNP may affect gene expression is by disrupting binding of specific transcription factors [159]. For each of the 981 vertebrate TF motifs annotated in the TRANSFAC database [160], we quantified (see Methods) the TF binding score difference between two alleles of eeSNP. We only considered the SNPs for which the score was significant for at least one of the

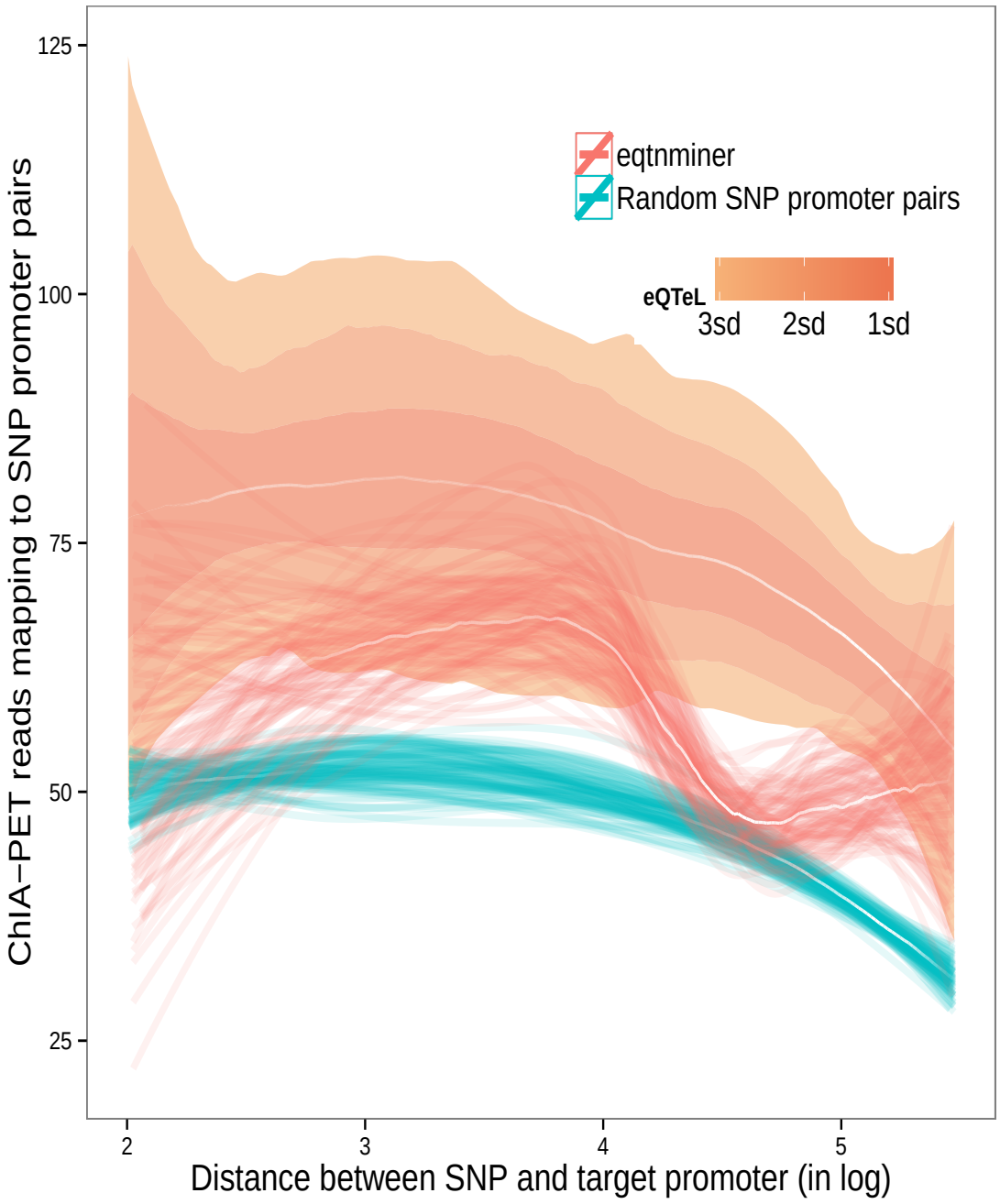

Figure 3.7: eeSNP-gene pairs are spatially proximal. X axis: the rank of eeSNP-gene distance (log 10), Y axis: ChIA-pet support. SNPs from eQTeL and eqtnminer are selected as in Fig 8. The random SNP-gene pairs were selected so as to have the same distance distribution as for eeSNPs. SNP-gene pair closer to 100bps were excluded. The median white lines represent LOESS (local regression) for each method. Confidence was estimated for each method just as in Fig. 3.6.

alleles. As shown in Fig. 3.8, the core cardiac TF motifs (such as FOX, NKX, GATA) are among the TF binding motifs that are most likely to be disrupted by eeSNPs. This observation indicates that functional consequence of regulatory SNP might be heart specific. The disruption of STAT, MEF2, FOX, NKX and GATA transcription factor families are known to play important role in cardio-vascular diseases [47, 161–163]. This suggests that identified eeSNPs may have a specific transcriptional role in the heart.

3.11 Proportion of eeSNPs that are causal

In the absence of extensive experimental data, it is difficult to estimate the proportion of eeSNPs that are causal. However, similar to a previous approach [139], we used the proportion of eeSNPs that disrupt potential TF binding relative to the same for high-confidence putatively causal SNPs, as an independent estimate of proportion of eeSNPs likely to be causal (see Methods). Based on each TF motif, that was found to be preferentially disrupted by eeSNPs above, the proportion of eeSNPs estimated to be causal varied from 17% to 93%, with a mean estimate of 58% (Methods, Appendix A Fig. 12). Lastly, based on mammalian conservation data, we found that eeSNPs are more conserved than control SNPs (Appendix A Fig. 13).

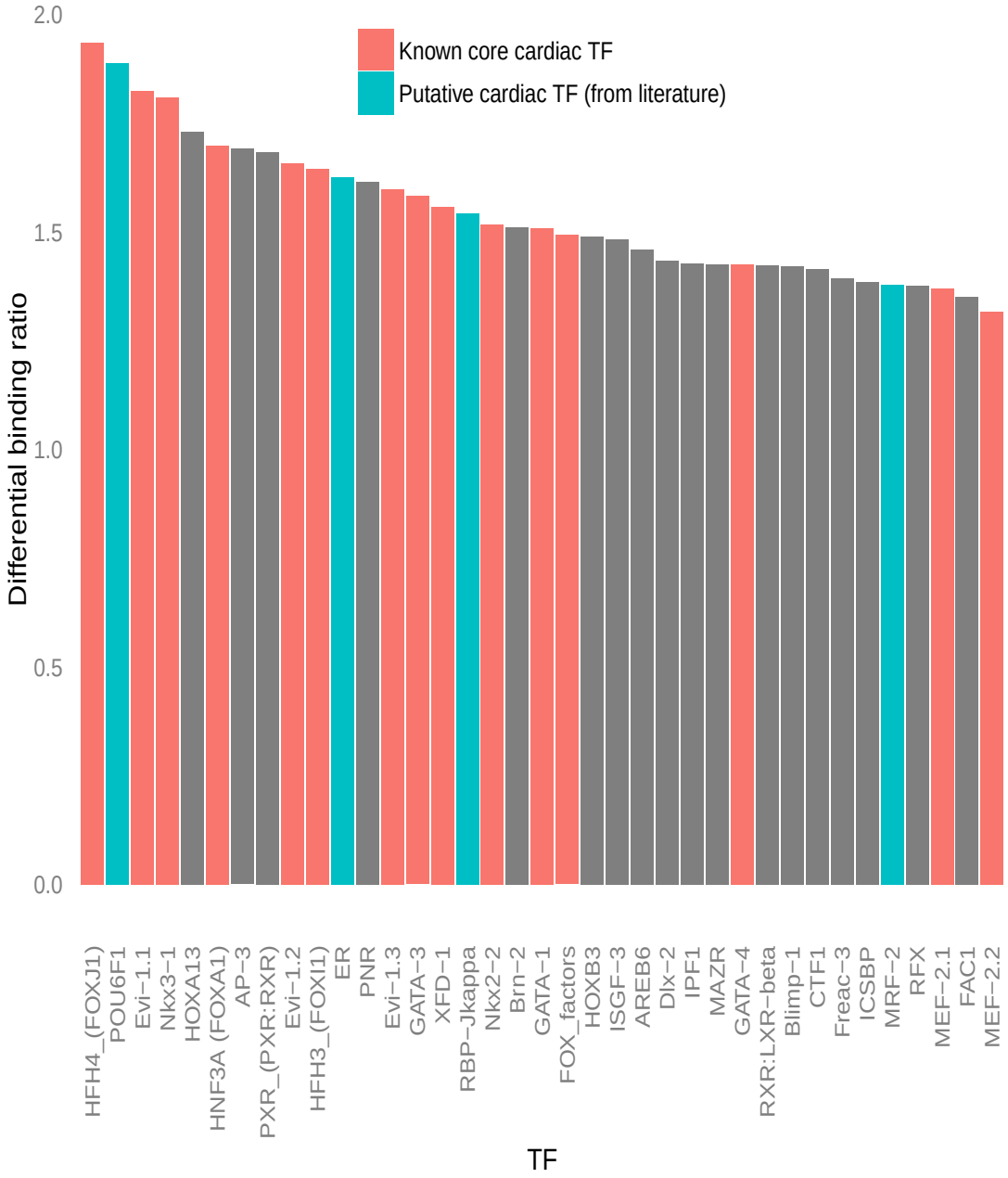

Figure 3.8: Regulatory motifs disrupted by eeSNP include several cardiac TFs. Only the motifs with average allele-specific binding score ratio ¿ 1.5 and Wilcoxon test p-value < 0.05 are shown, ordered by the ratio. Motifs corresponding to known cardiac TF families are shown in red and additional motifs with literature evidence of involvement in cardiac development or function are shown in blue.

3.12 Methods

3.12.1 Modeling regulatory-interaction potential:

There are R_1 epigenetic features $\mathbf{E}_i$ that were used to predict if a SNP i lies in a regulatory region. In addition, we also have R_2 interaction features $\mathbf{P}_{ij}$ that are predictive of the interaction between SNP i and gene j. We refer to a SNP that has high regulatory potential and high interaction potential as *interacting-regulator*, regardless of whether it associates with gene expression. Further, if the SNP is associated with gene expression, we refer to that SNP as *expression-regulator*. In our eQTeL approach, we model the regulatory-interaction potential θ_{ij} between SNP i and gene j as a combined function of epigenetic features $\mathbf{E}_i$ and interaction features $\mathbf{P}_{ij}$. Specifically, we use a Bayesian logistic regression model:

$$\theta_{ij} \sim \mathcal{B}ern(\mathtt{logistic}(\mathbf{F}_{ij} \cdot \boldsymbol{\alpha}))$$

, where $\mathbf{F}_{ij}$ is a concatenated set of features consisting of both $\mathbf{E}_i$ and $\mathbf{P}_{ij}$, and $\mathcal{B}ern$ is the Bernoulli distribution. The coefficients $\boldsymbol{\alpha}$ are shared across all genes.

3.12.2 Modeling Gene Expression:

In our model, the expression of gene j depends not only on the allele status of candidate SNPs, but also on the estimated regulatory-interaction potential of the SNP i and gene j pair. Specifically, given gene expression in n samples $\mathbf{Y}_j =$

$(Y_{j1}, \ldots, Y_{jn})$, we model the vector of expression $\mathbf{Y}_j$ for gene j as a linear function of the allele status for all candidate SNPs, $\mathbf{X} = \{X_1, \cdots, X_p\}$ where X_i is allele status of SNP i over the n samples:

$$\mathbf{Y}_j|\boldsymbol{\beta}_j, \mathbf{X}, \boldsymbol{\gamma}_j \sim \mathcal{N}(\mathbf{X}_{\boldsymbol{\gamma},j} \cdot \boldsymbol{\beta}_{\boldsymbol{\gamma},j}, \sigma_j^2 I), \tag{3.1}$$

where the effect β_{ij} of SNP i on the expression of gene j is nonzero only when indicator variable $\gamma_{ij} = 1$. In other words, $\gamma_{ij} = 1$ signifies whether SNP i is associated with the expression of gene j. $\mathbf{X}_{\boldsymbol{\gamma},j}$ (and $\boldsymbol{\beta}_{\boldsymbol{\gamma},j}$) refers to a subset of SNPs for which $\gamma_{ij} = 1$.

If a SNP lies within a genomic region that is deemed to be (i) a regulator, and (ii) interacting with the target gene, then the SNP is likely to affect the gene's expression. Thus, the regulatory-interaction potential for each pair of SNP i and gene j enters our gene expression model through the prior distribution on the indicator variables γ_{ij},

$$\gamma_{ij}|\phi(\theta_{ij}) \sim \mathcal{B}ern(\phi(\theta_{ij})) \quad \forall \quad \text{SNPs } i \tag{3.2}$$

where the function $\phi(\theta)$ is defined so that $\phi(\theta) = \pi^{\theta}\pi_0^{1-\theta} = \pi/\rho^{1-\theta}$ with π being our prior probability for each SNP to be expression-regulator and let $\pi_0 = \pi/\rho$ be the prior probability when the SNP does not reside in such a region, where ρ is an amplification factor. An uniform prior for $\pi \in (m/e, M/e)$ is defined where m and M are respectively the minimum and the maximum number of expected

expression-regulators. However, no substantial difference in results was observed when we just fixed $\pi = \bar{m}/e$ where $\bar{m}$ is expected number of expression regulators. A value of $\rho = 100$ was used because performance of model was insensitive to choice of $\rho \in (100, 1000)$.

Due to severe multiple testing corrections, association studies miss many potential causal regulators that have relatively small effect on expression. In our eQTeL model, overall sparsity is controlled by two factors: (a) the fraction of SNPs which are interacting-regulators i.e. $E(\theta)$ and (b) the fraction of interacting-regulators which are expression-regulators i.e. π. This is because the overall sparsity is a product of the two factors i.e. $\log E(\phi(\theta)) \approx E(\theta)\log\pi$ assuming $\rho >>> 1$. Thus, the effective sparsity constraints are less conservative on SNPs that lie within an interacting-regulator in our eQTeL model, which allows us to capture potential causal expression-regulator SNPs with small (but non-zero) effects on expression variance (Fig. 3.4 and Appendix A Fig. 3.6; refer to Supplementary Note 5).

We also employ a standard prior distribution, Zeller's g-prior [146], for our linear model parameters,

$$\boldsymbol{\beta}_\gamma | \boldsymbol{\gamma}, \sigma, c \;\sim\; \mathcal{N}(0, c\sigma^2(\mathbf{X}_\gamma^T\mathbf{X}_\gamma)^{-1}), \quad p(\sigma^2) \propto 1/\sigma^2 \tag{3.3}$$

and we also define the following prior distributions for the rest of the parameters as

$$\begin{aligned} c &\sim IG(\frac{1}{2}, \frac{n}{2}) \\ \boldsymbol{\alpha} &\sim \mathcal{N}(\mathbf{b}, 100 \cdot \mathbf{I}) \end{aligned} \tag{3.4}$$

The first element of $\boldsymbol{\alpha}$, α_0 is the bias term, and $\mathbf{b}$ is the prior for $\boldsymbol{\alpha}$, and is set to 0, except for b_0 (the prior for α_0), which can be used to control the sparsity on the number of interacting-regulators. We expect 1% of all SNPs to be regulators. To achieve this level of sparsity in number of regulators, b_0 was set to $\log(e/(p-e))$, where e is expected number of interacting-regulators, and was set to $p/100$. That is, $b_0 = \log(1/99)$.

Refer to Supplementary Note 1 for the eQTeL's inference algorithm, initialization and convergence criteria.

3.12.3 Cardiac expression data (MAGNet):

Samples of cardiac tissue ($n = 313$) were acquired from patients from the Myocardial Applied Genomics Network (MAGNet; www.med.upenn.edu/magnet). Left ventricular free-wall tissue was harvested at the time of cardiac surgery from subjects with heart failure undergoing transplantation and from unused donor hearts. Genomic DNA was extracted using the Gentra Puregene Tissue Kit (Qiagen, CA) according to manufacturer's instructions. Total RNA was extracted using the miRNeasy Kit (Qiagen) including DNAse treatment. RNA concentration and quality was determined using the NanoVue Plus^{TM} spectrophotometer (GE Healthcare) and the Agilent 2100 RNA Nano Chip (Agilent). To assess gene expression, RNA was hybridized with Affymetrix Genechip ST1.1 arrays using manufacturer instructions. CEL files were normalized with the robust multiarray analysis (RMA) using the oligo package in Bioconductor [164]. To remove potential batch effects, expression

values were further adjusted using ComBat, an empirical Bayes method that estimates parameters for location and scale adjustment of each batch for each gene independently [165]. Probe sets were removed if they displayed RMA expression values < 4.8 on all arrays. This filtering yielded sets of genes present well above background levels in the human heart. Probeset showing no annotated cross hybridization potential were kept, leaving 15,395 probes for final analysis.

3.12.4 Selection of genes:

The genes were selected such that they had at least one significantly associated SNPs based on univariate-eQTL (Matrix eQTL). 1880 genes were thus selected using FDR threshold of 1E-6 using Matrix-eQTL (Lappalanien et. al.). We have no reason to believe that this selection is favorable to eQTeL.

3.12.5 Pre-procession of gene-expression:

It has been found that removing technical biases and confounding factors can greatly improve the association studies. Normalization of gene-expression data to remove confounding factors have been studied extensively ([166,167]). In association studies the comparison is across individual and not across genes, and therefore main aim of the normalization is to make the gene-expression distribution across samples comparable. Similar to Lappalainen et. al., we use PEER [166] to remove the confounding factors from expression data as pre-processing. Given expression data for multiple individuals, PEER identifies hidden factors that explain a large

proportion of global expression variability. Factors represent covariates that affect multiple gene and are therefore most likely to be confounding factors or technical biases. The factors are then regressed out from the expression and residual are used for performing association studies. In certain cases, such in trans-eQTL, a genetic-factor can affect multiple SNPs and PEER might remove biologically relevant signal. However, since the aim of the paper is to identify cis-eQTL, i.e. local effects, we can safely use PEER.

To determine number of factors (K) to be removed using PEER, we used approach similar to Lappalaninen et. al. We ran PEER for 16,271 Affymetrix gene probes from MagNet using parameter K=0, 3, 5, 10, 15 and 20; then we compared number of genes (eGenes) that have at least one SNPs significantly associated with expression (p-value $<$ 1 E -6). We chose K=10 because number of eGenes plateaued at K=10. Factors from PEER were regressed out from the expression and residual expression was used for further analyses.

Linear regression assumes normality of the expression data. Residual data from PEER was standardized to normal distribution before performing the association analysis.

3.12.6 Genotypes and imputation for cardiac samples:

DNA samples were genotyped using Affymetrix Genome Wide SNP Array 6.0 and analyzed per manufactures instructions. We applied quality control (QC) filters to exclude unreliable samples, samples with cryptic relatedness and samples

that were not genetically inferred Caucasian. After QC filtering, 313 individuals remained. All analyses were conducted using software package PLINK [140]. For the analysis reported here, we eliminated SNPs with genotype call rate $< 95\%$, with minor allele frequency (MAF) $< 15\%$, or if there was significant departure from Hardy-Weinberg equilibrium ($p < 10^{-6}$). A total of 360,046 SNPs passed QC and were available for analysis. To improve cross study comparisons, genotype imputation was performed using the Minimac (v 2012.11.16) [153] program. Imputation results were filtered at an imputation quality threshold of 0.5 and a MAF threshold of 0.15.

PLINK [140] was used to infer LD block for the genotypes. Default setting of SNPs within 200Kb was used to estimate it.

3.12.7 Epigenetic data and Interaction features:

Epigenetic data were obtained from ENCODE, Roadmap epigenome project and GEO database for following heart tissues: AoAF, HCM, HCF, Fetal-hearts, Adult-hearts, Left Ventricle, Right Ventricle, Arota, and Right Atrium. Because DNAse I footprints were used to validate eeSNPs, they were excluded from the feature importance ($\boldsymbol{\alpha}$) estimation of eQTeL. Appendix A Fig. 2 lists the epigenetic and interaction features, that were critical for identification of interacting-regulators. We assessed the importance of epigenetic factors directly overlapping each SNP within 50 bps flanking region (suffix .50 in Appendix A Fig. 2). We also assessed the importance of epigenetic factors in broader context of each SNP within 500 bps

flanking region (suffix .500 in Appendix A Fig. 2). Interaction features between a gene-promoter and a region containing SNP were calculated using RNASeq and DHS data from 15 cell types (A549, Bj, H1hesc, Hepg2, Hsmm, K562, Nhek, Ag04450, Gm12878, Helas3, Hmec, Huvec, Mcf7, Nhlf, and Sknshra). These features include: a)correlation and absolute correlation between DHS of the region and DHS of the promoter b) correlation and absolute correlation between DHS of the region and RNASeq FPKM of the gene.

Both epigenetic and interaction features were normalized to mean of 0 and standard deviation of 1. This implies that distribution of each of these features for a set of random SNPs were expected to have zero mean and one standard deviation. Therefore, y-axis in Appendix A Fig. 2 shows absolute enrichment over random-SNPs with units in standard deviation.

3.12.8 Estimating fraction of putatively causal eeSNP:

Using an approach similar to Lappalanien et. al. [139], we estimated proportion of eeSNP that are putatively causal. Clearly, an independent estimation of proportion of causal SNPs cannot rely on features used to identify eeSNPs, or any other potentially correlated feature, such as footprints. Thus, for an independent estimate of the proportion of causal SNPs, we used potential TF binding disruption by a SNP allele. Following Lappalanien et. al., using Matrixeqtl [151], we first identified *causal* SNPs as follows. For each gene we identified best and second best associated SNPs, and the best SNP was deemed *causal* if (i) the best SNP associa-

tion was significant ($FDR < 10^{-6}$) and (ii) the difference in association score (-log10 pvalue) between the best and the second best SNPs was greater than a threshold (conservatively, 2.5, a la Lappalanien et al.).

For each TF motif, we obtained the disruption at each SNP (decrease in motif match scores due minor allele relative to major allele) thus obtaining two distributions, one for *causal* SNPs and another for the presumed non-functional background. Using distribution of motif disruption score for causal SNP, we identified TF motifs that are preferentially disrupted by *causal* SNPs. For each of such motif y, we calculated an enrichment score $c_{causal,y}$ which is the ratio of means of TF motif disruption score between the causal and a set of presumed non-causal SNPs. For motif y, we similarly calculated the enrichment score for eeSNPs $c_{eeSNP,y}$. Following Lappalainen et. al., we then estimated the fraction of eeSNPs likely to be causal as $\frac{c_{eeSNP,y}-1}{c_{causal,y}-1}$. Appendix A Fig. 14 shows these proportion of eeSNP that is likely to be causal for all selected motifs, suggesting that overall 58% of eeSNPs are putatively causal.

Functional explained variance and expression predictability was defined as explained variance by subset of expression-regulators that mapped to a DNAse I footprint.

3.12.9 Simulation study:

Simulation was done on 200 genes. We used 174800 SNPs (874 SNPs per each gene) for 313 samples from MAGNet genotype data. 1% of total SNPs were declared

as enhancers. We estimated, number of causal regulatory SNPs and distribution of explained expression variance by genotype by running eQTeL in MAGNet data. Using estimated number of causal regulators from MAGNet, expression-regulators were selected among enhancer per gene. Effect-size of each expression regulator was generated from $\sim \mathcal{N}(0, 1)$, that is finally being used to generate expression for each gene using a linear model. Finally a random noise was added such that explained variance by expression-regulators will be same as estimated from MAGNet data. For each regulator SNP, 7 epigenetic features (DNAse, H3K4me1, H3K4me3, P300, H3K27me3, H3K36me3 and H3K9me3) for heart were generated from distribution derived from validated heart enhancers [47]. For all other SNPs epigenetic features were generated from random SNP background.

3.12.10 Motif binding score differential:

For each of the 981 vertebrate TF motif from TRANSFAC database [168], we scanned the 50 bps flanking eeSNPs (and for 10,000 control SNPs randomly sampled from 300,000 SNPs) for the presence of motif using pwmscan tool [169], separately for the major and the minor allele. Only the cases where at one of the two alleles had a motif hits ($p - value < 0.0002$) were further considered. For each such case, the difference in the binding score for the two alleles was computed, as the difference in log(p-value). For each motif, the binding differential score for eeSNPs and the control SNPs were compared using Wilcoxon test and the motifs which had at least 1.5 fold greater differential among eSNPs and a $p - value < 0.05$ were identified.

3.12.11 DNAse footprint enrichment:

From [157] we obtained a list of genomic locations, for 41 different cell-types, where significant evidence of in-vitro protein binding event were detected using DNAse-footprint. For each tissue, we calculated fraction of number of SNP that have a footprint in the 50 bps flanking it.

3.12.12 Allelic imbalance and ChIA-PET analysis:

DNAse hypersensitivity (DHS-seq) reads for heart cells (HCM sample) were obtained and mapped to eeSNPs (and control SNPs). Heterozygousity at each SNP locus was ascertained by the presence of multiple alleles among the reads mapping to the SNP location. For each such locus, the allelic imbalance was calculated as the difference in the number of reads mapped to each allele. The allelic imbalance was plotted against the overall signal intensity rank.

ChIA-pet assay identified spatially proximal genomic regions where at least one of the region is bound by PolII. Because ChiA-pet data is unavailable for heart-related cell types, we pooled multiple ChiA-pet data from *K562, Hela, Nb4 and MCF7*. For each 50 bps flanking an eeSNP (or control SNP) and the target promoter pair, number of ChIA-pet reads supporting the spatial proximity of the two loci were recorded. The ChiA-pet support for each SNP-gene pair was then compared for different methods after controlling for the genomic distance between the SNP and its target gene.

In Fig. 3.6 and 7, median "white" lines represent LOESS (local regression) for

each method. Confidence interval for each median line is estimated using bootstrapping and they are shown in the s using either of following two ways: by thin lines representing LOESS of each bootstrap, or by colored regions representing confidence intervals in terms of standard deviation of bootstraps.

3.13 Software availability

The implementation of eQTeL with its source code is freely available at (www.cbcb.umd.edu/software/goal) as a R-package under MIT license.

For details of other eQTL methods (Supplementary Note 3); expression explained variance and predictability (Supplementary Note 6); and scalability of eQTeL (Supplementary Note 7) refer to Supplementary Notes.

Synthetic rescue determinants in cancer

Chapter 4: Synthetic rescue determinants of resistance and response to cancer therapy

4.1 Introduction

Resistance to therapy in cancer may arise due to diverse mechanisms including drug efflux, mutations in drug targets and adaptive responses in downstream molecular pathways [61]. The latter cellular reprogramming alterations mainly involve network-wide changes in the DNA sequence, copy number, expression, epigenetics and phosphorylation of proteins that buffer the disrupted function of the drug targets. Indeed, numerous recent transcriptomic and sequencing studies have identified different molecular signatures underlying the variable response and emergence of resistance to specific drugs in cancer patients, and potential interventions to improve the effectiveness of therapies [83, 84, 170–179].

During cancer progression, fitness-reducing alterations in a particular gene may be compensated by subsequent alterations in the activity of another gene, restoring cancer progression and proliferation. In this type of genetic interaction, we term the former gene a vulnerable gene, the latter gene a rescuer gene, and the functional relation between them a synthetic rescue (SR). There are potentially four basic types

of SRs: (1) down-regulation of both the vulnerable and the rescuer gene (DD); (2) down-regulation of the vulnerable gene and up-regulation (i.e., over-activation) of the rescuer (DU); (3) up-regulation of the vulnerable gene and down-regulation of the rescuer (UD); and (4) up-regulation of both vulnerable and rescuer genes (UU) (see Extended Data Figure 1a-d).

Recent years have seen a surge of interest in studying an inherently different class of genetic interactions termed synthetic lethality (SL) [180, 181] in which the inactivation of both SL partner genes is lethal but the inactivation of either gene alone is viable (see Extended Data Figure 1e). A tumor may become insensitive to a drug treatment because activity of the SL partner of its drug target is maintained at wild-type levels to escape conditional lethality [72]. However, cancer cells may also further over-activate a rescuer gene of the drug target far beyond its wild-type activity levels to escape lethality [60, 83, 84, 170–173] (DU-type SR). While the role of SL interactions in cancer has received tremendous attention [71, 181–183]18,21-24, only a few instances of SR interactions have been reported in cance [60, 83, 84, 170–173] (and very few reported in micro-organisms [184–186]). Specifically, a genome-wide approach to identify SR interactions has not been reported.

4.2 Background

Before proceeding further, we briefly revisit some background of genetic interactions in cancer.

4.2.1 Synthetic lethality

Synthetic lethal (SL) interaction between a pair of genes defines an interaction between two genes when concomitant inactivation of two gene is lethal to cell, while inactivation of each of gene is not [71]. As shown in a figure an example of SL interactions between genes BRCA and PARP [187]. In a cell, individual knockdown of either BRCA or PARP genes are not lethal to cell. However, simultaneous knockdown of BRCA and PARP genes are lethal to cell. Fig 4.1b. illustrates the concept of SL in terms on a functional truth table of gene activities. We will use the functional truth table representation throughout the document to represent any genetic interaction between two genes. In the functional table samples are divided based on each of the genes activity. We assume tri-state of gene activity i.e, in-active (under-expressed), wild-type, over-active (over-expressed).

Synthetic lethality was first noticed first by Cavin bridge in 1922, when he observed a combination of mutation confer lethality in melanogaster [188]. The term synthetic lethality was later coined in 1945 [188]. Synthetic lethality offers a unique opportunity to develop anticancer drugs that will target genes whose Synthetic Lethal (SL)-partners are inactivated in the specific cancer being treated. SL-based drugs are therefore expected to kill cancer cells selectively, sparing normal healthy cells [72, 73, 189]. Towards the realization of this potential, screening technologies have been developed to detect SL-interactions in numerous model organisms [180] and in human cell lines [62–70]. However, as every pair of genes can potentially interact in synthetically lethal manner, the combinatorial search space consists of

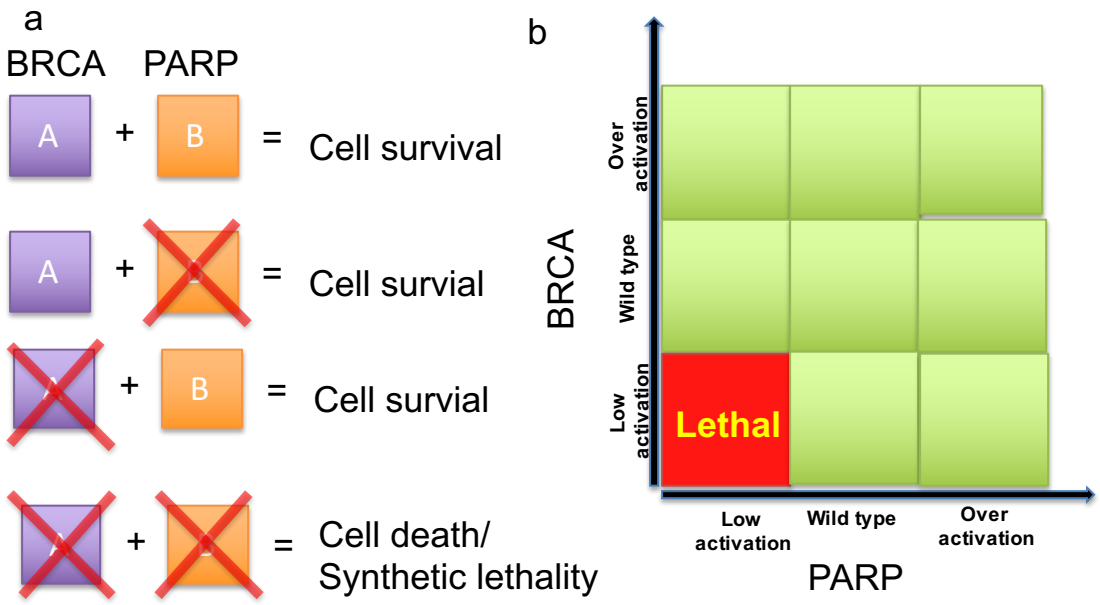

Figure 4.1: A example of synthetic lethal between genes BRCA and PARP. (a) Two genes form an SL pair if the combined inhibition of both gene products is lethal to the cells, while the inhibition of either gene product alone is not lethal. (b). Synthetic lethal functional truth tables: The truth table denotes the cell viability states - viable (green), lethal (red) - as a function of the activity state of each of the SL pair genes (down regulated, wild-type and up-regulated).

more than 500 million pairs that ideally should be examined in more than just one experimental system. Current experimental technologies at our disposal are hence yet far from being able to address the challenge of identifying the SL interactions across different cancers on a genome-scale. New bioinformatics approaches are hence been called for to guide and complement the experimental search for SL-interactions in cancer.

Previous computational approaches developed to systematically study synthetic lethality in cancer have aimed to infer SL pairs by mapping SL-interactions in yeast to their human orthologs [190, 191]or by utilizing metabolic models and evolutionary characteristics of metabolic genes [192–194]. In a recent study Jerby

et. al. harnessed large cancer genomic data that have been rapidly accumulating to identify candidate SL-interactions via a direct data-driven approach, termed the DAta-mIning SYnthetic-lethality-identification pipeline (DAISY) [71].

4.2.2 Computation identification of SL network in cancer (DAISY)

DAISY identifies candidate SL interactions employing three independent statistical tests

1. Molecular survival of the fittest: DAISY mines gene expression and SCNA of tumor samples from TCGA and cell lines data to identify SL gene pairs A and B having the property that tumor samples with co-inactivation the genes are significantly less frequent than than what would be expected by observing the genes individual inactivation rates in the data.

2. The second inference strategy, "shRNA-based functional examination", is closely related to the first. It is based on the notion that the essentiality of a synthetically lethal gene manifests itself when a gene is knocked down in cancer cells where its SL-partner(s) are inactive (that is, with a markedly low copy-number and expression). Accordingly, the SL-pairs of a given gene can be identified by searching for partner genes whose under-expression and low copy-number induce its essentiality.

3. The third procedure, "pairwise gene co-expression", is based on the notion that SL-pairs tend to participate in closely related biological processes and

hence are likely to be co-expressed [180].

They show that a genome-wide cancer-SL-network can be robustly identified from these datasets, and then utilized to successfully predict both gene essentiality and drug response in cancer cell lines, as well as patient survival [71].

4.2.3 Synthetic dosage lethality

Synthetic dosage lethal interaction between a pair of genes defines an (asymmetric) interaction such that the over-activity of one of them renders the other gene essential, i.e independent knockdown of gene A is not lethal to cell, however knockdown of A in cells where B is over-expresssed is lethal [74]. The concept of synthetic dosage lethality, although not explored as extensively as SL, may hold therapeutic potential, especially in case of cancer. One of the hallmark of caner is over-expression of oncogenes. The over-expression of oncogenes such as MYC help cells to overcome apoptosis and proliferate rapidly. However, over-expression of oncogenes creates additional vulnerabilities in cells, specifically in such cells if SDL partner of the oncogenes are knockdown it will selectively kill the cancer cells. Therefore, the over-activation associated with oncogenes, unlike loss-of-function associated with tumor suppressor, can be therapeutically exploited by SDL.

4.2.4 Synthetic rescue

We define synthetic rescue (SR) interactions between a vulnerable gene V and rescuer gene R as (asymmetric) interactions in which change in activity of V is lethal,

but subsequent perturbation in gene R makes the cell viable again. Depending on direction of perturbation there can be following four kinds of SR.

4.2.5 Down-Down (DD) synthetic rescue

In this kind of interaction, inactivation of vulnerable gene is lethal to cell, however subsequent inactivation of rescuer gene make cell viable. Fig **??** illustrates the DD interaction. SR interaction have three possible state: (i) "viable" (green): active vulnerable gene active , (ii) "lethal" (red): inactive vulnerable gene and rescuer gene active and (iii) "rescue" (blue): inactive vulnerable gene and inactive rescuer gene. At first glance it might seem that viable and rescue state should be phenotypically similar, however as we shall see in case of cancer they are phenotypically very different. In cancer while viable state represent normal poliferation of cancer cell, on the other hand rescue state represents resistant state (i.e cells still proliferate with drug treatment).

Such kind of interaction in are also referred as extragenic suppressor mutations [195]. However, suppressor mutation definition are limited to mutations, where mutation in one gene reverses the phenotypic effect due to mutation in other gene. For eg. mutation in gene UNC-54 can be rescued by mutation in UNC-22 in C. elegans [196].

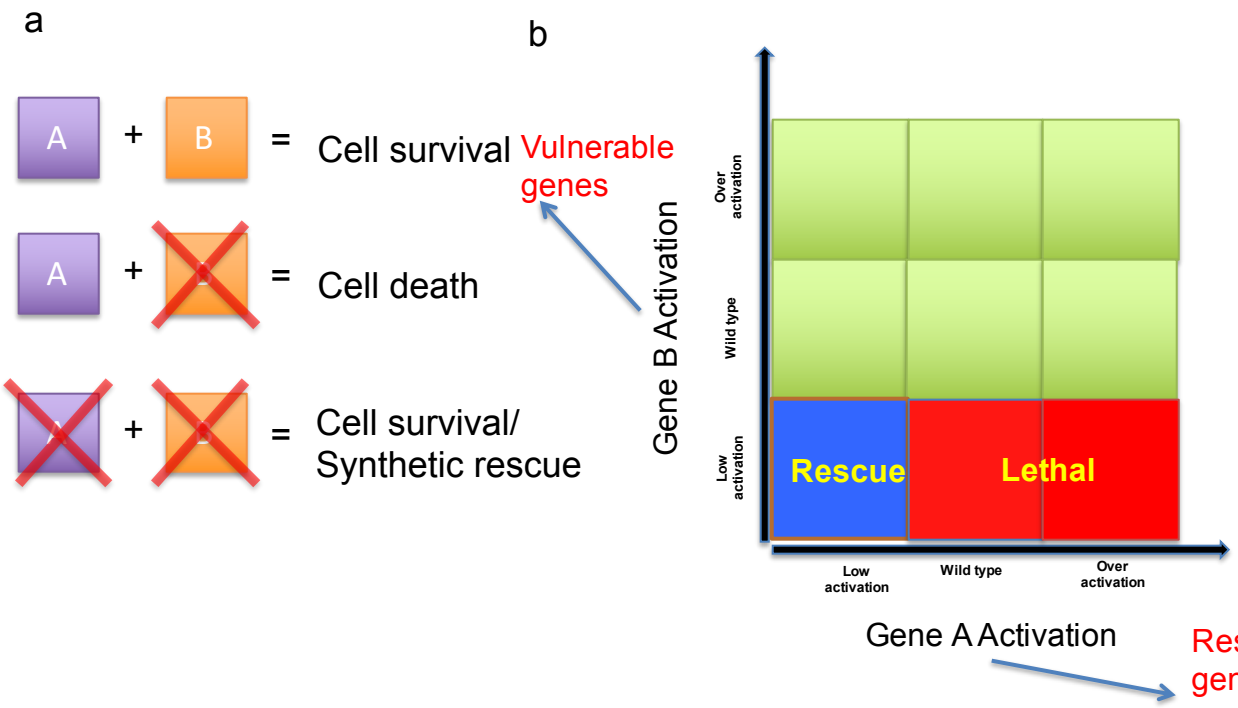

Figure 4.2: Definition of DD type SR: (a) A vulnerable gene and a rescuer gene form an DD SR pair if the inhibition of the vulnerable gene is lethal unless it is rescued by inhibition of the rescuer gene. (b) The truth table denotes the cell viability states - viable (green), non-rescued (i.e., lethal – red), and rescued (blue) - as a function of the activity state of each of the DD SR pair genes (down regulated, wild-type and up-regulated).

4.2.6 Down-Up (DU) synthetic rescue

In this kind of interaction, inactivation of vulnerable gene is lethal to cell, however subsequent **over-expression** of rescuer gene make cell viable. Fig 4.3 illustrates the DU interaction. Analogous to DD interaction DU have three possible state.

Other SR interactions are Up-Down(UD) SR and Up-Up SR, where over-expression of vulnerable gene is lethal and rescued by rescuer in-activation in case of UD and over-activation in case of UU.

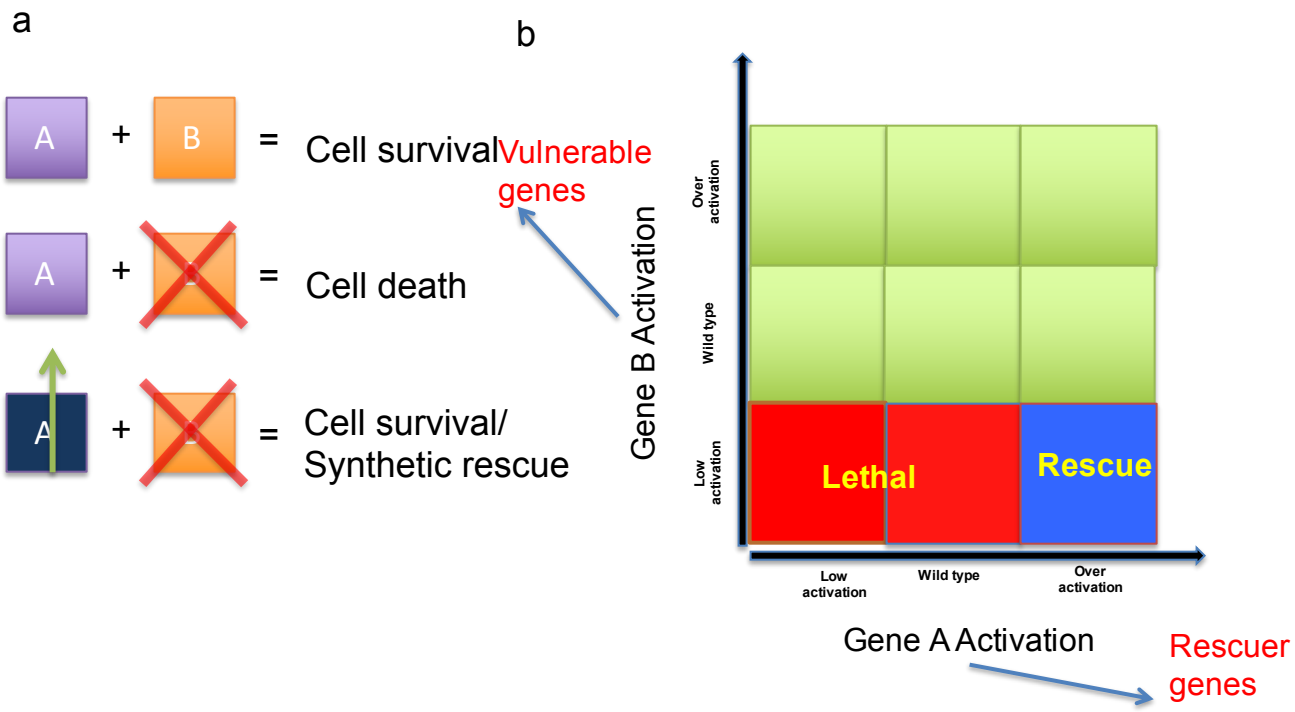

Figure 4.3: Definition of DU type SR: (a) A vulnerable gene and a rescuer gene form an DU SR pair if the inhibition of the vulnerable gene is lethal unless it is rescued by over-activation of the rescuer gene. (b) The truth table denotes the cell viability states - viable (green), non-rescued (i.e., lethal – red), and rescued (blue) - as a function of the activity state of each of the DU SR pair genes (down regulated, wild-type and up-regulated).

Although all four types of SR interactions are important, in the presented work we concentrate on DU SR interactions because (i) they are most intituive of SR interaction, (ii) most clinically relevant in cancer and (iii) can be used to devise anti-resistant cancer therapies.

4.3 INCISOR

Here we set out to study the potential role that SR interactions play in determining drug resistance in cancer, mediated by altered activity of SR rescuer

partners of drug targets. We developed a new statistical pipeline, termed IdeNtification of ClinIcal Synthetic Rescues in cancer (INCISOR) to identify genome-wide SR networks in cancer. Mining tumor molecular and survival data of cancer patients, INCISOR predicts SR pairs through a series of four inference steps that together capture the salient features of an SR pair. We provide a brief overview of INCISOR for the DU-SR type (see Methods for a comprehensive description and refer to Appendix B for other types): (1) The first step, termed Molecular survival of the fittest (SoF) uses molecular data (somatic copy number alterations (SCNA) and transcriptomics data) and examines the fraction of tumor samples that display a given candidate SR pair of genes in its DU rescued state that is, where the vulnerable gene is down-regulated and the rescuer gene is up-regulated. Scanning all possible gene pairs it selects pairs that appear in the rescued state (respectively non-rescued state) significantly more (respectively less) frequently than expected, testifying to their rescue effect on the tumor fitness. The next three steps examine patient survival data to further narrow down the SR candidate pairs (identified in the first step based on molecular data) by eliminating potential false positives: (2) Vulnerable gene screening aims to identify the vulnerable genes by searching for genes whose down-regulation improves patient survival (i.e., reduces tumor fitness) in the subset of tumors where the rescuer partner (as predicted from the first step) is not up-regulated. (3) Robust rescue effect studies the subset of tumors where the vulnerable gene is down-regulated. It aims to select the SR pairs where the rescue of the vulnerable gene is robustly associated with worse patient survival than its non-rescued state. Finally (4) Oncogene rescuer screening removes false positive

candidate SR pairs whose rescuers show worse survival when up-regulated regardless of the inactivation of the vulnerable gene partners (thus likely to have oncogenic effects on their own).

More specifically, INCISOR identifies candidate SR interactions employing four independent statistical tests, each tailored to test a distinct property of SR pairs. We describe here the identification process for the DU-type SR interactions. The methods to detect other patterns are analogous and described in the Appendix B. We identified pan-cancer SRs analyzing gene expression, SCNA, and patient survival data of TCGA from 7,995 patients in 28 different cancer types. As reviewed in the main text, INCISOR is composed of four sequential steps (see Extended Data Figure 1a):

1. Molecular survival of the fittest: We mine gene expression and SCNA of multiple tumor samples to identify vulnerable gene (V) and rescuer gene (R) pairs having the property that tumor samples in non-rescued state (that is samples with underactive gene V and non-overactive gene R shown in red in Extended Data Figure 1a) are significantly less frequent than expected (due to lethality), whereas samples in rescues state (that is samples with under-active gene V but over-active gene R shown in blue in Extended Data Figure 1a) appear significantly more than expected (testifying to an explicit rescue from lethality). Specifically, we performed multiple one-sided Wilcoxon rank-sum tests to identify the pairs that have the above properties (see Appendix B).

   The next three steps utilize patient survival data to narrow down which of

the SR candidate pairs from step 1 are the most promising candidates (Note that in doing that we take into account both FDR adjusted log-rank p-value and effect size, $\Delta\mathcal{AUC}$, which quantifies the difference in the Area Under the Curves in the KM survival plot of the two compared groups):

2. Vulnerable gene screening: This step aims to selects vulnerable genes V by searching genes whose down regulation conditionally improves patient survival, that is it examines the samples where the gene R is not unregulated and tests whether the candidate vulnerable gene V is detrimental to cancer progression (when not rescued by candidate rescuer gene R). Specifically, we perform two KM analyses testing if the inactivation of vulnerable gene V (without rescue) improves patient survival (test I) and if the over-activation of candidate rescuer gene R when V is inactivated decreases patient survival (test II). Among candidate pairs that are significant in test I (after FDR correction), we calculate ΔAUC in tests I and II, and then we calculate the difference in these two ΔAUC values. Gene pairs with top 25 percentile of these differences will be selected for further testing in steps 3 and 4.

3. Robust rescue effect: This step examines the samples where the gene V is not down-regulated and aims to identify candidate SR pairs where the rescue (blue in Extended Data Figure 1a) of the vulnerable gene is robustly associated with worse patient survival than its non-rescued state (red in Extended Data Figure 1a). We compare the survival of patients whose tumors show rescued versus non-rescued activation patterns for a given SR pair. Based on KM analysis,

candidate SR pairs where the rescued state is associated more strongly with worse survival than the non-rescued state are considered likely SR candidates and are passed to the final, 4th step. In order to augment the robustness of the rescue effect we employed bootstrapping within TCGA samples, which improves cross-dataset generalizability of rescue effect of SR pairs. Specifically, we aggregated the results over 50 bootstraps of the samples set to identify robust rescue effects [152].

4. Oncogene rescuer screening: Some pairs found significant in step 3 might show an effect on patient survival simply because the rescuer gene is an oncogene, irrespective of any synergy between the rescuer and the vulnerable gene. This step aims to correct for such false positives by eliminating the SR pairs with the lowest 90% of rescue effect (measured by ΔAUC in KM patient survival curves) among all pairs that include a given rescuer gene.

Finally, INCISOR tailors a log-rank statistical test (two-sided) for the three survival analyses (steps 2-4) to account for differences in survival time between cancer types. Specifically, to compare survival of any two groups, we estimate the expected number of deaths in each group for each cancer type separately assuming a hypergeometric distribution. We then sum the cancer-specific estimates of expected and observed number of deaths to infer pan-cancer expected and observed number of deaths. Finally a 2-test (two-sided) comparing the pan-cancer expected and observed death gives the final pan-cancer survival difference between any two groups tested.

4.4 Validations of INCISOR

We applied INCISOR to mine the TCGA data, which spans 7,995 samples across 28 different cancer types [197]. We focus our description on DU-SR analysis as it has the greatest survival predictive power and most importantly, DU rescuer genes can be targeted to reduce emerging resistance to cancer drug therapies. The resulting pancaner DU-SR network has 2,033 interactions involving 686 rescuer genes and 1,513 vulnerable genes (Figure 4.4 , Extended Data Figure 1g). The Gene Ontology (GO) distance (Appendix B) between pairs of vulnerable and rescuer genes is less than that of random pairs (Wilcoxon rank-sum P $<$ 4.4E-05) and shuffled DU-SR pairs (Wilcoxon rank-sum P $<$0.03), suggesting that SR partners are functionally related. An interesting example involves RPL23, which suppresses tumor progression by stabilizing P53 protein. It is a moonlighting gene, having two additional secondary functions as a ribosomal protein and an inhibitor of cell cycle arrest. A GO analysis of its 12 predicted rescuer partners shows that they indeed span such secondary functions, compensating the loss of RPL23 (Appendix B Table 2). Only a small fraction (2.5%) of the DU protein pairs physically interact with each other, indicating that more complex and indirect regulatory and signaling mechanisms mediate most SR functional interactions. The relative significance of each of the four screening steps in determining the final DU-SR network was benchmarked in an independent gastric cancer dataset, showing that each step of INCISOR significantly contributes to the final prediction accuracy (Extended Data

Figure 4j,k) [175]. Descriptions of the other pan-cancer DD (Extended Data Figure 6a), UD (Extended Data Figure 6d) and UU (Extended Data Figure 6g) SR networks are provided in Appendix B.

We tested the clinical significance of the DU-SR network in an independent METABRIC breast cancer (BC) dataset [198] by comparing the survival of patients that have many vs. few (top vs. bottom 10%) SR pairs in their DU rescued state in tumor (Methods, Extended Data Figure 1a). We find that tumors with many rescued SRs have markedly worse patient survival than tumors bearing a low load of rescued SRs (true for all four SR types; see Figure 4.5a-d), and that this is not merely due to differential activation of vulnerable genes (Figure 4.5e, Extended Data Figure 8e, Extended Data Figure 8f) or other confounding factors (Cox regression in Appendix B Table 1). The pancancer DU-SR network predicts patient survival also in other cancer types, as determined by cross validation evaluation over different TCGA cancer types (Extended Data Figure 2a) and in another independent (ovarian) cancer dataset with a sufficiently large number of samples33 (Extended Data Figure 2b). Combining INCISOR-inferred SL interactions (Extended Data Figure 5e, Appendix B) with SR interactions further improves survival predictive power (Figure 2f). Finally, we find that the copy number of DU rescuer genes is significantly higher when their vulnerable genes are mutated vs wild type (data not used in the INCISOR inference, Wilcoxon rank-sum P <1.2E-100), and so is the rescuers gene expression (Wilcoxon rank-sum P < 1.1E-17, Extended Data Figure 2c,d). Breast cancer specific SR networks inferred using TCGA breast cancer samples only are also predictive of patient survival in the METABRIC dataset (Ex-

tended Data Figure 8a-d, Appendix B). Patient outcomes were also predictable by SR networks built specifically for each of four major BC subtypes (HER2, Luminal A, Luminal B and TNBC, Extended Data Figure 10).

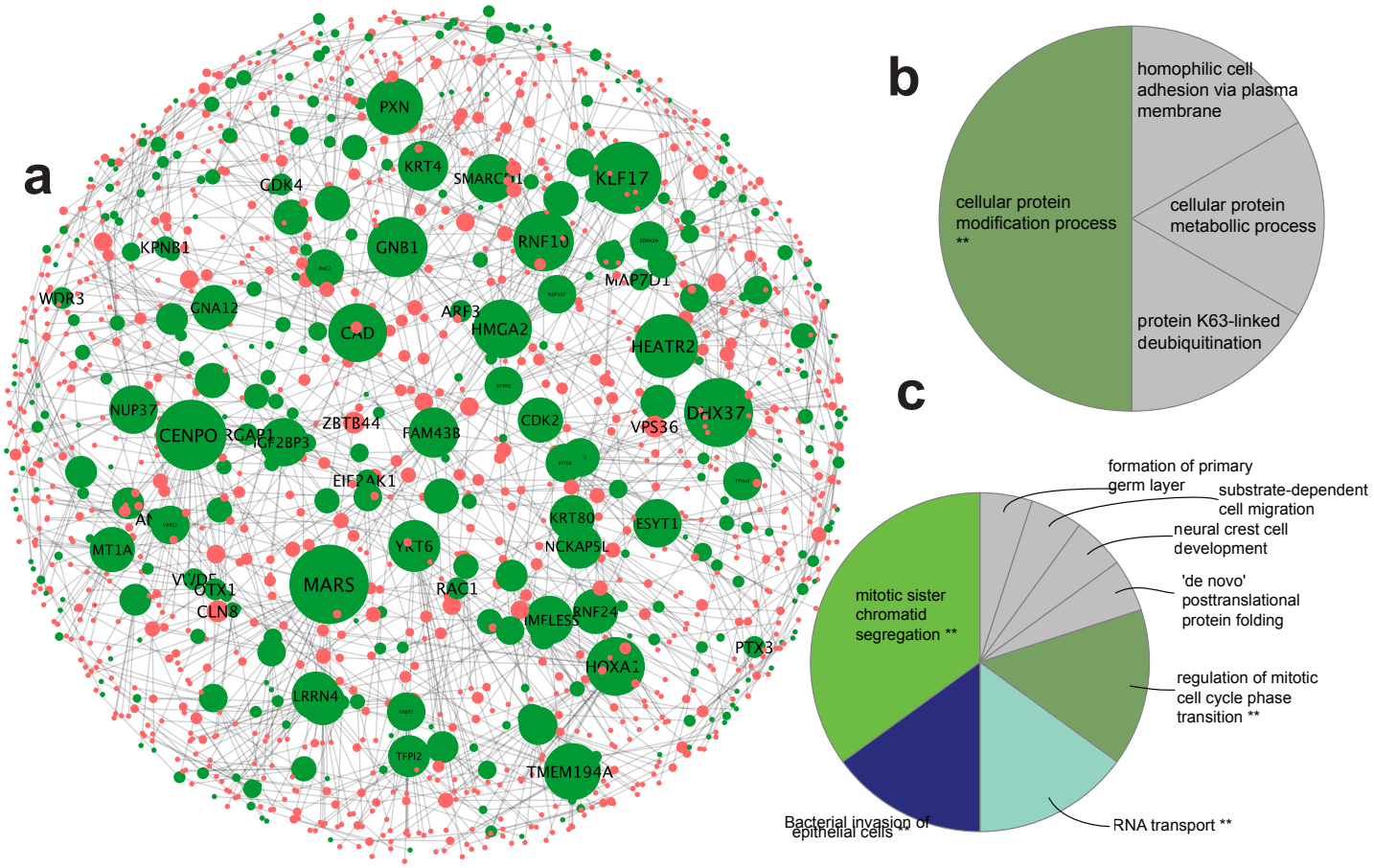

Figure 4.4: Pan-cancer DU-type SR network. (a) Pan-cancer DU-type synthetic rescues network with 686 rescuer genes (green) and 1,513 vulnerable genes (red) encompassing 2,033 interactions. The size of nodes indicates their degree in the network. (b,c): Gene Ontology enrichment of vulnerable and rescuer genes. (b) The vulnerable genes are enriched with cell adhesion, protein modification, metabolism and deubiquitination. (c) The rescuer genes are enriched with mitotic cell cycle phase transition, chromatid segregation, cell migration and RNA transport. Only significant pathways (one-sided hypergeometric FDR adjusted $P<0.05$) are shown in the figure.

We next investigated the dynamics of SR pairwise activity as cancer progresses. We stratified the BC patients in the METABRIC dataset into six different cancer progression bins based on their survival data and quantified the number of rescued DU-SR pairs in samples in each bin. We find that tumors associated with shorter survival times (i.e., likely to be more advanced) have a higher fraction of rescued DU-SR pairs (Extended Data Figure 8g,h). Based on the patient stratification, we further distinguished between two kinds of DU-SR interactions: reprogrammed SRs (rSR), where the rescuer gene up regulation (over-activation) is inferred to follow after the down-regulation (inactivation) of the paired vulnerable gene (and hence likely to occur in response to it), and buffered SR (bSR), where the rescuer gene up-regulation is inferred to precede the down-regulation of the vulnerable gene (Appendix B). Indeed, we find that while SRs carry a significant predictive survival signal irrespective of their order of occurrence (as shown throughout and also in Extended Data Figures 8a-d,10), the emerging resistant-associated responsive rSRs have a significantly stronger predictive survival signal than bSRs (Appendix B).

Interestingly, a DU-SR analysis may also provide insights to carcinogenesis, since the cellular response to the inhibition of a vulnerable gene may result in the

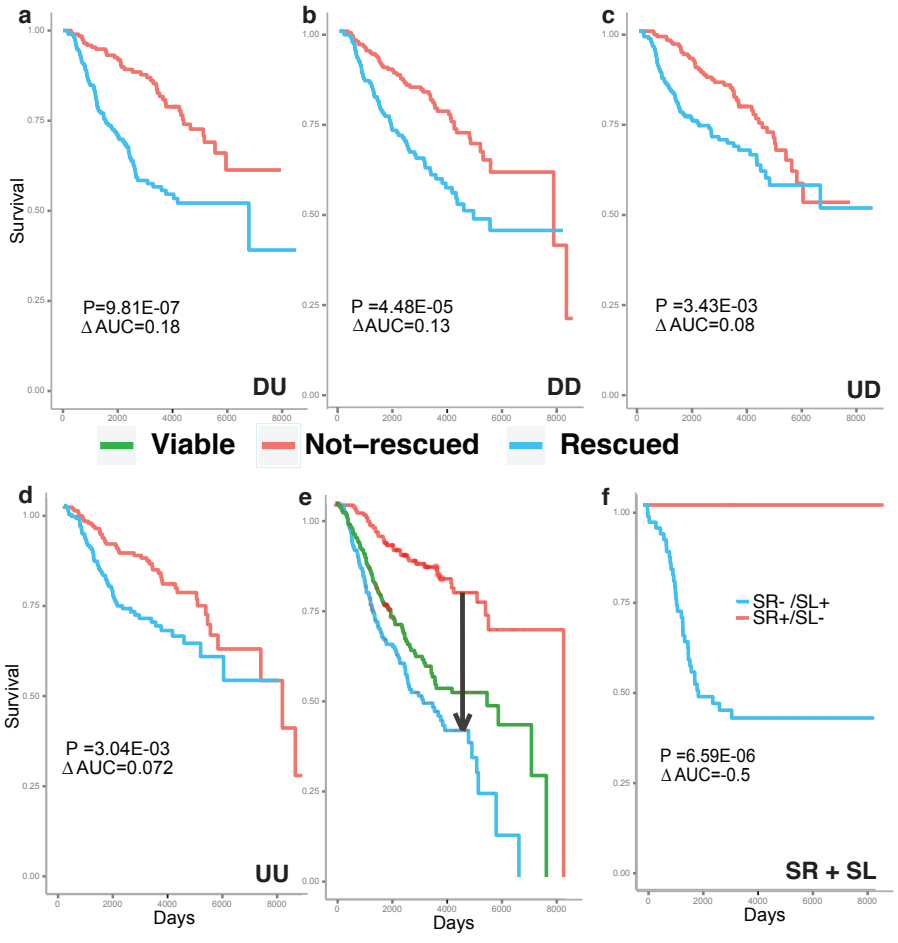
a
b
c
Survival
P=9.81E-07
ΔAUC=0.18
DU
P =4.48E-05
ΔAUC=0.13
DD
P =3.43E-03
ΔAUC=0.08
UD
Viable
Not−rescued
Rescued
d
e
f
Survival
P =3.04E-03
ΔAUC=0.072
UU
Days
Days
SR- /SL+
SR+/SL-
P =6.59E-06
ΔAUC=-0.5
SR + SL
Days

Figure 4.5: The four types of SR networks successfully predict cancer patients survival. (a-d) A Kaplan-Meier (KM) analysis comparing the survival of patients whose tumors have many rescued SRs (top 10 percentile (N=800), rescued) to those with the few (bottom 10 percentile (N=800), non-rescued). The difference in the areas under the curve between rescued (blue) and non-rescued (red) samples (δAUC) and their logrank p-values are denoted. (e) Patients with tumors having a large fraction of vulnerable genes that are not down-regulated (termed viable, green curve) have only intermediate levels of survival, less than those patients whose tumors are highly rescued. (f) Survival prediction by integrating both SL and SR networks. The subset of non-rescued patients in Figure 4.5a that also have many functionally active SLs (top 10 percentile (N=87); Appendix B) show remarkably better survival than the subset of rescued patients that also have few functionally active SLs (bottom 10 percentile (N=158)).

up-regulation of oncogenic rescuers. Indeed, by mining the data of carcinogenic agents and their targets [199, 200], we found that drugs that inhibit vulnerable partners of known oncogenes [189] are known to be carcinogenic (hypergeometric $P<0.03$, Appendix B). For instance, Lindane, which inhibits GLRB, is shown in the literature to be carcinogenic through the activation of RAS/MAPK/ERK pathway [201, 202] which in turn activates MDM2 [203, 204]. Nitric oxide, which targets guanylyl cyclase (GUCY1A2), is known to be closely associated with KRAS-driven tumorigenesis [203, 205]. These observations are consistent with our predictions of DU-SR interactions between GLRB and KRAS/MDM2 and between GUCY1A2 and KRAS, suggesting that screening for agents targeting vulnerable genes rescued by oncogenes may offer a new way for identifying carcinogens on a pan cancer, genome scale.

We next set out to experimentally test our SR predictions in vitro focusing on a subset of the predicted SRs involving mTOR, a major kinase regulating cancer growth and survival. We studied rSR and bSR predictions of the DD-SR type as they can be readily validated by in vitro knockdown (KD) experiments. Our investi-

gation was performed in a head and neck squamous cell carcinoma (HNSC) cell-line, where mTOR is known to be essential for cancer progression and its inhibition by Rapamycin interferes with cancer progression [206, 207] (also confirmed in our analysis, Wilcoxon rank-sum P < 4.5E-15, Appendix B). In difference from its overall effect, we hypothesized that when mTORs predicted vulnerable DD-SR partners are knocked down, Rapamycin treatment will not inhibit but induce cancer progression as per the DD definition (Extended Data Figure 1b). To test this predicted reversal of effect, we tested 10 (pan-cancer) DD-rSR pairs where mTOR is the predicted rescuer gene via shRNA knockdowns of the vulnerable partner gene followed by Rapamycin treatment (Methods). The KD of mTORs vulnerable partners hampers tumor proliferation both in an in vitro tissue culture (Paired Wilcoxon rank-sum P <1.3E-5) and in an in vivo mouse model (Paired Wilcoxon rank-sum P < 6.5E-6, see Appendix B). We observed a significant reversal effect of Rapamycin treatment on proliferation in 6 out of 10 vulnerable gene KDs (Figure 4.6a, aggregate Wilcoxon rank-sum P< 2.1E-8). The experiments testing the shRNA KD of five different sets of control (non-vulnerable) genes followed by mTOR treatment reassuringly failed to produce a significant rescue signal (see Figure 4.6a,b). A similar but less marked rescue effect is observed when mTOR is the vulnerable gene in DD-bSR interactions (Figure 4.6b, P<4.3E-4 across 9 predicted SR interactions), consistent with the observation of superior predictive power of rSR above. An experimental testing of the predicted HNSC-specific DD-type rescuers of mTOR yielded an additional validation of the predicted mTOR DD partners in an analogous manner (Extended Data Figure 5g, Methods).

As an additional validation test we investigated the extent to which SR interactions can provide a unified network-level account of transcriptome resistance signatures that have been published recently (Methods, Figure 4.6c). One prominent case involves resistance emerging to treatments targeting BET and AR; the predicted SR rescuers of the BET inhibitor (hypergeometric FDR P< 1.9E-5) and the AR inhibitor (FDR P< 5E-7) are enriched with Wnt signaling pathways, in line with recent reports [83, 84]. Further, we identified MYC as a common rescuer of BET and AR, which confirms its known association with the resistance to both AR and BET inhibition [84,171]. In another recently published case involving resistance to an EGFR inhibitor, the predicted SR rescuers are enriched with signaling pathways associated with the hepatocyte growth factor receptor (hypergeometric FDR P< 1E-3), including PI3KCA that has been associated with the resistance to EGFR inhibition [171]. A detailed description of this analysis is provided in Methods.

To test the utility of SRs in predicting emergence of resistance we analyzed longitudinal expression and sequencing data from tumors of 81 ovarian cancer patients (OC81 dataset), some of whom initially responded to drug treatment but later relapsed. The patients had been treated with two drugs: Taxane, which has 18 rescuer genes linked to 3 drug targets in the treatment specific DU-SR network, and Cisplatin (Figure 4.7a)16. We find a significantly higher expression of the 18 rescuer genes in initial non-responder versus responder patients (Wilcoxon rank-sum P<1.5E-4; expression and copy number alterations were significantly higher than those observed in randomly selected genes, empirical P<0.045; Extended Data Figure 5a). The SR network successfully predicts patient-specific gene activation al-

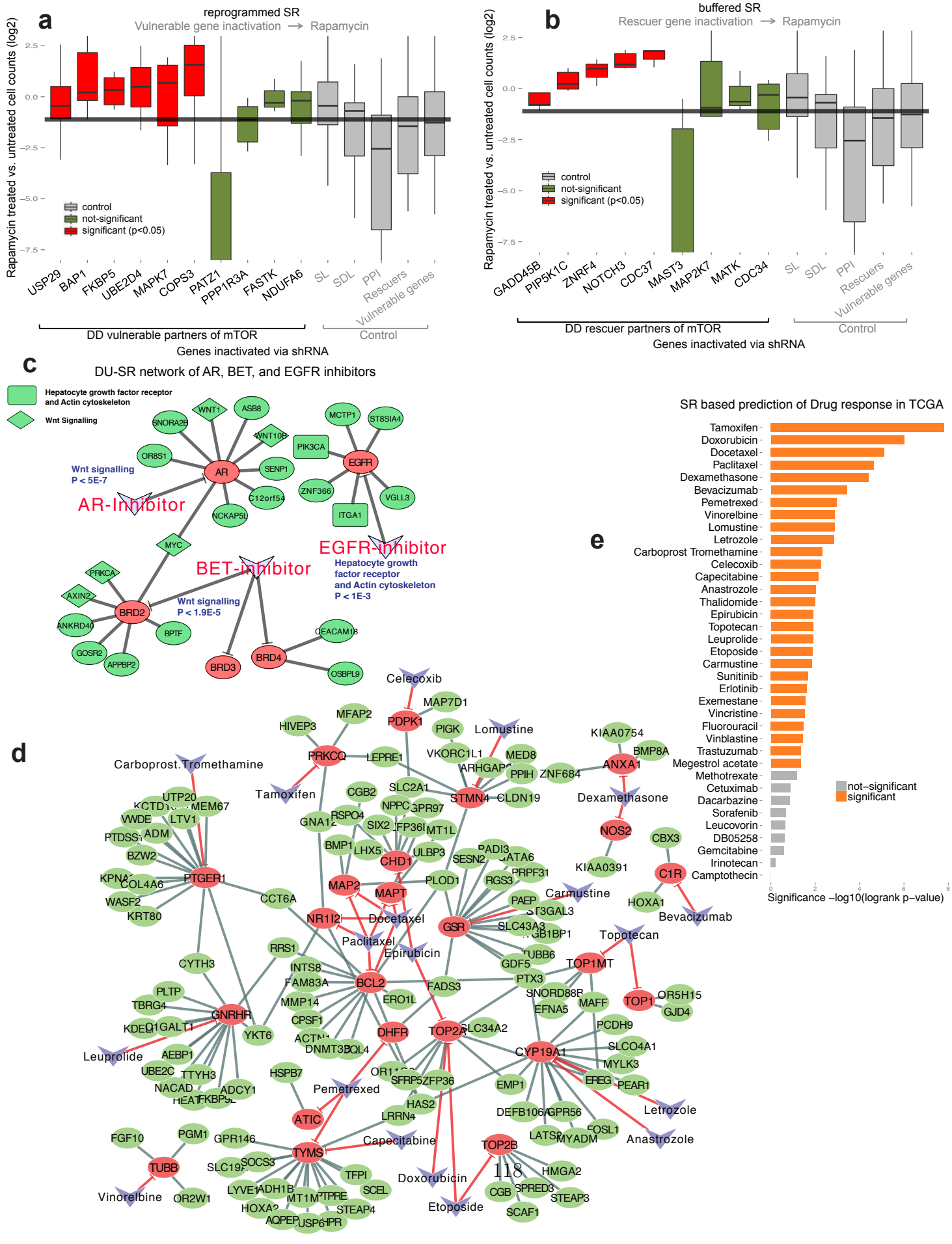
a
reprogrammed SR
Vulnerable gene inactivation → Rapamycin
Rapamycin treated vs. untreated cell counts (log2)
control
not-significant
significant (p<0.05)
USP29
BAP1
FKBP5
UBE2D4
MAPK7
COPS3
PATZ1
PPP1R3A
FASTK
NDUFA6
SL
SDL
PPI
Rescuers
Vulnerable genes
DD vulnerable partners of mTOR
Control
Genes inactivated via shRNA
b
buffered SR
Rescuer gene inactivation → Rapamycin
GADD45B
PIP5K1C
ZNRF4
NOTCH3
CDC37
MAST3
MAP2K7
MATK
CDC34
DD rescuer partners of mTOR
c
DU-SR network of AR, BET, and EGFR inhibitors
Hepatocyte growth factor receptor and Actin cytoskeleton
Wnt Signalling
Wnt signalling P < 5E-7
AR-Inhibitor
BET-inhibitor
EGFR-inhibitor
Hepatocyte growth factor receptor and Actin cytoskeleton P < 1E-3
Wnt signalling P < 1.9E-5
d
e
SR based prediction of Drug response in TCGA
Tamoxifen
Doxorubicin
Docetaxel
Paclitaxel
Dexamethasone
Bevacizumab
Pemetrexed
Vinorelbine
Lomustine
Letrozole
Carboprost Tromethamine
Celecoxib
Capecitabine
Anastrozole
Thalidomide
Epirubicin
Topotecan
Leuprolide
Etoposide
Carmustine
Sunitinib
Erlotinib
Exemestane
Vincristine
Fluorouracil
Vinblastine
Trastuzumab
Megestrol acetate
Methotrexate
Cetuximab
Dacarbazine
Sorafenib
Leucovorin
DB05258
Gemcitabine
Irinotecan
Camptothecin
not−significant
significant
Significance −log10(logrank p−value)
118

Figure 4.6: Experimental shRNA screening validates the predicted DD-SR rescue interactions involving mTOR in a head and neck cancer cell-line: Predicted DD-SR pairs involving mTOR both as (a) a rescuer gene and as (b) a vulnerable gene were tested (Methods). The vertical axis shows the cell count fold change in Rapamycin treated vs. untreated (i.e., in the rescued versus the non-rescued state), and the significance was quantified using one-sided Wilcoxon rank-sum test for three technical replicates with at least 2 independent shRNAs per each gene in each condition. Several sets of control genes (5 genes in each set that is total of 25 genes) that are not predicted as SR partners of mTOR were additionally knocked down and screened for comparison. These control sets include proteins known to physically interact with mTOR, computationally predicted SL and SDL partners of mTOR, predicted DD-SR vulnerable partners of non-mTOR genes, and DD-SR predicted rescuer partners of non-mTOR genes. The horizontal black line indicates the median effect of Rapamycin treatment in these controls as a reference point. Experiments were carried with at least 2 independent shRNAs for each gene of interest and controls. (c-e) The SR network successfully predicts the response to cancer drug treatments. (c) The SR network of a few cancer drugs whose resistance mechanisms were recently published (see text). The network includes the drug targets (red) and their rescuers (green). The rescuers are involved in Wnt signaling (diamond), and hepatocyte growth factor receptor and actin cytoskeleton (box). (d) The drug-DU-SR network includes 170 interactions between 36 cancer drug targets genes (red) and a 103 rescuer genes interacting with them (green). The drugs (purple) are linked to their targets. (e) Logrank p-values per drug denote how well treatment response (measured by survival) is predicted (KM plots for each drug are provided in Extended Data Figure 3).

terations after treatment, where patients that initially responded but then relapsed had increased rescuers activation in the relapsed tumors relative to the primary tumors (testified by gene expression and SCNA alterations, overall Wilcoxon rank-sum P< 5.8E-5, empirical P<4.0E-4; Figure 4.7b). Many but not every single rescuers show significant difference above, which may be at least partially due to the heterogeneity between and within tumors.

Remarkably, the rescuers gene expression at the pretreatment stage already provides a clear predictive signal for future emergence of resistance (AUC=0.77 for SVM predictor, P<2.2E-16, Extended Data Figure 5b, markedly superior to the predictive performance obtained using the predicted SL partners of these drug targets for this task (AUC=0.52, Extended Data Figure 5c)). The expression of the multidrug resistance (MDR) genes inversely correlates with the expression levels of the predicted rescuers in resistant samples (Spearman = -0.63 (P<0.03), Figure

4.7c), suggesting a complementary relationship between these two resistance mechanisms. A similar resistance prediction analysis of 155 primary breast cancer patients treated with Tamoxifen45 shows that the expression of 13 rescuers of Tamoxifens targets can significantly predict patient relapse also in this dataset (AUC=0.74, P <2.2 E-16, Extended Data Figure 5d).

4.5 Application of SR

Next we assessed whether SR interactions can help predict drug efficacy in a specific tumor based on the active SR partners of the drugs target. The original SR networks are based on highly stringent significance criteria and hence do not include many of the target genes of current cancer drugs. We hence applied INCISOR to build a drug-DU-SR network that includes a large number of drug targets and their rescuer genes by using lower significance cut-offs to select the interactions (though still highly significant after multiple hypotheses correction, see Methods and Figure 4.6d). We next used the drug-DU-SR network alongside with gene expression data from cancer patients to predict the response of 3873 patients (from the TCGA dataset) to 37 common anticancer drugs ($\geq$ 30 treated patients per drug). Specifically, patients with tumors having many up-regulated DU rescuers of a given drug target(s) were predicted as non-responder to that drug, and patients with just few such up-regulated rescuers were predicted as responders. By comparing our predictions to the actual patient survival data we confirmed that we correctly classified the patients to responders and non-responders in a significant manner for

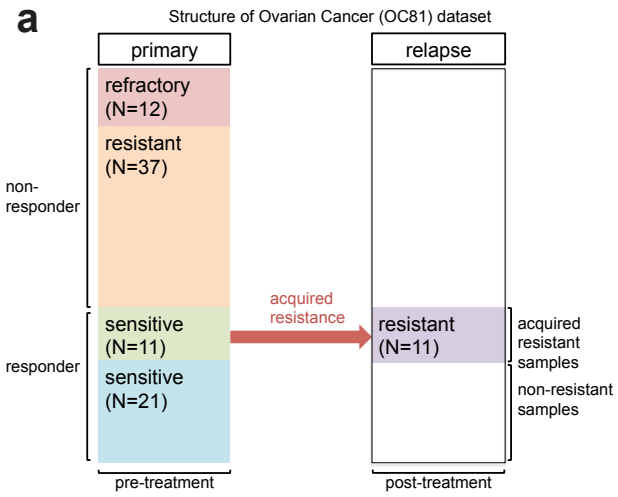
a
Structure of Ovarian Cancer (OC81) dataset
primary
relapse
refractory (N=12)
resistant (N=37)
non-responder
sensitive (N=11)
responder
sensitive (N=21)
acquired resistance
resistant (N=11)
acquired resistant samples
non-resistant samples
pre-treatment
post-treatment

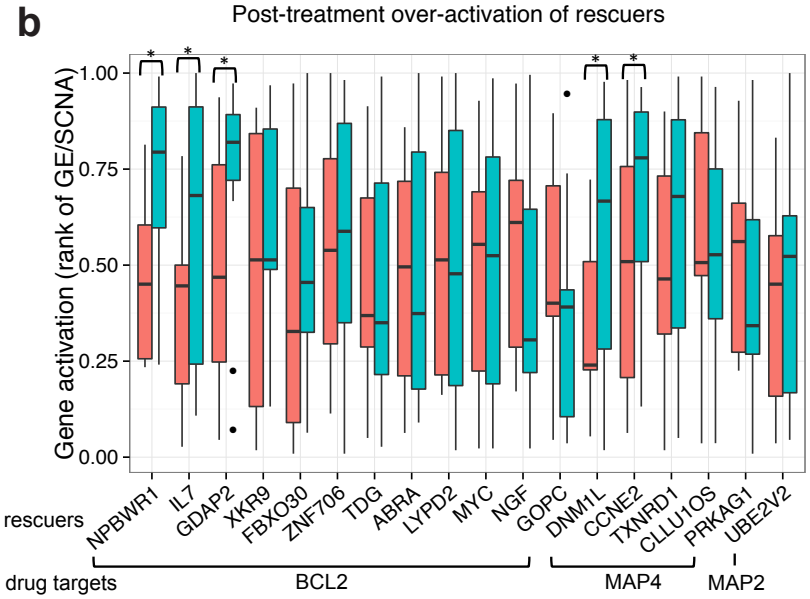
b
Post-treatment over-activation of rescuers
Gene activation (rank of GE/SCNA)
1.00
0.75
0.50
0.25
0.00
rescuers
NPBWR1
IL7
GDAP2
XKR9
FBXO30
ZNF706
TDG
ABRA
LYPD2
MYC
NGF
GOPC
DNM1L
CCNE2
TXNRD1
CLLU1OS
PRKAG1
UBE2V2
drug targets
BCL2
MAP4
MAP2

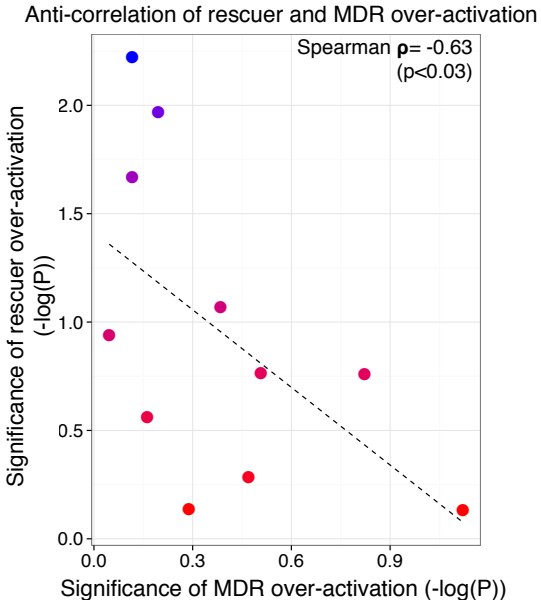
Anti-correlation of rescuer and MDR over-activation
c
Spearman ρ= -0.63
(p<0.03)
Significance of rescuer over-activation (-log(P))
2.0
1.5
1.0
0.5
0.0
0.0
0.3
0.6
0.9
Significance of MDR over-activation (-log(P))

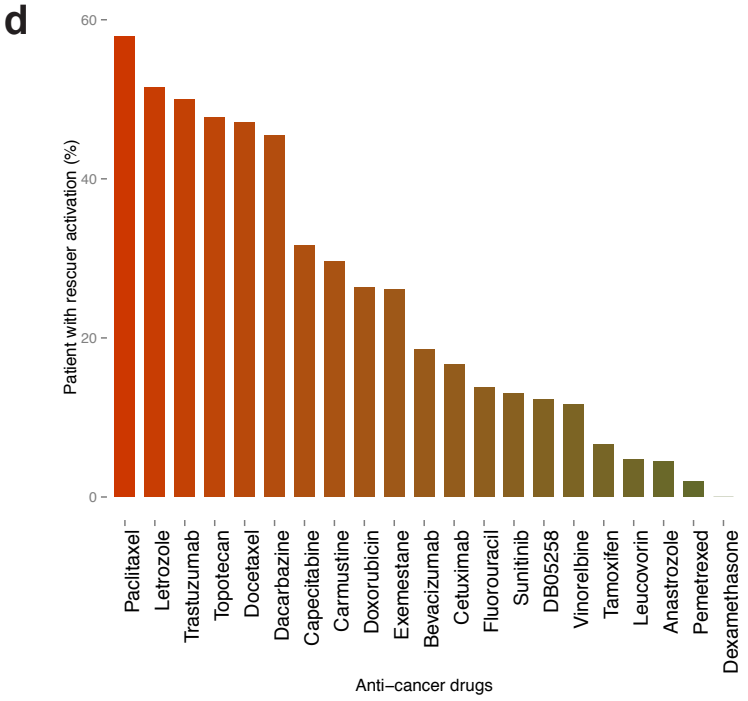
d
Patient with rescuer activation (%)
60
40
20
0
Paclitaxel
Letrozole
Trastuzumab
Topotecan
Docetaxel
Dacarbazine
Capecitabine
Carmustine
Doxorubicin
Exemestane
Bevacizumab
Cetuximab
Fluorouracil
Sunitinib
DB05258
Vinorelbine
Tamoxifen
Leucovorin
Anastrozole
Pemetrexed
Dexamethasone
Anti−cancer drugs

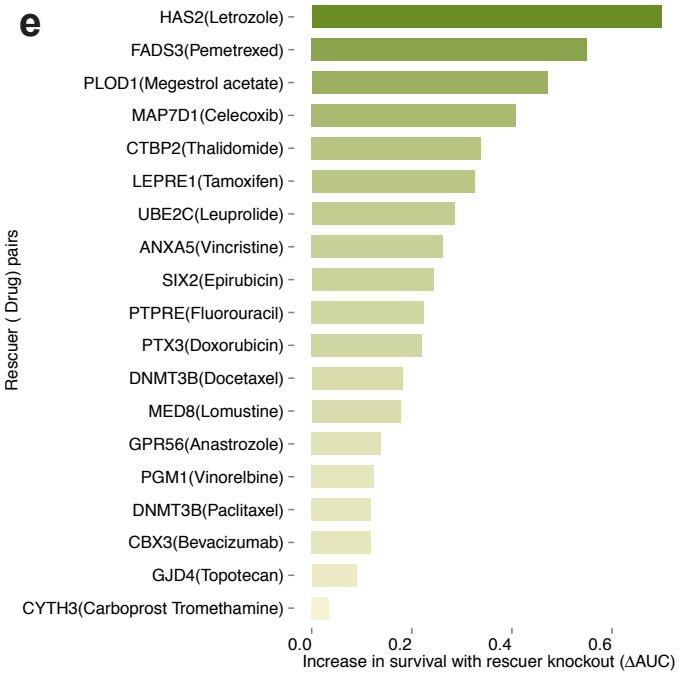
e
HAS2(Letrozole)
FADS3(Pemetrexed)
PLOD1(Megestrol acetate)
MAP7D1(Celecoxib)
CTBP2(Thalidomide)
LEPRE1(Tamoxifen)
UBE2C(Leuprolide)
ANXA5(Vincristine)
SIX2(Epirubicin)
PTPRE(Fluorouracil)
PTX3(Doxorubicin)
DNMT3B(Docetaxel)
MED8(Lomustine)
GPR56(Anastrozole)
PGM1(Vinorelbine)
DNMT3B(Paclitaxel)
CBX3(Bevacizumab)
GJD4(Topotecan)
CYTH3(Carboprost Tromethamine)
Rescuer (Drug) pairs
0.0
0.2
0.4
0.6
Increase in survival with rescuer knockout (ΔAUC)

Figure 4.7: The DU-SR network identifies key molecular alterations associated with tumor relapse after Taxane treatment. (a) The OC81 dataset includes gene expression, copy number, and mutational information for primary (N=81) and relapsed (N=11) tumors. The tumors were classified as refractory (N=12), resistant (N=37), and sensitive (N=32). (b) Post-treatment activation in the relapsed tumors (blue) of rescuer genes compared to their activation level in pre-treatment primary tumors (red) of the 11 patients. Significant genes are marked by stars (one-sided Wilcoxon rank-sum P¡0.05). (c) SR- (blue) and MDR- (red) mediated responses co-vary in the patients developing resistance to Taxane treatment in the 11 patients: The horizontal axis denotes the extent (-log10(one-sided Wilcoxon rank-sum P)) of post-treatment increase in MDR genes activation and the vertical axis represents the extent of post-treatment increase in the predicted rescuers activation (-log10(one-sided Wilcoxon rank-sum P)) (d) The likelihood of developing drug SR-mediated resistance following treatments. (e) The predicted clinical impact of rescuer gene down-regulation: Key rescuer genes and their corresponding drugs are listed on the vertical axis, and the survival increase associated with suppression of rescuer over-activation is presented on the horizontal axis. (d,e) are generated via an SR mediated data-driven analysis of the TCGA collection (see main text).

28 of the 37 drugs (Figure 4.63), a result that was reconfirmed in several additional datasets (see Appendix B).

To test the utility of SRs in predicting emergence of resistance we analyzed longitudinal expression and sequencing data from tumors of 81 ovarian cancer patients (OC81 dataset), some of whom initially responded to drug treatment but later relapsed. The patients had been treated with two drugs: Taxane, which has 18 rescuer genes linked to 3 drug targets in the treatment specific DU-SR network, and Cisplatin (Figure 4.7a) [179]. We find a significantly higher expression of the 18 rescuer genes in initial non-responder versus responder patients (Wilcoxon rank-sum P<1.5E-4; expression and copy number alterations were significantly higher than those observed in randomly selected genes, empirical P<0.045; Extended Data Figure 5a). The SR network successfully predicts patient-specific gene activation alterations after treatment, where patients that initially responded but then relapsed had increased rescuers activation in the relapsed tumors relative to the primary tumors (testified by gene expression and SCNA alterations, overall Wilcoxon rank-sum

P< 5.8E-5, empirical P<4.0E-4; Figure 4.7b). Many but not every single rescuers show significant difference above, which may be at least partially due to the heterogeneity between and within tumors.

Remarkably, the rescuers gene expression at the pretreatment stage already provides a clear predictive signal for future emergence of resistance (AUC=0.77 for SVM predictor, P<2.2E-16, Extended Data Figure 5b, markedly superior to the predictive performance obtained using the predicted SL partners of these drug targets for this task (AUC=0.52, Extended Data Figure 5c)). The expression of the multidrug resistance (MDR) genes inversely correlates with the expression levels of the predicted rescuers in resistant samples (Spearman = -0.63 (P<0.03), Figure 4.6c), suggesting a complementary relationship between these two resistance mechanisms. A similar resistance prediction analysis of 155 primary breast cancer patients treated with Tamoxifen45 shows that the expression of 13 rescuers of Tamoxifens targets can significantly predict patient relapse also in this dataset (AUC=0.74, P <2.2 E-16, Extended Data Figure 5d).

Uncovering cancer SR networks raises new treatment strategies options in which rescuer hubs can be targeted in a specific manner alongside traditional chemotherapy to enhance treatment response and counteract resistance. As a first step, by quantifying the number of samples in the TCGA dataset with rescued interactions among the patients that receive a specific drug, we provide estimates of the emergence of DU SR-mediated resistance following each current cancer treatment (Figure 4.7d, Methods). Interestingly, microtubule-destabilizing therapy (Vinorelbine) has a much lower likelihood of resistance emerging with rescuer activation than

microtubule-stabilizing therapies (Paclitaxel, Docetaxel). Next, we analyzed the TCGA collection and provide a list of cancer type-specific rescuer hubs (Appendix B Table 3), many of which have been already associated with resistance (see Appendix B). Interestingly, none of these predicted rescuer hubs are targeted by current anti-cancer therapies. We estimated the effect of targeting each of these key rescuer genes following specific contemporary cancer treatments on patient survival by comparing the survival time of the treated-patients with and without up-regulation of the DU rescuers (Figure 4.6e, Methods). Notably, a considerable fraction of the DU rescuers are housekeeping genes [208] (27.3%, hypergeometric $P<0.03$) and hence their complete inhibition is likely to have adverse side-effects. However, as they are up-regulated their rescue effect may be abolished by inhibiting their activation to moderate levels, potentially thus having lesser effects on healthy cells.

In summary, this work presents a new concept of synthetic rescue interactions in cancer, and a data-driven framework INCISOR for inferring genome-wide SR networks. We find that SR reprogramming is widespread across cancer types and is predictive of patient survival and drug response. Previous studies of cancer resistance to therapy have been typically conducted in a supervised manner by identifying gene signatures that differentiate between responders and non-responders, requiring exhaustive clinical studies. In difference, INCISOR is the first approach capable of predicting drug response and resistance utilizing the growing body of publicly available tumor data to this end in a universal and unsupervised manner. As we have shown, given the extent of SR interactions, resistance may potentially emerge due to alterations in any of the multiple alternative rescuers. The actual rescuers that

lead to resistance may vary across patients (or even within a heterogeneous tumor), calling for the integration of personalized tumor omics data with the SR networks to devise an optimal treatment [209]. Indeed, we show that the down regulation of specific individual rescuers of some specific drugs may have considerable clinical value. Ideally, on the longer run, one would strive to devise new drugs whose targets have as few rescuers as possible. Therefore, identifying SR interactions in cancer networks, which is likely to further improve with the incoming flux of cancer data sets, bears considerable future translational importance, mainly: (a) for assessing the likelihood that resistance will emerge; this is relevant both to optimizing the treatment of individual patients and for prioritizing new drug targets in specific cancer types, and (b) for targeting key rescuer genes in a new class of adjuvant cancer therapies aimed at counteracting resistance.

4.6 Additional Methods

4.6.1 Evaluating the predictive survival signal of the inferred SR networks

To evaluate the aggregate survival predictive signal of the pan-cancer SRs we applied INCISOR to pan-cancer TCGA samples (training set) to identify the SR pairs and tested their clinical significance in a completely independent METABRIC dataset (test set) to avoid potential risk of over-fitting, which includes the gene expression, SCNA, and survival of 1981 breast cancer patients. Based on the number

of functionally active SRs in each tumor sample, the top 10 percentile of samples were considered as rescued and the bottom 10 percentile as non-rescued. We then estimated the significance of improvement of survival in the rescued vs non-rescued samples using a logrank test.

4.6.2 Tracing the number of functionally active SR pairs in tumors during cancer progression

To study the functional activation of SRs as cancer progresses we divided the breast cancer patients in METABRIC dataset into 6 classes of cancer progression (removing censored data), by dividing them equally into 6 bins according to their survival times (N=627). First, in each bin, we counted the mean fraction of functionally active SRs. Such pairs are defined by the under-activation of the vulnerable gene and the over-activation of the rescuer gene, where the latter are determined based on their SCNA and gene expression values (Extended Data Figure 8g). Second, we defined a vulnerable gene as rescued if more than N number of rescuers are over-activated with the threshold N running from 0 to 4, and counted the mean fraction of rescued vulnerable genes in the six progression bins (Extended Data Figure 8h).

4.6.3 Identifying the clinical significance of reprogrammed SR and buffered SR

Using the cancer progression classes described above, we classified the DU SRs identified by INCISOR based on the relations of three frequency values: rescuer over-activation (fr), vulnerable gene inactivation (fv), and functional activation of SR (fSR). An SR pair is defined as reprogrammed SR (rSR) if the inactivity of the vulnerable gene A occurs first (in an earlier stage) and is followed by the over-activation of rescuer gene B (i.e., occurring in a later stage). Accordingly, we classified an SR pair as an rSR if fr and fSR are highly correlated while fv and fSR are not, and fSR increases as cancer progresses. Similarly, an SR was classified as buffered (bSR) when the over-activation of rescuer gene B precedes the inactivation of vulnerable gene A. We classified as an SR pair as a bSR if fv and fSR are highly correlated while fr and fSR are not, and fSR increases as cancer progresses.

4.6.4 The Cancer-Drug SR Network (drug-DU-SR) and predicting pan-cancer drug response

To show the utility of SR network in predicting drug resistance and response we constructed a cancer-drug DU SR network (drug-DU-SR) using pan-cancer TCGA data. Gene targets of 37 drugs that are included drug-DU-SR were identified using Drugbank database [210]. In identifying the original genome-wide DU-SR network, we have applied a very conservative criteria (FDR $< .01$ wherever applicable) at each

steps of INCISOR. As a result, the network contained only 2033 interactions (3.5E-4 % of all possible gene pairs), leaving out many potential rescuers of many drug targets. To capture DU-type rescuers of anti-cancer drug targets in a more comprehensive manner we modified INCISOR as follows: (i) Vulnerable gene screening was eliminated (because inhibition of the cancer drug targets that we studied are by definition known to hamper cancer progression) (ii) An FDR correction was applied only at the last step, and (iii) The SR significance P-value threshold were relaxed to accommodate weaker SR interactions. The resultant network drug-DU-SR includes the targets of most of the 37 cancer drugs that were administered to TCGA patients, encompassing 170 interactions between 36 vulnerable genes (drug targets) and 103 rescuer genes (Figure 4.6d). A pathway enrichment analysis shows that the rescuers are highly enriched with lipid storage/transport, thioester/fatty acid metabolism, and drug efflux transporters (Extended Data Figure 4.5g). Using the drug-DU-SR, we analyzed 3,873 TCGA patient samples that have been treated [197], including drugs that were used to treat at least 30 patients. For each drug tested, we divided the treated samples into rescued (predicted non-responders) and non-rescued (predicted responders) groups based on the number of over-active rescuers of the drug target genes in the drug-DU-SR network. We then analyzed patient survival data of treated patients to evaluate the predictive power of drug-DU-SR by comparing the decrease in survival in the rescued group compared to the non-rescued group using a logrank test (Figure 4.6e, Extended Data Figure 3).

4.6.5 Charting molecular mechanism underlying drug resistance using SR networks

We analyzed multiple drug response and resistance datasets where gene expression (and SCNA for limited cases) was measured from the patients treated with targeted therapy [175–178]. For each dataset we identified drug targets from Drugbank [210] and the rescuer genes were specifically inferred by applying the relaxed condition described above in the section The Cancer-Drug SR Network (drug-DU-SR) and predicting pan-cancer drug response to the specific treatment of interest. To check the over-activation of rescuers in post-treatment samples (relative to pre-treatment), we performed a paired one-sided Wilcoxon rank-sum test. To associate the over-activation of rescuers in non-responders (compared to responders) we first divided samples into rescued and not-rescued groups based on the number of over-active rescuers, and performed a one-sided Wilcoxon rank-sum test between the two groups. When information on patient survival is available (instead of drug response) we performed a logrank test between the two groups using progression free survival and/or overall survival. To predict emergence of resistance based on pre-treatment gene-expression (and/or SCNA) in an unsupervised manner, we divided the samples into predicted resistant and sensitive groups based on the number of over-activated rescuers in pre-treatment samples, and then performed a one-sided Wilcoxon rank-sum test. The supervised predictor was built using SVM with rescuer expression profile as input feature, and the accuracy of the supervised predictor was determined using cross validation. To compare the resistance arising from multidrug resistance

and synthetic rescues, we considered the post-treatment increase of gene activation level of the rescuer partners of the given drug targets with the gene expression levels of 12 MDR-associated genes [211] in relapsed tumors. To validate our SR network with the recent findings on pathways associated with the resistance of 4 different drug treatments (BET [83, 84], AR [170], EGFR [171] and BRAF [172] inhibitors), we first applied INCISOR to identify treatment-specific DU-SR rescuers. We then performed a pathway enrichment analysis of them, and observed that there are significant overlaps in the cellular processes to which these rescuers belong and the resistance gene sets reported in these studies. The details and additional analysis for each such dataset are provided in Appendix B.

4.6.6 Experimental analyses

We used Rapamycin because it is a highly specific mTOR inhibitor and hence enables targeting of a predicted rescuer gene by a highly specific drug, combined with the ability to knock down predicted vulnerable genes in a clinically-relevant lab setting. We used HNSC cell-line HN12, which, like most HNSC cells, is highly sensitive to Rapamycin [207]. For this we applied INCISOR to identify top 10 vulnerable partners and 9 rescuer partners of mTOR in a pan-cancer scale. We also identified HNSC-specific DD-type vulnerable partners of mTOR (see Appendix B for complete description).

We performed the shRNA knockout and mTOR inhibition in the following steps (Extended Data Figure 5f). Each of these mTORs vulnerable/rescuer part-

ners together with the controls were knocked down in HN12 cell lines, after which mTOR was inactivated via Rapamycin treatment. HN12 cells were infected with a library of retroviral barcoded shRNAs at a representation of 1,000 and a multiplicity of infection (MOI) of 1, including at least 2 independent shRNAs for each gene of interest and controls. 25 genes were included as controls (71 shRNA in total). At day 3 post infection cells were selected with puromycin for 3 days (1g/ml) to remove the minority of uninfected cells. After that, cells where expanded in culture for 3 days and then an initial population-doubling 0 (PD0) sample was taken. For in vitro testing, the cells were divided into 6 populations, 3 were kept as a control and 3 where treated with Rapamycin (100nM). Cells where propagated in the presence or not of drug for an additional 12 doublings before the final, PD13 sample was taken. For in vivo testing, cells were transplanted into the flanks of athymic nude mice (female, four to six weeks old, obtained from NCI/Frederick, MD), and when the tumor volume reached approximately 1cm3 (approximately 18 days after injection) tumors where isolated for genomic DNA extraction. Mice studies were carried out according to National Institutes of Health (NIH) approved protocols (ASP # 10569 and 13695) in compliance with the NIH Guide for the Care and Use of Laboratory Mice. shRNA barcode was PCR-recovered from genomic samples and samples sequenced to calculate abundance of the different shRNA probes. From these shRNA experiments, we obtained cell counts for each gene knock-down at the following three time points: (a) post shRNA infection (PD0, referred as initial count), (b) shRNA treatment followed by either Rapamycin treatment (PD13, referred as treated count, 3 replicates) or control (PD13, referred as untreated count,

3 replicates) (c) shRNA infected cell injected to mice (tumor, referred as in-vivo count, 2 replicates). To obtain normalized counts at each time point, cell counts of each shRNA at each time point were divided by corresponding total number of cell count. To estimate cell growth rate at treated, untreated and in vivo time points for each gene X, normalized counts were divided by initial normalized count as follow:

$$\text{growth rate}(\mathsf{X}) = \frac{\text{normalized count}(\mathsf{X})}{\text{initial normalized count}(\mathsf{X})} \tag{4.1}$$

Effect of Rapamycin treatment on cell growth on knockdown of gene X was calculated as:

$$\text{rapamycin effect}(\mathsf{X}) = \frac{\text{treated growth rate}(\mathsf{X})}{\text{mean treated growth rate}(\mathsf{X})} \tag{4.2}$$

To quantify the lethality of vulnerable knockdown, we performed a one-sided Wilcoxon rank-sum test between initial normalized count with in vivo normalized count for in vivo lethality (and with untreated normalized count for in vitro lethality). To compare rescue effect of Rapamycin treatment between shRNA knockdown of mTORs vulnerable gene partner and control gene knockdown, we performed a one-sided Wilcoxon rank-sum test between Rapamycin effects of mTOR partner vulnerable genes and control genes.

4.6.7 Predicting adjuvant therapy candidates for counteracting the emergence of resistance via DU-SR interactions

Down-regulating DU-SR rescuers provides a unique opportunity to mitigate drug-resistance. For each drug in TCGA collection, we first identified all DU-SR rescuer partners of its drug targets. We then investigated the impact of the down-regulation of these rescuers by comparing the survival of patients whose rescuer activation is low vs. high (using a logrank test) per each drug treatment. We selected the top rescuers of each drug that show the highest improvement in patient survival when inactivated, and reported 19 drug-rescuer pairs that have significant clinical impacts.

4.6.8 Estimating the likelihood of developing resistance to anti-cancer drug treatments via DU-SR interactions

The proportion of patients who have over-activated rescuers provides an estimate of likelihood of developing SR-mediated resistance. For 25 anti-cancer drugs, whose response is predictable by SR network, we estimated the drugs likelihood to develop resistance by the fraction of patients whose tumors harbor significantly over-activated DU-SR rescuers of the drug targets.

Chapter 5: Discussion and perspective

The presented thesis addresses emerging challenges in the improving detection and therapy of diseases, focusing on cardio-vascular diseases and cancer. To this end we developed novel computational methods for the integration of high-throughput data, and utilized them to study the genetic and molecular determinants of disease onset and drug resistance. The prediction of disease onset was accomplished, as described in Chapter 3., via a Bayesian integration of epigenetic and genetic data that enable the prediction of regulatory elements in genome and in turn the regulatory variants that drive transcriptome variations. The prediction of drug resistance in cancer was accomplished by proposing and identifying a novel type of gene interaction, synthetic rescue.

The first part of the thesis begins with the presentation of a simple scheme to improve association studies. The scheme was further extended and leveraged in a Bayesian framework in Chapter 3 that significantly improved the association studies. The second part of the thesis, in order to understand cancer-drug-resistance, defined synthetic rescue gene interactions and proposed a data driven approach, INCISOR, to identify the interactions. It concludes with presenting an array of translation applications of synthetic rescue.

Below we provide in details discussion and future perspective of these parts of the thesis.

5.1 Discussion

5.1.1 Association studies

In Chapter 3, we introduce a novel Bayesian approach, eQTeL, that integrates genetic and epigenetic data in a statistically consistent manner to identify putatively causal genetic variants underlying the expression variance. We have shown that (i) eQTeL identifies combinations of SNPs (eeSNPs) that, compared to other methods, explain substantially greater portion of expression variability, (ii) eQTeL is especially effective in identifying SNPs with small effect sizes, (iii) 58% of the identified eeSNPs are likely to be causal, (iv) eeSNPs can predict sample specific expression much more accurately, (v) eeSNPs are much more likely to be bound by a regulatory factor in an allele-specific manner, (vi) eeSNPs preferentially disrupt core cardiac transcription factor binding, and (vii) eeSNPs tend to be spatially proximal to their target genes. Taken together, our results strongly suggest that eQTeL captures a substantial proportion of putative causal regulatory genetic determinants underlying transcriptomic variance.

It is important to note limitations of eQTeL. First, eQTeL can only detect cis-eQTL and not trans-eQTL. Second, like other model-based association methods, eQTeL's computational speed is a bottleneck; however, using parallel cores and cer-

tain reasonable compromises in parameter estimation procedure, the computational burden can be substantially reduced. Third, eQTeL assumes normality of expression data, therefore the expression data needs to be pre-processed accordingly, which can be particularly problematic for certain kinds of high throughput data. Fourth, eQTeL can only detect SNPs with small effect sizes if they have high regulatory potential. Finally, eQTeL statistically infers the potentially causal SNPs and further experimental validations are required to establish causality.

eQTeL can effectively resolve LD and discriminate putative regulatory SNPs from myriad associated SNPs. This lays a foundation for future experimental studies to characterize genetic variants underlying disease risk. Finally, eQTeL can be extended by integrating additional layer of molecular data – easily achieved in Bayesian framework – to directly infer SNPs that cause disease.

5.1.2 Synthetic rescue in cancer

In Chapter 4 we introduce and rigorously define a new concept of synthetic rescue reprogramming occurring in cancer. We developed INCISOR, a data-driven framework to infer genome-wide SR networks. We extensively studied evolutionary properties of SR pertaining to cancer. Our study reveals that cellular reprogramming is widespread across cancer types, shows significant clinical importance and is associated with patient survival, drug sensitivity and emergence of resistance.

SR provides multiple therapeutic opportunities. The functional activity of SL and SR networks determines tumor aggressiveness and patient survival. We

demonstrated that the clinical impact of the combined SR and SL networks is more significant than their individual impacts (Figure 4.5f). The SL network provides information on the selectivity and efficacy of a given drug [71]. On the other hand, the SR network provides complementary information on the likelihood to incur resistance. Combining SL and SR networks, we can predict a drug that has the highest efficacy/selectivity and lowest chance of developing resistance.

SR reprogramming can be used to develop two novel classes of sequential treatment regimens of anticancer therapies. First, almost all cancer patients who initially respond to a drug, have the potential to develop resistance to the treatment and experience tumor relapse. Currently, we do not have the ability to access and prepare for the second line of treatment for the relapsed tumors, till it happens to the patients, which is often too late. SR provides a way to infer, together with pretreatment expression screening, whether resistance will emerge quickly and, more importantly, the possible mechanisms of the emergence of resistance and how they can be mitigated by subsequent treatments (as demonstrated in Figure 4.7d). Therefore, SR can guide decisions on the second line of action without biopsies from the relapsed tumors.

Second, some of the gene-targeting drugs are known to be more efficient and effective in treating cancer (eg. kinase inhibitors) than other drugs, provided tumors are homogeneously addicted to the target gene. In such a scenario, using concept of SR reprogramming, it is possible to first induce homogeneous addiction to such targetable genes by first targeting vulnerable partner of the targetable gene. In order to survive the cell will over-activate the targetable genes which will lead to oncogenic

(or non-oncogenic) addiction. In the second line of treatment, the targetable gene can be targeted to eradicate the homogeneously addicted tumor population, thus efficiently treating cancer.

INCISOR has limitations arising from the scarcity of available data, the specific design of the pipeline, and the diverse mechanisms of the emergence of drug resistance. It is well-known that many genes are correlated based on their expression and the proximal genes have correlated SCNA values, which make it difficult to identify the true rescuers from spurious ones. INCISOR mitigates some of these problems by selecting pairs only when they are supported by both gene expression and SCNA, however, it may not completely resolve this issue. INCISOR is also based on patient survival data, which is known to be noisy. INCISOR does not incorporate other genetic, epigenetic and post-transcriptional mechanism of gene inactivation partly due to the unavailability of these data for cancer patients.

INCISOR is designed to identify the rescuer genes for targeted therapies, so it cannot be used to predict drug response/resistance analysis for non-targeted therapies such as generic chemotherapy (e.g. Cisplatin). By definition, SR reprogramming events are context-specific to a cancer type or a sub-type. Our pancancer SR network focuses on the generic SR interactions that are prevalent across multiple cancer types, and the same pipeline can be applied to specific cancer types or sub-types as presented in the main text and Supplementary Information for specific cancer types and subtypes.

It must be noted that resistance does not always emerge due to SR reprogramming. This is because there are multiple mechanisms for development of resistance

including drug efflux via multi-drug resistance mechanism or the modification of drug target that makes drug ineffective. We nonetheless note that SR interactions are so widespread in multiple cancers that they are highly likely to be a contributing factor. Our analysis shows that only a small subset of SR interactions are mediated by physical contacts, and further studies are needed to identify the mechanism of SR reprogramming in giving rise to drug resistance.

We expect the fast growth of the publically available omics/survival patient data, both within the TCGA collection and beyond would help us designing a better pipeline and improving our identification of the SR interactions, and lead to a deeper understanding of their mechanism in a context-specific manner.

It is necessary to be aware of the difference between SL and SR. First, as revealed in Extended Figure 1a-e, their molecular states are different. In SR, the inactivation of the vulnerable gene is lethal, only over-activation of rescuers retains the cell viability under the condition (i.e. normal expression level is not enough to rescue the cell). However, in SL, the inactivation of one of the SL partners is not lethal unless the other partner is inactivated (i.e. normal expression level does not lead to a lethal state). In other words, the inactivation of a vulnerable gene is in general lethal in SR, unless it is rescued, but the inactivation of a single gene is not lethal in SL pairs. In our analysis we made a clear distinction between SL and SR. In ovarian and breast cancer analysis, the activation profile of SL partners of the drug target genes have poor predictive potential for tumor relapse (Extended Data Figure 5c), while over-activation profile of rescuers show great predictive potential (Extended Data Figure 5b,d). Also, the predictive power for drug response is sig-

nificantly reduced if a vulnerable gene is defined rescued when its rescuer partner is not over-activated but only normally activated (Extended Data Figure 2f).

Second, in SL, if any two partner genes are both inactive, it will be lethal irrespective of activity of any other genes. But in SR, the inactivation of a rescuer partner of a vulnerable gene does not guarantee lethality because an alternative rescuer may have been over-activated to rescue the cell. Third, while SL has two cellular states of viable and lethal; SR have additional third state rescued, where cancer is often more aggressive than in both viable and lethal states (see Figure 4.5e). Fourth, both SL and SR may play roles in determining effectiveness of cancer therapy. In SL, targeted treatments, which inactivate one of the SL partners, lead to the activation of the other partner from inactive state to escape conditional lethality. On the other hand in SR, in response to the inactivation of the vulnerable gene due to targeted therapies, a cancer cell rewires the pathways associated with the targeted cellular function by changing wild-type activity of its rescuer gene (to over-active or inactive state) to escape lethality. In sum, SL is an inherent property of the system, but SR is an adaptive cellular response, where cells reprogram their molecular activity state to evade lethality.

These differences have therapeutic implications. Unlike SL, therapy based on SR is likely to be used only in combination with other primary therapies. While SL-based therapy can selectively kill cancer cells, SR based therapy, on other hand, may not be selective. However, if the primary therapy is selective and SR interaction is highly synergistic (implying selectivity), then the combined therapy will be also selective.

The inference from SL and SR can be combined to identify drugs that target cancer cells (and not normal cells) and that are not likely to develop resistance (as shown in Fig. 4.5). In particular, SL gene pairs with no rescuers would be best drug targets.

Our analysis reveals a frightening aspect of SR reprogramming, namely that critical vulnerable genes for cancer progression have not one but multiple rescuers, implying the presence of multiple ways of developing resistance. Thus, targeting a single rescuer may not be enough. This has been already known in the case of Lapatinib resistance, where ERBB3 over-expression leads to resistance but inhibiting ERBB3 can be overcome by over-expression of other kinases. Many patients that go through sequential treatments, where each treatment targets a new gene, show initial response; however cancer relapse after every treatment might be due to the fact that many of target genes have multiple rescuers. In this light, it is necessary to chart a complete SR network to avoid emergence of resistance by focusing on drug targets that have little chance of being rescued (a limited number of rescuers).

Synthetic rescue reprogramming has a considerable translational importance. Targeting the rescuer hubs can offer a new class of treatments for adjuvant cancer therapies aimed at counteracting resistance and may also be efficient in treating heterogeneous tumor cells. This is because targeting rescuer hubs makes cancer cells vulnerable to the inactivation of different vulnerable genes. Alternatively, vulnerable genes with few or no rescuer can be important drug targets because targeting such genes would be least likely to evolve resistance due to SR reprogramming. Further, the probability of a new drug to develop resistance can be efficiently eval-

uated using SR, which will significantly reduce the time and cost of clinical trials or enable to assess long-term effect of a drug, which is often impossible. Finally, SR reprogramming can predict mechanism of emerging resistance using pre-treatment gene expression. By periodically monitoring patients gene expression, we can predict when resistance will emerge, and accordingly develop a sequential regimen for patients.

SR reprogramming can contribute to precision and personalized cancer medicine in the following manner: (i) ranking drugs by its likelihood to develop resistance, (ii) recommending a drug for patients based on their gene expression before treatment, (iii) predicting (aggressiveness of) emerging resistance in patients, time of relapse and second line of action (iv) drug-repurposing to target rescuer hubs or vulnerable genes that have no rescuer. (v) identifying new drugs that target rescuer hubs and can lead to development of a new class of anti-resistance drugs. (vi) SR network can be combined with SL prediction to identify drugs that only target cancer cells and at the same time are unlikely to develop resistance.

5.2 Perspective

We conclude the thesis by placing it in a wider academic perspective, and exploring some unresolved questions. Finally, we point out potential follow up and new exciting projects that emerged from the thesis but are beyond the scope of this work.

In Chapter 4, at the regulatory mechanism level, eQTeL uncovers genetic

regulatory network that controls gene expression in cells. Specifically, it provides genomic regions that regulate the genes such that a variation within one of the regions changes the expression of its target. The analysis also reveals many of the regulatory elements are far away from its target, pointing out that most of the variation that causes transcriptomic changes are distal regulators.

Because some of the identified SNPs are common in the population, the analysis suggests that these genomic variations are not deleterious (since they can accumulate in the population). The expression variance associated with this set of genomic variation also does not manifest into deleterious phenotypes.

Our analysis in Chapter 4 provides a basis to find contributions of each epigenetic factor in regulatory element. In particular, whether presence of an epigenetic factor activates regulators (in turn having activating effect on expression of target genes), or in-activates them. Thus the framework can be used to identify marker of different regulatory elements and also their functional characterizations.

The human heart data (MAGNet) is composed of data for individuals with and without heart failure, therefore a major portion of expression variance in the samples will be due to heart failure. Consequently, the identified genomic variants by eQTeL that explain the major portion of expression variance will explain a portion of phenotypic variance due to heart failure. Thus, these variants will be associated with cardiovascular disease risk to a large extent. Importantly, identified variants are likely to be causal in expression regulation, and thus they are likely to be causal with regards to cardio-vascular disease risk as well.

eQTeL is important from a translational point of view, because it not only

provides regulatory variants, but also identifies specific genes that are highly disrupted by the regulatory variants. This gives us an opportunity to devise therapies in a personalized manner. For example, if a eeSNP over-expresses its target gene in a cardio-vascular patient, targeting the gene by an inhibitory drug may mitigate the risk of the heart failure. eQTeL also provides epigenetic and regulatory mediators thus providing additional means to mitigate the risk by targeting those mediators.

In Chapter 5 we introduce a concept of synthetic rescues that dictates extensive cellular reprogramming in tumors. Our analysis also reveals that multiple types of SR participate in the reprogramming. As cancer advances, synthetic rescuing becomes increasingly rampant. This indicates that cancer cells become increasingly refractory, confirming Darwinian kind of evolution of cancer cells in tumors. Tumors undergo gradual but extensive cellular reprogramming, each conferring additional advantage to cancer in terms of proliferation and viability in the event of external onslaughts.

Synthetic rescues will change the current paradigm of how anti-cancer interventions are devised. It illustrates at molecular level how resistance to a therapy emerges in a cell. Synthetic rescuing plays the role of a double-edged sword for cancer cells because it not only develops additional refractoriness, but also develops many additional vulnerabilities that can be capitalized on for cancer therapies against resistance.

For instance, if a kinase is a (DU) rescuer of a vulnerable gene, inhibiting vulnerable gene in cells will not only over-express the kinase, but also will make the cells addicted to the kinase. Targeting such kinases with our repertoire of available

kinase inhibitors will efficiently eliminate the cancer cells. Thus SR raises very promising therapeutic possibilities.

From a computational point of view, the thesis demonstrates that Bayesian approaches can be used to integrate diverse set of data in a statistically consistent manner. eQTeL harnessed two advantages of Bayesian approaches : (i) seamless integration of different type of data through belief propagation, and (ii) developing bottom-up computational framework that can leverage known mechanisms and hierarchies of information flow.

Therefore the approaches are ideally suited to tackle myriad of biological datasets that are being generated with ever increasing pace and building computational framework to obtain superior inferences.

The thesis also proposes simple means to control various confounding factors in statistical tests. These include controlling cancer type confounders in Kaplan-Meier survival analyses. Such simple techniques can also be utilized and extended to remove confounding factors in many of published genomic studies.

5.2.1 Alternatives

There is a number of ways the proposed methods can be improved. for instance, a Bayesian approach in INCISOR will significantly improve the SR prediction algorithm. Another elegant alternative to Kaplan-Meier analysis used in INCISOR is Cox regression, which resolves the issue of individual gene effect to uncover genetic interactions. In SR analysis, the emphasis was on introducing the concept of

synthetic rescues and consequently we choose to sacrifice elegance over simplicity of the method used in INCISOR.

Bayesian approach used in eQTeL needs a complicated and computationally intense algorithm. In case of eQTeL, an alternative approach that can be used for data integration is a simple empirical approach. In fact, it was employed in the initial phase, showing superior performance over than existing association methods. However, the performance of empirical approach was inferior with respect to eQTeL (refer to Appendix A).

5.2.2 Unresolved question

The analyses in the presented thesis opened up some interesting, yet unanswered questions that require further follow up analyses:

- In enrichment analysis of eeSNP in section 3.10, regions around eeSNPs were enriched with two types of transcription factor motifs: (i) core-cardiac motifs and (ii) enhancer specific motifs. However, only core-cardiac TFs were preferentially disrupted by eeSNP and not enhancer specific TFs. This indicates the possibility that enhancer specific motifs are avoided by regulatory SNPs. The landscape of transcription is enriched with regulatory variants and it is currently unexplored which ones among them are disrupted by regulatory variants. The variation of the landscape across different tissues and other disease might be an interesting direction to pursue.

- In SR analyses, we identified many genes that have multiple rescuers. A

natural question that arises in such cases is if activation of any single rescuer suffices for the rescue, or the rescue occurs with collective over-expression of all rescuers. The rescue behavior may be variable across genes; for certain genes the rescue may occur by over-expression of any rescuer and for others over-expression of multiple rescuers may be required. For instance, genes with multiple functions require all their functions to be rescued to promote cell viability (see chap 4).

- Another intriguing question that was raised with our analyses is based on cancer heterogeneity. Our analyses suggest that resistance landscape is quite heterogeneous and resistance to a drug can arise through multiple routes. There is large variation among patients in terms of molecular causes of resistance. Does the variance of resistance mechanism also tranlate into tumors due to heterogeneity? Does a different set of cell activates a different set of rescuers to avoid lethality due to the inactivation of the same gene?

5.2.3 Potential follow up and new project

The thesis opens up and provides a basis for several new research directions. We are currently pursuing some of them.

- **Extending eQTeL to GWAS** eQTeL model can be easily extended to GWAS. Based on the causal SNPs identified by eQTeL a hierarchical model can be developed for genotype-phenotype relationship that includes additional layers corresponding to gene expression and biological pathways mediating the

genotype-phenotype relationships.

- **Drug response prediction by eQTeL** Tissue specific predicted transcriptome by eQTeL can be harnessed to predict drug efficacy in a personalized manner. Using eQTeL tissue specific expression before and after drug treatment can be predicted for each individual. Relating the pre and post-treatment transcriptome to phenotype [212], drug efficacy can be evaluated in a personalized manner.

- **Predicting anti-biotic/anti-microbial resistance by synthetic rescue** Emerging microbial resistance to antibiotics is as a serious challenge in the effective prevention and treatment of infections caused by microbes including bacteria, viruses and fungi. It is already proving to be a serious menace and expected to keep growing rapidly in the next decade, poseing a serious challenge to all nations. In 2014, alarming increase in resistance cases to HIV drugs were also reported [82].

  Applying INCISOR to a large dataset of bacterial transcriptome data, we will be able to predict synthetic rescue landscape specific to the infectious bacteria. Similarly to cancer, this will enable us to predict molecular mechanisms of emergence of antibiotics resistance.

- **Devising new targeted cancer therapies by estimating clinical essentiality of a gene** One of the popular approaches of precision oncology [213] is mouse transgenics. Tumor samples from a patient are first inserted into immuniodeficient transgenic mice and then treated with an array of anti-cancer

drugs, finally recommendation is provided to the patient based on the drug response in the mice. There are multiple shortcoming of these approache, including the fact that mice are immunodeficient and conclusion in mice does not translate to human patients completely. A major limitations is also it takes around 6 months to get back a recommendation.

The analysis of estimating SR activation on patient's survival (section 4.5) can be simplified to identify genes that are essential for cancer progression in patients (i.e whose independent inhibition improves patient survival). Thus it provides an alternative to mouse transgenic precision oncology with added advantages: (i) the effects are predicted directly in clinics and (ii) much faster prediction (compared to transgenic mice that takes around six months).

- **Carcinogen identification**: Our SR analysis in section 4.4 suggests that carcinogenicity of many agents are mediated by synthetic rescues. Given our SR network, not only we can detect mechanism of carcinogenicity of existing carcinogens, but also discover unknown carcinogenic agents (or estimate risk of a chemical to show long term carcinogenic effect in an unbiased manner).

- **Genetic interaction**: Until now, including in the presented work, the spotlight was focused on three types of genetic interaction(SL, SDL, SR), however the genetic perturbations that rewire the complex molecular networks toward malignancy are likely to involve other types of GIs that are waiting to be discovered. In the context of cancer as a competing population of autonomous cells, the emergence of beneficial novel GIs leading to greater fitness during

cancer evolution is highly plausible and indeed expected. There are potentially 512 different types of additional interactions! Clearly, many of those are probably infrequent and have no functional role, but it is likely that several new GI types, which have not yet been even defined, let alone searched for, may play a critical role in cancer.

A statistical approach similar to INCISOR can be used to identify other patterns. However, there are many challenges remaining in the identification of all possible genetic interactions including:

1. Multiple hypothesis correction testing becomes complicated.
2. It is difficult to control for individual gene effect.
3. It is not clear how to assign a pair to the best gene interaction pattern. In such case maximum likelihood approaches might be required for the model selection.
4. It will be hard to biologically interpret many of the genetic interaction patterns.

- **Experimental method of inducing gene inhibition indirectly**: Our SR analysis suggests that if a pair of genes have SR-DD interaction, inhibiting the vulnerable gene will inhibit the rescuer. Therefore, genes which are not efficiently inhibited by existing experimental technologies, call for SR-DD based experimental methods to be indirectly inhibited.

Appendix

Appendix A: Bayesian integration of genetics and epigenetics detects causal regulatory SNPs underlying expression variability

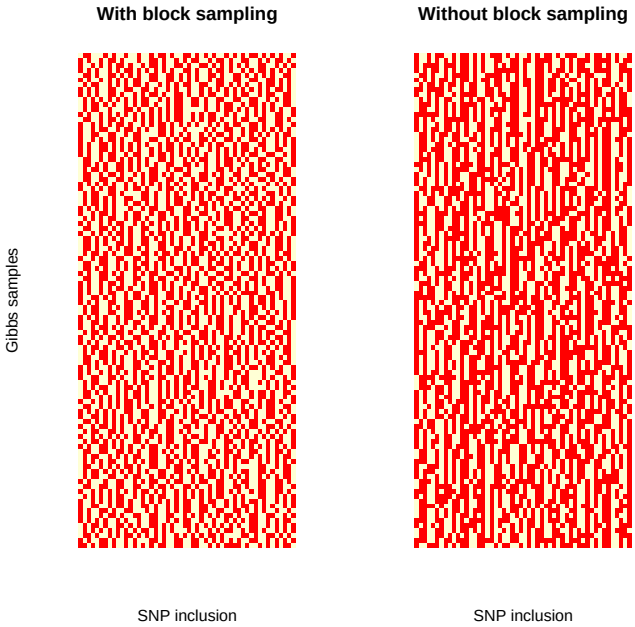

Figure A.1: Mixing rate of eQTeL with and without block sampler. (Note: regulatory and interaction priors were removed for this exposition). The block sampler leverages information of Linkage disequilibrium (LD) blocks to choose sparse set of SNPs within each LD block. In the current example, there are two (identical) SNPs within each LD block. The sampler without block sampler are more often stuck at previously selected SNPs in consecutive MCMC iterations compared to the block sampler. This problem will exponentially increase with growing number of SNPs in LD block. On the other hand, block sampler chooses subset of SNPs with a LD from their full posterior distribution in each iteration independently using a MH sampler. Relatively higher number of combinations of SNPs will be explored by block sampler. The block sampler chooses comparatively better subset of SNPs since it explores relatively larger fraction of the model space.

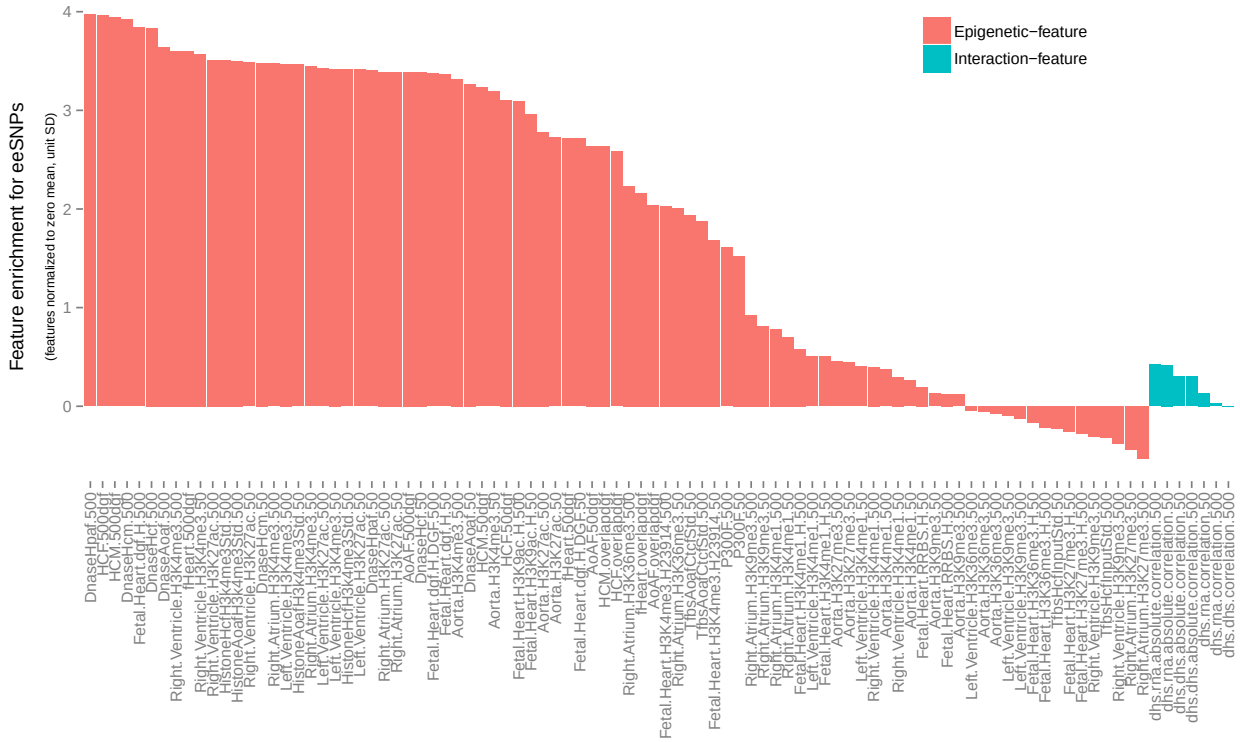

Figure A.2: Feature-analysis: Significant features ($p - value < 10^{-6}$) are sorted by their enrichment in eeSNPs relative to random SNPs (Note: features are not independent). Lists the epigenetic and

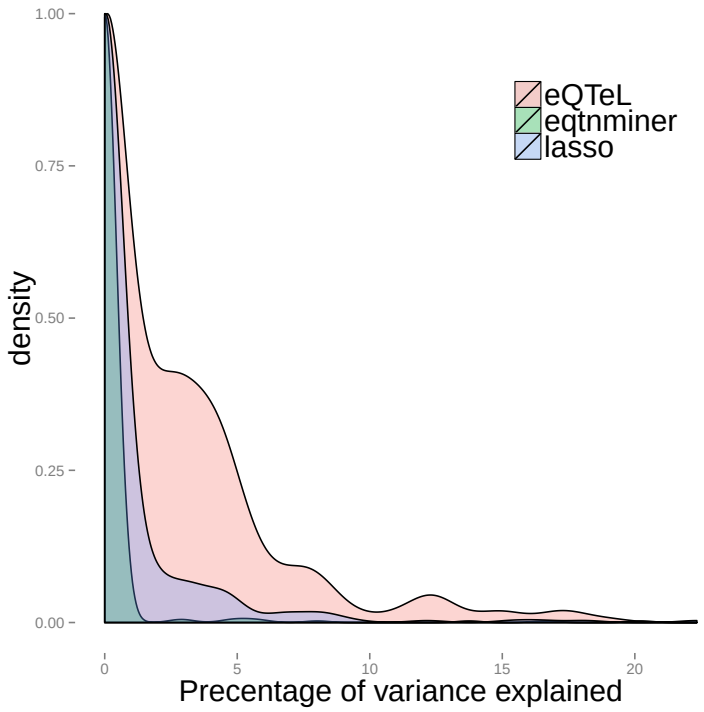

Figure A.3: Validation of eeSNPs in GTEx: Comparative performance of SNPs detected by eQTeL, LASSO and eqtnminer in terms of explained variance. Number of SNPs were controlled for each method (as in Fig 2). SNPs from eQTeL were selected using posterior probability > 0.5. The figure shows (5 fold) cross-validated explained variance and correlation between predicted expression using alleles of identified SNPs for each methods.

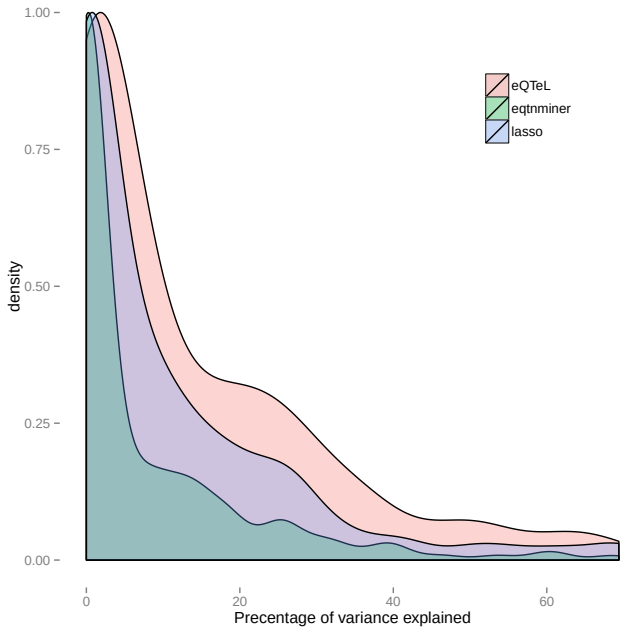

Figure A.4: Comparative performance of eQTeL in terms of explained variance in simulated data: Number of SNPs were controlled for each method (as in Fig 2). SNPs from eQTeL were selected using posterior probability > 0.5. SNPs from eQTeL were identified with posterior probability > 0.5. The figure shows (10 fold) cross-validated explained variance for each method.

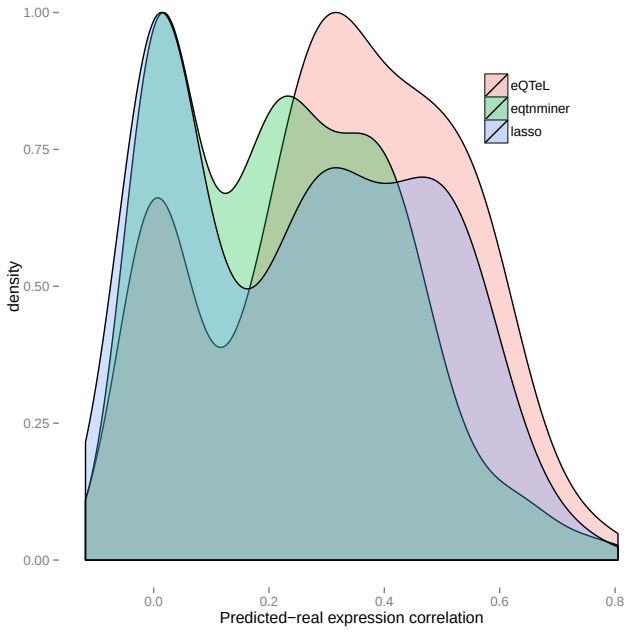

Figure A.5: Comparative performance of eQTeL in terms of expression predictability in simulated data: Number of SNPs were controlled for each method (as in Fig 2). SNPs from eQTeL were selected using posterior probability > 0.5. The figure shows (10 fold) cross-validated correlation between predicted expression using alleles of identified SNPs for each method.

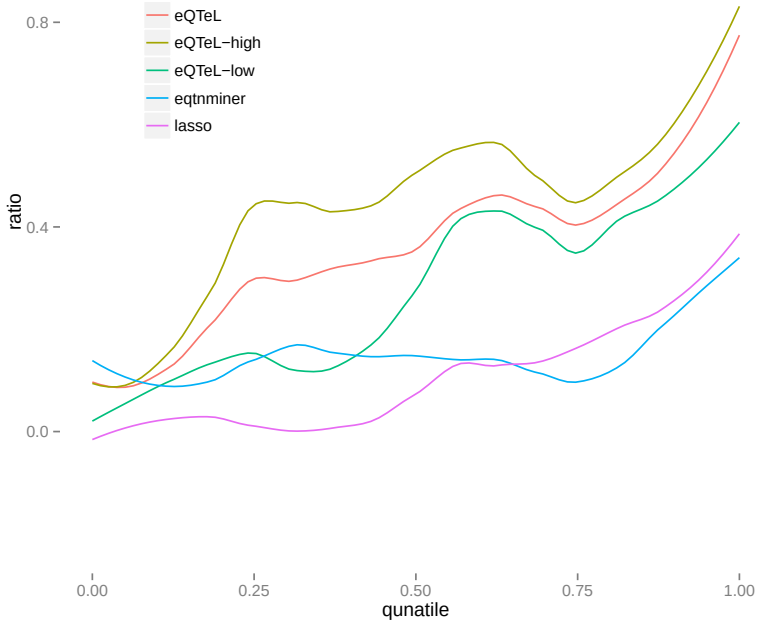

Figure A.6: Comparison of recall-rate of different methods (controlled for overall effective sparsity). eQTeL-high is eeSNPs with high regulatory potential (above 75 quantile). eQTeL-low is eeSNPs with low regulatory potential in lower 25% quantile.

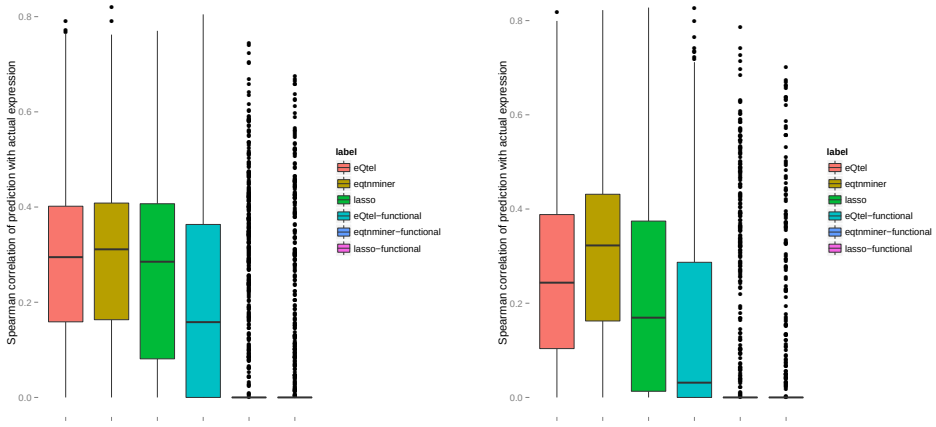

(a) top 1 per gene

(b) top 2 SNPs per gene

//

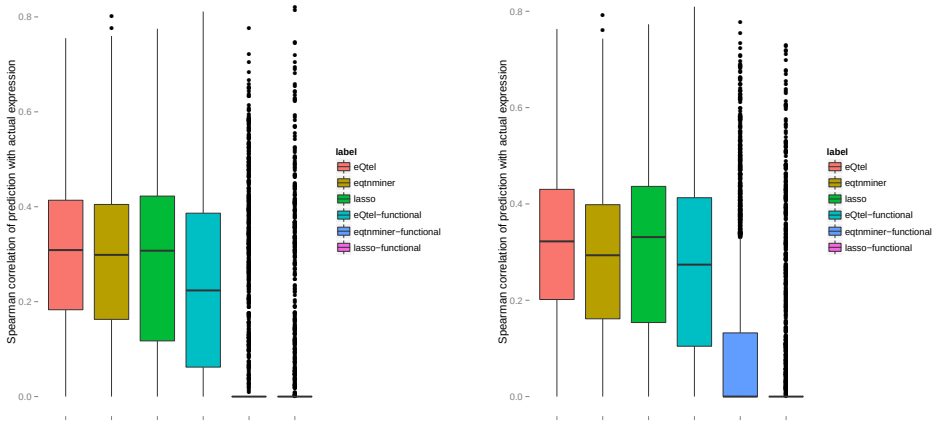

(c) top 3 SNPs per gene

(d) top 5 SNPs per gene

Figure A.7: Comparative performance of eQTeL as number of SNP per genes are increased in imputed data.

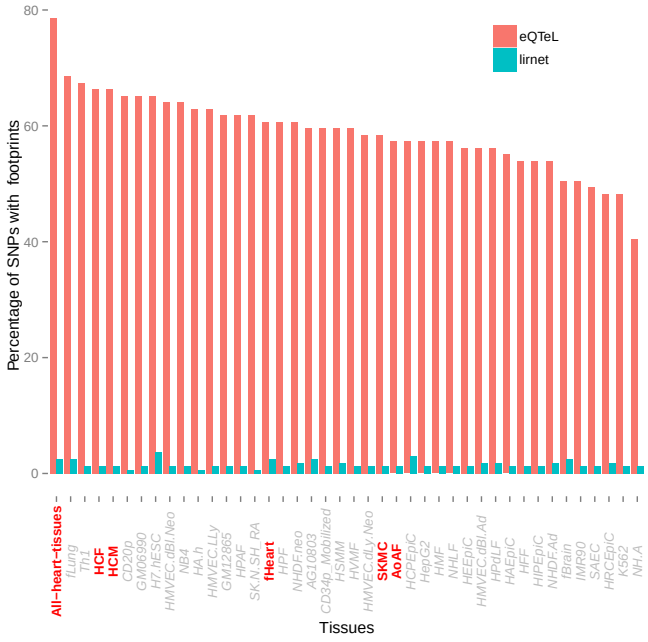

Figure A.8: Lirnet enrichment of DGF footprint: This analysis is based on 162 SNPs identified by eQTeL and Lirnet. We analyzed footprint in 42 cell lines from Neph et. al. overlapping the SNP within 25 bps the SNP loci by using bedtools for each of the method. The heart-related-tissues are highlighted in red in the figure. The left-most bar represents pooled data from all heart-related cell types.

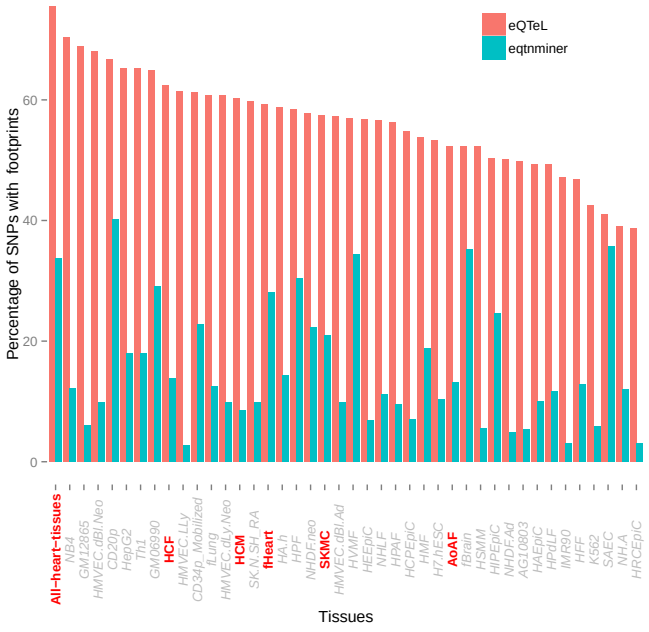

Figure A.9: Eqtnminer subset selection. The eqtnminer with 8 dimensional features (from 95 dimensional features), selected based on feature importance estimated by eQTeL. Non-redundant features were chosen. The performance of eqtnminer improves substantially compared to 95 dimensional eqtnminer.

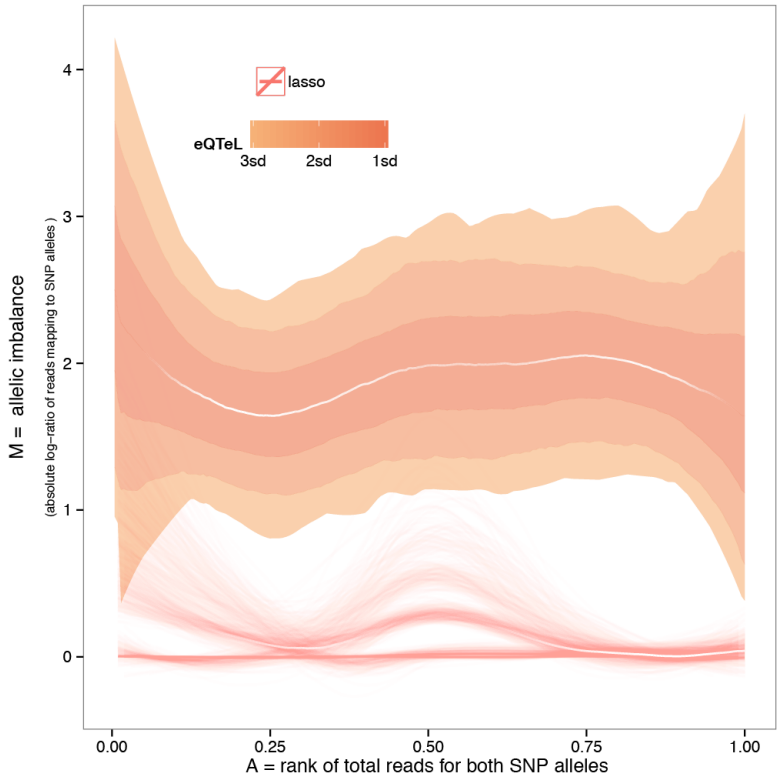

Figure A.10: DNAse hypersensitivity at eeSNPs shows greater allele specificity in HCM. X axis: rank of DHS read counts, Y axis: absolute log-ratio of read counts mapping to the two alleles at a SNP. SNPs from different methods are selected similar to Fig 5. The median white lines represent LOESS (local regression) for each method. Confidence interval for each median line is estimated using bootstrapping and are represented either by thin lines representing LOESS of each bootstrap, or by colored shades representing confidence intervals in terms of standard deviation of bootstraps. Note the allele-specificity at SNPs detected by eQTeL and eqtnminer remains same even if we control for number of SNPs per gene.

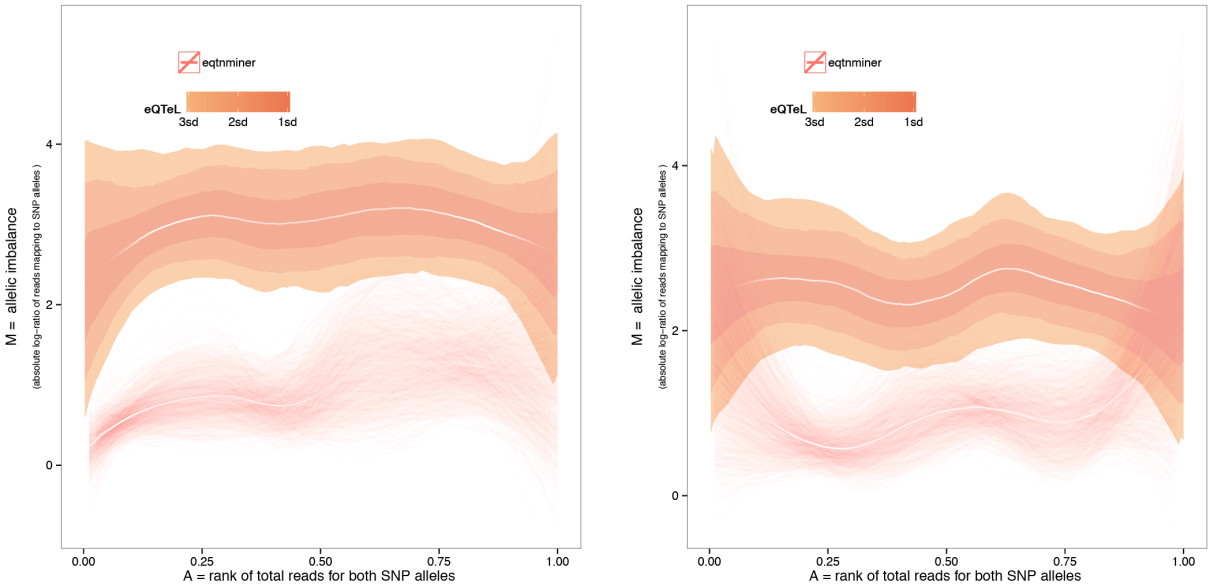

(a) SKMC (b) HCF

Figure A.11: Relative allele specificity (in terms of DHS reads) by SNPs identified by different methods: X axis: rank of DHS read counts, Y axis: absolute log-ratio of read counts mapping to the two alleles at a SNP. SNPs from different methods are selected similar to fig 5. The median white lines represent LOESS (local regression) for each method. Confidence interval for each median line is estimated using bootstrapping and they are shown in the figures using either of following two ways: by thin lines representing LOESS of each bootstrap, or by colored shades representing confidence intervals in terms of standard deviation of bootstraps. Note the allele-specificity at SNPs detected by eQTeL and eqtnminer remains same even if we control for number of SNPs per gene.

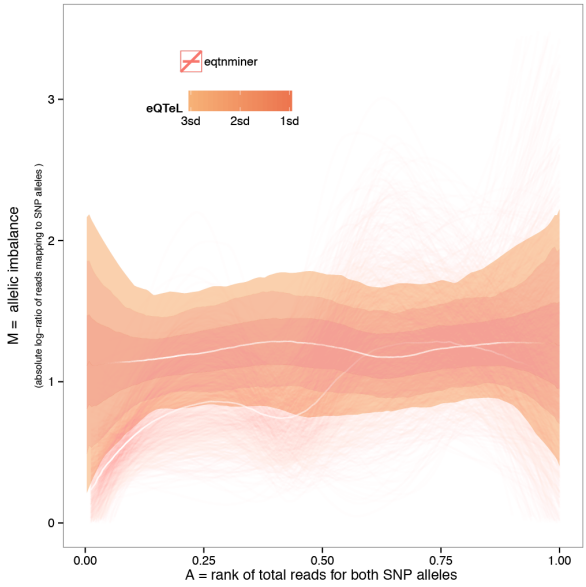

Figure A.12: Relative allele specificity by SNPs (in terms of H3K4me3) identified by different methods: X axis: rank of DHS read counts, Y axis: absolute log-ratio of read counts mapping to the two alleles at a SNP. SNPs from different methods are selected similar to fig 5. The median white lines represent LOESS (local regression) for each method. Confidence interval for each median line is estimated using bootstrapping and they are shown in the figures using either of following two ways: by thin lines representing LOESS of each bootstrap, or by colored shades representing confidence intervals in terms of standard deviation of bootstraps. Note the allele-specificity at SNPs detected by eQTeL and eqtnminer remains same even if we control for number of SNPs per gene.

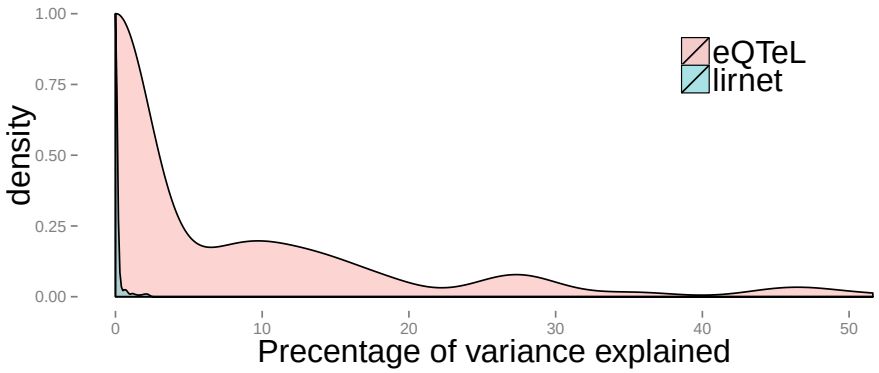

(a) Explained variance

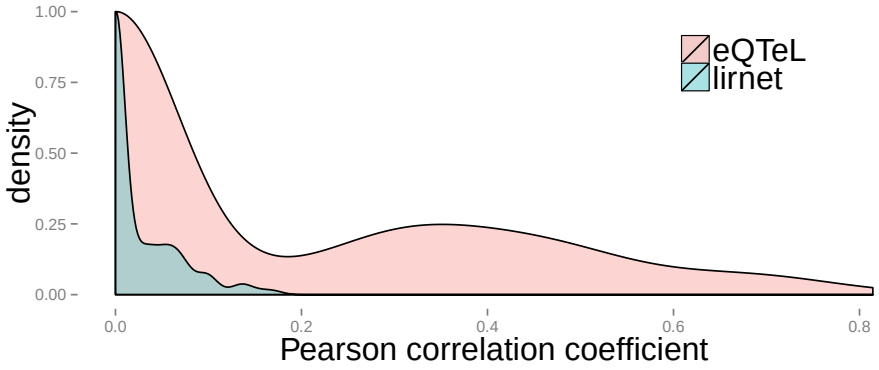

(b) Expression predictiblity

Figure A.13: Comparative performance of Lirnet: Comparative performance of Lirnet in terms of explained variance and expression predictability for 200 genes. Number of SNPs were controlled for each method (as in Fig 2). SNPs from eQTeL were selected using posterior probability > 0.5. The figure shows (10 fold) cross-validated correlation between predicted expression using alleles of identified SNPs for each method.

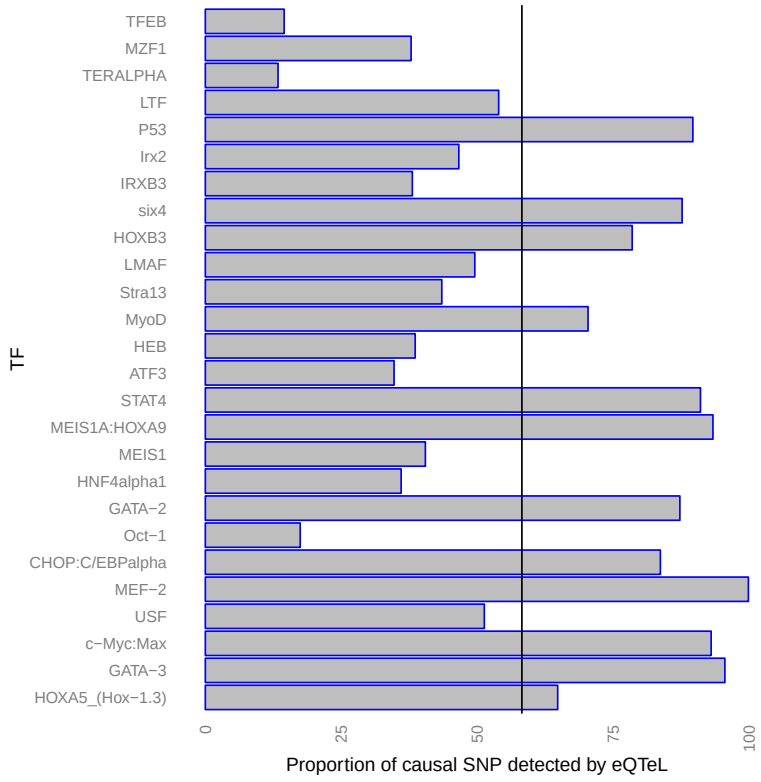

Figure A.14: Proportion of causal SNPs detected by eQTeL: Highly putatively *causal* were identified SNPs using difference in association between best-associated SNP and second-associated SNP for each gene. Y axis shows mammalian TF motifs that are preferetially disrupted by *causal* SNPs. For each of these motifs, proportion of causal SNPs among eeSNPs was estimated using ratio of relative enrichment (over background) of motif disruption score (differential binding score between major allele and minor allele of SNP) between eeSNPs and *causal SNPs*.

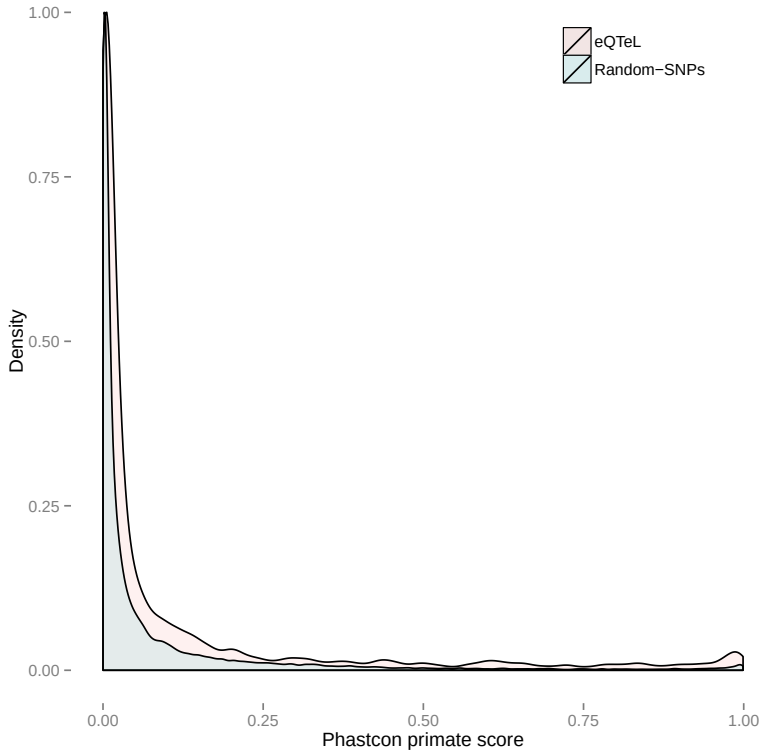

Figure A.15: Conseravation of eeSNPs. Distribution of mammalian PhasCons scores for eeSNPs and the control SNPs. The ratio of the two means is 1.49 and Wilcoxon test p-value $< 5 * 10^{-5}$.

Inference

We used a combination of Gibbs and Metropolis-Hasting sampling [214] to jointly estimate the full posterior distribution of our model parameters.

Sampling γ parameters accounting for Linkage Disequilibrium

We estimated linkage disequilibrium block using PLINK [140], by using default setting of SNPs within 200kb. The effects of SNPs in Linkage Disequilibrium are dependent on each other because the SNP alleles are highly correlated. Gibbs or Metropolis-Hastings samplers that ignore the LD structure of SNPs can get stuck in local minima while failing to explore high probability combinations of $\boldsymbol{\gamma}$ (Fig. S15). To overcome these poor mixing properties, we devise a block MCMC sampler that explicitly uses LD-block information to sample from the posterior probability of a LD-block i.e.

$$p(\boldsymbol{\gamma}_{LD}|.) = \frac{P(\boldsymbol{Y}|\boldsymbol{\gamma}_{LD}, \boldsymbol{\gamma}_{-LD}) \prod_i p(\gamma_i|\theta_i)}{\sum_{\gamma'_{LD}} P(\boldsymbol{Y}|\boldsymbol{\gamma}'_{LD}, \boldsymbol{\gamma}_{-LD}) \prod_i p(\gamma'_i|\theta_i)}$$

where, $\boldsymbol{\gamma}_{LD}$ and $\boldsymbol{\gamma}_{-LD}$ are γ of set of SNPs respectively within and outside the LD-block. The resulting sampler mixed much faster (Fig. S15) by exploring high probability models in a hierarchical fashion: we use a Gibbs sampler to sample highly-probable combinations of LD blocks and within these sampled LD block, and then a Metropolis-Hasting sampler is used to sample a sparse combination of SNPs that explain expression variance.

Sampling $\boldsymbol{\alpha}$ and θ parameters

We follow the latent variable Gibbs sampling strategy of [144] to sample the logistic regression parameters $\boldsymbol{\alpha}$. Specifically, we can sample latent variables from a Pólya-gamma distribution,

$$w_i|\boldsymbol{\alpha} \sim \mathcal{PG}(1, E_i\boldsymbol{\alpha}) \tag{A.1}$$

and then sample $\boldsymbol{\alpha}$ from a normal distribution,

$$\boldsymbol{\alpha} \sim N(m_w, V_w)$$

where, $V_w = (\mathbf{F}^T\Omega\mathbf{F} + B^{-1})^{-1}$, $m_w = V_w(\mathbf{F}^T\kappa(\theta) + \mathbf{B}^{-1}\mathbf{b})$ with $\kappa(\theta) = (\theta - .5)$ and Ω being a diagonal matrix of the w_i's. Then, for each SNP i and gene j, the regulatory-interaction potential θ_{ij} is sampled from its posterior distribution as

$$P(\theta_{ij} = 1) = \frac{\phi(\gamma_{ij})\mathrm{logistic}(E_i\boldsymbol{\alpha})}{\phi(\gamma_{ij})\mathrm{logistic}(E_i\boldsymbol{\alpha}) + (1 - \phi(\gamma_{ij}))(1 - \mathrm{logistic}(E_i\boldsymbol{\alpha}))} \tag{A.2}$$

where $\phi(\gamma) = \pi^{\gamma}\pi_0^{1-\gamma}$. If θ were estimated based only on whether the corresponding SNP was an expression-regulator (i.e based on value of γ), then the resulting estimation of regulatory-interaction potential would be equivalent to supervised learning. On the other hand, if θ were sampled on posterior that depended only on current estimate of $\boldsymbol{\alpha}$ and not on γ, the resulting estimation be equivalent to clus-

tering. eQTeL, however, uses both in its posterior sample and therefore induces a semi-supervised clustering of genomic regions into interacting regulator and neutral regions. This approach to model θ induces a semi-supervised clustering of genomic-region into interacting-regulators and noninteracting-regulators, since each MCMC iteration produces a sample of θ_{ij} for each SNP that depends on its γ_{ij} in addition to its current estimate of regulatory and interaction potentials.

Inference of β, σ^2 and c

For simplifying the notations, in the section we only consider subset of SNPs which were selected by the model so that $\mathbf{X}$ represents $\mathbf{X}_\gamma$ (this is $n \times q$ matrix, where n is number of samples and q is total number of SNP selected in the model). The generative model for β, σ^2 and c are:

$$\begin{aligned} Y|\boldsymbol{\beta}, X, \gamma &\sim N(X^T\boldsymbol{\beta}, \sigma^2 I) \\ \boldsymbol{\beta}|c, \sigma &\sim N(0, c\sigma^2(X^TX)^{-1}) \\ \sigma^2 &\sim IG(\nu/2, \nu\lambda/2) \\ c &\sim IG(\frac{1}{2}, \frac{n}{2}) \end{aligned} \tag{A.3}$$

For Zellner's g-prior ν is usually assumed to be zero. β, σ^2 and c are sampled from the full posterior distribution as:

$$\begin{aligned} P(\beta, \sigma^2, c|Y, X) &\propto c^{3/2} exp(-n/2c) \\ &\quad \sigma^{-2(\nu/2+1)} \sigma^{-n} (c\sigma^2)^{-q/2} \\ &\quad exp\{-\frac{1}{2\sigma^2}\nu\lambda \\ &\quad -\frac{1}{2\sigma^2}(Y - X\hat{\beta})^T(Y - X\hat{\beta}) \\ &\quad -\frac{1}{2\sigma^2}(\beta - \hat{\beta})^T X^T X(\beta - \hat{\beta}) \\ &\quad -\frac{1}{2c\sigma^2}\beta^T X^T X\beta\} \end{aligned} \tag{A.4}$$

Where, $\hat{\beta} = (X^T X)^{-1} X^T Y$

$$\begin{aligned} P(\sigma^2/.) &\propto \sigma^{-2(\frac{\nu+n+q}{2}+1)} \\ &\quad exp\{-\frac{1}{2\sigma^2}\left((Y - X\beta)^T(Y - X\beta) + \frac{\beta^T X^T X\beta}{c} + \nu\lambda\right)\} \\ \sigma^2|. &\sim IG\left(\frac{\nu+n+q}{2}, \frac{1}{2}(Y - X\beta)^T(Y - X\beta) + \frac{\beta^T X^T X\beta}{2c} + \frac{\nu\lambda}{2}\right) \end{aligned} \tag{A.5}$$

$$\begin{aligned} P(c/.) &\propto c^{-(q+1)/2-1} \\ &\quad exp\{-\frac{1}{2c}\left(n + \frac{\beta^T X^T X\beta}{\sigma^2}\right)\} \\ c|. &\sim IG\left(\frac{q+1}{2}, \frac{\beta^T X^T X\beta}{2\sigma^2} + n/2\right) \end{aligned} \tag{A.6}$$

$$
\begin{aligned}
P(\beta, |.) &\propto exp\{-\frac{1}{2\sigma^2}(\beta-\hat{\beta})^T X^T X(\beta-\hat{\beta}) - \frac{1}{2c\sigma^2}\beta^T X^T X\beta\} \\
\beta|. &\sim N\left(\frac{c}{c+1}\hat{\beta}, \frac{c\sigma^2}{c+1}(X^T X)^{-1}\right) \qquad \text{(A.7)}
\end{aligned}
$$

Convergence of sampler

Convergence of the MCMC sampler was assessed by running 10 independent chains and diagnostics of MCMC chain was performed using R-package "coda". In general, we found that the Markov chains converge within 5000 iterations of the sampler.

Initialization

We use univariate-eQTL to initialize different parameter of the eQTeL model.

Further investigation into the reasons for eQTeL's performance gain

In this paper, we have chosen to compare performance of eQTeL against eqtnminer since it is the only method that mostly explicitly incorporated epigenomic data in eQTL as opposed to traditional eQTL approaches. First eqtnminer estimates Bayesian factor (likelihood of association) of each SNP, assuming at most one SNP per gene to be causal; this assumption can be limiting, because it cannot

identify combination of SNPs that jointly explain the expression variance. It then estimates posterior probability of each SNP to be causal regulator by modeling prior probability as a function of epigenetic data. However, eqtnminer parameter estimation relies on maximizing a likelihood function, which is prone to get stuck in local maxima due to correlation among different types of epigenetic data (demonstrated in supplementary note 6 and Fig S9). Further, they do not explicitly model relative weights of genetic and epigenetic factors in determining causality of SNPs. Another approach by Lee et al. [2], does not have the limiting assumption of single causal SNP per gene but it does not incorporate epigenomic data, making comparison infeasible. Recently, Lappalainen et al. [139] uses Matrix-eQTL (essentially a univariate eQTL method) to find associated SNPs, and estimates the proportion of causal SNPs by comparing their epigenomic profiles with that of the most associated SNP per gene as a gold standard (which is a strong assumption). Since they do not explicitly identify causal SNPs amongst associated SNP (the only estimate proportion of causal SNPs), this method is not directly comparable with our method.

To assess performance of eQTeL, we also chose LASSO as a representative of multivariate regression eQTL approaches, because of its good performance and scalability to larger datasets. Other approaches to date [215–217] that identify causal variants in GWAS, but not in eQTL studies and therefore are not directly comparable.

eQTeLs performance gain is potentially due to two main factors (i) integration of epigenetic data, (ii) allowing multiple causal variants per gene (cite http://www.ncbi.nlm.nih.gov/pubmed/25104515). In quantifying the relative con-

tribution of each of these factors, we note that the mean correlation between actual and predicted eQTeL-predicted gene expression, when a single causal SNP per gene is allowed, is 0.154. This correlation improved substantially to 0.289 when 5 causal SNPs per gene are allowed in eQTeL (Fig S8). However, in the absence of epigenomic data, i.e., when using standard LASSO, we do not see any such performance gain, and in general, the performance is substantially worse than that for eQTeL. This strongly suggests that allowing multiple SNP per gene is useful in identifying regulatory SNP specifically when functional information is used.

Another advantage of eQTeL is that it models heterogeneity in epigenetic signatures of expression regulators. eQTeL is a hierarchical Bayesian model as opposed to empirical Bayes model. Unlike empirical Bayes, hyper-parameters of model are drawn from unparameterized distributions. For this reason in eQTeL all parameters are estimated using MCMC sampling and EM approximation was not required. Empirical prior models [2, 49, 218, 219] assumes a single signature for all regulators and therefore cannot account heterogeneity in the type of regulators of different genes. The eQTeL accommodates such heterogeneity because it allows variation in parameter combinations.

Other methods for comparison

Eqtnminer

The software tool related to Gaffney et. al. was downloaded from http://eqtnminer.sourceforge.net. For each of the comparative analysis, the initial set of SNPs per gene was kept same for both eqtnminer and eQTeL for fair comparison. We obtained Bayesian factor for each SNPs using eqtnminer. The parameters to calculate epigenetic prior were estimated using maximizing equation (9) of Veyrieras et. al. The parameters were initialized as recommended by Veyrieras et. al.

To generate Fig 2, we controlled for total number of SNPs selected by eQTeL and eqtnminer. To do so, we sorted SNPs based on eqtnminer prior probability and selected top 2428 SNPs. As Gaffney et. al. recommend the eqtnminer for single SNP per gene, we compared the performance of eqtnminer in main manuscript (Fig 5, 6 and 8) using single SNP per gene for footprint enrichment, allele-specificity and ChiA-PET enrichment analyses. We repeated that analysis by controlling for number of SNPs per gene between eQTeL and eqtnminer; the eQTeL still outperform eqtnminer in that case. To generate Fig S8, for each gene we selected N (= 1,2, 3 and 5) top SNP(s) based on eqtnminer posterior probability.

LASSO

R-package GLMNET was used for L1 regulaizer multivariate regression (LASSO). LASSO estimates effect size (regression coefficient), for the SNP included in the

model. We used 10-fold cross validation to estimate the hyper-parameter (lambda, regularization parameter). For each of the comparative analysis, the initial set of SNPs per gene was kept the same for both LASSO and eQTeL for fair comparison.

To generate Fig 2, we controlled for total number of SNPs selected by eQTeL and LASSO. To do so, we sorted SNPs based on absolute value of effect size estimated by LASSO-selected top 2428 SNPs. To generate Fig S8, for each gene we selected N (=1,2,3 and 5) top SNP(s) based on absolute value of estimated effect size estimated by LASSO.

Matrix-eQTL /univariate-eQTL (Lappalainen et. al.)

We used R package matrix-eQTL (http://www.bios.unc.edu/research/genomic_software/Matrix_eQTL/), to perform univariate-eQTL as recommended by Lappalainen et. al.

Epigenetic-only model

In simulation study, $\boldsymbol{\alpha}$ parameters were learned, in supervised manner, by using enhancers as training example. Bayesian logistic regression [144] was used to learn $\boldsymbol{\alpha}$. Based on learned $\boldsymbol{\alpha}$, SNPs were sorted based on their regulatory potential.

Known-epigenetic-prior-eQTeL

Known-epigenetic-prior-eQTeL, is a version of eQTeL (for simulation study only) where instead of estimating $\boldsymbol{\alpha}$, the $\boldsymbol{\alpha}$ used to generate regulatory potential for

simulation study was used. Thus it is a theoretically best model for eQTeL.

Variable selection method

Variable selection model was implemented by modifying eQTeL model as follows: (a) informative prior was changed to uninformative priors. (b) hierarchical sampling SNP (based on LD block) was switched off; each SNP were processed sequentially, similar to Liang et. al. [146].

Lirnet

Lirnet was downloaded from (http://homes.cs.washington.edu/~suinlee/lirnet/). Because of computational limitation of lirnet (it takes 13 days of CPU processing in a 64 core machine to process 200 genes), this analysis was limited to 200 random genes. Hyper-parameter of the model was set by cross-validation as recommended in Lee et. al. [2]. For comparing the performance of Lirnet with eQTeL we ran eQTeL with same set of 200 genes.

Figure A.13 demonstrates that eQTeL outperforms Lirnet in terms of explained variance and prediction accuracy (we controlled for number of SNPs selected by each methods). Figure A.8 also demonstrates that higher fraction of of SNPs detected by eQTeL overlaps with footprints, suggesting eeSNPs are more likely to be functional compared to SNPs detected by Lirnet.

Eqtnminer subset selection

We used 95 dimensional epigenetic and interaction features, (Fig A.2) to learn interacting-regulatory potential by eQTeL. Many of the features have very high correlation between them. When the 95 dimensional features were used for learning prior in eqtnminer, the alpha parameters (feature importance) were not learned accurately. This is most probably due extreme correlation between different input features that might cause the maximization function to stuck in a local maximum. To analyze this further, we used 8 features of the 95 dimensional features, which were given high feature importance by eQTeL and does not have extreme correlation. The performance improved substantially, although eQTeL performed better compared to eqtnminer(Supplementary Fig. A.9).

Multiple hypothesis correction/sparsity constrains

Here we demonstrate that eQTeL model can detect causal expression-regulatory SNP even if they have small effect size by analyzing sparsity constraints by association methods on the simulated dataset. Normally, due to multiple-hypothesis test correction (equivalent to sparsity constraint in Bayesian models), expression-regulators with small effect on expression are missed. Fig. A.6. shows effect-size distribution of identified causal SNPs by univariate-eQTL and eQTeL when the same number of SNPs is selected by each methods. Univariate-eQTL cannot identify causal SNPs with low effect-size because of severe multiple-hypothesis correction.

eQTeL, however, detects causal SNPs with small effect-size. Although the recall-rate decreases with the effect size for eQTeL it can more effectively retrieve causal SNP with small effect size, particularly those with relatively high interacting-regulator potential. Since there are fewer SNPs which are within an interacting-regulator, selection of expression regulators among those SNPs can be made under a relatively less severe sparsity constraint (or equivalently, multiple hypothesis correction). This is evident from from Fig. A.6. Moreover, recall rate of eQTeL is relatively higher for top 50% causal SNPs with stronger interacting-regulatory potential (eQTeL-high) than for the bottom 50%. This suggests that eQTeL applies a relatively lower sparsity constraint on interacting-regulators.

Explained variance and expression predictability

Different methods are known have biases in estimating effect size β. For instance, LASSO is know to over-shrink the parameters, therefore it is recommended that first LASSO be used for feature selection and then β be estimated independently for selected features [79]. To remove such biases and compare performance of different methods in an unbiased manner, each methods were used for regulatory SNPs identification only and β was independently estimated using cross-validation training set as follows.

For each method, explained variance and expression predictability was estimated using k fold cross-validation. Samples were randomly partitioned into k subsamples. $k-1$ of subsamples were used for estimating β for selected SNPs as

$\hat{\beta}_{train} = (X^T X)^{-1} X^T Y$, while retaining one subsample for validation. In the validation subsample expression was predicted as $\hat{Y}_{test} = X^T \hat{\beta}_{train}$. Expression predictability was defined as Pearson correlation between Y_{test} and $\hat{Y}_{test}$. Explained variance was calculated as $1 - \frac{var(Y_{test} - \hat{Y}_{test})}{var(Y_{test})}$. This process is repeated k times, using each k subsamples for validation exactly once. The mean and standard deviation of explained variance of expression predictability and explained variance was calculated for k test subsamples.

Scalability and computation

eQTeL uses shared memory multiprocessing to process genes in parallel. This makes it feasible to run Gibbs sampler to process thousands of genes with million of putative SNPs. In order to calculate Bayesian factor of SNP, we use fast Choleksy-update algorithm described in Dongarra et al. (Ch 10. [220]). Further, while calculating feature importance $\boldsymbol{\alpha}$ at each Gibbs iteration we randomly sample subset of interacting-regulator and non-regulators to: a) speed up the eQTeL model and b) avoid over-fitting while estimating $\boldsymbol{\alpha}$.

The software GOAL that implements the eQTeL model uses the multiple cores to speed up the process. In addition, we use several efficient algorithms from LAPACK to efficiently update the Choleskythe most computation intensive part of eQTeL. GOAL can efficiently handle million of SNPs for thousand of genes because it process each genes in parallel in a separate thread. In addition, the epigenetic importance can be estimated using subset of genes; and given the importance esti-

mated each of genes could be processed independently.

Appendix B: Synthetic rescue determinants of resistance and response to cancer therapy

Extended data figures

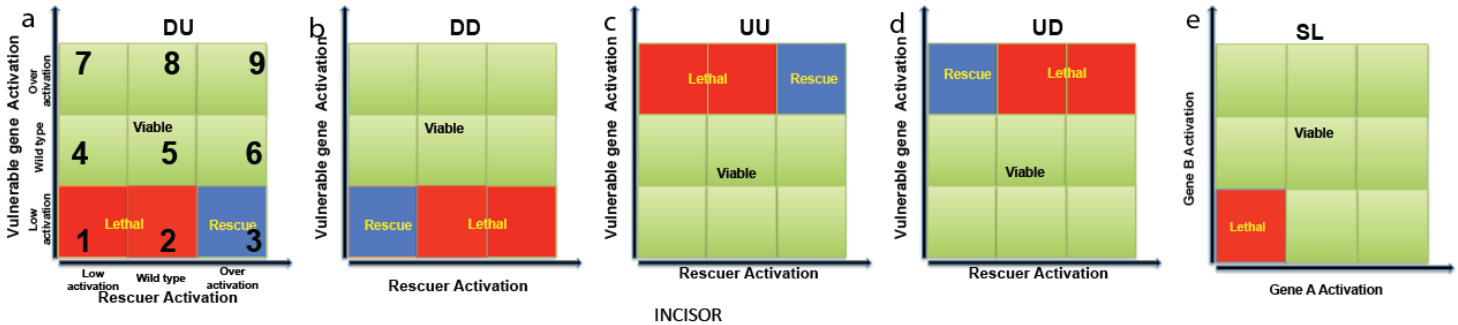
a
DU
Vulnerable gene Activation
Over activation
Wild type
Low activation
7
8
9
Viable
4
5
6
Lethal
1
2
Rescue
3
Low activation
Wild type
Over activation
Rescuer Activation
b
DD
Vulnerable gene Activation
Viable
Rescue
Lethal
Rescuer Activation
c
UU
Vulnerable gene Activation
Lethal
Rescue
Viable
Rescuer Activation
d
UD
Vulnerable gene Activation
Rescue
Lethal
Viable
Rescuer Activation
e
SL
Gene B Activation
Viable
Lethal
Gene A Activation

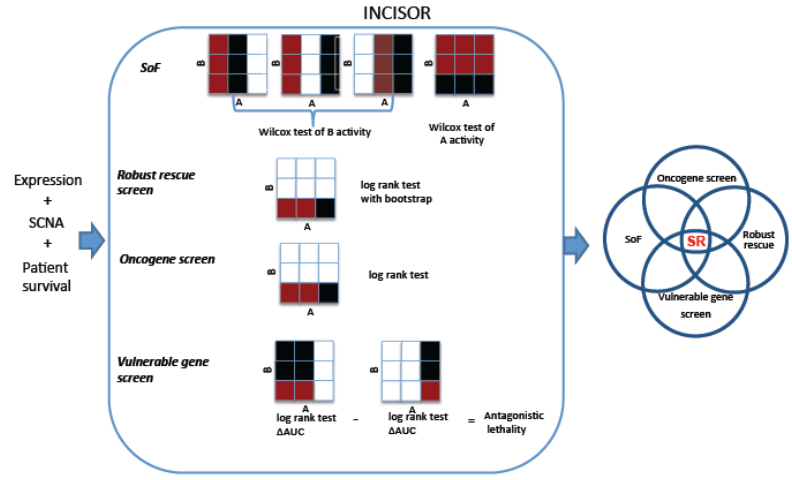
f
INCISOR
SoF
B
A
Wilcox test of B activity
Wilcox test of A activity
Expression
+
SCNA
+
Patient survival
Robust rescue screen
log rank test with bootstrap
Oncogene screen
log rank test
Vulnerable gene screen
log rank test ΔAUC
log rank test ΔAUC
Antagonistic lethality
Oncogene screen
SoF
SR
Robust rescue
Vulnerable gene screen

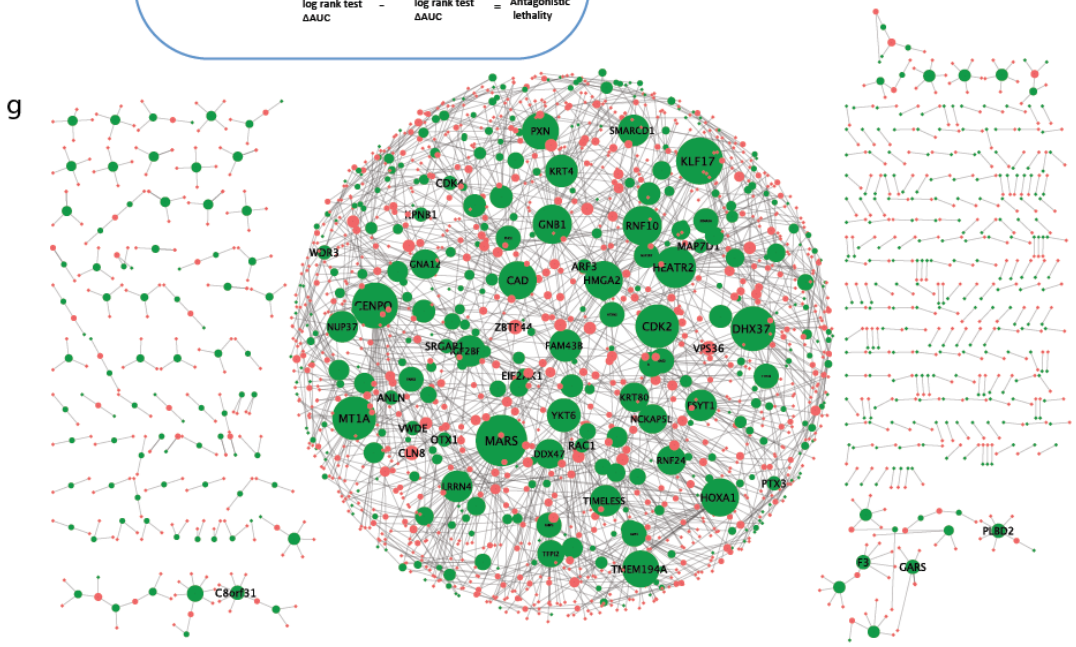
g
PXN
SMARCD1
KLF17
KRT4
CDH1
KPNB1
GNB1
RNF10
MAP7D1
WDR3
GNA14
ARF3
HMGA2
HEATR2
CAD
CENPO
NUP37
ZBTB44
CDK2
DHX37
SRCAP
FAM43B
VPS36
EIF1AX
ANLN
KRT80
GYT1
MT1A
YKT6
NCKAP1L
VWDE
OTX1
MARS
RAC1
CLN8
DDX42
RNF24
RRN4
TIMELESS
HOXA1
PTX3
TMEM194A
PLOD2
CARS
C8orf31

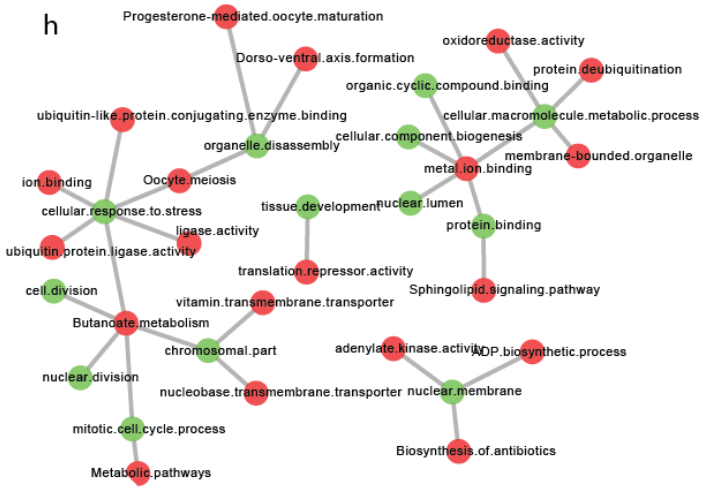
h
Progesterone-mediated.oocyte.maturation
Dorso-ventral.axis.formation
oxidoreductase.activity
protein.deubiquitination
organic.cyclic.compound.binding
ubiquitin-like.protein.conjugating.enzyme.binding
cellular.macromolecule.metabolic.process
organelle.disassembly
cellular.component.biogenesis
membrane-bounded.organelle
metal.ion.binding
ion.binding
Oocyte.meiosis
cellular.response.to.stress
tissue.development
nuclear.lumen
protein.binding
ligase.activity
ubiquitin.protein.ligase.activity
translation.repressor.activity
cell.division
Sphingolipid.signaling.pathway
vitamin.transmembrane.transporter
Butanoate.metabolism
chromosomal.part
adenylate.kinase.activity
ADP.biosynthetic.process
nuclear.division
nucleobase.transmembrane.transporter
nuclear.membrane
mitotic.cell.cycle.process
Biosynthesis.of.antibiotics
Metabolic.pathways

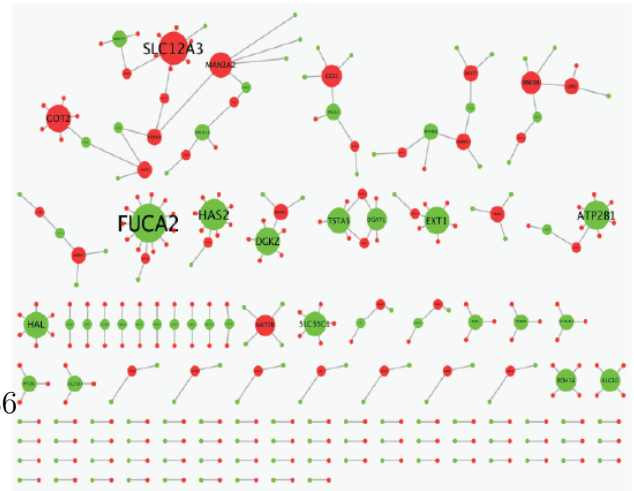
i
SLC12A3
MAN2A2
GOT2
FUCA2
HAS2
ATP2B1
EXT1
DGK2
HAL

Figure B.1: (a-e) Synthetic rescues functional truth tables: The truth tables of the four SR and SL interaction types. Each truth table denotes the cell viability states - viable (green), non-rescued (i.e., lethal – red), and rescued (blue) - as a function of the activity state of each of the SR pair genes (down regulated, wild-type and up-regulated). The states are enumerated as state 1 to state 9.: (a) (DU-SR): Down-regulation of a vulnerable gene is lethal but the cancer cell is rescued (retains viability) by the up-regulation of its rescuer partner; (b-d): Analogous functional truth tables for (DD, UD, and UU) SR types. (e) In an SL interaction, in difference, the down-regulation of either gene alone is viable but the down-regulation of both genes together is lethal. (f) Overview of INCISOR. INICISOR takes inputs as expression, somatic copy number of alternations (SCNA) and survival of patients sample as input and output SR pairs. It composes of 4 steps: SoF performs 4 Wilcoxon test to compare expression between groups highlighted in red and black (and similar 4 wilcox test for SCNA). Next three step survival data uses survival data and perform KM analyses to compare survival between the groups highlighted in red and black. (g-i) DU-type SR network and functional characterization. (f) Pairwise gene enrichment analysis: The Extended Data Figure shows relationship between vulnerable gene biological processes (red) and rescuer gene biological processes. Edges between a vulnerable process and rescuer process represents enrichment of the vulnerable process in vulnerable gene partner of rescuer process genes. (g) SR-DU network of metabolic genes and functional characterization. The figure depicts synthetic rescues network with 152 vulnerable genes (green) and 210 rescuer genes (red) of 131 metabolic genes (diamond) encompassing 258 interactions. The size of nodes indicates their degree in the network as in (c).


a
Fraction of pancancer SR with significant rescue
Cancer Type
KIRC KIRP CESC PRAD LGG GBM COAD PAAD LAML LUSC UCS SKCM BRCA SARC UCEC LIHC UVM OV LUAD CHOL HNSC TGCT DLBC STAD KICH THCA ESCA BLCA
b
not-rescued
rescued
P =1.74E-02
Δ AUC=0.4
Survival
Days
c
mRNA
scna
Wilcox P−value (−log10)
HYDIN CDH11 MCM3AP FLI1 HPSE2 SLC44A2 TTC18 TERF2IP MYH9 C10orf129 CDH8 ASAH2 OR13A1 CNTN3 PLCE1 HERC4 ARMC4 CDH13 SLC7A2 VCL GPC5
d
mRNA
scna
Wilcox P−value (−log10)
CAD UBXN2A OPRD1 MSH2 MAD2L2 EIF2B4 SLC2A1 OST4 C2orf44 LRRC69 MTOR FAM60A MRPL33 DDX11 MMACHC COX7A2L
e
not-rescued
rescued
Survival
P=4.32E−05
AUC=0.44
Days
f
not−significant
significant
logRank P−value (−log10)
DB05258 Irinotecan Leucovorin Carmustine Methotrexate Topotecan Erlotinib Bevacizumab Gemcitabine Vinblastine Camptothecin Fluorouracil Paclitaxel Doxorubicin Pemetrexed Anastrozole Exemestane Capecitabine Carboprost Trometh Lomustine Celecoxib Cetuximab Dacarbazine Dexamethasone Docetaxel Epirubicin Etoposide Lefrozole Trastuzumab Leuprolide Megestrol acetate Vinorelbine Sorafenib Sunitinib Tamoxifen Thalidomide Vincristine
g
%Genes / Term
AU-rich element binding
mRNA 3'-UTR binding
mRNA 3'-UTR AU-rich region binding
chondrocyte proliferation
endoderm development
somatic stem cell population maintenance
endoderm formation
chondrocyte differentiation
cell fate commitment involved in formation of primary ge...
embryonic skeletal system morphogenesis
endodermal cell differentiation
embryonic cranial skeleton morphogenesis
chondrocyte proliferation_1
somatic stem cell population maintenance_1
digestive tract morphogenesis
regulation of cartilage development
chondrocyte differentiation_1
'de novo' protein folding
'de novo' posttranslational protein folding
keratinocyte proliferation
smooth muscle cell differentiation
regulation of cell junction assembly
cell-substrate junction assembly
regulation of cell-substrate junction assembly
regulation of adherens junction organization
regulation of Notch signaling pathway
adherens junction assembly
cell-substrate adherens junction assembly
focal adhesion assembly
regulation of focal adhesion assembly
Collagen formation
Collagen biosynthesis and modifying enzymes
cellular modified amino acid biosynthetic process
regulation of substrate adhesion-dependent cell spreading
regulation of cyclin-dependent protein kinase

Figure B.2: (a) Pan-cancer clinical significance of SR network. X axis shows 23 different cancer types, and Y axis shows the fraction of significant pan-cancer SR in each cancer type. Pan-cancer TCGA dataset was divided into two halves. DU-SR network was identified by applying INCISOR using one half of the data, and clinical significance was determined in the other half of the data. (b) Clinical predictive power of pancancer DU-SR pairs in an independent ovarian cancer dataset. The KM plot compared the survival of rescued (top 5-percentile; blue) vs non-rescued (bottom 5-percentile; red) ovarian cancer samples (N=92). The rescued samples show worse patient survival (logrank p-value<0.017, Δ AUC=0.4). (c-e) Rescuer activation associated with the vulnerable gene inactivation due to somatic mutations. (c) Rescuer activation per each vulnerable gene. The horizontal axis lists vulnerable genes with somatic mutations in TCGA samples, and the vertical axis denotes the significance of rescuer gene-activity between samples with vs. without vulnerable gene mutations. (d) Rescuer activation per each rescuer. The horizontal axis lists rescuer genes with somatic mutations in TCGA samples and the vertical axis denotes the significance of rescuer gene-activity between samples with vs. without vulnerable gene mutations. (e) The KM plot depicts the aggregate clinical predictive power of rescuers of CDH11 gene, among patient with CDH11 mutation. (f) Predictive power of SR when they are treated as SL. In this predictor an activation of SR as defined as when a rescuer expression is wild type and vulnerable gene is inactive Specifically, for each patients we count number of rescuer activity is wild-type, patients with the higher count (top 10 percentile) were considered as non-responder and lower count (bottom 10 percentile) were considered as non-responder. (g) GO-term enrichment analysis with rescuers of the drug targets. Rescuers are enriched with lipid storage/transport, thioester/fatty acid metabolism, and drug efflux transporters.

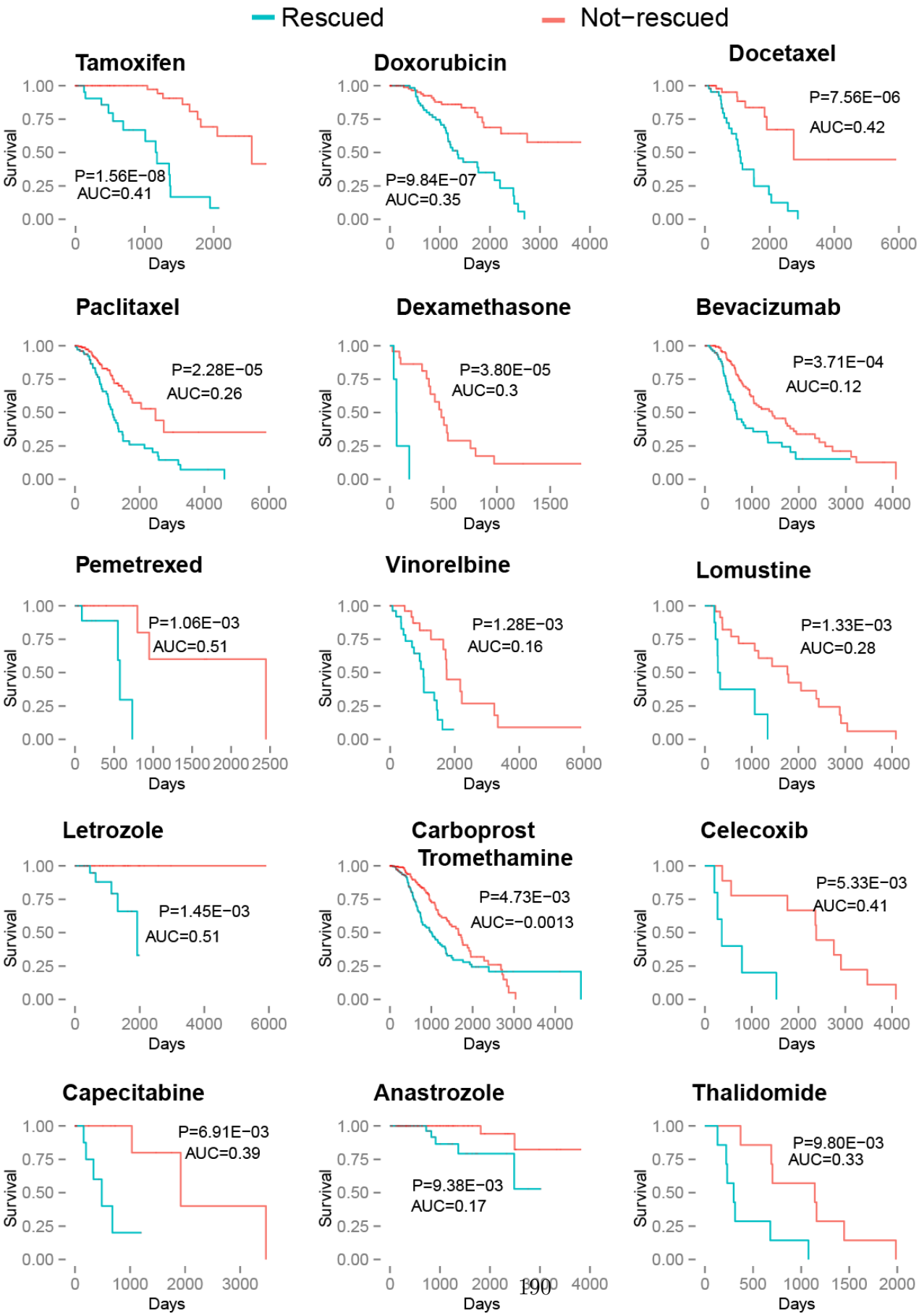
Rescued
Not−rescued
Tamoxifen
P=1.56E−08
AUC=0.41
Doxorubicin
P=9.84E−07
AUC=0.35
Docetaxel
P=7.56E−06
AUC=0.42
Paclitaxel
P=2.28E−05
AUC=0.26
Dexamethasone
P=3.80E−05
AUC=0.3
Bevacizumab
P=3.71E−04
AUC=0.12
Pemetrexed
P=1.06E−03
AUC=0.51
Vinorelbine
P=1.28E−03
AUC=0.16
Lomustine
P=1.33E−03
AUC=0.28
Letrozole
P=1.45E−03
AUC=0.51
Carboprost Tromethamine
P=4.73E−03
AUC=−0.0013
Celecoxib
P=5.33E−03
AUC=0.41
Capecitabine
P=6.91E−03
AUC=0.39
Anastrozole
P=9.38E−03
AUC=0.17
Thalidomide
P=9.80E−03
AUC=0.33
Survival
Days

Figure B.3: TCGA drug response. Drug response of top 15 anti-cancer drugs using drug- DU-SR in TCGA data. Each subplot represents a KM analysis of responder (red) v/s non-responders (blue) for a drug. The name of drug, log-rank p-value and ΔAUC is indicated in each subplot.

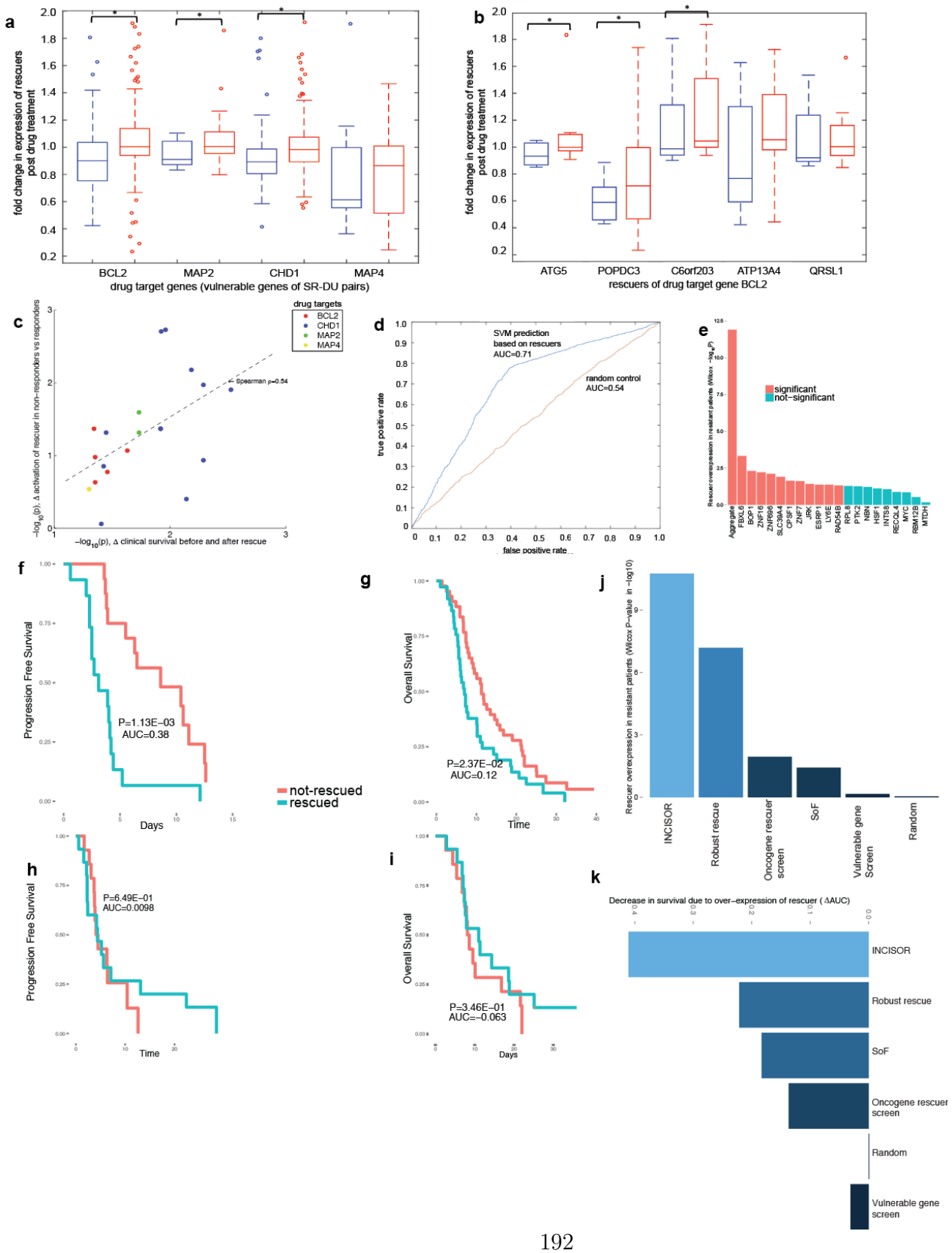
a
fold change in expression of rescuers post drug treatment
BCL2
MAP2
CHD1
MAP4
drug target genes (vulnerable genes of SR-DU pairs)
b
fold change in expression of rescuers post drug treatment
ATG5
POPDC3
C6orf203
ATP13A4
QRSL1
rescuers of drug target gene BCL2
c
drug targets
BCL2
CHD1
MAP2
MAP4
Spearman ρ=0.54
−log10(p), Δ activation of rescuer in non−responders vs responders
−log10(p), Δ clinical survival before and after rescue
d
SVM prediction based on rescuers AUC=0.71
random control AUC=0.54
true positive rate
false positive rate
e
significant
not−significant
Rescuer overexpression in resistant patients (Wilcox −log10(p))
Aggregate
FBXL6
BOP1
ZNF16
ZNF696
SLC39A4
CPSF1
ZNF7
JRK
ESRP1
LY6E
RAD54B
RPL6
PTK2
NBN
HSF1
NUP98
RECQL4
MYC
RBM12B
MTDH
f
Progression Free Survival
P=1.13E−03
AUC=0.38
Days
not−rescued
rescued
g
Overall Survival
P=2.37E−02
AUC=0.12
Time
h
Progression Free Survival
P=6.49E−01
AUC=0.0098
Time
i
Overall Survival
P=3.46E−01
AUC=−0.063
Days
j
Rescuer overexpression in resistant patients (Wilcox P−value in −log10)
INCISOR
Robust rescue
Oncogene rescuer screen
SoF
Vulnerable gene Screen
Random
k
Decrease in survival due to over−expression of rescuer (ΔAUC)
INCISOR
Robust rescue
SoF
Oncogene rescuer screen
Random
Vulnerable gene screen

Figure B.4: (a-d) SR network successfully predicts the response to cancer drug treatments in breast cancer. (a) Expression fold change (pre- versus post- drug treatment) is shown for the rescuer genes of the four vulnerable genes that are targeted by a drug cocktail in a cohort of 25 clinical breast cancer patients (i.e., from the BC25 dataset). Box plots aggregate rescuer expression changes for all rescuers of a given vulnerable target across patients that are clinical responders (blue) and non-responders (red). Ranksum p-values denote differences in overall rescuer fold change between these responder groups for each target gene. (b) Expression fold changes are shown for clinical responders and non-responders of BC25 for the 5 rescuers of the gene target BCL2. In (a) and (b) significant genes are marked by stars (ranksum p-value$<$0.05). (c) The 20 DU gene pairs active in the BC25 dataset are ranked by degree of potency (i.e., by the ranksum p-value denoting differential responder- versus non-responder pre- to post- drug fold change) (y-axis), and also ranked by their rescue effect (as calculated using the BC-DU-SR network as in step 2 of INCISOR) (x-axis). These measures correlate (Spearman = -0.54, p$<$1e-3). (d) Receiver Operating Characteristic (ROC) curve for an SVM predictor of patient treatment response, trained on the BC25 dataset. Area under the curve (AUC) is 0.71 for the predictor (blue), as compared to 0.54 for a random predictor (red). (e-k) SR network successfully predicts the response to cancer drug treatments in gastric cancer (e) The bar plot shows the significance of over-expression of 15 rescuers of THYMS in the tumors of patients who acquired resistance to Cisplatin and Fluorouracil compared to the patients who did not acquire resistance. (f,g) The KM plots depict the clinical significance of rescuer over-expression in patient tumors in terms of progression free survival (f) and overall survival (g). The patients with highly rescued tumors ($>$90 percentile) have significantly worse survival compared the patients with lowly rescued tumors ($<$10 percentile). The KM plot compares the difference in survival rates between rescued patients with many rescuers over-expressed (top 10 percentile) and non-rescued patients with fewer rescue events (bottom 10 percentile) for random chosen rescuer genes (h) for over-all survival and (i) progression-free survival. Both figures show no statistical significance.(continued in the next page). (j) The contribution of the 4 steps of INCISOR in predicting over-activation of rescuers. The rescuers identified by combining 4 steps of INCISOR show the highest significance, and this is followed by significances of rescuers over-expression identified with each of the step separately: robust rescue effect (step 3), oncogene rescuer screening (step 4), molecular survival of the fittest (step 1), vulnerable gene screening (step 2), and random control.

Figure B.4: (continued in the previous page): (k) The clinical significance of the rescuer up-regulation (rescue effect) of the 4 steps of INCISOR (estimated in ΔAUC). The rescuers identified by all 4 steps of INCISOR have the most significant clinical impact, and this is followed by those identified by robust rescue effect (step 3), molecular survival of the fittest (step 1), oncogene rescuer screening (step 4), and vulnerable gene screening (step 2).

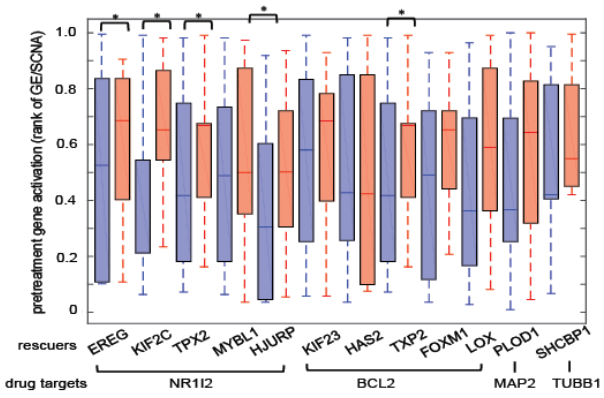
pretreatment gene activation (rank of GE/SCNA)
rescuers
EREG
KIF2C
TPX2
MYBL1
HJURP
KIF23
HAS2
TXP2
FOXM1
LOX
PLOD1
SHCBP1
drug targets
NR1I2
BCL2
MAP2
TUBB1

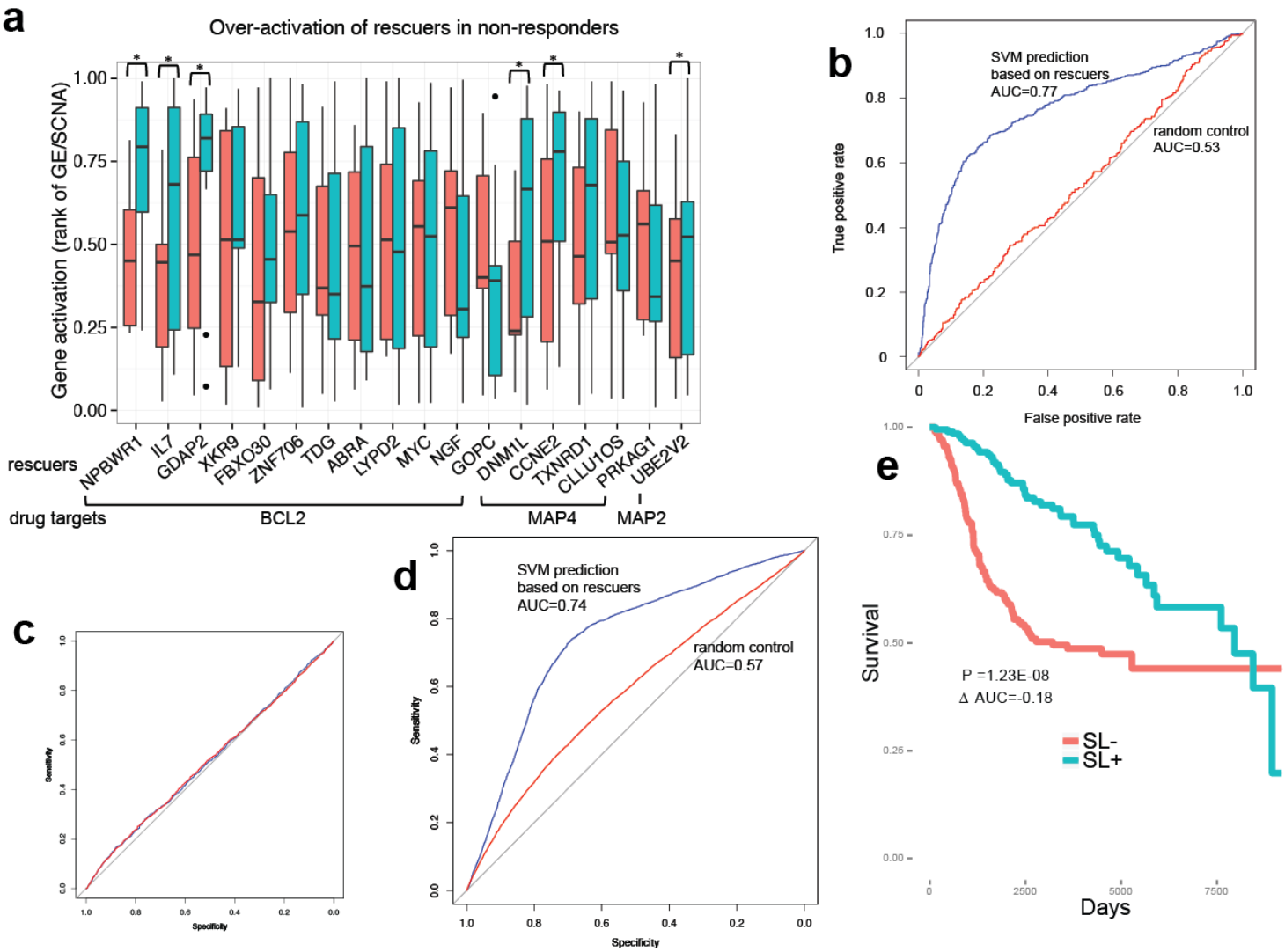
a
Over-activation of rescuers in non-responders
Gene activation (rank of GE/SCNA)
rescuers
NPBWR1
IL7
GDAP2
XKR9
FBXO30
ZNF706
TDG
ABRA
LYPD2
MYC
NGF
GOPC
DNM1L
CCNE2
TXNRD1
CLLU1OS
PRKAG1
UBE2V2
drug targets
BCL2
MAP4
MAP2
b
SVM prediction
based on rescuers
AUC=0.77
random control
AUC=0.53
True positive rate
False positive rate
c
Sensitivity
Specificity
d
SVM prediction
based on rescuers
AUC=0.74
random control
AUC=0.57
Sensitivity
Specificity
e
Survival
P =1.23E-08
Δ AUC=-0.18
SL-
SL+
Days

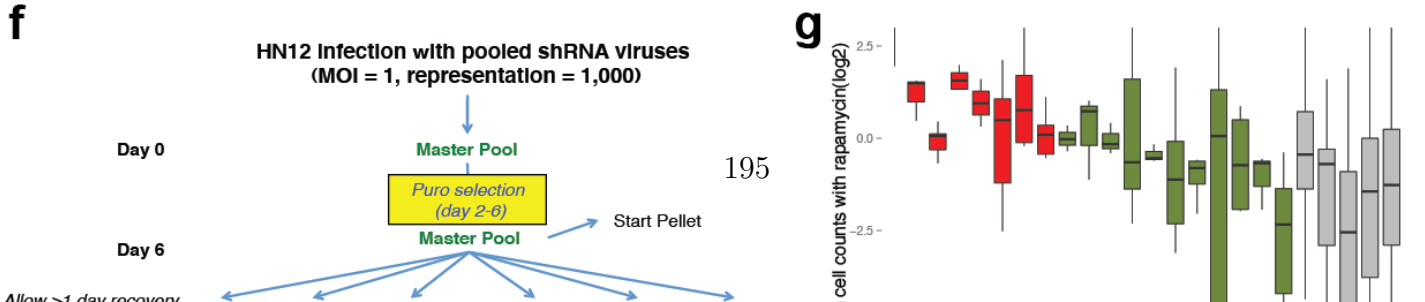
f
HN12 infection with pooled shRNA viruses
(MOI = 1, representation = 1,000)
Day 0
Master Pool
Puro selection
(day 2-6)
Start Pellet
Day 6
Master Pool
g
cell counts with rapamycin(log2)

Figure B.5: Extended Data Figure 5. (a,c) Synthetic rescue interaction in ovarian cancer dataset: (a) Rescuers are up regulated in non-responders: We compared activation of 18 rescuer genes (of the treatment drugs 3 targets) in non-responders (blue) vs. responders (red) before primary treatments. Ranksum p-values denote significant non-responder vs. responder expression differences. Significant genes are marked by stars (ranksum p-value$<$0.05). (b) A binary classifier based on pre-treatment rescuer gene expression predicts patient relapse among 32 initial responders (AUC=0.77 (blue), vs. AUC=0.53 (red) for an 18-gene random classifier). (c) Pre-treatment SL partners expression is insufficient to predict future relapse among initial responders in ovarian cancer. An ROC plot showing the prediction accuracy obtained by a linear SVM based on 18 SL partners (AUC=0.52) compared to the accuracy obtained based on 18 random genes (red line, AUC=0.52) in ovarian cancer. (d) Pre-treatment rescuers expression successfully predicts future relapse among initial responders in breast cancer. An ROC plot in breast cancer shows the prediction accuracy obtained by a linear SVM (AUC=0.74) compared to the accuracy obtained based on 13 random genes (red line, AUC=0.57). (e) Clinical significance of SL pairs identified by INCISOR Patients were scored based on number of functionally active SL pairs. Kaplan-Meier analysis shows the survival of patients who belong to top 10 percentile (SL+) is better than the survival of those belonging to bottom 10 percentile (SL-). (f-g) Experimental shRNA screening validates (DD) rescue effects of mTOR. (f) Summary of pooled shRNA experiment. Time points, treated and control samples are explained in the figure. (g) 19 predicted vulnerable partners for mTOR are knocked down using shRNA. Next, Rapamycin is used to inhibit mTOR. The vertical axes show fold change in cell counts after versus before Rapamycin treatment (i.e., in the non-rescued versus the rescued state). SR partners of mTOR are compared to several control genes that are not in SR pairs with mTOR.

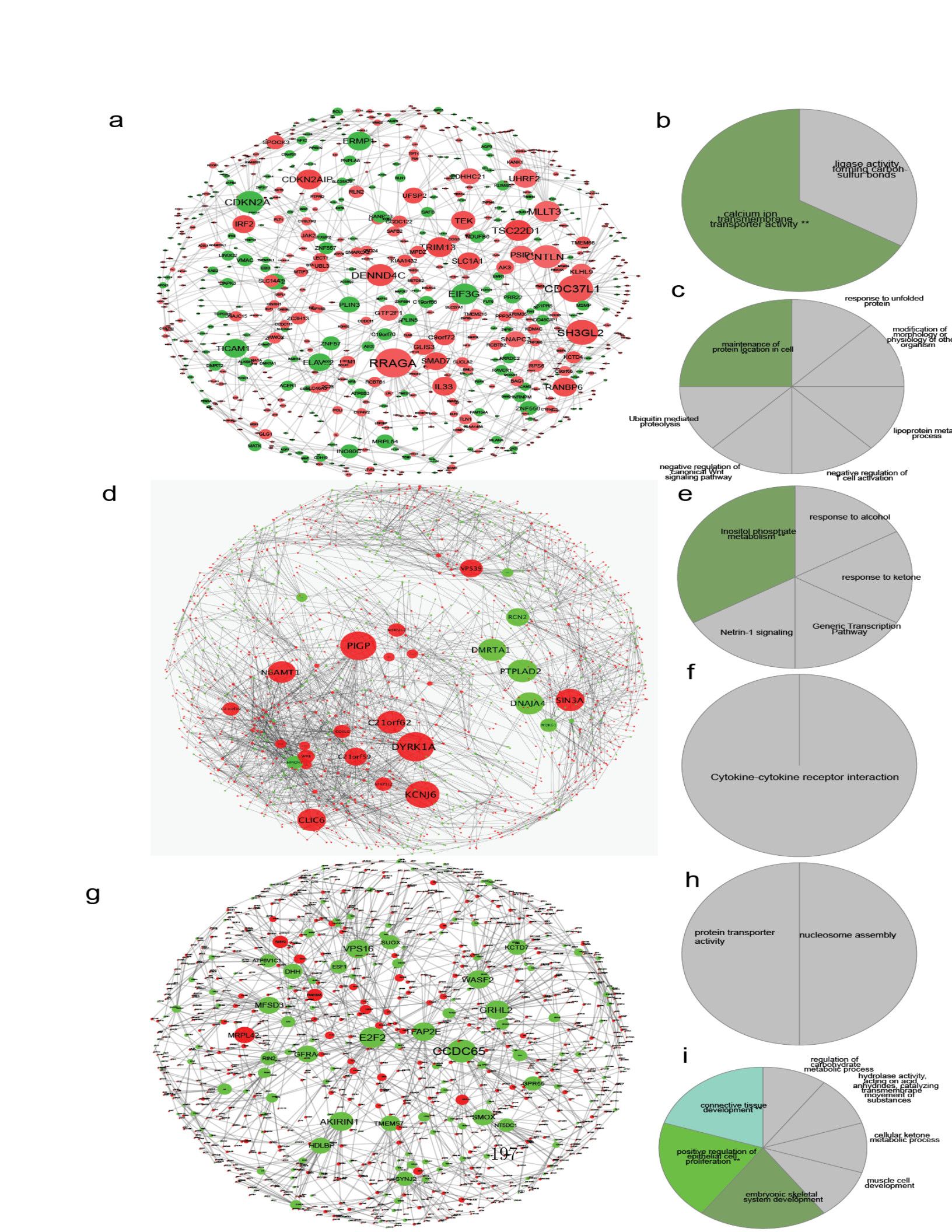
a
b
ligase activity forming carbon-sulfur bonds
calcium ion transmembrane transporter activity **
c
response to unfolded protein
modification of morphology or physiology of other organism
maintenance of protein location in cell **
Ubiquitin mediated proteolysis
lipoprotein meta process
negative regulation of canonical Wnt signaling pathway
negative regulation of T cell activation
d
e
response to alcohol
Inositol phosphate metabolism **
response to ketone
Netrin-1 signaling
Generic Transcription Pathway
f
Cytokine-cytokine receptor interaction
g
h
protein transporter activity
nucleosome assembly
i
regulation of carbohydrate metabolic process
hydrolase activity, acting on acid anhydrides, catalyzing transmembrane movement of substances
connective tissue development
cellular ketone metabolic process
positive regulation of epithelial cell proliferation **
muscle cell development
embryonic skeletal system development

Figure B.6: DD-type SR network and functional characterization (a) The figure depicts synthetic rescues network with 531 vulnerable genes (green), 422 rescuer genes (red) encompassing 977 interactions. Red denotes vulnerable genes and green denoted rescuers genes, while the size of nodes indicates their degree in the network, such that large nodes point to major vulnerable and rescuer hub genes. (b) Vulnerable genes are enriched with transmembrane ion transport signaling. (c) Rescuers are enriched protein location processes, WNT signaling, T cell regulation, protein folding and proteolysis. (d-f) UD-type SR network and functional characterization (d) The figure depicts synthetic rescues network with 1134 vulnerable genes, 789 rescuer genes (red) encompassing 2637 interactions. Red denotes vulnerable genes and green denoted rescuers genes, while the size of nodes indicates their degree in the network, such that large nodes point to major vulnerable and rescuer hub genes. (e) Gene enrichment analyses of vulnerable genes. (f) Gene enrichment analyses of rescuer genes. (g-i) UU-type SR network and functional characterization (g) The figure depicts synthetic rescues network with 1083 vulnerable genes, 430 rescuer genes (red) encompassing 1515 interactions. Red denotes vulnerable genes and green denoted rescuers genes, while the size of nodes indicates their degree in the network, such that large nodes point to major vulnerable and rescuer hub genes. (h) Gene enrichment analyses of vulnerable genes. (i) Gene enrichment analyses of rescuer genes.

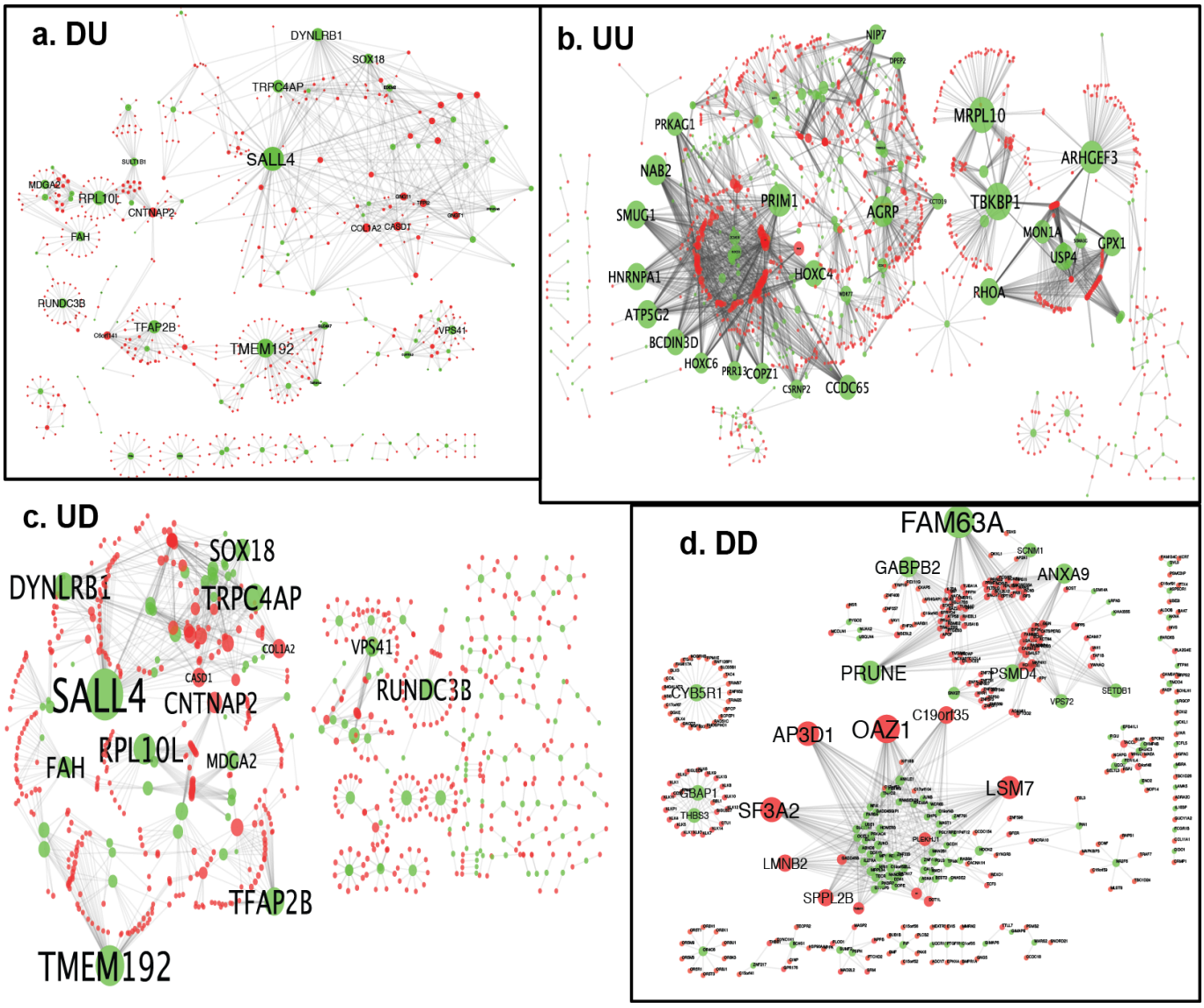
a. DU
DYNLRB1
SOX18
TRPC4AP
SALL4
MDGA2
RPL10L
CNTNAP2
FAH
COL1A2
CASD1
RUNDC3B
TFAP2B
TMEM192
VPS41
b. UU
NIP7
PRKAG1
NAB2
SMUG1
PRIM1
AGRP
HNRNPA1
HOXC4
ATP5G2
BCDIN3D
HOXC6
PRR13
COPZ1
CSRNP2
CCDC65
MRPL10
ARHGEF3
TBKBP1
MON1A
GPX1
USP4
RHOA
c. UD
SOX18
DYNLRB1
TRPC4AP
COL1A2
SALL4
CASD1
CNTNAP2
FAH
RPL10L
MDGA2
TFAP2B
TMEM192
VPS41
RUNDC3B
d. DD
FAM63A
GABPB2
ANXA9
PRUNE
PSMD4
SETDB1
VPS72
CYB5R1
C19orf35
AP3D1
OAZ1
GBAP1
THBS3
SF3A2
LSM7
LMNB2
SPPL2B

Figure B.7: BC-SR network and its functional characterization. (a) DU: The figure depicts synthetic rescues network among 433 vulnerable genes (green) and 583 rescuer genes (red), encompassing 2298 interactions. Rescuers are enriched with lipoprotein metabolism and G-protein coupled and chemokine receptor pathways. Vulnerable genes are enriched with linoleic acid metabolism and IL2 signaling pathway. (b) UU: The figure depicts synthetic rescues network with 1056 vulnerable genes (green), 311 rescuer genes (red) encompassing 3096 interactions. Rescuers are enriched with negative regulation of immune response and histone phosphorylation. Vulnerable genes are enriched with GTPase activity and extracellular matrix organization. (c) UD: The figure depicts synthetic rescues network with 635 vulnerable genes (green), 176 rescuer genes (red) encompassing 1189 interactions. Rescuers are enriched with cell morphogenesis. Vulnerable genes are enriched with cytochrome P450 and fatty acid metabolism. (d) DD: The figure depicts synthetic rescues network with 244 vulnerable genes (green), 110 rescuer genes (red) encompassing 781 interactions. Rescuers are enriched with proteasome complex and IL6 pathway. Vulnerable genes are enriched with protein folding and methytransferase.

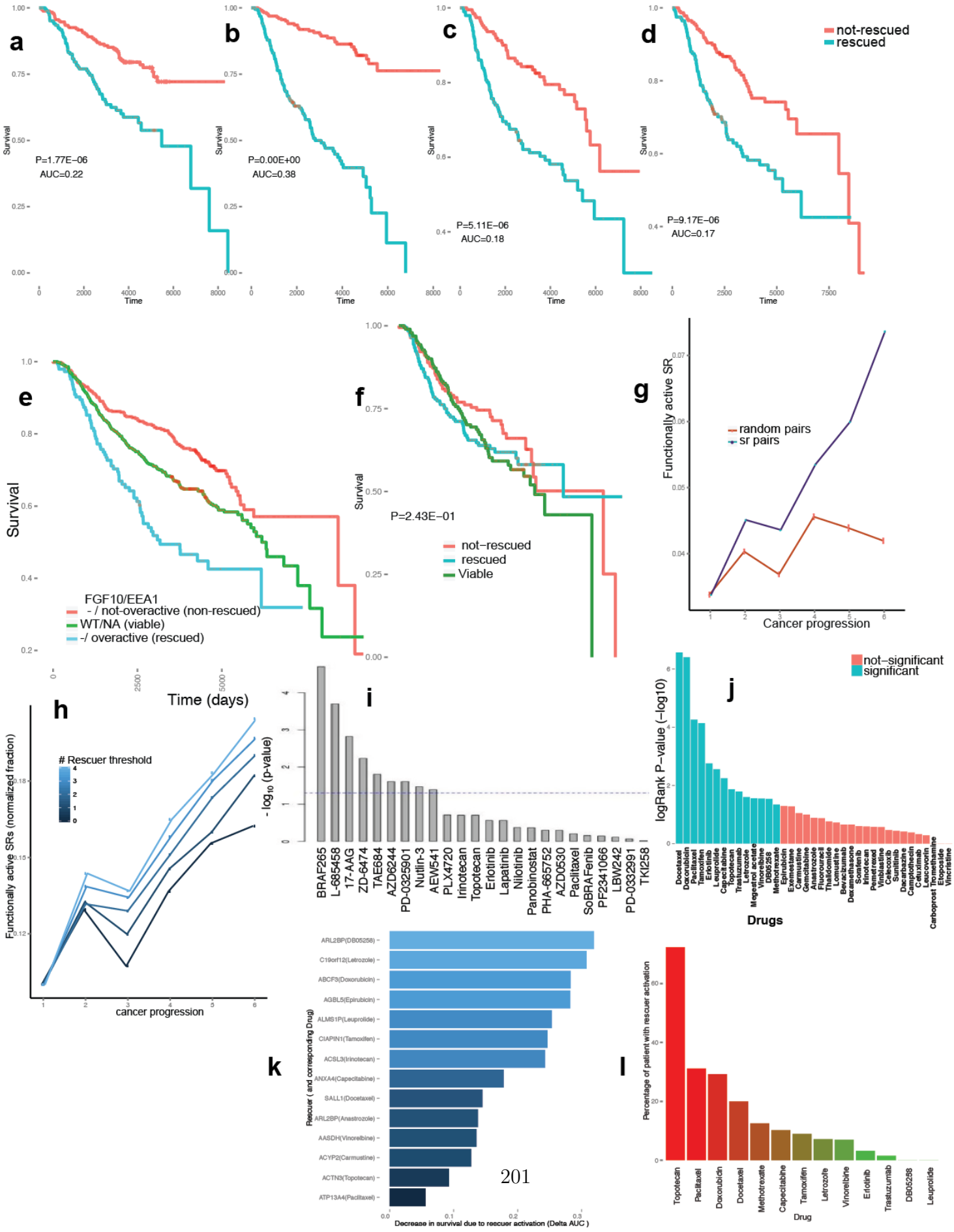
a
P=1.77E−06
AUC=0.22
b
P=0.00E+00
AUC=0.38
c
P=5.11E−06
AUC=0.18
d
P=9.17E−06
AUC=0.17
not-rescued
rescued
Survival
Time
e
FGF10/EEA1
- / not-overactive (non-rescued)
WT/NA (viable)
-/ overactive (rescued)
f
P=2.43E−01
not−rescued
rescued
Viable
g
random pairs
sr pairs
Functionally active SR
Cancer progression
h
Time (days)
Rescuer threshold
Functionally active SRs (normalized fraction)
cancer progression
i
- log10 (p-value)
BRAF265
L-685458
17-AAG
ZD-6474
TAE684
AZD6244
PD-0325901
Nutlin-3
AEW541
PLX4720
Irinotecan
Topotecan
Erlotinib
Lapatinib
Nilotinib
Panobinostat
PHA-665752
AZD0530
Paclitaxel
SoBRAFenib
PF2341066
LBW242
PD-0332991
TKI258
j
not−significant
significant
logRank P−value (−log10)
Drugs
k
Rescuer (and corresponding Drug)
ARL2BP(DB05258)
C19orf12(Letrozole)
ABCF3(Doxorubicin)
AGBL5(Epirubicin)
ALMS1P(Leuprolide)
CIAPIN1(Tamoxifen)
ACSL3(Irinotecan)
ANXA4(Capecitabine)
SALL1(Docetaxel)
ARL2BP(Anastrozole)
AASDH(Vinorelbine)
ACYP2(Carmustine)
ACTN3(Topotecan)
ATP13A4(Paclitaxel)
Decrease in survival due to rescuer activation (Delta AUC)
l
Percentage of patient with rescuer activation
Topotecan
Paclitaxel
Doxorubicin
Docetaxel
Methotrexate
Capecitabine
Tamoxifen
Letrozole
Vinorelbine
Erlotinib
Trastuzumab
DB05258
Leuprolide
Drug

Figure B.8: a-d) Clinical significance of 4 types of SR interactions in breast cancer: The Kaplan Meier (KM) plot depicts the difference in clinical prognosis between patients with rescued tumors (>90-percentile of number of functionally active SR pairs, blue) vs patients with non-rescued (<10- percentile of number of functionally active SR, red) samples. As predicted, a large number of functionally active rescuer pairs renders significantly marked worse survival based on all four different SR networks: (a) DD, (b) DU (c) UD and (d) UU. The logrank p-values and ΔAUC are marked, and DU shows the strongest clinical significance. (e) Illustration of effect of non-rescued, viable and rescued states on survival due to SR interaction between FGF10 (vulnerable gene) and EEA1 (rescuer gene) SR interaction. Patients were divided based on state of FGF10/EEA1 SR interaction: i) in viable state EEA1 was WT in patients, ii) in non-rescued state EEA1 was inactive and FGF10 was not over-active, and iii) in rescued stated EEA1 was inactive and FGF10 was over-active. (f) Rescue effect of SR network is due to interaction: Shuffling the vulnerable genes in SR network and KM analysis similar to Figure 4.5e. (g-h) The functional activity of SR increases as cancer progresses. (g) The number of functionally active SRs (green) and random gene pairs (red) as cancer progresses. (h) The number of rescued inactive vulnerable genes with varying number of active rescuers (from single rescuer with darkest blue line to five rescuers with the lightest blue line) as cancer progresses. (i-l) The breast cancer SR-DU network predicts drug response in cell lines and cancer patients. (i) The rescuer activity profiles of individual cell-lines predict drug response of 9 out of 24 drugs. We compared the experimentally measured drug response (IC50 values) between predicted rescued vs. non-rescued cell lines using a ranksum test. The horizontal axis represents the 24 drugs in CCLE database, and the vertical axis denotes the ranksum p-values. (j) The rescuer activity profiles successfully predict the survival of patients whose tumors are rescued vs. those whose tumors are non- rescued (the latter patients have better survival) for 15 out of 37 drugs as quantified by a logrank test. The horizontal axis lists the 37 drugs in TCGA BC dataset, and the vertical axis represents the logrank p-values examining the separation between predicted rescued and non-rescued tumors. (k) The expected clinical impact of rescuer genes knockdown: Key rescuer genes and their corresponding drugs (in parenthesis) are listed on the vertical axis, and the expected clinical benefit of the rescuer knockdown is presented in the horizontal axis. The clinical impact was measured by comparing the survival of drug-treated patients with and without the corresponding over-active rescuer (l) The likelihood of developing drug resistance: The probability of developing SR mediated resistance (vertical axis) for each drug (horizontal axis) is estimated by the fraction of samples that have non-zero over-activation of rescuers.

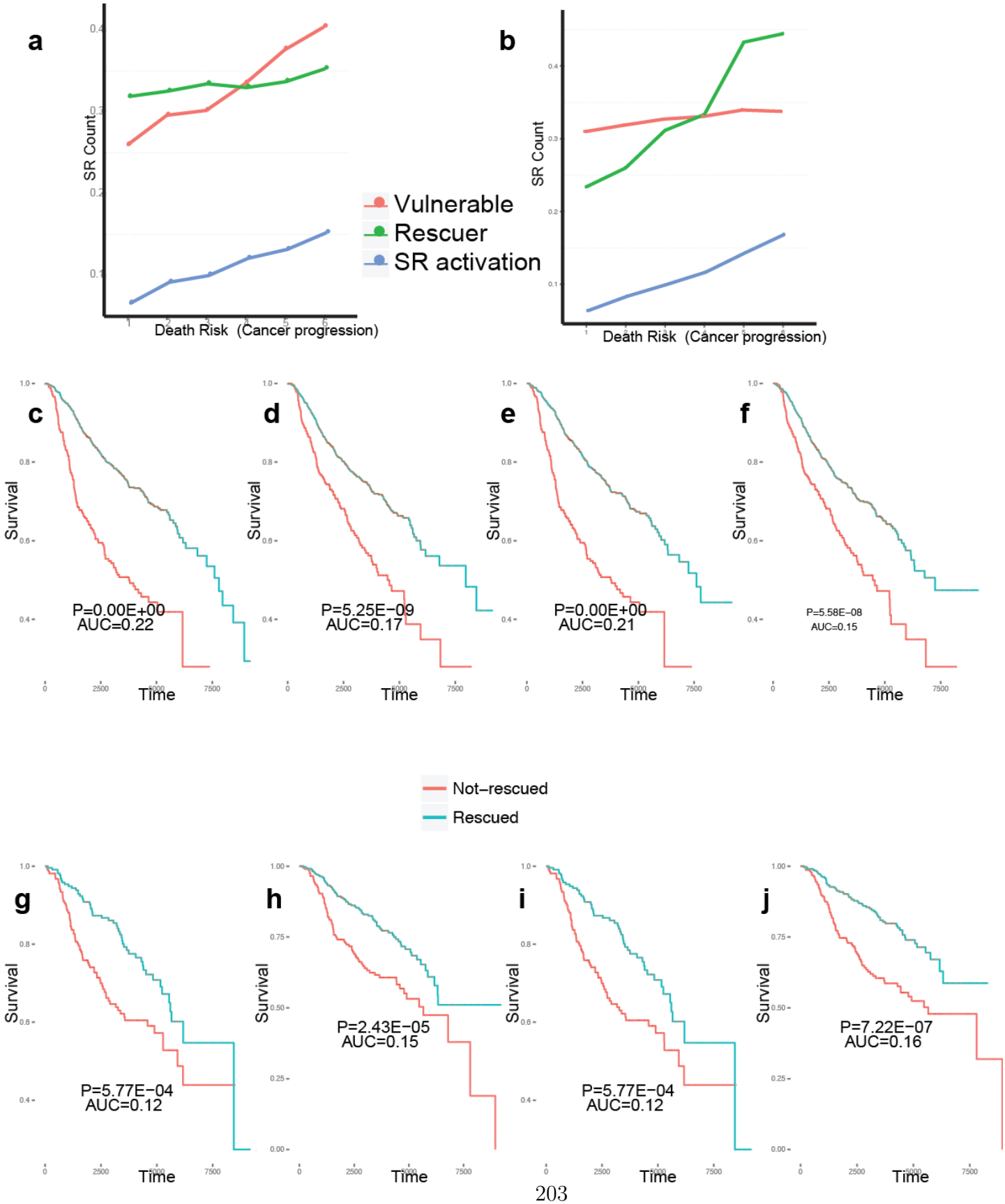
a
b
SR Count
Death Risk (Cancer progression)
Vulnerable
Rescuer
SR activation
c
d
e
f
Survival
Time
P=0.00E+00
AUC=0.22
P=5.25E−09
AUC=0.17
P=0.00E+00
AUC=0.21
P=5.58E−08
AUC=0.15
Not−rescued
Rescued
g
h
i
j
P=5.77E−04
AUC=0.12
P=2.43E−05
AUC=0.15
P=5.77E−04
AUC=0.12
P=7.22E−07
AUC=0.16

Figure B.9: (a-b) Characterization of rSR and bSR. (a) We identified rSR by selecting SR pairs whose rescuer activation (green) consistently drives the functional activation of SR (blue) as cancer progresses. (b) We identified bSR pairs by selecting SR pairs whose vulnerable gene inactivation (red) drives the functional activation. (c-j) Clinical impact of rSR and bSR (c,d) The KM plots depict the patients with highly rescued tumors (red; >90 percentile) have worse survival than the patients with lowly rescued tumors (blue; <10 percentile). The rSR shows more significant clinical rescue effect (logrank p- value<1E-300) than bSR (logrank p-value <1E-8) in comparison to rescuer controls (g) and (h). (e,f) The KM plots depict the difference in the survival between two groups of patients whose tumors are highly vulnerable (red; >90 percentile) vs. lowly vulnerable (blue; <10 percentile) given over-activation of rescuer genes. The rSR shows more significant impact (logrank p-value<1E-300) than bSR (logrank p-value <1E- 8) in comparison to vulnerable controls (i) and (j).

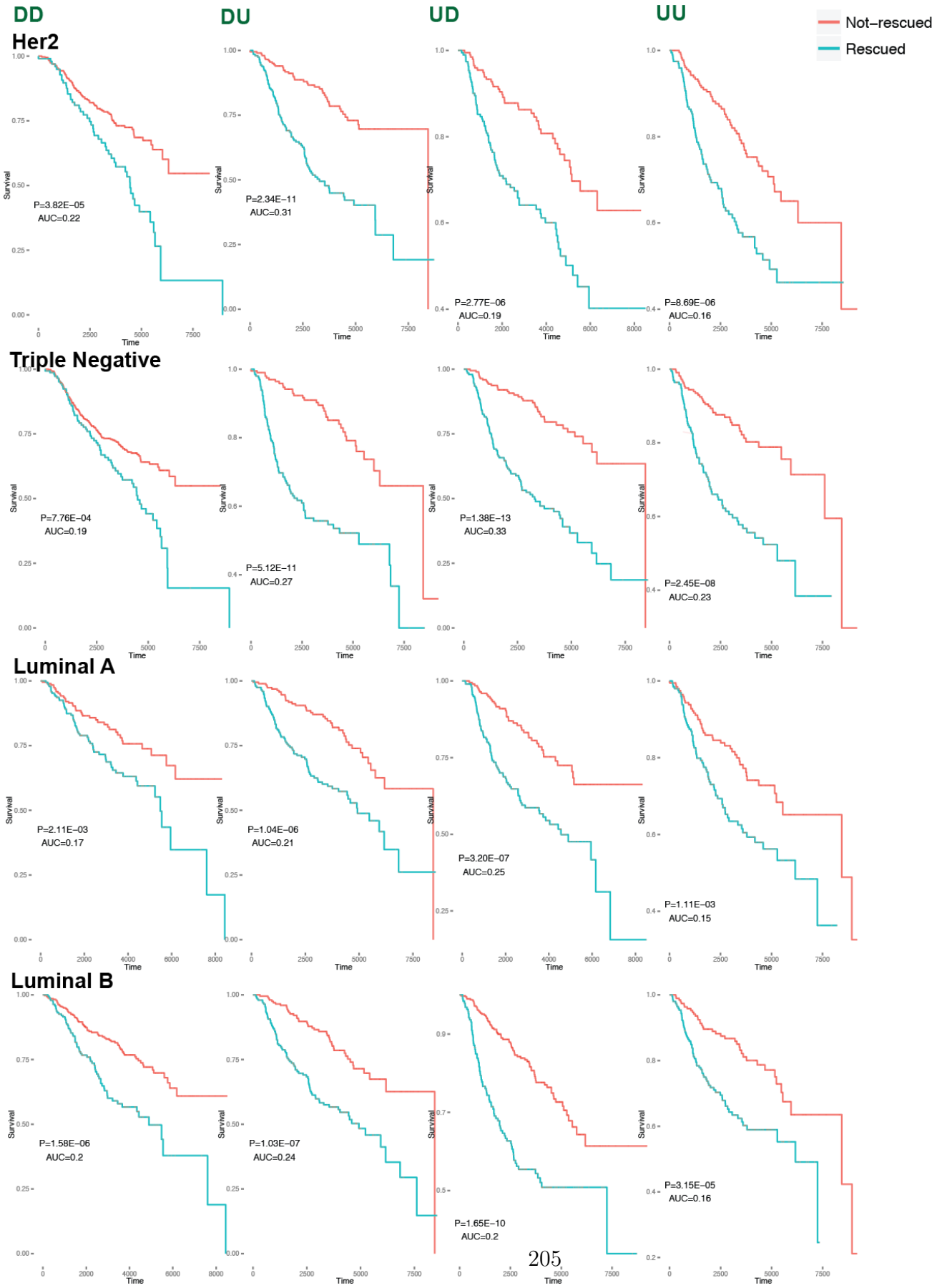
DD
DU
UD
UU
Not−rescued
Rescued
Her2
P=3.82E−05
AUC=0.22
P=2.34E−11
AUC=0.31
P=2.77E−06
AUC=0.19
P=8.69E−06
AUC=0.16
Triple Negative
P=7.76E−04
AUC=0.19
P=5.12E−11
AUC=0.27
P=1.38E−13
AUC=0.33
P=2.45E−08
AUC=0.23
Luminal A
P=2.11E−03
AUC=0.17
P=1.04E−06
AUC=0.21
P=3.20E−07
AUC=0.25
P=1.11E−03
AUC=0.15
Luminal B
P=1.58E−06
AUC=0.2
P=1.03E−07
AUC=0.24
P=1.65E−10
AUC=0.2
P=3.15E−05
AUC=0.16
Survival
Time

Figure B.10: Clinical significance of SR network in breast cancer subtypes The KM plot depicting the differences in clinical prognosis between rescued (>90-percentile of number of functionally active SR, blue) vs non-rescued (<10-percentile of number of functionally active SR, red) samples in her2 subtype (first row), triple-negative (second row), luminalA (third row), and luminalB (fourth row). The high fraction of rescue renders worse survival in all 4 different types of SR: DD (first column), DU (second column), UD (third column), and UU (fourth column). Their logrank p-values and the ΔAUC are represented.

The INCISOR pipeline

INCISOR identifies candidate synthetic rescue (SR) interactions with four independent statistical tests, each tailored to test distinct properties of SR pairs. We describe here in detail the identification procedure of four types of SR interaction (Extended Data Figure 1f).

Molecular survival of the fittest (SoF) (Step 1):

To reliably define the activity of a gene, we used gene expression (GE) and somatic copy number alteration (SCNA). A gene is inactive (respectively, overactive) if its expression level is less (greater) than the 20th-percentile (80th-percentile) across samples and its SCNA is less (greater) than -0.1 (0.1). A gene has its normal activation level if its expression level is between the 25th and 75th percentile (across samples).

To identify an SR pair from cancer molecular data, we performed the following four Wilcoxon tests, examining all possible pairs of a vulnerable gene V and a rescuer gene R.

For DU (DD) type, we confirmed if: (a) the SCNA levels of vulnerable gene V are not significantly different in samples with wild-type levels of rescuer R from its levels in samples where rescuer R is inactive (respectively, over-active) [Test I]; (b) the SCNA levels of vulnerable gene V are significantly lower (higher) in the samples where rescuer gene R is over-activated (inactivated) than in the samples where

rescuer R is inactivated (over-activated) [Test II] and in the samples with wild-type levels of rescuer gene R [Test III] test I, III distinguish DU- (DD-) type SR from SL (SDL); and (c) the SCNA levels of rescuer genes R are significantly higher (lower) in samples when the vulnerable gene V is inactive compared to samples where gene V is not inactive [Test IV]. (Here SDL stands for synthetic dosage lethality, where over-activation of one gene renders lethality to another gene.)

For UU (UD) type, we confirmed if: (a) the SCNA levels of vulnerable gene V are not significantly different in samples with wild types levels of rescuer R from its levels in samples where rescuer R is inactive (over-active) [Test I]; (b) the SCNA levels of vulnerable gene V are significantly higher (lower) in the samples where rescuer gene R is over-activated (inactivated) than in samples where rescuer R is inactivated (over-activated) [Test II] and in the samples with wild-type levels of rescuer gene R [Test III]; and (c) the SCNA levels of rescuer genes R are significantly higher (lower) in samples when the vulnerable gene V is overactive compared to samples where gene V is not overactive [Test IV].

For each type, we performed, analogously, four Wilcoxon tests examining the corresponding activity of candidate genes V and R at the gene-expression level. The molecularly inferred SR candidates were defined as those gene pairs that pass all 4 tests.

Vulnerable gene screen (Step 2)

This step tests whether the candidate vulnerable gene A is actually lethal when not specifically rescued by candidate rescuer gene B: we performed two Kaplan-Meier (KM) analyses testing if vulnerable gene A inactivation for DU/DD (over-activation for UU/UD) without rescue improves patient survival [test I]; and if vulnerable gene A inactivation for DU/DD (over-activation for UU/UD) with rescue decreases patient survival [test II]. Specifically, we calculated ΔAUC due to vulnerable gene A inactivation in DU/DD (over-activation in UU/UD) for the patients with rescuer B over-activated in DU/UU (inactivated in DD/UD), and for the patients where rescuer gene B is not over-activated in DU/UU (not inactivated in DD/UD), and then we calculated the difference in the ΔAUCs. Gene pairs with top 25percentile of these differences were selected as final SR pairs.

Robust rescue effect (Step 3):

This step selects the candidate gene pairs that provide consistently high predictive patient survival signal across multiple datasets and across multiple cancer types. For DU-type, we compared the survival of rescued inactive vulnerable gene A (rescuer gene B over-activated; state 3 in Extended Data Figure 1a) vs non-rescued gene A (states 1, 2). For DD-type, we compared the survival of rescued inactive vulnerable gene A (rescuer gene B inactive; state 1) vs non-rescued gene A (states 2, 3). For UU-type, we compared the survival of rescued over-active vulnerable gene A (rescuer gene B over-activated; state 9) vs non-rescued gene A (states 7, 8). For

UD-type, we compared the survival of rescued over-active vulnerable gene A (rescuer gene B inactive; state 7) vs non-rescued gene A (states 8, 9). The extent of decrease in survival of rescued samples from non-rescued is termed as rescue effect. We aggregated the results over 50 bootstraps of the samples set to identify robust rescue effect across datasets [221].

Oncogene rescuer screen (Step 4):

This step tests whether the rescue effect observed so far for a given pair A-> B is mediated by true synergy between the genes as desired or is just a false positive effect caused by a single gene, candidate rescuer B, that is not pair specific. For each candidate rescuer gene B we calculated its rescue effect (ΔAUC) when each of the candidate vulnerable genes is inactivated for DU/DD-types (over-activated for UU/UD-types). For the analyses only those SR pairs that show significant rescue after FDR correction are considered. The top 10-percentile of vulnerable genes A among those vulnerable genes with significant rescue effect was labeled as having synergistic effect with the rescuer gene B.

Pan-cancer KM analyses: combining survival analysis of different cancer types.

INCISOR was applied to pan-cancer TCGA (the Cancer Genome Atlas) data [76], and breast cancer and its four subtypes. For pan-cancer analysis INCISOR tailors a log-rank statistical test for the three survival analyses (steps 2-4) to ac-

count for differences in survival time between cancer types. Specifically, to compare survival of any two groups, we estimate expected number of deaths in each group for each cancer type separately assuming a hypergeometric distribution. We then sum the cancer-specific estimates of expected and observed number of deaths to infer pan-cancer expected and observed number of deaths. Finally a 2-test comparing the pan-cancer expected and observed deaths gives the final pan-cancer survival difference between any two groups tested. For cancer type-specific analysis (breast cancer (BC) and BC subtypes), we performed a regular log-rank test.

Pan-cancer SR network

DU network

We applied INCISOR to the pan-cancer TCGA data spanning 7,995 samples across 28 different cancer types. SR interactions are overwhelmingly asymmetric, where only 10 genes (ARL2BP, FOXL1, GLDN, JAM2, MT1A, PLEKHM2, SLC19A3, TMEM39B, UACA, UBE3B) are both rescuers and vulnerable genes. The pan-cancer DU-SR network has 2,033 interactions involving 686 rescuer genes and 1,513 vulnerable genes (Figure 4.4a, full network Extended Data Figure 1g interactive network in Supplementary Data 1). We carried out gene enrichment analyses using ClueGO [222] (refer to Supplementary Information Sec 3.1). Vulnerable genes are enriched with cellular process regulation, protein metabolic and developmental processes and the rescuers are enriched with mitotic cellular, macromolecule

metabolic and embryo development processes (Figure 4.4b,c), and in pairwise the inactivation of genes involved in metabolism and adenylate kinase activity is rescued by genes in mitotic cell cycle, and nuclear membrane, respectively (Extended Data Figure 1h). To check whether SR interaction is mediated by physical contact of proteins, we compared a protein-protein interaction (PPI) network [223] and our SR network. We found a small fraction (2.5%) of SR-DU interactions (hypergeometric p-value=0.70) are mediated by physical protein interactions.

If a cellular response to the inhibition of a vulnerable gene results in overactivation of an oncogenic rescuer, such inhibition will be carcinogenic. Indeed, by mining the data of carcinogenic agents and their targets [199,200,224] we found that drugs that inhibit vulnerable partners of known oncogenes [189] are known to be carcinogenic (hypergeometric P<0.03, Supplementary Information). We considered the DU-rescuer oncogenes that have more than 5 vulnerable partners, and identified their association with the drug targets of the carcinogenic agents identified above using DrugBank [210].

Clinical significance of SR DU network across cancer types

To determine clinical significance of DU-type network across different cancer types, we divided the TCGA dataset by half for each cancer type into a training set and a testing set. We first identified SR pairs by applying INCISOR to the training set, and we tested the clinical significance of the pairs by the fraction of SR pairs that are individually significant in testing set. Extended Data Figure 2a shows the fraction of significant SR pairs in each different cancer types. This is a natural way

Factors	coef	exp(coef)	se(coef)	z	Pr(>|z|)	Significance
Synthetic rescue	1.45E-01	1.16E+00	1.85E-02	7.826	5.00E-15	***
Age at diagnosis	1.33E-02	1.01E+00	3.41E-03	3.908	9.30E-05	***
Size	1.30E-02	1.01E+00	1.80E-03	7.182	6.87E-13	***
Lymph nodes positive	6.65E-02	1.07E+00	5.50E-03	12.083	<2.00E-16	***
Genomic instability	1.27E-05	1.00E+00	2.39E-05	0.53	0.5961	
ERBB2	-6.66E-01	5.14E-01	3.34E-01	-1.992	0.0464	*
ESR1	2.34E-01	1.26E+00	9.72E-02	2.402	0.0163	*
ESR2	-5.67E-02	9.45E-01	2.22E-01	-0.256	0.7981	
PGR	-4.71E-01	6.24E-01	2.97E-01	-1.584	0.1132	

Table B.1: Survival Cox regression in METABRIC dataset with features as DU-SR network and other confounding factors. The table summarizes the Cox regression analysis of patient survival based on DU-SR network and other factors in METABRIC dataset. DU-SR is significant ($p - value < 5E - 15$) even after controlling for other confounding factors.

to estimate the clinical significance in each cancer type because many of the cancer types have lower than 200 samples in TCGA.

Clinical significance of SR DU network in other cancer types

In the main text, we identified DU-SR network (and others) using TCGA data, and validated it in an independent METABRIC breast cancer cohort dataset [198]. We compared the survival of patients whose tumors have many vs. few functionally active DU-SRs, and found that rescued tumor samples typically accompany worse patient survival (Figure 2a). This collective clinical significant in METABRIC data is not simply due to lower expression or copy number of the vulnerable genes in the rescued samples. The mRNA expression and SCNA of the 1,513 DU-SR vulnerable genes are in fact higher in non-rescued samples than rescued samples (overall

ranksum P<2.2E-16 for both), and found 108 (166) of them are significantly up-regulated (amplified) and 700 (1,036) of them are significantly down-regulated (lost their copies) in rescued samples (ranksum p-value<0.05). This shows that the clinical rescue effect is not simply mediated by differential activation of the vulnerable partners.

We also tested the clinical significance of the pan-cancer DU-SR network in another independent dataset for an ovarian cancer patient cohort from International Cancer Genome Consortium (ICGC) [225]. We analyzed copy number alteration, gene expression and patient survival data of 81 patients, and compared the survival of rescued vs non-rescued tumor samples. We observed rescued samples show worse survival compared to non-rescued samples (logrank p-value<0.017, ΔAUC=0.4) (Extended Data Figure 2b). We also observed 9.5% of the individual pan-cancer SR-DU pairs show significance (logrank p-value<0.05) in this dataset.

TCGA (single nucleotide) mutation analysis

We examined the TCGA mutation profile to infer causality of SR interaction (DU-type) in pancancer-scale. (The single nucleotide polymorphism mutation profile has not been used in the SR prediction pipeline and hence can serve for independently validating INCISOR predictions.). If the vulnerable genes inactivation leads to selection for rescuer activation, we expect more rescuers will be active (over-expressed and/or increased copy number) when their vulnerable partner suffers deleterious mutation. We tested this hypothesis using TCGA mutation profile that spans 5,031 patients of 23 cancer types, and we considered SR interactions

of 341 genes that have mutations in at least 30 patients. We identified the rescuers of the 341 genes by applying less conservative INCISOR. Using Wilcoxon test, we statistically compared the GE and SCNA of the rescuers in patients with and without vulnerable gene mutations. Indeed, we found that the copy number of rescuers were significantly higher in samples with mutated vulnerable genes than without such mutation (Wilcoxon P <1.2e-100). The expression of rescuer genes was also significantly higher in samples with mutations in vulnerable genes than in those where they are intact (Wilcoxon P < 1.1E-17). Overall, 81% of 341 mutated vulnerable genes showed higher copy number of rescuers in the event they were mutated; with 33% of the genes having such a statistically significant increase in their rescuers copy number (Wilcoxon $p < 0.05$). Only 2.8% of the genes showed statistically significant decrease in rescuers copy number. In terms of mRNA, 17% of the mutated vulnerable genes showed significant under-expression of corresponding rescuers. Extended Data Figure 2c shows the key vulnerable genes, when mutated, whose rescuers show significant increase both in copy number and gene-expression. Extended Data Figure 2d shows the key rescuer genes that show significant increase both in copy number and gene-expression when their vulnerable gene partners are mutated.

Interestingly, we also identified 7 vulnerable genes whose rescuers have significantly lower copy number variation in mutated samples. We suspected that somatic mutations in these 7 genes might increase its activity. Indeed we found that 3 genes mutations are significantly associated with higher copy number variation or higher gene-expression. In particular, samples with mutations in GATA3 have both higher

copy number and gene expression variance.

Our analysis revealed that CDH11, a membrane protein that mediates cell-cell adhesion and is related to ERK signaling pathways [226], is highly rescued when mutated. It was mutated in 2.1% of TCGA samples. INCISOR predicts IFT172 and MSH2 as DU rescuers of CDH11. MSH2 protein is part of mismatch repair complex (MutS), whose deregulation is associated with emergence of drug resistance. In samples where CHD11 is mutated, these rescuers shows significant increase in copy number (Wilcoxon P<2.6E-6) and expression (Wilcoxon P<0.03). To investigate whether the cells are indeed functionally rescued by over-expression of rescuers genes, we examined the patients with CDH11 mutation and compared the survival of these patients when rescuers of CDH11 are highly activated to their survival when they are not. As anticipated, patients whose inactivated CHD11 is rescued show much poorer survival (Extended Data Figure 2e). This analysis demonstrates that a somatic mutation that inactivates a key cancer driver gene can be buffered/rescued by activation of rescuer genes.

Cancer-drug DU SR network

In identifying the original genome-wide SR-DU network, we have applied a very conservative criterion (FDR < .01 wherever applicable) at each steps of INCISOR. As a result, the network contained only 2033 interactions (6.2E-4 % of all possible gene pairs), leaving out many potential rescuers of many drug targets. To capture DU-type rescuers of anti-cancer drug targets in a more comprehensive manner we modified INCISOR as follows: (i) Vulnerable gene screening was eliminated

(because gene targets are by definition known to inhibit cancer progression) (ii) An FDR correction was applied only at the last step, and (iii) The SR significance P-value threshold were relaxed to accommodate weaker SR interactions. The resultant network cancer drug SR network (drug-DU-SR) includes the targets of the majority of 37 key cancer drugs administered to patients in TCGA. drug-DU-SR network includes 170 interactions that consists of 103 rescuers of 36 targets (vulnerable genes) of 37 anti-cancer drugs (Figure 4.6d). A pathway enrichment analysis shows the rescuers are highly enriched with lipid storage/transport, thioester/fatty acid metabolism, and drug efflux transporters (Extended Data Figure 2g).

Drug response prediction in breast cancer patients

To verify that DU rescue is an adaptive response of cancer (as opposed to occurring in some cells simply because there is higher basal expression of rescuer genes), we sought to determine if drug treatment stimulates a larger change in rescuer gene expression in clinical non-responder patients versus in responder patients. We used a dataset of 25 breast cancer patients (BC25 dataset) for which expression data was available before and after they were treated with a cocktail of three drugs (epirubicine, cyclophosphamide, and docetaxel), which collectively target four vulnerable genes in our treatment-specific SR-DU network [177]. Remarkably, we found a significantly higher expression fold change (pre- versus post- drug treatment) among the 19 predicted rescuer genes for clinical non-responders vs. responders (17 and 8 patients per group; ranksum p-value<1E-7 when pooling expression of all rescuers across all targets per group; see Extended Data Figure 4a,b for per-target

breakdown). By next re-calculating this fold change metric on a per-rescuer-gene basis, we were able to rank DU pairs (there were 20 total, incorporating the 19 rescuers) by degree of potency (i.e., by their p-values). We found this ranking to be highly consistent with the rescue effect of the same DU pairs calculated using the BC-DU-SR network (as in step 3 of INCISOR) (Spearman =0.54, p<1E-3; see Extended Data Figure 4c), a reassuring cross-check.

Identification of markers to predict drug response is a key challenge. To address this using our insights from the SR expression data, we built an SVM predictor of treatment response of the BC25 patients based on the pre-treatment expression of the 19 rescuer genes (AUC of 0.71, Extended Data Figure 4d). We specifically used the rescuer overexpression profile (a binary vector specifying whether the 19 rescuers are overexpressed or not) as input for the SVM classifier. Feature selection revealed two genes, ATAD2 and PBOV1, that are the most predictive of patient drug responsiveness. ATAD2 is required to induce the expression of a subset of target genes of estrogen receptor including MYC [227], and is also known to be associated with drug resistance to Tamoxifen and 5-Fluorouracil [228, 229]. PBOV1 is overexpressed in prostate and breast cancer, and its knockout was reported to disrupt the emergence of resistance to Taxane treatment in prostate cancer.

Survival prediction in gastric cancer patients

We further studied pre-treatment and post-treatment expression from 22 gastric cancer patients that acquired resistance to chemotheraphy regiment of Cisplatin and Fluorouracil [81]. INCISOR identified 15 rescuers of TYMS gene, a target of

Fluorouracil using pancancer TCGA data. The expression of the rescuers was significantly over-expressed in post-treatment samples compared to the pre-treatment samples (Wilcoxon p $<$ 1.3e-12). Out of 15 rescuers, 11 were significantly over-expressed while the expression of only one rescuer was significantly down regulated ($P < 0.05$, Extended Data Figure 4e). Next, we analyzed a larger cohort of 123 gastric cancer patients treated with Cisplatin and Fluorouracil for which we have the pre-treatment tumors gene expression and the patients progression-free and overall survival rates. Based on the number of highly over-expressed rescuers in each sample, we divided the samples into predicted rescued samples and not-rescued samples. Indeed, we found that overall survival was significantly worse in predicted rescued samples compared with non-rescued samples (Extended Data Figure 4f), and the progression-free survival of the patients was significantly worse in rescued samples as compared to non-rescued samples (Extended Data Figure 4g). Reassuringly, overall-survival and progression-free survival were not associated with randomly chosen rescuer genes (Extended Data Figure 4h,i).

In order to benchmark the four steps of INCISOR, we identified SR pairs individually by each step of SR using TCGA and analyzed their molecular and clinical significance in the gastric cancer dataset. Specifically, for each INCISORs step we ranked all possible DU rescuer of TYMS gene using TCGA pan-cancer data and identified the top 20 most significant DU rescuer genes of TYMS gene for each step separately. We then analyzed the over-expression of predicted rescuer in post-treatment (acquired resistant) samples of gastric cancer relative to pre-treatment samples (Extended Data Figure 4j). Rescuer genes identified by Robust rescue ef-

fect, Oncogene rescuer screening and SoF shows significant over-expression in post-treatment samples. Expectedly rescuer genes identified by Vulnerable gene screening and random genes does not show any over-expression. Next, in order to analyze clinical significance of each rescuer, we analyzed expression and progression-free survival of 123 gastric cancer patients. Analogous to Extended Fig 4f, we compute the decrease in patients progression free survival (ΔAUC) in rescued samples over non-rescued samples separately for each step (Extended Data Figure 4k). The expression of rescuer genes identified by each of the 4 steps predicts progression free survival.

Predicting acquired resistance in breast and ovarian cancer patients

Beyond initial drug response, our overarching hypothesis suggests that SR circuits might contribute to adaptive evolution in tumors after a drug insult, and thus to tumor relapse. To test this, we analyzed longitudinal expression and sequencing data of 81 stage-II, III ovarian cancer patients (OC81 dataset), who were treated with platinum-based therapy and Taxane [179] (Figure 4.7a), focusing on the activation level of Taxanes 18 identified rescuer genes (of its 3 drug targets), which includes MYC known to play an important role in Taxane resistance in ovarian cancer. Here, the gene activation is measured by the rank of gene expression (GE) or SCNA across all samples in the dataset. In line with our previous observations, we first found significantly higher expression of the 18 rescuer genes in initial non-responder versus responder patients (Wilcoxon rank-sum p-value<1.5E-4; expression and copy number were also significantly higher than for random genes, empirical p-value<0.045, Extended Data Figure 5a). Six out of 18 rescuers (respec-

tively, none) showed significant higher (lower) activation in non-responders than in responders (individual Wilcoxon rank-sum p-value<0.05, which is not expected for 18 random genes, empirical p-value<0.036). We then went further and analyzed the patients that initially responded but then relapsed, and found remarkably that rescuer genes became over-active in these relapsed resistant tumors (overall ranksum p-value< 5.8E-5), and to a significantly higher degree than 18 random genes (empirical p-value<4.0E-4, Figure 4.7b). Five out of 18 rescuers (respectively, none) showed significant post-treatment increase in gene activation (decrease) compared to pretreatment (individual Wilcoxon rank-sum p-value<0.05, which is not expected for 18 random genes, empirical p-value<0.05). Characteristically high expression profiles of the 18 rescuer genes at the pretreatment stage gave a clear predictive signal for future emergence of resistance (AUC=0.77 for SVM predictor, Extended Data Figure 5b).

To get more insight into the rescuer-relapse relationship in the OC81 dataset, we examined the rescuer genes that most contributed to the accuracy of our SVM relapse predictor. The most important rescuer, CLLU1OS is known to be up-regulated in chronic lymphocytic leukemia [230], and the second most predictive rescuer, XKR9, plays an important role in apoptosis [231], and the methylation of the third most predictive rescuer, NPBWR1, is a key prognostic factor for lung cancer patient survival [232].

Notably, an analysis of multidrug resistance (MDR) genes expression shows a marked inverse correlation between their activation and the level of rescue reprogramming occurring in Taxane resistant samples (Spearman correlation = -0.63

(p-value<0.03)). Specifically, we considered the gene activation level of 12 MDR genes [211], and the gene expression level of 18 rescuers. Our analysis classifies two different groups of patients who develop resistance through either MDR activation or SR reprogramming (Figure 4.7c).

We further analyzed the expression data of 155 primary breast cancer patients who were treated with Tamoxifen [233], where tumor relapsed in 52 patients within 5 years. With the activity states of 13 rescuers of Tamoxifens 6 drug targets, our binary classifier was able to predict the patients whose tumor will recur (AUC=0.74, Extended Data Figure 5d). The strongest predictor of acquired resistance, RAN, associated with RAS oncogene and androgen receptor (AR), is known to play a role in the resistance to anti-androgen drugs [234]. The third strongest predictor, MAN1C1, is known to be over-activated in cancer cell lines, which would later develop resistance [235]. The function of the second strongest predictor, TMEM200B, a trans-membrane protein, is not known well, indicating its potential role in emerging drug resistance.

It is expected that the synthetic lethal partners of the drug targets will also become active in response to the drug treatment; however, our analysis shows that the activation profile of SL partners does not carry information on tumor relapse. To distinguish the predictive power of SR-DU partners versus SL partners, we built an SVM classifier based on the activity states of 18 SL partners of Taxanes 3 drug targets in ovarian cancer. The accuracy of our classifier was not higher at all compared to the accuracy of 18 random genes (AUC=0.52, Extended Data Figure 5c).

Recent resistance data analysis

Due to the limited number of samples of colorectal, acute myeloid leukemia (AML), prostate cancer, and melanoma in TCGA dataset; we combined samples from all cancer types for identifying DU rescuers of BET, AR, EGFR, and BRAF inhibitors [83, 84, 170–172]. To account for cancer type specific mRNA and CNV differences, we normalized omics data within each cancer types. We then applied INCISOR to the normalized TCGA pan-cancer data.

Gene ontology distance and moonlight gene analysis

In order to estimate functional relationship between a rescuer and its vulnerable gene partner, we used most common gene ontology (GO) distance measure [236], which quantifies semantic similarity between GO terms. When multiple GO terms were associated with a single gene similarity score, maximum similarity score was taken as combined similarity score (when we change the combining method to average we obtain similar significance). For each SR-DU pair (Extended Data Figure 1g), we computed the similarity measure. The significance of the similarity measure was determined with two set of controls: (a) SR-DU pairs were shuffled to break the original SR-DU interaction. (b) Random pairs. For each set of control we determined the similarity measure in analogous manner. Rank-Sum Wilcoxon test provided the significance of similarity. A particularly interesting case involves RPL23, which suppresses tumor progression by stabilizing P53 protein. It is a moonlighting gene [237], having two additional secondary functions as a ribosomal protein

and an inhibitor of cell cycle arrest [238]. A GO analysis of its 12 predicted rescuer partners shows that they include its secondary functions (Table B2).

Deliverables

Cancer-specific Rescuer hubs Targeting the rescuer hubs, the rescuers that have a large number of vulnerable partners, will reduce likelihood of developing resistance and should supplement current chemotherapy. For each cancer type, we identified the rescuer hub whose activation was best associated with a decrease in survival of patients (in TCGA). The list of genes provided in Table B3, can serve as target whose inhibition will reduce the likelihood of developing resistance. ODCI is a rescuer hub in general across cancer types, and specifically kidney cancer, acute myeloid leukemia (AML), and prostate cancer. Its over-expression is known to cause chemoresistance by overcoming drug-induced apoptosis and promoting proliferation [239]. Similarly many other rescuer hubs are reported to be associated with resistance. Interestingly, none of the rescuer hubs are targeted by current anticancer therapies. This may be due to the fact that rescuers become critical for cell proliferation only after vulnerable gene knockdown in cells. This also underscores that targeting rescuers has not been harnessed and SR can provide an entirely new class of drugs.

Second line of therapy against emergence of resistance Currently, there is no mechanistic approach to recommend a second line of therapy in case patients acquire resistance to a therapy. SR network provides a unique opportunity to recommend such therapy based on molecular mechanism. We provide a list of

drug targets rescuers that get over-expressed to bypass progression lethality of drug that can serve as an effective second line of action to the relapsed tumors for each drug (Figure 4.7d). For each drug, we identified a rescuer of the drug target that is most clinically significant.

Estimating the likelihood of emergence of resistance to anti-cancer drug treatments If resistance emerges for a drug through the mechanism of SR activation, then the proportion of patients who have rescuer over-activation will provide a conservative estimate of the likelihood of developing resistance. To that end, for the drug whose response is predicted by the SR network, we estimated the drugs likelihood to foster resistance. Figure 4.7e shows the proportion of patients with an over-activated rescuer for each drug whose response was predicted by the SR network (Figure 4.6e). For each drug this proportion provides the likelihood that a patient treated with the drug will acquire resistance.

SR partners of cancer drivers and metabolic genes Next, we provide a list of SR interactions that involve main oncogenic driver genes. A rescuer or vulnerable partner of a cancer driver gene can play an important role in cancer, specifically in resistance emergence or drug effectiveness. These partner genes might be a viable target for a drug to mitigate cancer progression or resistance. First we compiled a list of oncogenic driver genes from three sources (i) CancerQuest (http://www.cancerquest.org/), (ii) Tumor Portal [240], and (iii) oncogenic drivers and associated genes8, summing up to 327 genes. Next, using the INCISOR pipeline, we identified rescuers of 33 cancer genes, and the vulnerable partners of 32 cancer genes (Table B4).

We also provide a list of SR interactions that involve metabolic genes. Deregulated metabolism is a hallmark of cancer, and their SR partners may play important roles in the process and offer key information on how to counteract cancer progression or resistance. We analyzed the DU-SR network of 1496 metabolic genes using INCISOR pipeline, and identified rescuers of 83 metabolic genes, and the vulnerable partners of 52 metabolic genes (Extended Data Figure 1g).

Pancancer DD, UD and UU networks

Next, we applied INCISOR to pancaner TCGA to identify the genome-wide DD-SR network. The resultant network has 317 interactions that are composed of 159 vulnerable and 197 rescuer genes (Extended Data Figure 6a). Gene enrichment analysis revealed that the vulnerable genes are enriched with processes associated with Tolllike receptor signaling pathways and nerve development (Extended Data Figure 6b). These vulnerable genes are rescued by extracellular matrix disassembly, neuromuscular process and glutathione transferase activity (Extended Data Figure 6c).

In a similar manner, we identified and analyzed the UD (Extended Data Figure 6d, interactive network as Supplementary Data 3) and UU (Extended Data Figure 6g, interactive network available as Supplementary Data 4) SR networks. The UD SR network contains 505 vulnerable genes and 371 rescuer genes, encompassing 926 interactions. The UU SR network contains 169 vulnerable genes and 68 rescuer genes, encompassing 212 interactions. Gene enrichment of the UD network revealed

that vulnerable genes were enriched with processes associated with ion transport and eNOS trafficking (Extended Data Figure 6e), which were rescued by the activation of regulators of biosynthesis process and CD4 T-cell differentiation (Extended Data Figure 6f). On the other hand, in the UU network vulnerable genes were associated with cell cycle (S-phase) and beta-catenin binding (Extended Data Figure 6h); the rescuers were associated with process associated with differentiation cell proliferation (Extended Data Figure 6i).

Pancancer SL network and combined clinical impact of SL and SR

We identified SL interactions in an analogous manner to SR with slight modifications. Since SL is a symmetric interaction, we performed the false positive control of step 3 for both genes, and eliminated step 2 in the INCISOR pipeline. The procedure led to 304 SL pairs with logrank p-value<1.23E-8.

The functional activity of SL and SR networks determines tumor aggressiveness and patient survival. We found that the clinical impact of the combined SR and SL networks is more significant than any of their individual impacts (Figure 4.5f, compare Figure 4.5a-d, Extended Data Figure 5e). We assigned a SL/SR score to each patient, which adds the number of functionally active SL/SRs. We confirmed that the patients (87 samples)with both higher SL score (>90 percentile) and low SR score (<10 percentile) have significantly better survival than the patients (158 samples) with both lower SL score (<10 percentile) and high SR score (>90 per-

centile) (logrank p-value<6.59E-6) . This combined impact is stronger than any single interactions.

Breast cancer SR network

SR networks

We applied INCISOR to TCGA 1098 breast cancer (BC) patient data to identify the four different types of SR networks specific to breast cancer. We have chosen breast cancer as it has the largest numbers of samples in the TCGA collection, and also has a large independent cohort METABRIC on which we could test the emerging predictions in an independent manner. Extended Data Figure 7a shows the resulting BC-DU-SR cancer network, on which we focus most of the section, as it is probably the most intuitive one and, more importantly, it displays the strongest predictive signal, successfully predicting patients survival in METABRIC BC cohort [198].

We next used TCGA BC data to identify DD (Extended Data Figure 7d), UD (Extended Data Figure 7c) and UU (Extended Data Figure 7b) type SR networks that are specific to breast cancer (interactive networks are provided as Supplementary Data 5-8). DD network contains 244 vulnerable genes and 110 rescuer genes, encompassing 781 interactions. UD network contains 635 vulnerable genes and 176 rescuer genes, encompassing 1189 interactions. Finally UU network contains 1056 vulnerable genes and 311 rescuer genes, encompassing 3096 interactions.

Interestingly, BC-DU-SR pairs are enriched with several immune processes: vulnerable genes are enriched for tolerance against natural killer cells (the inactivation of which will make cancer cells more susceptible to the immune system), while rescuer genes are enriched for negative regulation of cytokines (which could subsequently prevent cytokine-driven immune cell recruitment).

UU rescuers are enriched with macromolecular metabolism, and the vulnerable genes are enriched with protein carboxylation (p-value <1E-4). DD vulnerable genes are enriched with zinc-ion response and negative regulation of growth (p-value<1E-5), and DD rescuers are enriched with nitrobenzene metabolism and detoxification (p-value<1E-7). DU vulnerable genes are enriched with chemokine receptor binding and DNA binding (p-value<1E-5), and DU rescuers are enriched with mitochondrial organization and metabolic process (p-value<1E-4). The UD network is associated with immune response: UD vulnerable genes are enriched with antigen processing (p-value<1E-5), and UD rescuers are enriched with T-cell receptor signaling pathway (p-value<1E-3). UU vulnerable genes are enriched with phosphatidylserine metabolism and antigen process (p-value<1E-3), and UU rescuers are enriched with post-translational protein folding and cell-cell adhesion (p-value<1E-3). Interestingly, BC SR-DU shows a strong involvement of immune-related processes : while vulnerable SR-DU genes are enriched with tolerance against natural killer cells (the inactivation of which will increase the cancer cells susceptibility to the immune system), the rescuer genes are enriched with negative regulation of cytokines (which may prevent immune cells from being recruited by cytokines).

Patient survival prediction using SR networks

To generate these SR-dependent survival predictions we quantified the number of functionally active SRs in each tumor sample - that is, the number of DU-SR pairs where a vulnerable gene is inactive and its rescuer partner is over-activated in the given sample. As expected, we find that breast cancer samples with a large number of functionally active pairs have significantly worse survival than samples with fewer active pairs, as the former are rescued (Extended Data Figure 8a-d). This finding is true for each of the other three SR types, albeit to a lesser extent than the DU-SR type. Combining SR with SL interactions slightly improves the survival predictive power further (logrank p-value <1E-300, ΔAUC=0.42).

The three inherent states of SR interaction i.e. viable, non-rescued (lethal) and rescued states display different effects on cancer progression and consequently on patients clinical prognosis (Figure 4.5e). For example, insofar as the SR-DU interaction between a vulnerable gene FGF10 and a rescuer EEA1: patients with either FGF10 WT (viable state) or EEA1 over-activation (rescued state) have lower survival than patients with non-rescued EEA1 knockdown (Extended Data Figure 8e). However, patients with the SR pair in rescued state have even lower survival than those patients in viable state. Similarly, patients whose tumor has many SR pairs in non-rescued state have better survival compared to those patients whose tumor has many SR pairs in viable state. As shown in the main text, patients harboring tumors with extensive SR reprogramming have collectively worse survival than the other two groups of patients (Figure 4.5e), suggesting the three states of

SR have distinct clinical prognoses and are significantly different from each other.

Impact of inactivation of a vulnerable gene can be estimated by comparing the survival of patients in whose tumors the gene is inactivated (non-rescued state) to patients in whose tumors the gene is active (rescued state) (using logrank test). In case a vulnerable gene has more than one rescuer, we collectively compared the patient survival of rescued vs. non-rescued samples. Our analysis shows that the vulnerable genes whose inactivation leads to much better patient survival are more highly rescued in breast cancer. In particular, they have a larger number of rescuer partners (Spearman $= 0.11$, p-value<0.02).

SR levels increase as cancer progresses

To study the dynamics of SR functional activity as cancer progresses, we stratified the BC patients in the METABRIC dataset into six different cancer progression bins by their survival times. As expected, cancer progression is accompanied by an increase in the number of functionally active SRs in the tumors (Extended Data Figure 8g) and by an increase in the number of inactive vulnerable genes that are rescued (Extended Data Figure 8h).

Reprogrammed and buffered SRs

We distinguished between reprogrammed SRs (rSR), where the rescuer gene over-activation occurs after the inactivation of its paired vulnerable gene, to buffered SR (bSR), where the rescuer gene over-activation precedes the inactivation of the

vulnerable gene.

In order to infer if an SR pair is reprogrammed or buffered, we analyzed the fraction of samples with over-active rescuers (fr), inactive vulnerable genes (fv), and functional activation of SR (fSR) at each of 6 cancer progression bins used in Supplementary Information Section 3.3. We classified an SR pairs as an rSR if fr and fSR are highly correlated (Spearman correlation>0.3, p-value<0.05) while fv and fSR are not (Spearman correlation<0 or Spearman correlation p-value>0.05), and fSR is increasing as cancer progresses as shown in Extended Data Figure 9a. Similarly, an SR pair was classified as bSR if fv and fSR are highly correlated while fr and fSR are not (analogous to the conditions for rSR above), and fSR is increasing as cancer progresses (Extended Data Figure 9b).

While in general SRs carry clinical significance irrespective of their order of occurrence (Figure 4.5), rSRs have a significantly stronger survival predictive signal than bSRs (Extended Data Figure 9c-j). We first considered the clinical impact of rSR activation the decrease in survival due to rescuer over-activation given its vulnerable partner is inactivated (which we define as rescue effect in the main text). We confirmed that rSRs have highly significant rescue effect (Extended Data Figure 9c), and this effect arises from the pairwise interaction rather than a consequence of single gene (rescuer) over-activation (Extended Data Figure 9g), demonstrated by much lower p-value and higher ΔAUC ($\Delta(\Delta\text{AUC})$=0.22-0.12). The rescue effect of bSR, conversely, is not much more significant compared to the rescuer control (Extended Data Figure 9d,h).

We then considered the clinical impact of bSR activation the decrease in

survival due to vulnerable gene inactivation given its rescuer partner is already over-active. The inactivation of the bSR vulnerable gene is expected to be inconsequential because its rescuer partner is already over-active. We confirmed that the clinical impact of bSR is indeed minimal (Extended Data Figure 9f,j). However, we still observed a very strong impact of rSR even in this case (Extended Data Figure 9e,i). This means the compensating rescuer activation in response to the loss of the vulnerable gene drives the patient into an even worse state than before the loss. This is consistent with our observation in Figure 2e and Extended Data Figure 8e, and points to the active role of SR in the emergence of drug resistance.

SR networks predict drug response of cancer cell lines and breast cancer patients (TCGA)

We next investigated the ability of the DU-SR network to predict the response of cancer cell lines to treatment with commonly used anticancer drugs. The predictions are obtained in a straightforward unsupervised manner (no training data is involved) by analyzing the cell-lines transcriptomics data to determine cell-line specific gene activity and quantify how many of the SR rescuer partners of the inhibited target(s) of a specific drug tested are over-activated in a given cell line. We analyzed the response of 24 common anti-cancer drugs in 488 cancer cell lines in the CCLE database [65]. The SR network accurately classifies the cell lines into responder and non-responders for 9 drugs (Extended Data Figure 8i).

Next, we used breast cancer DU SR network to predict the clinical response of

3873 (pan cancer) patients in the TCGA dataset, focusing on 37 common anticancer drugs. Using the network and transcriptomics data of cancer patients we classified each patient to be a non-responder (or a responder) to a given drug if one or more of the rescuer partners of that drug target are over-active (and as a responder otherwise). We then compared the survival rates of predicted responders to those of non-responders, to examine how well our predictions separated true responders and non-responders. As demonstrated, we quite accurately classify patients into responder and non-responders for 15 of the drugs (Extended Data Figure 8j).

The SR network can be used to identify key genes, whose targeting will mitigate emergence of resistance in cancer therapies. To this end we provide a list of major rescuers and their expected clinical utility following treatment targeting their associated vulnerable genes (Extended Data Figure 8k), as estimated from their effects on patients survival in the TCGA. Further, by quantifying the number of samples with functionally active rescuers among the patients that receive a specific drug we provide estimates of the likelihood that resistance will emerge following treatment if these rescuers are not targeted, too (Extended Data Figure 8l).

SR buffers the lethal impact of essential genes

We identified the essential genes in breast cancer using the essentiality screening data of their knockdown in cancer cell lines [241]. Specifically, we selected those genes that mark top 5% essentiality score in each cell line for more than 20 out of 30 breast cancer cell lines (N=304). We then checked if their inactivation leads to

better patient survival using mRNA, SCNA and survival data of TCGA BC and METABRIC. We selected 118 nominal essential genes, which are essential in cell line screening but do not significantly improve patient survival when inactivated (logrank p-value>0.5). As control, we selected 124 actual essential genes, which show significance in patient samples (logrank p-value<0.05). A pathway enrichment analysis shows nominal essential genes are enriched with translation initiation and actual essential genes with cell-cycle regulation (hypergeometric p-value<1.3E-4).

We identified the SR-DU rescuers of the nominal and actual essential genes to compare the number of their rescuer partners and clinical significance. We observed nominal essential genes have a higher number of rescuers (t-test p-value<0.03) and higher collective clinical significance (nominal essential genes: logrank p-value<3.5E-10, control logrank p-value<1.2E-5).

We further tested if an advanced tumor shows higher prevalence of the SR pairs specific to the nominal essential genes than the control SR pairs. We selected aggressive breast cancer samples (N=103) from the most advanced progression step in the tumor evolution analysis (Supplementary Information Section 3.3). The SR pairs of nominal essential genes indeed show higher level of activation in advanced tumors than in the control (ranksum p-value<1.1E-9) in a more significant manner than three other groups of tumor samples: early stage breast cancer samples from the earliest progression step, all breast cancer samples in METABRIC, and all other cancer samples in TCGA (ranksum p-value>0.2). In particular, the difference between the clinical impact and essentiality in cell lines measured by the ratio of essentiality to clinical significance, positively correlates with the functional activity

of SR in aggressive tumors (Spearman =0.24, p-value<9.2E-4).

SR partners of cancer associated genes

We analyzed the DU-type rescuer partners of cancer driver genes. Cancer driver genes include the genes strongly associated with cancer that are reported in (http://www.cancerquest.org/) and Tumor Portal42, and strongly clinically relevant genes whenover-active or under-active, based on Kaplan-Meier analysis a total of 45 genes. Using INCISOR pipeline, we identified rescuers of 13 cancer genes in breast cancer (Table B5).

SR partners of cancer associated genes

We analyzed the DU-type rescuer partners of cancer driver genes. Cancer driver genes include the genes strongly associated with cancer that are reported in (http://www.cancerquest.org/) and Tumor Portal42, and strongly clinically relevant genes whenover-active or under-active, based on Kaplan-Meier analysis a total of 45 genes. Using INCISOR pipeline, we identified rescuers of 13 cancer genes in breast cancer (Table B5).

Breast cancer subtypes SR network

We applied our INCISOR pipeline to identify specific SR specific networks for four classical subtypes of breast cancer including Her2, triple-negative, luminal-A, and luminal-B (Supplementary Data 9-24), based on analyzing the TCGA BC data.

In Her2 subtype, DU vulnerable genes are enriched with cell migration and toll-like receptor pathway, and the rescuers are enriched with non-coding RNA metabolism, DNA recombination, and p53 binding. In basal subtype, DU vulnerable genes are enriched with gamma-aminobutyric acid signaling, and the rescuers are enriched with phosphatidylglycerol metabolism. In luminal-A subtype, DU vulnerable genes are enriched with chemokine, cytokine, G-protein coupled receptor pathway, and the rescuers are enriched with lipoprotein receptor pathway and telomere maintenance. In luminal-B subtype, DU vulnerable genes are enriched with dicarboxylic acid catabolism, and rescuers are enriched with cell growth.

The sub-type specific networks derived show significant predictive signal in predicting patients survival (Extended Data Figure 10), even though it is less than the predictive signal of all BC samples together (Extended Data Figure 10, due to the much smaller sample size). Comparing different type of SRs, DU has the highest predictive power in all cancer subtypes.

Identifying treatment-specific SR interactions

To capture DU-type rescuers of the drug targets of each drug treatment dataset, we modified INCISOR as follows: (i) Vulnerable gene screening was eliminated (because gene targets are, by definition, known to inhibit cancer progression) (ii) An FDR correction was applied only at the last step, and (iii) The SR significance P-value threshold was relaxed to accommodate weaker SR interactions. In case the survival data is available in the given drug treatment dataset, we then

quantified the clinical significance of each of the candidate SR (e.g. in case of drug response, survival difference between responders and non-responders or in case of resistance, survival difference of resistant vs sensitive samples). In case survival data was not available, we used relaxed criteria as in the drug-DU-SR network without the cross-validation against METABRIC data. The intersection of clinically significant SR and the SR pairs from each of four steps of our pipeline constitute the final set of SR. If there were no overlaps, thresholds of each step were adjusted such that there was at least one SR in the intersection.

Functional enrichment

For the network level functional enrichment analysis, we used ClueGO [222] (a Cytocscape plugin) with default settings except: (a) GO, KEGG and reactome ontologies were included, (b) network specificity was set to medium, (c) Bonferroni correction for multiple hypothesis correction, (d) Pathways with p-values < 0.05 were included. To perform pairwise GO analysis for an SR network, we first identified GO terms that are enriched in rescuer genes (using standard parameters in GOFunction package [242]). To determine GO processes rescued by a set of rescuers in an enriched GO term, we created a gene set composed of vulnerable partners of the rescuers. Finally, we identified GO terms significantly enriched in the vulnerable gene set (FDR < 0.05).

In-vitro validation in HNSC

To test our ability to predict and experimentally validate a key rescuer gene, we studied the role of mTOR as a predicted rescuer gene in head and neck squamous cell carcinoma (HNSC), where is it thought to play an important role [206]. Rapamycin is a highly specific mTOR inhibitor [207] and hence enables to target a predicted rescuer gene by a highly specific drug, combined with the ability to knock down predicted vulnerable genes in a clinically-relevant lab setting. To this end we studied SR-DD predictions in a HNSC cell-line HN12, which, like most HNSC cells, is highly sensitive to rapamycin [243]. For this we applied INCISOR to identify top 10 vulnerable partners and 9 rescuer partners of mTOR in a pancancer scale. We also identified HNSC-specific DD-type vulnerable partners of mTOR. In addition to the pancancer SRs, we tested the 19 HNSC specific vulnerable DD-SR partners of mTOR.

Extended Data Figure 5f summarizes the experimental procedure. Each of the mTORs vulnerable/rescuer partners together with the controls were knocked down in HN12 cell lines, after which mTOR was inactivated via Rapamycin treatment. HN12 cells were infected with a library of retroviral barcoded shRNAs at a representation of 1,000 and a multiplicity of infection (MOI) of 1, including at least 2 independent shRNAs for each gene of interest and controls. At day 3 post infection cells were selected with puromycin for 3 days (1g/ml) to remove the minority of uninfected cells. After that, cells where expanded in culture for 3 days and then

an initial population-doubling 0 (PD0) sample was taken. For in vitro testing, the cells were divided into 6 populations, 3 were kept as a control and 3 where treated with rapamycin (100nM). Cells where propagated in the presence or not of drug for an additional 12 doublings before the final, PD13 sample was taken. For in vivo testing, cells were transplanted into the flanks of athymic nude mice (female, four to six weeks old, obtained from NCI/Frederick, MD), and when the tumor volume reached approximately 1cm3 (approximately 18 days after injection) tumors where isolated for genomic DNA extraction. Mice studies were carried out according to National Institutes of Health (NIH) approved protocols (ASP 10569 and 13695) in compliance with the NIH Guide for the Care and Use of Laboratory Mice. shRNA barcode was PCR-recovered from genomic samples and samples sequenced to calculate abundance of the different shRNA probes. From these shRNA experiments, we obtained cell counts for each gene knock-down at the following three time points: (a) post shRNA infection (PD0, referred as initial count), (b) shRNA treatment followed by either Rapamycin treatment (PD13, referred as treated count, 3 replicates) or control (PD13, referred as untreated count, 3 replicates) (c) shRNA infected cell injected to mice (tumor, referred as in-vivo count, 2 replicates). To obtain normalized counts at each time point, cell counts of each shRNA at each time point were divided by corresponding total number of cell count.

Since our in vitro experimental analyses were carried out in HNSC cell lines, we also performed experimentally testing for HNSC specific SRs. Specifically, we studied rSR of the HNSC specific DD type as they can be readily validated by in vitro knockdown (KD) experiments. We obtained reversal of rapamycin treatment

when vulnerable partner of mTOR is knocked out (Extended Data Figure 5g; paired Wilcoxon P <1.1E-06 for 19 pairings). This implies rapamycin treatment that is generally not beneficial for tumor progression becomes beneficial when mTORs vulnerable partners are knocked out.

MOONLIGHTING GENE		RESCUER GENES	
RPL23	1. Constructs part of 60S subunit, ribosomal protein 2. Binds to and inhibits a ubiquitin ligase HDM2, which stabilizes of tumor suppressor p53[39]. 3. Binds nucleophosmin and sequesters it in the nucleolus to block its binding to Miz1 (a transcriptional activator and repressor), playing a role in inhibiting cell-cycle arrest[40].	**ARNTL2**	circadian and hypoxia factors
		BCAT1	enzyme catalyzes the reversible transamination of branched-chain alpha-keto acids to branched-chain L-amino acids essential for cell growth
		BHLHE41	control of circadian rhythm and cell differentiation. can interact with ARNTL
		CASC1	Cancer Susceptibility Candidate 1
		FGFR1OP2	Signaling by FGFR
		LMRP	major histocompatibility complex (MHC) class I molecules
		MRPS35	Mitochondrial Ribosomal Protein
		PPFIBP1	axon guidance and mammary gland development. found to interact with S100A4, a calcium-binding protein related to tumor invasiveness and metastasis
		REP15	Regulates transferrin receptor recycling from the endocytic recycling compartment
		STK38L	regulation of structural processes in differentiating and mature neuronal cells.

Table B.2: Synthetic rescue interaction of moonlight gene RPL23. The table lists the 10 rescuer partners of moonlighting gene RPL23, marking the similarity in their cellular processes.

Cancer type	Rescuer	Hub size	Vulnerable partner genes
pancancer	ODC1	16	ATP6V0D1,BBS2,CCDC79,CETP,CMTM4,DDX19A,DHX38,GABARAPL2,GLG1,GNAO1,MT1E,PSMB10,RANBP10,TRADD,TSNAXIP1,VPS4A
CESC	BCL11A	14	CDH16,CES2,COTL1,DHX38,FTSJD1,FUK,KLHDC4,NOL3,PHKB,RNF166,SPATA2L,TK2,TMED6,TMEM208
CHOL	C1orf122	7	ANAPC16,ANK3,ARFGAP2,DNAJB12,GPRIN2,MYBPC3,OR13A1
COAD	APITD1	1	CLRN3
DLBC	C2orf16	13	ARL2BP,CDH5,CES2,CMTM2,DPEP2,FUK,GFOD2,HERPUD1,IL34,LCAT,NRN1L,TRADD,VPS4A
GBM	LRRC69	3	CCDC151,EPOR,RGL3
HNSC	PMFBP1	4	ADAMTSL3,AP3B2,MRPL46,SNURF
KICH	BCL11A	11	CDH16,CES2,DHX38,FTSJD1,KLHDC4,NOL3,PHKB,RNF166,SPATA2L,TK2,TMEM208
KIRC	C1orf122	8	ANAPC16,ANK3,DNAJB12,ERCC6,GPRIN2,HKDC1,HNRNPH3,OR13A1
KIRP	ODC1	16	ATP6V0D1,BBS2,CCDC79,CETP,CMTM4,DDX19A,DHX38,GABARAPL2,GLG1,GNAO1,MT1E,PSMB10,RANBP10,TRADD,TSNAXIP1,VPS4A
LAML	ODC1	16	ATP6V0D1,BBS2,CCDC79,CETP,CMTM4,DDX19A,DHX38,GABARAPL2,GLG1,GNAO1,MT1E,PSMB10,RANBP10,TRADD,TSNAXIP1,VPS4A
LGG	LY6K	6	HDHD2,PIAS2,SLC14A1,SLC14A2,SMAD7,ST8SIA5
LIHC	CCDC30	7	DCTN6,MTMR9,MTUS1,PCM1,PHYHIP,SLC18A1,SLC25A37
LUAD	RLF	14	ADAMTSL1,ATP8B4,DENND4A,FAM96A,IGDCC4,INTS10,LIPC,MTMR9,RAB11A,RAB8B,SECISBP2L,SNX1,TLN2,TRIP4
LUSC	GREB1	2	HP,KLHL36
OV	RLF	11	DENND4A,FAM96A,IGDCC4,INTS10,LIPC,MTMR9,RAB11A,RAB8B,SNX1,TLN2,TRIP4
PAAD	C1orf122	7	ANAPC16,DNAJB12,ERCC6,GPRIN2,HKDC1,HNRNPH3,OR13A1
PRAD	ODC1	16	ATP6V0D1,BBS2,CCDC79,CETP,CMTM4,DDX19A,DHX38,GABARAPL2,GLG1,GNAO1,MT1E,PSMB10,RANBP10,TRADD,TSNAXIP1,VPS4A
SARC	PEX14	5	C10orf131,HPSE2,PDCD4,PIK3AP1,SFXN2
SKCM	RLF	11	ATP8B4,DENND4A,FAM96A,IGDCC4,LIPC,RAB11A,RAB8B,SECISBP2L,SNX1,TLN2,TRIP4
STAD	RDH16	5	ACTR3B,KCNH2,PTN,TBXAS1,UBN2
TGCT	CTNNBIP1	4	C10orf131,FBXL15,LGI1,NDUFB8
UCEC	SAMHD1	3	COG4,NRN1L,SLC12A4
UCS	ARHGEF10L	5	ANXA7,PRKG1,RUFY2,SEC24C,SLC25A16
UVM	FAM136A	3	COG8,NFATC3,VPS4A
BRCA-all	NFYC	3	JAK2,NARG2,RAB27A
BRCA-LuminalB	ACN9	2	CDH5,DPEP2
BRCA-Basal	BCL11A	3	FTSJD1,FUK,TMED6
BRCA-Her2	POU3F1	6	C10orf111,DNAJC24,FAM180B,JRKL,PTER,TRAF6

Table B.3: Cancer type-specific rescuer hubs. For pancancer, each cancer type, and breast cancer subtype, we identified the rescuer gene that has largest number of vulnerable partners. The number (hub size) and identities of vulnerable partners are listed.

Cancer genes	Vulnerable partners	Cancer genes	Rescuer partners
ACVR1B	EWSR1	ACVR1B	CCIN, HRCT1
AKT2	INSR	APOL2	CSPP1, PVT1
ARID1B	COL23A1, FAM153A, FLT4, GJD3, KRT222, KRT27, NBR1, PTRF, WNK4	BCL2	C8orf33, DYNLT1, FBXO30, PLAGL1, RNASET2, T, TFB1M, ZNF250, ZNF706
ARID2	PRODH	BMPR1A	C1orf94, FAM159A
ASXL1	C22orf34, FA2H	CSF1R	C5orf28, HTR1E
CBFB	KLF13, SCG5	CYLD	ATP6V0A2, BHLHE41, BRAP, CPSF7, CTDSP2, DDB1, EPYC, ERP27, FAM60A, LRRTM4, NUP107, OAS3, PAPOLG, RASSF9, RFC5, VPS37C
CCND1	MT1L	EP300	CPSF1, FOXH1, KCNV1, LRRC14, SARNP, TAC3
CDH1	CYP4X1, MRPS15, OSCP1, TRAPPC3	EWSR1	ACVR1B, RNF139
CDK4	CDH13	FBXW7	FUCA2, HBS1L, KLHL32
CDKN2C	ARAP1, CACNB2, CXCL12, FAM188A, IPMK, PTER, RHOD, SPAG6, SUV420H1, ZNF485	FUS	STEAP1
CTCF	INSC, TRIM68	GATA3	HSPA13, NTNG1, OPRD1
CYLD	ACSBG1, CTSH, TSPAN3	JAK3	SLC16A6
EXT1	CNDP2, GPR124, KIAA1328, KLB, RPL9, SLC14A1, SPATA18, TMX3, ZNF236, ZNF407	KEAP1	C17orf64
EXT2	BBS4, CALML4, CCPG1, DMXL2, IQCH, MAP2K5, MEGF11, RNF111, SLC24A1, TMOD2, TSPAN3	KIT	SALL4, SLPI
FANCF	ARRDC4	KLF4	DPY19L4
KRAS	BTNL9, ELF2, IQGAP2, SAP30L	LYL1	HOXB8, KIAA0391
MDM2	ZNF253	MAP3K1	IRX4
MSH6	UMOD	MLLT1	NT5C, RNF168
MUTYH	GLB1L, IHH, OBSL1	NPM1	COL12A1, ZDHHC5
MYB	ARL4D, LRRC41, PLEKHM1, TBX21	PDGFB	CS, RPS26, TAC3
MYC	CBLN2, CCDC102B, CHST9, FAM69C, SALL3, SLC39A6, SMAD4, ZNF407	PDGFRA	CASC1
MYCN	ACSF3, CBFA2T3, GGT5, KLHL36, NOL3, TRADD	PRDM1	RSPO2
PMS1	CCL22, CDK10, CX3CL1, DEF8, GLG1, GNAO1, GPR56, TEPP, ZFP90	PTEN	FIZ1, NLRP11, ZNF580
POLE	ZNF676, ZNF91	SETBP1	EIF3H, EZR, FAM91A1, POU5F1B, RAET1E
PRDM1	ARFIP1, NR3C2, RPS3A, TIGD4	SMAD2	C6orf70, TFB1M
RARA	CDH15, EPM2A, GCDH, JDP2, JUNB, OR7C1, RNF166, SNAI3, TCF21, TCF25, ZNF430	SMAD4	ANXA13, MYC, RAD21, UTP23
RET	HMHA1	SMARCB1	PKHD1L1
RPL5	RASSF4	SMO	CNGB1
SRC	THUMPD1	TET2	GTF2H5, MTRF1L, PCMT1
TAL1	SVIL	TIAM1	OSMR
TNFAIP3	COL25A1, GUCY1A3, MGST2, MMAA, SH3RF1	TSC1	SLC25A32
WT1	ABHD2, PEX11A	XPC	CYP2B7P1, LYRM2
ZHX2	CARD10, HDAC10, TTC38		

Table B.4: SR interactions of cancer associated genes. The table lists the vulnerable and rescuer partners of cancer associated genes.

Cancer Genes	Rescuers
CBFB	TNFRSF21
CCNE2	CYP20A1, DUSP18, PAX3, ZNF454
CDKN1B	MDH1, NCOA7, ODC1, PTPRK, STX7, TRMT11, UGP2
CTCF	TNFRSF21
ESRP1	CCDC89, PAX3, ZNF454
FGF3	BNIP2, MYO5A, NRP1, USP6NL
FGF4	C6orf123, USP6NL
GATA3	PIK3R4, TNFAIP1
KRAS	AIM1, AMD1, AMIGO1, CLIC4, FAM101B, IRAK2, KCNA2, PARD3B, PAX6, RSC1A1, SLC22A25, SOS1, TAF13, TCEB3, TCP11L1
NRAS	ABCE1, ACSL1, CASP3, KIAA0922, PAQR3, SLC10A6
PIK3CA	ACSL1, ARHGAP10, MGST1, MID1, MRPL13, NDRG1, TMEM40
BRCA1	ANKRD40, ORMDL3, SPAG9
HER2	C6orf195, RABGAP1, RC3H2, UBXN2A, PRPSAP1

Table B.5: DU-type rescuer partners of cancer genes in breast cancer. The table lists the rescuer partners of 13 cancer genes in breast cancer DU-SR network.

Bibliography

[1] John Lonsdale, Jeffrey Thomas, Mike Salvatore, Rebecca Phillips, Edmund Lo, Saboor Shad, Richard Hasz, Gary Walters, Fernando Garcia, Nancy Young, et al. The genotype-tissue expression (gtex) project. *Nature genetics*, 45(6):580–585, 2013.

[2] Su-In Lee, Aimée M Dudley, David Drubin, Pamela a Silver, Nevan J Krogan, Dana Pe'er, and Daphne Koller. Learning a prior on regulatory potential from eQTL data. *PLoS genetics*, 5(1):e1000358, January 2009.

[3] B Alberts, A Johnson, J Lewis, M Raff, K Roberts, and P And Walter. *Molecular Biology of the Cell*, volume 54. 2008.

[4] Eric C Schirmer, Laurence Florens, Tinglu Guan, John R Yates, and Larry Gerace. Nuclear membrane proteins with potential disease links found by subtractive proteomics. *Science*, 301(5638):1380–1382, 2003.

[5] Francis Collins. *The language of life: DNA and the revolution in personalised medicine*. Profile Books, 2010.

[6] David Eisenberg, Edward M Marcotte, Ioannis Xenarios, and Todd O Yeates. Protein function in the post-genomic era. *Nature*, 405(6788):823–826, 2000.

[7] T Töpel, R Hofestädt, D Scheible, and F Trefz. RAMEDIS: the rare metabolic diseases database. *Appl Bioinformatics*, 5:115–118, 2006.

[8] Melvin B Heyman. Lactose intolerance in infants, children, and adolescents. *Pediatrics*, 118(3):1279–1286, 2006.

[9] F Crick. Central dogma of molecular biology. *Nature*, 227(5258):561–563, 1970.

[10] Gene-Wei Li and X Sunney Xie. Central dogma at the single-molecule level in living cells. *Nature*, 475(7356):308–315, 2011.

[11] Melissa S Jurica and Melissa J Moore. Pre-mrna splicing: awash in a sea of proteins. *Molecular cell*, 12(1):5–14, 2003.

[12] Stefan Stamm, Shani Ben-Ari, Ilona Rafalska, Yesheng Tang, Zhaiyi Zhang, Debra Toiber, TA Thanaraj, and Hermona Soreq. Function of alternative splicing. *Gene*, 344:1–20, 2005.

[13] Jonathan MW Slack. Metaplasia and transdifferentiation: from pure biology to the clinic. *Nature Reviews Molecular Cell Biology*, 8(5):369–378, 2007.

[14] James M Ntambi and Kim Young-Cheul. Adipocyte differentiation and gene expression. *The Journal of Nutrition*, 130(12):3122S–3126S, 2000.

[15] Marilena V Iorio, Manuela Ferracin, Chang-Gong Liu, Angelo Veronese, Riccardo Spizzo, Silvia Sabbioni, Eros Magri, Massimo Pedriali, Muller Fabbri, Manuela Campiglio, et al. Microrna gene expression deregulation in human breast cancer. *Cancer research*, 65(16):7065–7070, 2005.

[16] Stephen T Smale and James T Kadonaga. The rna polymerase ii core promoter. *Annual review of biochemistry*, 72(1):449–479, 2003.

[17] Robert E Thurman, Eric Rynes, Richard Humbert, Jeff Vierstra, Matthew T Maurano, Eric Haugen, Nathan C Sheffield, Andrew B Stergachis, Hao Wang, Benjamin Vernot, Kavita Garg, Sam John, Richard Sandstrom, Daniel Bates, Lisa Boatman, Theresa K Canfield, Morgan Diegel, Douglas Dunn, Abigail K Ebersol, Tristan Frum, Erika Giste, Audra K Johnson, Ericka M Johnson, Tanya Kutyavin, Bryan Lajoie, Bum-Kyu Lee, Kristen Lee, Darin London, Dimitra Lotakis, Shane Neph, Fidencio Neri, Eric D Nguyen, Hongzhu Qu, Alex P Reynolds, Vaughn Roach, Alexias Safi, Minerva E Sanchez, Amartya Sanyal, Anthony Shafer, Jeremy M Simon, Lingyun Song, Shinny Vong, Molly Weaver, Yongqi Yan, Zhancheng Zhang, Zhuzhu Zhang, Boris Lenhard, Muneesh Tewari, Michael O Dorschner, R Scott Hansen, Patrick a Navas, George Stamatoyannopoulos, Vishwanath R Iyer, Jason D Lieb, Shamil R Sunyaev, Joshua M Akey, Peter J Sabo, Rajinder Kaul, Terrence S Furey, Job Dekker, Gregory E Crawford, and John a Stamatoyannopoulos. The accessible chromatin landscape of the human genome. *Nature*, 489(7414):75–82, September 2012.

[18] Bradley E. Bernstein, Alexander Meissner, and Eric S. Lander. The Mammalian Epigenome. *Cell*, 128(4):669–681, 2007.

[19] Anna Portela and Manel Esteller. Epigenetic modifications and human disease. *Nature biotechnology*, 28(10):1057–1068, 2010.

[20] Randy L Jirtle and Michael K Skinner. Environmental epigenomics and \ndisease susceptibility. *Nature reviews. Genetics*, 8(4):253–62, 2007.

[21] a. Bird. DNA methylation patterns and epigenetic memory. *Genes and Development*, 16(1):6–21, 2002.

[22] Jue D Wang and Petra A Levin. Metabolism, cell growth and the bacterial cell cycle. *Nature Reviews Microbiology*, 7(11):822–827, 2009.

[23] Károly Mirnics, Frank A Middleton, David A Lewis, and Pat Levitt. Analysis of complex brain disorders with gene expression microarrays: schizophrenia as a disease of the synapse. *Trends in neurosciences*, 24(8):479–486, 2001.

[24] Yael T Aminetzach, J Michael Macpherson, and Dmitri a Petrov. Pesticide resistance via transposition-mediated adaptive gene truncation in Drosophila. *Science (New York, N.Y.)*, 309(July):764–767, 2005.

[25] Vincent Burrus and Matthew K Waldor. Shaping bacterial genomes with integrative and conjugative elements. *Research in microbiology*, 155(5):376–86, 2004.

[26] Stanley a Sawyer, John Parsch, Zhi Zhang, and Daniel L Hartl. Prevalence of positive selection among nearly neutral amino acid replacements in Drosophila. *Proceedings of the National Academy of Sciences of the United States of America*, 104(16):6504–6510, 2007.

[27] Nils Weinhold, Anders Jacobsen, Nikolaus Schultz, Chris Sander, and William Lee. Genome-wide analysis of noncoding regulatory mutations in cancer. *Nature Genetics*, 46(11):1160–5, 2014.

[28] Soili Kytölä, Brita Nord, Elisabeth Edström Elder, Tobias Carling, Magnus Kjellman, Björn Cedermark, Claes Juhlin, Anders Höög, Jorma Isola, and Catharina Larsson. Alterations of the SDHD gene locus in midgut carcinoids, Merkel cell carcinomas, pheochromocytomas, and abdominal paragangliomas. *Genes, Chromosomes & Cancer*, 34(3):325–332, 2002.

[29] Franklin W Huang, Eran Hodis, Mary Jue Xu, Gregory V Kryukov, Lynda Chin, and Levi a Garraway. Highly recurrent TERT promoter mutations in human melanoma. *Science (New York, N.Y.)*, 339(6122):957–9, 2013.

[30] Axel Visel, Edward M Rubin, and Len a Pennacchio. Genomic views of distant-acting enhancers. *Nature*, 461(7261):199–205, 2009.

[31] Len a Pennacchio, Wendy Bickmore, Ann Dean, Marcelo a Nobrega, and Gill Bejerano. Enhancers: five essential questions. *Nature reviews. Genetics*, 14(4):288–95, 2013.

[32] Scott Smemo, Luciene C Campos, Ivan P Moskowitz, José E Krieger, Alexandre C Pereira, and Marcelo a Nobrega. Regulatory variation in a TBX5 enhancer leads to isolated congenital heart disease. *Human molecular genetics*, 21(14):3255–63, 2012.

[33] David C Rees, Thomas N Williams, and Mark T Gladwin. Sickle-cell disease. *The Lancet*, 376(9757):2018–2031, 2010.

[34] Nan M Laird and Christoph Lange. Family-based designs in the age of large-scale gene-association studies. *Nature Reviews Genetics*, 7(5):385–394, 2006.

[35] Peter M Visscher, Matthew a Brown, Mark I McCarthy, and Jian Yang. Five years of GWAS discovery. *American journal of human genetics*, 90(1):7–24, January 2012.

[36] Frank W Albert and Leonid Kruglyak. The role of regulatory variation in complex traits and disease. *Nature Reviews Genetics*, 16(4):197–212, 2015.

[37] Thomas a Pearson and Teri a Manolio. How to interpret a genome-wide association study. *JAMA : the journal of the American Medical Association*, 299(11):1335–44, 2008.

[38] T A Manolio, F S Collins, N J Cox, D B Goldstein, L A Hindorff, D J Hunter, M I McCarthy, E M Ramos, L R Cardon, A Chakravarti, J H Cho, A E Guttmacher, A Kong, L Kruglyak, E Mardis, C N Rotimi, M Slatkin, D Valle, A S Whittemore, M Boehnke, A G Clark, E E Eichler, G Gibson, J L Haines, T F Mackay, S A McCarroll, and P M Visscher. Finding the missing heritability of complex diseases. *Nature*, 461(7265):747–753, 2009.

[39] John Hardy and Andrew Singleton. Genomewide association studies and human disease. *The New England journal of medicine*, 360(17):1759–1768, 2009.

[40] Consortium. The international hapmap project. *Nature*, 426(6968):789–96, 2003.

[41] Danielle Welter, Jacqueline MacArthur, Joannella Morales, Tony Burdett, Peggy Hall, Heather Junkins, Alan Klemm, Paul Flicek, Teri Manolio, Lucia Hindorff, and Helen Parkinson. The NHGRI GWAS Catalog, a curated resource of SNP-trait associations. *Nucleic acids research*, 42(Database issue):D1001–6, 2014.

[42] Lucia a Hindorff, Praveen Sethupathy, Heather a Junkins, Erin M Ramos, Jayashri P Mehta, Francis S Collins, and Teri a Manolio. Potential etiologic and functional implications of genome-wide association loci for human diseases and traits. *Proceedings of the National Academy of Sciences of the United States of America*, 106(23):9362–7, 2009.

[43] Lucas D Ward and Manolis Kellis. Interpreting noncoding genetic variation in complex traits and human disease. *Nature biotechnology*, 30(11):1095–106, November 2012.

[44] Gregory M Cooper and Jay Shendure. Needles in stacks of needles: finding disease-causal variants in a wealth of genomic data. *Nature reviews. Genetics*, 12(9):628–640, 2011.

[45] Montgomery Slatkin. Linkage disequilibrium–understanding the evolutionary past and mapping the medical future. *Nature reviews. Genetics*, 9(6):477–85, 2008.

[46] Peter Kraft and DJ Hunter. Genetic risk prediction: are we there yet? *The New England journal of medicine*, pages 1701–1703, 2009.

[47] Avinash Das Sahu, Radhouane Aniba, Yen-Pei Christy Chang, Sridhar Hannenhalli, et al. Epigenomic model of cardiac enhancers with application to genome wide association studies. In *Pacific Symposium on Biocomputing. Pacific Symposium on Biocomputing*, pages 92–102. World Scientific, 2012.

[48] Konrad J Karczewski, Joel T Dudley, Kimberly R Kukurba, Rong Chen, Atul J Butte, Stephen B Montgomery, and Michael Snyder. Systematic functional regulatory assessment of disease-associated variants. *Proceedings of the National Academy of Sciences of the United States of America*, 110(23):9607–12, June 2013.

[49] Daniel J Gaffney, Jean-Baptiste Veyrieras, Jacob F Degner, Roger Pique-Regi, Athma A Pai, Gregory E Crawford, Matthew Stephens, Yoav Gilad, Jonathan K Pritchard, et al. Dissecting the regulatory architecture of gene expression qtls. *Genome Biol*, 13(1):R7, 2012.

[50] Jean-Baptiste Veyrieras, Sridhar Kudaravalli, Su Yeon Kim, Emmanouil T Dermitzakis, Yoav Gilad, Matthew Stephens, and Jonathan K Pritchard. High-resolution mapping of expression-QTLs yields insight into human gene regulation. *PLoS genetics*, 4(10):e1000214, October 2008.

[51] Ian Dunham, Anshul Kundaje, Shelley F Aldred, Patrick J Collins, Carrie a Davis, Francis Doyle, Charles B Epstein, Seth Frietze, Jennifer Harrow, Rajinder Kaul, Jainab Khatun, Bryan R Lajoie, Stephen G Landt, Burn-Kyu Lee, Florencia Pauli, Kate R Rosenbloom, Peter Sabo, Alexias Safi, Amartya Sanyal, Noam Shoresh, Jeremy M Simon, Lingyun Song, Nathan D Trinklein, Robert C Altshuler, Ewan Birney, James B Brown, Chao Cheng, Sarah Djebali, Xianjun Dong, Jason Ernst, Terrence S Furey, Mark Gerstein, Belinda Giardine, Melissa Greven, Ross C Hardison, Robert S Harris, Javier Herrero, Michael M Hoffman, Sowmya Iyer, Manolis Kelllis, Pouya Kheradpour, Timo Lassmann, Qunhua Li, Xinying Lin, Georgi K Marinov, Angelika Merkel, Ali Mortazavi, Stephen C J Parker, Timothy E Reddy, Joel Rozowsky, Felix Schlesinger, Robert E Thurman, Jie Wang, Lucas D Ward, Troy W Whitfield, Steven P Wilder, Weisheng Wu, Hualin S Xi, Kevin Y Yip, Jiali Zhuang, Bradley E Bernstein, Eric D Green, Chris Gunter, Michael Snyder, Michael J Pazin, Rebecca F Lowdon, Laura a L Dillon, Leslie B Adams, Caroline J Kelly, Julia Zhang, Judith R Wexler, Peter J Good, Elise a Feingold, Gregory E Crawford, Job Dekker, Laura Elinitski, Peggy J Farnham, Morgan C Giddings, Thomas R Gingeras, Roderic Guigó, Tomothy J Hubbard, Manolis Kellis, W James Kent, Jason D Lieb, Elliott H Margulies, Richard M Myers, John a Starnatoyannopoulos, Scott a Tennebaum, Zhiping Weng, Kevin P White, Barbara Wold, Yanbao Yu, John Wrobel, Brian a Risk, Harsha P Gunawardena, Heather C Kuiper, Christopher W Maier, Ling Xie, Xian Chen, Tarjei S Mikkelsen, Shawn Gillespie, Alon Goren, Oren Ram, Xiaolan Zhang, Li Wang, Robbyn Issner, Michael J Coyne, Timothy

Durham, Manching Ku, Thanh Truong, Matthew L Eaton, Alex Dobin, Andrea Tanzer, Julien Lagarde, Wei Lin, Chenghai Xue, Brian a Williams, Chris Zaleski, Maik Röder, Felix Kokocinski, Rehab F Abdelhamid, Tyler Alioto, Igor Antoshechkin, Michael T Baer, Philippe Batut, Ian Bell, Kimberly Bell, Sudipto Chakrabortty, Jacqueline Chrast, Joao Curado, Thomas Derrien, Jorg Drenkow, Erica Dumais, Jackie Dumais, Radha Duttagupta, Megan Fastuca, Kata Fejes-Toth, Pedro Ferreira, Sylvain Foissac, Melissa J Fullwood, Hui Gao, David Gonzalez, Assaf Gordon, Cédric Howald, Sonali Jha, Rory Johnson, Philipp Kapranov, Brandon King, Colin Kingswood, Guoliang Li, Oscar J Luo, Eddie Park, Jonathan B Preall, Kimberly Presaud, Paolo Ribeca, Daniel Robyr, Xiaoan Ruan, Michael Sammeth, Kuljeet Singh Sandu, Lorain Schaeffer, Lei-Hoon See, Atif Shahab, Jorgen Skancke, Ana Maria Suzuki, Hazuki Takahashi, Hagen Tilgner, Diane Trout, Nathalie Walters, Huaien Wang, Yoshihide Hayashizaki, Timothy J Hubbard, Alexandre Reymond, Stylianos E Antonarakis, Gregory J Hannon, Yijun Ruan, Piero Carninci, Cricket a Sloan, Katrina Learned, Venkat S Malladi, Matthew C Wong, Galt P Barber, Melissa S Cline, Timothy R Dreszer, Steven G Heitner, Donna Karolchik, Vaness M Kirkup, Laurence R Meyer, Jeffrey C Long, Morgan Maddren, Brian J Raney, Linda L Grasfeder, Paul G Giresi, Bum-Kyu Lee, Anna Battenhouse, Nathan C Sheffield, Kimberly a Showers, Darin London, Akshay a Bhinge, Christopher Shestak, Matthew R Schaner, Seul Ki Kim, Zhuzhu Z Zhang, Piotr a Mieczkowski, Joanna O Mieczkowska, Zheng Liu, Ryan M McDaniell, Yunyun Ni, Naim U Rashid, Min Jae Kim, Sheera Adar, Zhancheng Zhang, Tianyuan Wang, Deborah Winter, Damian Keefe, Vishwanath R Iyer, Kljeet Singh Sandhu, Meizhen Zheng, Ping Wang, Jason Gertz, Jost Vielmetter, E Christopher Partridge, Katherine E Varley, Clarke Gasper, Anita Bansal, Shirley Pepke, Preti Jain, Henry Amrhein, Kevin M Bowling, Michael Anaya, Marie K Cross, Michael a Muratet, Kimberly M Newberry, Kenneth McCue, Amy S Nesmith, Katherine I Fisher-Aylor, Barbara Pusey, Gilberto DeSalvo, Stephanie L Parker, Sreeram Balasubramanian, Nicholas S Davis, Sarah K Meadows, Tracy Eggleston, J Scott Newberry, Shawn E Levy, Devin M Absher, Wing H Wong, Matthew J Blow, Axel Visel, Len a Pennachio, Laura Elnitski, Hanna M Petrykowska, Alexej Abyzov, Bronwen Aken, Daniel Barrell, Gemma Barson, Andrew Berry, Alexandra Bignell, Veronika Boychenko, Govanni Bussotti, Claire Davidson, Gloria Despacio-Reyes, Mark Diekhans, Iakes Ezkurdia, Adam Frankish, James Gilbert, Jose Manuel Gonzalez, Ed Griffiths, Rachel Harte, David a Hendrix, Toby Hunt, Irwin Jungreis, Mike Kay, Ekta Khurana, Jing Leng, Michael F Lin, Jane Loveland, Zhi Lu, Deepa Manthravadi, Marco Mariotti, Jonathan Mudge, Gaurab Mukherjee, Cedric Notredame, Baikang Pei, Jose Manuel Rodriguez, Gary Saunders, Andrea Sboner, Stephen Searle, Cristina Sisu, Catherine Snow, Charlie Steward, Electra Tapanari, Michael L Tress, Marijke J van Baren, Stefan Washieti, Laurens Wilming, Amonida Zadissa, Zhang Zhengdong, Michael Brent, David Haussler, Alfonso Valencia, Alexandre Raymond, Nick Addleman, Roger P Alexander, Raymond K Auerbach, Suganthi Balasubramanian, Keith Bet-

tinger, Nitin Bhardwaj, Alan P Boyle, Alina R Cao, Philip Cayting, Alexandra Charos, Yong Cheng, Catharine Eastman, Ghia Euskirchen, Joseph D Fleming, Fabian Grubert, Lukas Habegger, Manoj Hariharan, Arif Harmanci, Susma Iyenger, Victor X Jin, Konrad J Karczewski, Maya Kasowski, Phil Lacroute, Hugo Lam, Nathan Larnarre-Vincent, Jin Lian, Marianne Lindahl-Allen, Renqiang Min, Benoit Miotto, Hannah Monahan, Zarmik Moqtaderi, Xinmeng J Mu, Henriette O'Geen, Zhengqing Ouyang, Dorrelyn Patacsil, Debasish Raha, Lucia Ramirez, Brian Reed, Minyi Shi, Teri Slifer, Heather Witt, Linfeng Wu, Xiaoqin Xu, Koon-Kiu Yan, Xinqiong Yang, Zhengdong Zhang, Kevin Struhl, Sherman M Weissman, Scott a Tenebaum, Luiz O Penalva, Subhradip Karmakar, Raj R Bhanvadia, Alina Choudhury, Marc Domanus, Lijia Ma, Jennifer Moran, Alec Victorsen, Thomas Auer, Lazaro Centarin, Michael Eichenlaub, Franziska Gruhl, Stephan Heerman, Burkard Hoeckendorf, Daigo Inoue, Tanja Kellner, Stephan Kirchmaier, Claudia Mueller, Robert Reinhardt, Lea Schertel, Stephanie Schneider, Rebecca Sinn, Beate Wittbrodt, Jochen Wittbrodt, Gaurav Jain, Gayathri Balasundaram, Daniel L Bates, Rachel Byron, Theresa K Canfield, Morgan J Diegel, Douglas Dunn, Abigail K Ebersol, Tristan Frum, Kavita Garg, Erica Gist, R Scott Hansen, Lisa Boatman, Eric Haugen, Richard Humbert, Audra K Johnson, Ericka M Johnson, Tattayana M Kutyavin, Kristin Lee, Dimitra Lotakis, Matthew T Maurano, Shane J Neph, Fiedencio V Neri, Eric D Nguyen, Hongzhu Qu, Alex P Reynolds, Vaughn Roach, Eric Rynes, Minerva E Sanchez, Richard S Sandstrom, Anthony O Shafer, Andrew B Stergachis, Sean Thomas, Benjamin Vernot, Jeff Vierstra, Shinny Vong, Hao Wang, Molly a Weaver, Yongqi Yan, Miaohua Zhang, Joshua a Akey, Michael Bender, Michael O Dorschner, Mark Groudine, Michael J MacCoss, Patrick Navas, George Stamatoyannopoulos, John a Stamatoyannopoulos, Kathryn Beal, Alvis Brazma, Paul Flicek, Nathan Johnson, Margus Lukk, Nicholas M Luscombe, Daniel Sobral, Juan M Vaquerizas, Serafim Batzoglou, Arend Sidow, Nadine Hussami, Sofia Kyriazopoulou-Panagiotopoulou, Max W Libbrecht, Marc a Schaub, Webb Miller, Peter J Bickel, Balazs Banfai, Nathan P Boley, Haiyan Huang, Jingyi Jessica Li, William Stafford Noble, Jeffrey a Bilmes, Orion J Buske, Avinash O Sahu, Peter V Kharchenko, Peter J Park, Dannon Baker, James Taylor, and Lucas Lochovsky. An integrated encyclopedia of DNA elements in the human genome. *Nature*, 489(7414):57–74, September 2012.

[52] Bradley E Bernstein, John a Stamatoyannopoulos, Joseph F Costello, Bing Ren, Aleksandar Milosavljevic, Alexander Meissner, Manolis Kellis, Marco a Marra, Arthur L Beaudet, Joseph R Ecker, Peggy J Farnham, Martin Hirst, Eric S Lander, Tarjei S Mikkelsen, and James a Thomson. The NIH Roadmap Epigenomics Mapping Consortium. *Nature biotechnology*, 28(10):1045–1048, 2010.

[53] Robert A Smith, Deana Manassaram-Baptiste, Durado Brooks, Vilma Cokkinides, Mary Doroshenk, Debbie Saslow, Richard C Wender, and Otis W

Brawley. Cancer screening in the united states, 2014: a review of current american cancer society guidelines and current issues in cancer screening. *CA: a cancer journal for clinicians*, 64(1):30–51, 2014.

[54] Douglas Hanahan and Robert A Weinberg. Hallmarks of cancer: the next generation. *Cell*, 144(5):646–74, 2011.

[55] Douglas Hanahan and Robert A Weinberg. The Hallmarks of Cancer. *Cell*, 100(1):57–70, jan 2000.

[56] R a Weinberg. The retinoblastoma protein and cell cycle control. *Cell*, 81(3):323–330, 1995.

[57] C C Harris. Structure and function of the p53 tumor suppressor gene: clues for rational cancer therapeutic strategies. *Journal of the National Cancer Institute*, 88(20):1442–1455, 1996.

[58] Yuri Lazebnik. What are the hallmarks of cancer? *Nature reviews. Cancer*, 10(4):232–233, 2010.

[59] D A Haber, N S Gray, and J Baselga. The evolving war on cancer. *Cell*, 145(1):19–24, 2011.

[60] TimothyJ. Stuhlmiller, SamanthaM. Miller, JonS. Zawistowski, Kazuhiro Nakamura, AdrianaS. Beltran, JamesS. Duncan, StevenP. Angus, KylaA.L. Collins, DeborahA. Granger, RachelA. Reuther, LeeM. Graves, ShawnM. Gomez, Pei-Fen Kuan, JoelS. Parker, Xin Chen, Noah Sciaky, LisaA. Carey, H.Shelton Earp, Jian Jin, and GaryL. Johnson. Inhibition of Lapatinib-Induced Kinome Reprogramming in ERBB2-Positive Breast Cancer by Targeting BET Family Bromodomains. *Cell Reports*, 11(3):390–404, 2015.

[61] Caitriona Holohan, Sandra Van Schaeybroeck, Daniel B Longley, and Patrick G Johnston. Cancer drug resistance: an evolving paradigm. *Nature Reviews Cancer*, 13(10):714–726, 2013.

[62] Elizabeth Iorns, Christopher J Lord, Nicholas Turner, and Alan Ashworth. Utilizing RNA interference to enhance cancer drug discovery. *Nature reviews. Drug discovery*, 6(7):556–568, 2007.

[63] Rachel Brough, Jessica R Frankum, Sara Costa-Cabral, Christopher J Lord, and Alan Ashworth. Searching for synthetic lethality in cancer. *Current Opinion in Genetics and Development*, 21(1):34–41, 2011.

[64] Archana Bommi-Reddy, Ingrid Almeciga, Jacqueline Sawyer, Christoph Geisen, Wenliang Li, Ed Harlow, William G Kaelin, and Dorre a Grueneberg. Kinase requirements in human cells: III. Altered kinase requirements in VHL-/- cancer cells detected in a pilot synthetic lethal screen. *Proceedings of the National Academy of Sciences of the United States of America*, 105(43):16484–16489, 2008.

[65] Jordi Barretina, Giordano Caponigro, Nicolas Stransky, Kavitha Venkatesan, Adam A Margolin, Sungjoon Kim, Christopher J Wilson, Joseph Lehár, Gregory V Kryukov, Dmitriy Sonkin, Anupama Reddy, Manway Liu, Lauren Murray, Michael F. Berger, John E. Monahan, Paula Morais, Jodi Meltzer, Adam Korejwa, Judit Jané-Valbuena, Felipa A Mapa, Joseph Thibault, Eva Bric-Furlong, Pichai Raman, Aaron Shipway, Ingo H Engels, Jill Cheng, Guoying K. Yu, Jianjun Yu, Peter Aspesi, Melanie de Silva, Kalpana Jagtap, Michael D Jones, Li Wang, Charles Hatton, Emanuele Palescandolo, Supriya Gupta, Scott Mahan, Carrie Sougnez, Robert C Onofrio, Ted Liefeld, Laura MacConaill, Wendy Winckler, Michael Reich, Nanxin Li, Jill P Mesirov, Stacey B Gabriel, Gad Getz, Kristin Ardlie, Vivien Chan, Vic E Myer, Barbara L Weber, Jeff Porter, Markus Warmuth, Peter Finan, Jennifer L Harris, Matthew Meyerson, Todd R Golub, Michael P Morrissey, William R Sellers, Robert Schlegel, and Levi A Garraway. The Cancer Cell Line Encyclopedia enables predictive modelling of anticancer drug sensitivity. *Nature*, 483(7391):603–307, 2012.

[66] M J Garnett, E J Edelman, S J Heidorn, C D Greenman, A Dastur, K W Lau, P Greninger, I R Thompson, X Luo, J Soares, Q S Liu, F Iorio, D Surdez, L Chen, R J Milano, G R Bignell, A T Tam, H Davies, J A Stevenson, S Barthorpe, S R Lutz, F Kogera, K Lawrence, A McLaren-Douglas, X Mitropoulos, T Mironenko, H Thi, L Richardson, W J Zhou, F Jewitt, T H Zhang, P O'Brien, J L Boisvert, S Price, W Hur, W J Yang, X M Deng, A Butler, H G Choi, J Chang, J Baselga, I Stamenkovic, J A Engelman, S V Sharma, O Delattre, J Saez-Rodriguez, N S Gray, J Settleman, P A Futreal, D A Haber, M R Stratton, S Ramaswamy, U McDermott, and C H Benes. Systematic identification of genomic markers of drug sensitivity in cancer cells. *Nature*, 483(7391):570–U87, 2012.

[67] Sarah A. Martin, Afshan McCarthy, Louise J. Barber, Darren J. Burgess, Suzanne Parry, Christopher J. Lord, and Alan Ashworth. Methotrexate induces oxidative DNA damage and is selectively lethal to tumour cells with defects in the DNA mismatch repair gene MSH2. *EMBO Molecular Medicine*, 1(6-7):323–337, 2009.

[68] Nicholas C Turner, Christopher J Lord, Elizabeth Iorns, Rachel Brough, Sally Swift, Richard Elliott, Sydonia Rayter, Andrew N Tutt, and Alan Ashworth. A synthetic lethal siRNA screen identifying genes mediating sensitivity to a PARP inhibitor. *The EMBO journal*, 27(9):1368–1377, 2008.

[69] C J Lord and A Ashworth. Mechanisms of resistance to therapies targeting BRCA-mutant cancers. *Nature Medicine*, 19(11):1381–1388, 2013.

[70] Michael C. Bassik, Martin Kampmann, Robert Jan Lebbink, Shuyi Wang, Marco Y. Hein, Ina Poser, Jimena Weibezahn, Max a. Horlbeck, Siyuan Chen,

Matthias Mann, Anthony a. Hyman, Emily M. Leproust, Michael T. McManus, and Jonathan S. Weissman. A systematic mammalian genetic interaction map reveals pathways underlying ricin susceptibility. *Cell*, 152(4):909–922, 2013.

[71] Livnat Jerby-Arnon, Nadja Pfetzer, YedaelY. Waldman, Lynn McGarry, Daniel James, Emma Shanks, Brinton Seashore-Ludlow, Adam Weinstock, Tamar Geiger, PaulA. Clemons, Eyal Gottlieb, and Eytan Ruppin. Predicting Cancer-Specific Vulnerability via Data-Driven Detection of Synthetic Lethality. *Cell*, 158(5):1199–1209, 2014.

[72] Alan Ashworth, Christopher J Lord, and Jorge S Reis-Filho. Genetic interactions in cancer progression and treatment. *Cell*, 145(1):30–38, 2011.

[73] Leland H Hartwell, Philippe Szankasi, Christopher J Roberts, Andrew W Murray, and Stephen H Friend. Integrating genetic approaches into the discovery of anticancer drugs. *Science (New York, N.Y.)*, 278(5340):1064–1068, 1997.

[74] Babu V Sajesh, Brent J Guppy, and Kirk J McManus. Synthetic genetic targeting of genome instability in cancer. *Cancers*, 5(3):739–61, 2013.

[75] I B Weinstein. Cancer. Addiction to oncogenes–the Achilles heal of cancer. *Science*, 297(5578):63–64, 2002.

[76] Kyle Chang, Chad J Creighton, Caleb Davis, Lawrence Donehower, Jennifer Drummond, David Wheeler, Adrian Ally, Miruna Balasundaram, Inanc Birol, Yaron S N Butterfield, Andy Chu, Eric Chuah, Hye-Jung E Chun, Noreen Dhalla, Ranabir Guin, Martin Hirst, Carrie Hirst, Robert a Holt, Steven J M Jones, Darlene Lee, Haiyan I Li, Marco a Marra, Michael Mayo, Richard a Moore, Andrew J Mungall, a Gordon Robertson, Jacqueline E Schein, Payal Sipahimalani, Angela Tam, Nina Thiessen, Richard J Varhol, Rameen Beroukhim, Ami S Bhatt, Angela N Brooks, Andrew D Cherniack, Samuel S Freeman, Stacey B Gabriel, Elena Helman, Joonil Jung, Matthew Meyerson, Akinyemi I Ojesina, Chandra Sekhar Pedamallu, Gordon Saksena, Steven E Schumacher, Barbara Tabak, Travis Zack, Eric S Lander, Christopher a Bristow, Angela Hadjipanayis, Psalm Haseley, Raju Kucherlapati, Semin Lee, Eunjung Lee, Lovelace J Luquette, Harshad S Mahadeshwar, Angeliki Pantazi, Michael Parfenov, Peter J Park, Alexei Protopopov, Xiaojia Ren, Netty Santoso, Jonathan Seidman, Sahil Seth, Xingzhi Song, Jiabin Tang, Ruibin Xi, Andrew W Xu, Lixing Yang, Dong Zeng, J Todd Auman, Saianand Balu, Elizabeth Buda, Cheng Fan, Katherine a Hoadley, Corbin D Jones, Shaowu Meng, Piotr a Mieczkowski, Joel S Parker, Charles M Perou, Jeffrey Roach, Yan Shi, Grace O Silva, Donghui Tan, Umadevi Veluvolu, Scot Waring, Matthew D Wilkerson, Junyuan Wu, Wei Zhao, Tom Bodenheimer, D Neil Hayes, Alan P Hoyle, Stuart R Jeffreys, Lisle E Mose, Janae V Simons, Mathew G Soloway, Stephen B Baylin, Benjamin P Berman, Moiz S Bootwalla, Ludmila Danilova, James G Herman, Toshinori Hinoue,

Peter W Laird, Suhn K Rhie, Hui Shen, Timothy Triche, Daniel J Weisenberger, Scott L Carter, Kristian Cibulskis, Lynda Chin, Jianhua Zhang, Gad Getz, Carrie Sougnez, Min Wang, Huyen Dinh, Harsha Vardhan Doddapaneni, Richard Gibbs, Preethi Gunaratne, Yi Han, Divya Kalra, Christie Kovar, Lora Lewis, Margaret Morgan, Donna Morton, Donna Muzny, Jeffrey Reid, Liu Xi, Juok Cho, Daniel Dicara, Scott Frazer, Nils Gehlenborg, David I Heiman, Jaegil Kim, Michael S Lawrence, Pei Lin, Yingchun Liu, Michael S Noble, Petar Stojanov, Doug Voet, Hailei Zhang, Lihua Zou, Chip Stewart, Brady Bernard, Ryan Bressler, Andrea Eakin, Lisa Iype, Theo Knijnenburg, Roger Kramer, Richard Kreisberg, Kalle Leinonen, Jake Lin, Yuexin Liu, Michael Miller, Sheila M Reynolds, Hector Rovira, Ilya Shmulevich, Vesteinn Thorsson, Da Yang, Wei Zhang, Samirkumar Amin, Chang-Jiun Wu, Chia-Chin Wu, Rehan Akbani, Kenneth Aldape, Keith a Baggerly, Bradley Broom, Tod D Casasent, James Cleland, Chad Creighton, Deepti Dodda, Mary Edgerton, Leng Han, Shelley M Herbrich, Zhenlin Ju, Hoon Kim, Seth Lerner, Jun Li, Han Liang, Wenbin Liu, Philip L Lorenzi, Yiling Lu, James Melott, Gordon B Mills, Lam Nguyen, Xiaoping Su, Roeland Verhaak, Wenyi Wang, John N Weinstein, Andrew Wong, Yang Yang, Jun Yao, Rong Yao, Kosuke Yoshihara, Yuan Yuan, Alfred K Yung, Nianxiang Zhang, Siyuan Zheng, Michael Ryan, David W Kane, B Arman Aksoy, Giovanni Ciriello, Gideon Dresdner, Jianjiong Gao, Benjamin Gross, Anders Jacobsen, Andre Kahles, Marc Ladanyi, William Lee, Kjong-Van Lehmann, Martin L Miller, Ricardo Ramirez, Gunnar Rätsch, Boris Reva, Chris Sander, Nikolaus Schultz, Yasin Senbabaoglu, Ronglai Shen, Rileen Sinha, S Onur Sumer, Yichao Sun, Barry S Taylor, Nils Weinhold, Suzanne Fei, Paul Spellman, Christopher Benz, Daniel Carlin, Melisssa Cline, Brian Craft, Kyle Ellrott, Mary Goldman, David Haussler, Singer Ma, Sam Ng, Evan Paull, Amie Radenbaugh, Sofie Salama, Artem Sokolov, Joshua M Stuart, Teresa Swatloski, Vladislav Uzunangelov, Peter Waltman, Christina Yau, Jing Zhu, Stanley R Hamilton, Scott Abbott, Rachel Abbott, Nathan D Dees, Kim Delehaunty, Li Ding, David J Dooling, Jim M Eldred, Catrina C Fronick, Robert Fulton, Lucinda L Fulton, Joelle Kalicki-Veizer, Krishna-Latha Kanchi, Cyriac Kandoth, Daniel C Koboldt, David E Larson, Timothy J Ley, Ling Lin, Charles Lu, Vincent J Magrini, Elaine R Mardis, Michael D McLellan, Joshua F McMichael, Christopher a Miller, Michelle O'Laughlin, Craig Pohl, Heather Schmidt, Scott M Smith, Jason Walker, John W Wallis, Michael C Wendl, Richard K Wilson, Todd Wylie, Qunyuan Zhang, Robert Burton, Mark a Jensen, Ari Kahn, Todd Pihl, David Pot, Yunhu Wan, Douglas a Levine, Aaron D Black, Jay Bowen, Jessica Frick, Julie M Gastier-Foster, Hollie a Harper, Carmen Helsel, Kristen M Leraas, Tara M Lichtenberg, Cynthia McAllister, Nilsa C Ramirez, Samantha Sharpe, Lisa Wise, Erik Zmuda, Stephen J Chanock, Tanja Davidsen, John a Demchok, Greg Eley, Ina Felau, Brad a Ozenberger, Margi Sheth, Heidi Sofia, Louis Staudt, Roy Tarnuzzer, Zhining Wang, Liming Yang, Jiashan Zhang, Larsson Omberg, Adam Margolin, Benjamin J Raphael, Fabio Vandin, Hsin-Ta Wu, Mark D M Leiserson, Stephen C Benz, Charles J Vaske, Houtan Noushmehr,

Denise Wolf, Laura Van't Veer, Eric a Collisson, Dimitris Anastassiou, Tai-Hsien Ou Yang, Nuria Lopez-Bigas, Abel Gonzalez-Perez, David Tamborero, Zheng Xia, Wei Li, Dong-Yeon Cho, Teresa Przytycka, Mark Hamilton, Sean McGuire, Sven Nelander, Patrik Johansson, Rebecka Jörnsten, Teresia Kling, Jose Sanchez, and Kenna R Mills Shaw. The Cancer Genome Atlas Pan-Cancer analysis project. *Nature genetics*, 45(10):1113–1120, 2013.

[77] Michael E Tipping. Bayesian Inference : An Introduction to Principles and Practice in Machine Learning From Least-Squares to Bayesian Inference. pages 1–19, 2006.

[78] E. T. Jaynes. *Probability theory: the logic of science*, volume 27. 2005.

[79] Trevor Hastie, Robert Tibshirani, Jerome Friedman, T Hastie, J Friedman, and R Tibshirani. *The elements of statistical learning*, volume 2. Springer, 2009.

[80] C E Rasmussen and Z Ghahramani. Occam's Razor. In *Advances in Neural Information Processing Systems 13*, pages 294–300, 2001.

[81] David J. C. MacKay. Bayesian Interpolation. *Neural Computation*, 4(3):415–447, 1992.

[82] WHO. Global status report on noncommunicable diseases 2014. Technical report, 2014.

[83] Chun Yew Fong, Omer Gilan, Enid Y N Lam, Alan F Rubin, Sarah Ftouni, Dean Tyler, Kym Stanley, Devbarna Sinha, Paul Yeh, Jessica Morison, George Giotopoulos, Dave Lugo, Philip Jeffrey, Stanley Chun-wei Lee, Christopher Carpenter, Richard Gregory, Robert G Ramsay, Steven W Lane, Omar Abdel-Wahab, Tony Kouzarides, Ricky W Johnstone, Sarah-Jane Dawson, Brian J P Huntly, Rab K Prinjha, Anthony T Papenfuss, and Mark A Dawson. BET inhibitor resistance emerges from leukaemia stem cells. *Nature*, 525(7570):538–542, sep 2015.

[84] Philipp Rathert, Mareike Roth, Tobias Neumann, Felix Muerdter, Jae-Seok Roe, Matthias Muhar, Sumit Deswal, Sabine Cerny-Reiterer, Barbara Peter, Julian Jude, Thomas Hoffmann, ukasz M. Bory, Elin Axelsson, Norbert Schweifer, Ulrike Tontsch-Grunt, Lukas E. Dow, Davide Gianni, Mark Pearson, Peter Valent, Alexander Stark, Norbert Kraut, Christopher R. Vakoc, and Johannes Zuber. Transcriptional plasticity promotes primary and acquired resistance to BET inhibition. *Nature*, 525(7570):543–547, sep 2015.

[85] A Bertotti, E Papp, S Jones, V Adleff, V Anagnostou, B Lupo, M Sausen, J Phallen, C A Hruban, C Tokheim, N Niknafs, M Nesselbush, K Lytle, F Sassi, F Cottino, G Migliardi, E R Zanella, D Ribero, N Russolillo, A Mellano, A Muratore, G Paraluppi, M Salizzoni, S Marsoni, M Kragh, J Lantto, A Cassingena, Q K Li, R Karchin, R Scharpf, A Sartore-Bianchi, S Siena, L A

Diaz Jr., L Trusolino, and V E Velculescu. The genomic landscape of response to EGFR blockade in colorectal cancer. *Nature*, 526(7572):263–267, 2015.

[86] D T Miyamoto, Y Zheng, B S Wittner, R J Lee, H Zhu, K T Broderick, R Desai, D B Fox, B W Brannigan, J Trautwein, K S Arora, N Desai, D M Dahl, L V Sequist, M R Smith, R Kapur, C L Wu, T Shioda, S Ramaswamy, D T Ting, M Toner, S Maheswaran, and D A Haber. RNA-Seq of single prostate CTCs implicates noncanonical Wnt signaling in antiandrogen resistance. *Science*, 349(6254):1351–1356, 2015.

[87] Avinash Das, Michael Morley, Christine S Moravec, WHW Tang, Hakon Hakonarson, Kenneth B Margulies, Thomas P Cappola, Shane Jensen, Sridhar Hannenhalli, MAGNet Consortium, et al. Bayesian integration of genetics and epigenetics detects causal regulatory snps underlying expression variability. *Nature communications*, 6, 2015.

[88] Avinash Das, Joo Sang Lee, Ramiro Iglesias-bartolome, Silvio J Jerby-arnon, Livnat, Sridhar Hannenhalli, and Eytan Ruppin. Synthetic rescue determinants of resistance and response to cancer therapy. *(In preparation)*, (1).

[89] G. A. Maston, S. K. Evans, and M. R. Green. Transcriptional regulatory elements in the human genome. *Annu Rev Genomics Hum Genet*, 7:29–59, 2006.

[90] R. J. White. Transcription by rna polymerase iii: more complex than we thought. *Nat Rev Genet*, 12(7):459–63, 2011.

[91] S. Naranjo, K. Voesenek, E. de la Calle-Mustienes, A. Robert-Moreno, H. Kokotas, M. Grigoriadou, J. Economides, G. Van Camp, N. Hilgert, F. Moreno, B. Alsina, M. B. Petersen, H. Kremer, and J. L. Gomez-Skarmeta. Multiple enhancers located in a 1-mb region upstream of pou3f4 promote expression during inner ear development and may be required for hearing. *Human genetics*, 128(4):411–419, 2010.

[92] L. A. Lettice, S. J. Heaney, L. A. Purdie, L. Li, P. de Beer, B. A. Oostra, D. Goode, G. Elgar, R. E. Hill, and E. de Graaff. A long-range shh enhancer regulates expression in the developing limb and fin and is associated with preaxial polydactyly. *Hum Mol Genet*, 12(14):1725–35, 2003.

[93] L. A. Hindorff, P. Sethupathy, H. A. Junkins, E. M. Ramos, J. P. Mehta, F. S. Collins, and T. A. Manolio. Potential etiologic and functional implications of genome-wide association loci for human diseases and traits. *Proc Natl Acad Sci U S A*, 106(23):9362–7, 2009.

[94] D. J. Gaffney, J. B. Veyrieras, J. F. Degner, R. Pique-Regi, A. A. Pai, G. E. Crawford, M. Stephens, Y. Gilad, and J. K. Pritchard. Dissecting the regulatory architecture of gene expression qtls. *Genome Biol*, 13(1):R7, 2012.

[95] V. Gotea, A. Visel, J. M. Westlund, M. A. Nobrega, L. A. Pennacchio, and I. Ovcharenko. Homotypic clusters of transcription factor binding sites are a key component of human promoters and enhancers. *Genome Res*, 20(5):565–77, 2010.

[96] J. Ernst and M. Kellis. Discovery and characterization of chromatin states for systematic annotation of the human genome. *Nat Biotechnol*, 28(8):817–25, 2010.

[97] G. E. Zentner, P. J. Tesar, and P. C. Scacheri. Epigenetic signatures distinguish multiple classes of enhancers with distinct cellular functions. *Genome Res*, 21(8):1273–83, 2011.

[98] R.Y. Birnbaum, E.J. Clowney, O. Agamy, M.J. Kim, J. Zhao, T. Yamanaka, Z. Pappalardo, S.L. Clarke, A.M. Wenger, L. Nguyen, et al. Coding exons function as tissue-specific enhancers of nearby genes. *Genome Research*, 22(6):1059–1068, 2012.

[99] J. Ernst, P. Kheradpour, T. S. Mikkelsen, N. Shoresh, L. D. Ward, C. B. Epstein, X. Zhang, L. Wang, R. Issner, M. Coyne, M. Ku, T. Durham, M. Kellis, and B. E. Bernstein. Mapping and analysis of chromatin state dynamics in nine human cell types. *Nature*, 473(7345):43–9, 2011.

[100] A. Visel, M. J. Blow, Z. Li, T. Zhang, J. A. Akiyama, A. Holt, I. Plajzer-Frick, M. Shoukry, C. Wright, F. Chen, V. Afzal, B. Ren, E. M. Rubin, and L. A. Pennacchio. Chip-seq accurately predicts tissue-specific activity of enhancers. *Nature*, 457(7231):854–8, 2009.

[101] M. P. Creyghton, A. W. Cheng, G. G. Welstead, T. Kooistra, B. W. Carey, E. J. Steine, J. Hanna, M. A. Lodato, G. M. Frampton, P. A. Sharp, L. A. Boyer, R. A. Young, and R. Jaenisch. Histone h3k27ac separates active from poised enhancers and predicts developmental state. *Proc Natl Acad Sci U S A*, 107(50):21932–6, 2010.

[102] Daniel D Lee, Bell Laboratories, Murray Hill, and H Sebastian Seung Ý. Algorithms for Non-negative Matrix Factorization. (1).

[103] M. Fernandez and D. Miranda-Saavedra. Genome-wide enhancer prediction from epigenetic signatures using genetic algorithm-optimized support vector machines. *Nucleic Acids Res*, 40(10):e77, 2012.

[104] R Jansen. Genetical genomics: the added value from segregation. *Trends in Genetics*, 17(7):388–391, 2001.

[105] Rachel B Brem, Gaël Yvert, Rebecca Clinton, and Leonid Kruglyak. Genetic dissection of transcriptional regulation in budding yeast. *Science (New York, N.Y.)*, 296(2002):752–755, 2002.

[106] D J Lunn, J C Whittaker, and N Best. A Bayesian toolkit for genetic association studies. *Genet Epidemiol*, 30(3):231–247, 2006.

[107] Jonathan Marchini, Bryan Howie, Simon Myers, Gil McVean, and Peter Donnelly. A new multipoint method for genome-wide association studies by imputation of genotypes. *Nature genetics*, 39(7):906–13, 2007.

[108] Robert J Klein, Caroline Zeiss, Emily Y Chew, Jen-Yue Tsai, Richard S Sackler, Chad Haynes, Alice K Henning, John Paul SanGiovanni, Shrikant M Mane, Susan T Mayne, Michael B Bracken, Frederick L Ferris, Jurg Ott, Colin Barnstable, and Josephine Hoh. Complement factor H polymorphism in age-related macular degeneration. *Science (New York, N.Y.)*, 308(5720):385–9, 2005.

[109] Albert O Edwards, Robert Ritter, Kenneth J Abel, Alisa Manning, Carolien Panhuysen, and Lindsay a Farrer. Complement factor H polymorphism and age-related macular degeneration. *Science (New York, N.Y.)*, 308(5720):421–424, 2005.

[110] Kaixin Zhou and Ewan R Pearson. Insights from genome-wide association studies of drug response. *Annual review of pharmacology and toxicology*, 53:299–310, 2013.

[111] Andrew R Harper and Eric J Topol. Pharmacogenomics in clinical practice and drug development. *Nature biotechnology*, 30(11):1117–24, 2012.

[112] Andrew R Wood. Defining the role of common variation in the genomic and biological architecture of adult human height. *Nature genetics*, 46(11), 2014.

[113] Mary Grace Goll and Timothy H Bestor. Eukaryotic cytosine methyltransferases. *Annual review of biochemistry*, 74:481–514, 2005.

[114] Raphael Margueron, Patrick Trojer, and Danny Reinberg. The key to development: Interpreting the histone code? *Current Opinion in Genetics and Development*, 15(2):163–176, 2005.

[115] Rudolf Jaenisch and Adrian Bird. Epigenetic regulation of gene expression: how the genome integrates intrinsic and environmental signals. *Nature genetics*, 33 Suppl(march):245–254, 2003.

[116] T R Haines, D I Rodenhiser, and P J Ainsworth. Allele-specific non-CpG methylation of the Nf1 gene during early mouse development. *Developmental Biology*, 240(2):585–598, 2001.

[117] B H Ramsahoye, D Biniszkiewicz, F Lyko, V Clark, a P Bird, and R Jaenisch. Non-CpG methylation is prevalent in embryonic stem cells and may be mediated by DNA methyltransferase 3a. *Proceedings of the National Academy of Sciences of the United States of America*, 97(10):5237–5242, 2000.

[118] A D Riggs. X inactivation, differentiation, and DNA methylation. *Cytogenetics and cell genetics*, 14(1):9–25, 1975.

[119] R Holliday and J E Pugh. DNA modification mechanisms and gene activity during development. *Science (New York, N.Y.)*, 187(4173):226–232, 1975.

[120] A P Wolffe and M A Matzke. Epigenetics: regulation through repression. *Science (New York, N.Y.)*, 286(5439):481–486, 1999.

[121] Fyodor D. Urnov and Alan P. Wolffe. Above and within the genome: Epigenetics past and present. *Journal of Mammary Gland Biology and Neoplasia*, 6(2):153–167, 2001.

[122] Leonie Ringrose and Renato Paro. Epigenetic regulation of cellular memory by the Polycomb and Trithorax group proteins. *Annual review of genetics*, 38:413–443, 2004.

[123] C.J.C. Burges. A tutorial on support vector machines for pattern recognition. *Data mining and knowledge discovery*, 2(2):121–167, 1998.

[124] V.N. Vapnik. *The nature of statistical learning theory*. Springer-Verlag New York Inc, 2000.

[125] C. Cortes and V. Vapnik. Support-vector networks. *Machine learning*, 20(3):273–297, 1995.

[126] D. May, M.J. Blow, T. Kaplan, D.J. McCulley, B.C. Jensen, J.A. Akiyama, A. Holt, I. Plajzer-Frick, M. Shoukry, C. Wright, et al. Large-scale discovery of enhancers from human heart tissue. *Nature genetics*, 2011.

[127] L. Narlikar, N.J. Sakabe, A.A. Blanski, F.E. Arimura, J.M. Westlund, M.A. Nobrega, and I. Ovcharenko. Genome-wide discovery of human heart enhancers. *Genome research*, 20(3):381–392, 2010.

[128] Mark Johnson, Thomas L Griffiths, Mark Johnsonbrownedu, and Tom Griffithsberkeleyedu. Bayesian Inference for PCFGs via Markov chain Monte Carlo.

[129] N. Frey and E. N. Olson. Cardiac hypertrophy: the good, the bad, and the ugly. *Annu Rev Physiol*, 65:45–79, 2003.

[130] S. Hannenhalli, M. E. Putt, J. M. Gilmore, J. Wang, M. S. Parmacek, J. A. Epstein, E. E. Morrisey, K. B. Margulies, and T. P. Cappola. Transcriptional genomics associates fox transcription factors with human heart failure. *Circulation*, 114(12):1269–76, 2006.

[131] I. Manukyan, J. Galatioto, E. Mascareno, S. Bhaduri, and M. A. Siddiqui. Cross-talk between calcineurin/nfat and jak/stat signalling induces cardioprotective alphab-crystallin gene expression in response to hypertrophic stimuli. *J Cell Mol Med*, 14(6B):1707–16, 2010.

[132] J. Schlesinger, M. Schueler, M. Grunert, J. J. Fischer, Q. Zhang, T. Krueger, M. Lange, M. Tonjes, I. Dunkel, and S. R. Sperling. The cardiac transcription network modulated by gata4, mef2a, nkx2.5, srf, histone modifications, and microrna. *PLoS Genet*, 7(2):e1001313, 2011.

[133] V. Matys, O. V. Kel-Margoulis, E. Fricke, I. Liebich, S. Land, A. Barre-Dirrie, I. Reuter, D. Chekmenev, M. Krull, K. Hornischer, N. Voss, P. Stegmaier, B. Lewicki-Potapov, H. Saxel, A. E. Kel, and E. Wingender. Transfac and its module transcompel: transcriptional gene regulation in eukaryotes. *Nucleic Acids Res*, 34(Database issue):D108–10, 2006.

[134] S. Levy and S. Hannenhalli. Identification of transcription factor binding sites in the human genome sequence. *Mamm Genome*, 13(9):510–4, 2002.

[135] A. G. West and P. Fraser. Remote control of gene transcription. *Hum Mol Genet*, 14 Spec No 1:R101–11, 2005.

[136] J. Chen, E. E. Bardes, B. J. Aronow, and A. G. Jegga. Toppgene suite for gene list enrichment analysis and candidate gene prioritization. *Nucleic Acids Res*, 37(Web Server issue):W305–11, 2009.

[137] K Beyer and J Goldstein. When is nearest neighbour meaningful? *Database TheoryICDT'99*, 1999.

[138] Joel N Hirschhorn. Genomewide association studies–illuminating biologic pathways. *The New England journal of medicine*, 360(17):1699–701, April 2009.

[139] Tuuli Lappalainen, Michael Sammeth, Marc R Friedländer, Peter ACt Hoen, Jean Monlong, Manuel A Rivas, Mar Gonzàlez-Porta, Natalja Kurbatova, Thasso Griebel, Pedro G Ferreira, et al. Transcriptome and genome sequencing uncovers functional variation in humans. *Nature*, 2013.

[140] Shaun Purcell, Benjamin Neale, Kathe Todd-Brown, Lori Thomas, Manuel AR Ferreira, David Bender, Julian Maller, Pamela Sklar, Paul IW De Bakker, Mark J Daly, et al. Plink: a tool set for whole-genome association and population-based linkage analyses. *The American Journal of Human Genetics*, 81(3):559–575, 2007.

[141] Richard M. Durbin, David L. Altshuler, Richard M. Durbin, Gonçalo R. Abecasis, David R. Bentley, Aravinda Chakravarti, Andrew G. Clark, Francis S. Collins, De La Vega, M. Francisco, Peter Donnelly, Michael Egholm, Paul Flicek, Stacey B. Gabriel, Richard a. Gibbs, Bartha M. Knoppers, Eric S. Lander, Hans Lehrach, Elaine R. Mardis, Gil a. McVean, Debbie a. Nickerson, Leena Peltonen, Alan J. Schafer, Stephen T. Sherry, Jun Wang, Richard K. Wilson, Richard a. Gibbs, David Deiros, Mike Metzker, Donna Muzny, Jeff Reid, David Wheeler, Jun Wang, Jingxiang Li, Min Jian, Guoqing Li, Ruiqiang Li, Huiqing Liang, Geng Tian, Bo Wang, Jian Wang,

Wei Wang, Huanming Yang, Xiuqing Zhang, Huisong Zheng, Eric S. Lander, David L. Altshuler, Lauren Ambrogio, Toby Bloom, Kristian Cibulskis, Tim J. Fennell, Stacey B. Gabriel, David B. Jaffe, Erica Shefler, Carrie L. Sougnez, David R. Bentley, Niall Gormley, Sean Humphray, Zoya Kingsbury, Paula Koko-Gonzales, Jennifer Stone, Kevin J. McKernan, Gina L. Costa, Jeffry K. Ichikawa, Clarence C. Lee, Ralf Sudbrak, Hans Lehrach, Tatiana a. Borodina, Andreas Dahl, Alexey N. Davydov, Peter Marquardt, Florian Mertes, Wilfiried Nietfeld, Philip Rosenstiel, Stefan Schreiber, Aleksey V. Soldatov, Bernd Timmermann, Marius Tolzmann, Michael Egholm, Jason Affourtit, Dana Ashworth, Said Attiya, Melissa Bachorski, Eli Buglione, Adam Burke, Amanda Caprio, Christopher Celone, Shauna Clark, David Conners, Brian Desany, Lisa Gu, Lorri Guccione, Kalvin Kao, Andrew Kebbel, Jennifer Knowlton, Matthew Labrecque, Louise McDade, Craig Mealmaker, Melissa Minderman, Anne Nawrocki, Faheem Niazi, Kristen Pareja, Ravi Ramenani, David Riches, Wanmin Song, Cynthia Turcotte, Shally Wang, Elaine R. Mardis, Richard K. Wilson, David Dooling, Lucinda Fulton, Robert Fulton, George Weinstock, Richard M. Durbin, John Burton, David M. Carter, Carol Churcher, Alison Coffey, Anthony Cox, Aarno Palotie, Michael Quail, Tom Skelly, James Stalker, Harold P. Swerdlow, Daniel Turner, Anniek De Witte, Shane Giles, Richard a. Gibbs, David Wheeler, Matthew Bainbridge, Danny Challis, Aniko Sabo, Fuli Yu, Jin Yu, Jun Wang, Xiaodong Fang, Xiaosen Guo, Ruiqiang Li, Yingrui Li, Ruibang Luo, Shuaishuai Tai, Honglong Wu, Hancheng Zheng, Xiaole Zheng, Yan Zhou, Guoqing Li, Jian Wang, Huanming Yang, Gabor T. Marth, Erik P. Garrison, Weichun Huang, Amit Indap, Deniz Kural, Wan-Ping Lee, Wen Fung Leong, Aaron R. Quinlan, Chip Stewart, Michael P. Stromberg, Alistair N. Ward, Jiantao Wu, Charles Lee, Ryan E. Mills, Xinghua Shi, Mark J. Daly, Mark a. DePristo, David L. Altshuler, Aaron D. Ball, Eric Banks, Toby Bloom, Brian L. Browning, Kristian Cibulskis, Tim J. Fennell, Kiran V. Garimella, Sharon R. Grossman, Robert E. Handsaker, Matt Hanna, Chris Hartl, David B. Jaffe, Andrew M. Kernytsky, Joshua M. Korn, Heng Li, Jared R. Maguire, Steven a. McCarroll, Aaron McKenna, James C. Nemesh, Anthony a. Philippakis, Ryan E. Poplin, Alkes Price, Manuel a. Rivas, Pardis C. Sabeti, Stephen F. Schaffner, Erica Shefler, Ilya a. Shlyakhter, David Neil Cooper, Edward Vincent Ball, Matthew Edwin Mort, Andrew David Phillips, Peter Daniel Stenson, Jonathan Sebat, Vladimir Makarov, Kenny Ye, Seungtai C. Yoon, Carlos D. Bustamante, Andrew G. Clark, Adam Boyko, Jeremiah Degenhardt, Simon Gravel, Ryan N. Gutenkunst, Mark Kaganovich, Alon Keinan, Phil Lacroute, Xin Ma, Andy Reynolds, Laura Clarke, Paul Flicek, Fiona Cunningham, Javier Herrero, Stephen Keenen, Eugene Kulesha, Rasko Leinonen, William M. McLaren, Rajesh Radhakrishnan, Richard E. Smith, Vadim Zalunin, Xiangqun Zheng-Bradley, Jan O. Korbel, Adrian M. Stütz, Sean Humphray, Markus Bauer, R. Keira Cheetham, Tony Cox, Michael Eberle, Terena James, Scott Kahn, Lisa Murray, Aravinda Chakravarti, Kai Ye, De La Vega, M. Francisco, Yutao Fu, Fiona C. L. Hyland, Jonathan M. Manning, Stephen F. McLaughlin,

Heather E. Peckham, Onur Sakarya, Yongming a. Sun, Eric F. Tsung, Mark a. Batzer, Miriam K. Konkel, Jerilyn a. Walker, Ralf Sudbrak, Marcus W. Albrecht, Vyacheslav S. Amstislavskiy, Ralf Herwig, Dimitri V. Parkhomchuk, Stephen T. Sherry, Richa Agarwala, Hoda M. Khouri, Aleksandr O. Morgulis, Justin E. Paschall, Lon D. Phan, Kirill E. Rotmistrovsky, Robert D. Sanders, Martin F. Shumway, Chunlin Xiao, Gil a. McVean, Adam Auton, Zamin Iqbal, Gerton Lunter, Jonathan L. Marchini, Loukas Moutsianas, Simon Myers, Afidalina Tumian, Brian Desany, James Knight, Roger Winer, David W. Craig, Steve M. Beckstrom-Sternberg, Alexis Christoforides, Ahmet a. Kurdoglu, John V. Pearson, Shripad a. Sinari, Waibhav D. Tembe, David Haussler, Angie S. Hinrichs, Sol J. Katzman, Andrew Kern, Robert M. Kuhn, Molly Przeworski, Ryan D. Hernandez, Bryan Howie, Joanna L. Kelley, S. Cord Melton, Gonçalo R. Abecasis, Yun Li, Paul Anderson, Tom Blackwell, Wei Chen, William O. Cookson, Jun Ding, Hyun Min Kang, Mark Lathrop, Liming Liang, Miriam F. Moffatt, Paul Scheet, Carlo Sidore, Matthew Snyder, Xiaowei Zhan, Sebastian Zöllner, Philip Awadalla, Ferran Casals, Youssef Idaghdour, John Keebler, Eric a. Stone, Martine Zilversmit, Lynn Jorde, Jinchuan Xing, Evan E. Eichler, Gozde Aksay, Can Alkan, Iman Hajirasouliha, Fereydoun Hormozdiari, Jeffrey M. Kidd, S. Cenk Sahinalp, Peter H. Sudmant, Elaine R. Mardis, Ken Chen, Asif Chinwalla, Li Ding, Daniel C. Koboldt, Mike D. McLellan, David Dooling, George Weinstock, John W. Wallis, Michael C. Wendl, Qunyuan Zhang, Richard M. Durbin, Cornelis a. Albers, Qasim Ayub, Senduran Balasubramaniam, Jeffrey C. Barrett, David M. Carter, Yuan Chen, Donald F. Conrad, Petr Danecek, Emmanouil T. Dermitzakis, Min Hu, Ni Huang, Matt E. Hurles, Hanjun Jin, Luke Jostins, Thomas M. Keane, Si Quang Le, Sarah Lindsay, Quan Long, Daniel G. MacArthur, Stephen B. Montgomery, Leopold Parts, James Stalker, Chris Tyler-Smith, Klaudia Walter, Yujun Zhang, Mark B. Gerstein, Michael Snyder, Alexej Abyzov, Suganthi Balasubramanian, Robert Bjornson, Jiang Du, Fabian Grubert, Lukas Habegger, Rajini Haraksingh, Justin Jee, Ekta Khurana, Hugo Y. K. Lam, Jing Leng, Xinmeng Jasmine Mu, Alexander E. Urban, Zhengdong Zhang, Yingrui Li, Ruibang Luo, Gabor T. Marth, Erik P. Garrison, Deniz Kural, Aaron R. Quinlan, Chip Stewart, Michael P. Stromberg, Alistair N. Ward, Jiantao Wu, Charles Lee, Ryan E. Mills, Xinghua Shi, Steven a. McCarroll, Eric Banks, Mark a. DePristo, Robert E. Handsaker, Chris Hartl, Joshua M. Korn, Heng Li, James C. Nemesh, Jonathan Sebat, Vladimir Makarov, Kenny Ye, Seungtai C. Yoon, Jeremiah Degenhardt, Mark Kaganovich, Laura Clarke, Richard E. Smith, Xiangqun Zheng-Bradley, Jan O. Korbel, Sean Humphray, R. Keira Cheetham, Michael Eberle, Scott Kahn, Lisa Murray, Kai Ye, De La Vega, M. Francisco, Yutao Fu, Heather E. Peckham, Yongming a. Sun, Mark a. Batzer, Miriam K. Konkel, Jerilyn a. Walker, Chunlin Xiao, Zamin Iqbal, Brian Desany, Tom Blackwell, Matthew Snyder, Jinchuan Xing, Evan E. Eichler, Gozde Aksay, Can Alkan, Iman Hajirasouliha, Fereydoun Hormozdiari, Jeffrey M. Kidd, Ken Chen, Asif Chinwalla, Li Ding, Mike D. McLellan, John W. Wallis, Matt E. Hurles, Donald F.

Conrad, Klaudia Walter, Yujun Zhang, Mark B. Gerstein, Michael Snyder, Alexej Abyzov, Jiang Du, Fabian Grubert, Rajini Haraksingh, Justin Jee, Ekta Khurana, Hugo Y. K. Lam, Jing Leng, Xinmeng Jasmine Mu, Alexander E. Urban, Zhengdong Zhang, Richard a. Gibbs, Matthew Bainbridge, Danny Challis, Cristian Coafra, Huyen Dinh, Christie Kovar, Sandy Lee, Donna Muzny, Lynne Nazareth, Jeff Reid, Aniko Sabo, Fuli Yu, Jin Yu, Gabor T. Marth, Erik P. Garrison, Amit Indap, Wen Fung Leong, Aaron R. Quinlan, Chip Stewart, Alistair N. Ward, Jiantao Wu, Kristian Cibulskis, Tim J. Fennell, Stacey B. Gabriel, Kiran V. Garimella, Chris Hartl, Erica Shefler, Carrie L. Sougnez, Jane Wilkinson, Andrew G. Clark, Simon Gravel, Fabian Grubert, Laura Clarke, Paul Flicek, Richard E. Smith, Xiangqun Zheng-Bradley, Stephen T. Sherry, Hoda M. Khouri, Justin E. Paschall, Martin F. Shumway, Chunlin Xiao, Gil a. McVean, Sol J. Katzman, Gonçalo R. Abecasis, Tom Blackwell, Elaine R. Mardis, David Dooling, Lucinda Fulton, Robert Fulton, Daniel C. Koboldt, Richard M. Durbin, Senduran Balasubramaniam, Allison Coffey, Thomas M. Keane, Daniel G. MacArthur, Aarno Palotie, Carol Scott, James Stalker, Chris Tyler-Smith, Mark B. Gerstein, Suganthi Balasubramanian, Aravinda Chakravarti, Bartha M. Knoppers, Gonçalo R. Abecasis, Carlos D. Bustamante, Neda Gharani, Richard a. Gibbs, Lynn Jorde, Jane S. Kaye, Alastair Kent, Taosha Li, Amy L. McGuire, Gil a. McVean, Pilar N. Ossorio, Charles N. Rotimi, Yeyang Su, Lorraine H. Toji, Chris Tyler-Smith, Lisa D. Brooks, Adam L. Felsenfeld, Jean E. McEwen, Assya Abdallah, Christopher R. Juenger, Nicholas C. Clemm, Francis S. Collins, Audrey Duncanson, Eric D. Green, Mark S. Guyer, Jane L. Peterson, Alan J. Schafer, Gonçalo R. Abecasis, David L. Altshuler, Adam Auton, Lisa D. Brooks, Richard M. Durbin, Richard a. Gibbs, Matt E. Hurles, and Gil a. McVean. A map of human genome variation from population-scale sequencing. *Nature*, 473(7348):544–544, May 2011.

[142] EI George and RE McCulloch. Approaches for Bayesian variable selection. *Statistica sinica*, 7:339–373, 1997.

[143] Yongtao Guan and Matthew Stephens. Bayesian variable selection regression for genome-wide association studies and other large-scale problems. *The Annals of Applied Statistics*, 5(3):1780–1815, September 2011.

[144] NG Polson, JG Scott, and Jesse Windle. Bayesian inference for logistic models using Polya-Gamma latent variables. *Journal of the American Statistical ...*, pages 1–42, 2013.

[145] EI George and RE McCulloch. Variable Selection via gibbs sampling. *Journal of the American ...*, 1993.

[146] Feng Liang, Rui Paulo, German Molina, Merlise a Clyde, and Jim O Berger. Mixtures of g Priors for Bayesian Variable Selection. *Journal of the American Statistical Association*, 103(481):410–423, March 2008.

[147] Radford M Neal. Probabilistic Inference Using Markov Chain Monte Carlo Methods. *Technical Report*, pages 1–144, 1998.

[148] Kevin P. Murphy. *Machine Learning: A Probabilistic Perspective*. MIT press, 1991.

[149] Xiaojin Zhu, Zoubin Ghahramani, and John D Lafferty. Semi-supervised learning using Gaussian fields and harmonic functions. *International Conference on Machine Learning - ICML 2003*, 20:912, 2003.

[150] David M Altshuler, Richard a Gibbs, Leena Peltonen, Emmanouil Dermitzakis, Stephen F Schaffner, Fuli Yu, Penelope E Bonnen, Paul I W de Bakker, Panos Deloukas, Stacey B Gabriel, Rhian Gwilliam, Sarah Hunt, Michael Inouye, Xiaoming Jia, Aarno Palotie, Melissa Parkin, Pamela Whittaker, Kyle Chang, Alicia Hawes, Lora R Lewis, Yanru Ren, David Wheeler, Donna Marie Muzny, Chris Barnes, Katayoon Darvishi, Matthew Hurles, Joshua M Korn, Kati Kristiansson, Charles Lee, Steven a McCarrol, James Nemesh, Alon Keinan, Stephen B Montgomery, Samuela Pollack, Alkes L Price, Nicole Soranzo, Claudia Gonzaga-Jauregui, Verneri Anttila, Wendy Brodeur, Mark J Daly, Stephen Leslie, Gil McVean, Loukas Moutsianas, Huy Nguyen, Qingrun Zhang, Mohammed J R Ghori, Ralph McGinnis, William McLaren, Fumihiko Takeuchi, Sharon R Grossman, Ilya Shlyakhter, Elizabeth B Hostetter, Pardis C Sabeti, Clement a Adebamowo, Morris W Foster, Deborah R Gordon, Julio Licinio, Maria Cristina Manca, Patricia a Marshall, Ichiro Matsuda, Duncan Ngare, Vivian Ota Wang, Deepa Reddy, Charles N Rotimi, Charmaine D Royal, Richard R Sharp, Changqing Zeng, Lisa D Brooks, and Jean E McEwen. Integrating common and rare genetic variation in diverse human populations. *Nature*, 467(7311):52–8, September 2010.

[151] Andrey a Shabalin. Matrix eQTL: ultra fast eQTL analysis via large matrix operations. *Bioinformatics (Oxford, England)*, 28(10):1353–8, May 2012.

[152] B Efron and T Hastie. LEAST ANGLE REGRESSION. *The Annals of statistics*, 32(2):407–499, 2004.

[153] Bryan Howie, Christian Fuchsberger, Matthew Stephens, Jonathan Marchini, and Gonçalo R Abecasis. Fast and accurate genotype imputation in genome-wide association studies through pre-phasing. *Nature genetics*, 44(8):955–959, 2012.

[154] Jason Ernst and Manolis Kellis. ChromHMM: automating chromatin-state discovery and characterization. *Nature methods*, 9(3):215–6, March 2012.

[155] Elin Grundberg, Kerrin S Small, Åsa K Hedman, Alexandra C Nica, Alfonso Buil, Sarah Keildson, Jordana T Bell, Tsun-Po Yang, Eshwar Meduri, Amy Barrett, James Nisbett, Magdalena Sekowska, Alicja Wilk, So-Youn Shin, Daniel Glass, Mary Travers, Josine L Min, Sue Ring, Karen Ho, Gudmar Thorleifsson, Augustine Kong, Unnur Thorsteindottir, Chrysanthi Ainali,

Antigone S Dimas, Neelam Hassanali, Catherine Ingle, David Knowles, Maria Krestyaninova, Christopher E Lowe, Paola Di Meglio, Stephen B Montgomery, Leopold Parts, Simon Potter, Gabriela Surdulescu, Loukia Tsaprouni, Sophia Tsoka, Veronique Bataille, Richard Durbin, Frank O Nestle, Stephen O'Rahilly, Nicole Soranzo, Cecilia M Lindgren, Krina T Zondervan, Kourosh R Ahmadi, Eric E Schadt, Kari Stefansson, George Davey Smith, Mark I McCarthy, Panos Deloukas, Emmanouil T Dermitzakis, and Tim D Spector. Mapping cis- and trans-regulatory effects across multiple tissues in twins. *Nature Genetics*, 44(10):1084–1089, 2012.

[156] F. Hormozdiari, E. Kostem, E. Y. Kang, B. Pasaniuc, and E. Eskin. Identifying Causal Variants at Loci with Multiple Signals of Association. *Genetics*, 198(October):genetics.114.167908–, 2014.

[157] Shane Neph, Jeff Vierstra, Andrew B Stergachis, Alex P Reynolds, Eric Haugen, Benjamin Vernot, Robert E Thurman, Sam John, Richard Sandstrom, Audra K Johnson, Matthew T Maurano, Richard Humbert, Eric Rynes, Hao Wang, Shinny Vong, Kristen Lee, Daniel Bates, Morgan Diegel, Vaughn Roach, Douglas Dunn, Jun Neri, Anthony Schafer, R Scott Hansen, Tanya Kutyavin, Erika Giste, Molly Weaver, Theresa Canfield, Peter Sabo, Miaohua Zhang, Gayathri Balasundaram, Rachel Byron, Michael J MacCoss, Joshua M Akey, M a Bender, Mark Groudine, Rajinder Kaul, and John a Stamatoyannopoulos. An expansive human regulatory lexicon encoded in transcription factor footprints. *Nature*, 489(7414):83–90, September 2012.

[158] Geet Duggal, Hao Wang, and Carl Kingsford. Higher-order chromatin domains link eQTLs with the expression of far-away genes. *Nucleic Acids Research*, 42(1):87–96, 2014.

[159] Graham McVicker, Bryce van de Geijn, Jacob F Degner, Carolyn E Cain, Nicholas E Banovich, Anil Raj, Noah Lewellen, Marsha Myrthil, Yoav Gilad, and Jonathan K Pritchard. Identification of genetic variants that affect histone modifications in human cells. *Science (New York, N.Y.)*, 342(6159):747–9, November 2013.

[160] V Matys, O V Kel-Margoulis, E Fricke, I Liebich, S Land, a Barre-Dirrie, I Reuter, D Chekmenev, M Krull, K Hornischer, N Voss, P Stegmaier, B Lewicki-Potapov, H Saxel, a E Kel, and E Wingender. TRANSFAC and its module TRANSCompel: transcriptional gene regulation in eukaryotes. *Nucleic acids research*, 34(7):D108–D110, 2006.

[161] Sridhar Hannenhalli and Klaus H Kaestner. The evolution of Fox genes and their role in development and disease. *Nature reviews. Genetics*, 10(April):233–240, 2009.

[162] Yuzhen Zhang, Nibedita Rath, Sridhar Hannenhalli, Zhishan Wang, Thomas Cappola, Shioko Kimura, Elena Atochina-Vasserman, Min Min Lu, Michael F

Beers, and Edward E Morrisey. GATA and Nkx factors synergistically regulate tissue-specific gene expression and development in vivo. *Development (Cambridge, England)*, 134:189–198, 2007.

[163] Mary E. Putt, Sridhar Hannenhalli, Yun Lu, Philip Haines, Hareesh R. Chandrupatla, Edward E. Morrisey, Kenneth B. Margulies, and Thomas P. Cappola. Evidence for coregulation of myocardial gene expression by MEF2 and NFAT in human heart failure. *Circulation: Cardiovascular Genetics*, 2:212–219, 2009.

[164] Rafael A Irizarry, Bridget Hobbs, Francois Collin, Yasmin D Beazer-Barclay, Kristen J Antonellis, Uwe Scherf, and Terence P Speed. Exploration, normalization, and summaries of high density oligonucleotide array probe level data. *Biostatistics*, 4(2):249–264, 2003.

[165] W Evan Johnson, Cheng Li, and Ariel Rabinovic. Adjusting batch effects in microarray expression data using empirical bayes methods. *Biostatistics*, 8(1):118–127, 2007.

[166] Oliver Stegle, Leopold Parts, Matias Piipari, John Winn, and Richard Durbin. Using probabilistic estimation of expression residuals (peer) to obtain increased power and interpretability of gene expression analyses. *Nature protocols*, 7(3):500–507, 2012.

[167] Andrew E Teschendorff, Joanna Zhuang, and Martin Widschwendter. Independent surrogate variable analysis to deconvolve confounding factors in large-scale microarray profiling studies. *Bioinformatics*, 27(11):1496–1505, 2011.

[168] Volker Matys, Olga V Kel-Margoulis, Ellen Fricke, Ines Liebich, Sigrid Land, A Barre-Dirrie, Ingmar Reuter, D Chekmenev, Mathias Krull, Klaus Hornischer, et al. Transfac® and its module transcompel®: transcriptional gene regulation in eukaryotes. *Nucleic acids research*, 34(suppl 1):D108–D110, 2006.

[169] Sridhar Hannenhalli and Samuel Levy. Promoter prediction in the human genome. *Bioinformatics*, 17(suppl 1):S90–S96, 2001.

[170] David T Miyamoto, Yu Zheng, Ben S Wittner, Richard J Lee, Huili Zhu, Katherine T Broderick, Rushil Desai, Douglas B Fox, Brian W Brannigan, Julie Trautwein, Kshitij S Arora, Niyati Desai, Douglas M Dahl, Lecia V Sequist, Matthew R Smith, Ravi Kapur, Chin-Lee Wu, Toshi Shioda, Sridhar Ramaswamy, David T Ting, Mehmet Toner, Shyamala Maheswaran, and Daniel A Haber. RNA-Seq of single prostate CTCs implicates noncanonical Wnt signaling in antiandrogen resistance. *Science*, 349(6254):1351–1356, sep 2015.

[171] Andrea Bertotti, Eniko Papp, Jillian Phallen, Carolyn A Hruban, Collin Tokheim, Noushin Niknafs, Monica Nesselbush, Karli Lytle, Francesco Sassi,

Francesca Cottino, Giorgia Migliardi, Eugenia R Zanella, Dario Ribero, Nadia Russolillo, Alfredo Mellano, Andrea Muratore, Gianluca Paraluppi, Mauro Salizzoni, Silvia Marsoni, Michael Kragh, Johan Lantto, Andrea Cassingena, Qing Kay Li, Rachel Karchin, Robert Scharpf, Andrea Sartore-bianchi, Salvatore Siena, and Luis A Diaz Jr. Then genomic landscape of response to EGFR blockade in colorectal cancer. 2015.

[172] Chong Sun, Liqin Wang, Sidong Huang, Guus J J E Heynen, Anirudh Prahallad, Caroline Robert, John Haanen, Christian Blank, Jelle Wesseling, Stefan M Willems, Davide Zecchin, Sebastijan Hobor, Prashanth K Bajpe, Cor Lieftink, Christina Mateus, Stephan Vagner, Wipawadee Grernrum, Ingrid Hofland, Andreas Schlicker, Lodewyk F a Wessels, Roderick L Beijersbergen, Alberto Bardelli, Federica Di Nicolantonio, Alexander M M Eggermont, and Rene Bernards. Reversible and adaptive resistance to BRAF(V600E) inhibition in melanoma. *Nature*, 508(7494):118–122, 2014.

[173] Willy Hugo, Hubing Shi, Lu Sun, Marco Piva, Chunying Song, Xiangju Kong, Gatien Moriceau, Aayoung Hong, KimberlyB. Dahlman, DouglasB. Johnson, JeffreyA. Sosman, Antoni Ribas, and RogerS. Lo. Non-genomic and Immune Evolution of Melanoma Acquiring MAPKi Resistance. *Cell*, 162(6):1271–1285, 2015.

[174] Reading List. C L Se m i n a r i n Ba y e si a n N on p a ra m e t ri c s. pages 12–14, 2007.

[175] Hark Kyun Kim, Il Ju Choi, Chan Gyoo Kim, Hee Sung Kim, Akira Oshima, Aleksandra Michalowski, and Jeffrey E. Green. A gene expression signature of acquired chemoresistance to cisplatin and fluorouracil combination chemotherapy in gastric cancer patients. *PLoS ONE*, 6(2), 2011.

[176] C. Hatzis, L. Pusztai, V. Valero, D. J. Booser, L. Esserman, a. Lluch, T. Vidaurre, F. Holmes, E. Souchon, H. Wang, M. Martin, J. Cotrina, H. Gomez, R. Hubbard, J. I. Chacon, J. Ferrer-Lozano, R. Dyer, M. Buxton, Y. Gong, Y. Wu, N. Ibrahim, E. Andreopoulou, N. T. Ueno, K. Hunt, W. Yang, a. Nazario, a. DeMichele, J. O'Shaughnessy, G. N. Hortobagyi, and W. F. Symmans. A Genomic Predictor of Response and Survival Following Taxane-Anthracycline Chemotherapy for Invasive Breast Cancer. *JAMA: The Journal of the American Medical Association*, 305(18):1873–1881, 2011.

[177] Elmar Stickeler, Dietmar Pils, Maximilian Klar, Marzenna Orlowsk-Volk, Axel Zur Hausen, Markus Jäger, Dirk Watermann, Gerald Gitsch, Robert Zeillinger, and Clemens B. Tempfer. Basal-like molecular subtype and HER4 up-regulation and response to neoadjuvant chemotherapy in breast cancer. *Oncology Reports*, 26(4):1037–1045, 2011.

[178] L Gonzalez-Malerva, J Park, L H Zou, Y H Hu, Z Moradpour, J Pearlberg, J Sawyer, H Stevens, E Harlow, and J LaBaer. High-throughput ectopic

expression screen for tamoxifen resistance identifies an atypical kinase that blocks autophagy. *Proceedings of the National Academy of Sciences of the United States of America*, 108(5):2058–2063, 2011.

[179] A M Patch, E L Christie, D Etemadmoghadam, D W Garsed, J George, S Fereday, K Nones, P Cowin, K Alsop, P J Bailey, K S Kassahn, F Newell, M C Quinn, S Kazakoff, K Quek, C Wilhelm-Benartzi, E Curry, H S Leong, Study Australian Ovarian Cancer, A Hamilton, L Mileshkin, G Au-Yeung, C Kennedy, J Hung, Y E Chiew, P Harnett, M Friedlander, M Quinn, J Pyman, S Cordner, P O'Brien, J Leditschke, G Young, K Strachan, P Waring, W Azar, C Mitchell, N Traficante, J Hendley, H Thorne, M Shackleton, D K Miller, G M Arnau, R W Tothill, T P Holloway, T Semple, I Harliwong, C Nourse, E Nourbakhsh, S Manning, S Idrisoglu, T J Bruxner, A N Christ, B Poudel, O Holmes, M Anderson, C Leonard, A Lonie, N Hall, S Wood, D F Taylor, Q Xu, J L Fink, N Waddell, R Drapkin, E Stronach, H Gabra, R Brown, A Jewell, S H Nagaraj, E Markham, P J Wilson, J Ellul, O McNally, M A Doyle, R Vedururu, C Stewart, E Lengyel, J V Pearson, N Waddell, A DeFazio, S M Grimmond, and D D Bowtell. Corrigendum: Whole-genome characterization of chemoresistant ovarian cancer. *Nature*, 2015.

[180] M Costanzo, A Baryshnikova, J Bellay, Y Kim, E D Spear, C S Sevier, H M Ding, J L Y Koh, K Toufighi, S Mostafavi, J Prinz, R P S Onge, B VanderSluis, T Makhnevych, F J Vizeacoumar, S Alizadeh, S Bahr, R L Brost, Y Q Chen, M Cokol, R Deshpande, Z J Li, Z Y Lin, W D Liang, M Marback, J Paw, B J S Luis, E Shuteriqi, A H Y Tong, N van Dyk, I M Wallace, J A Whitney, M T Weirauch, G Q Zhong, H W Zhu, W A Houry, M Brudno, S Ragibizadeh, B Papp, C Pal, F P Roth, G Giaever, C Nislow, O G Troyanskaya, H Bussey, G D Bader, A C Gingras, Q D Morris, P M Kim, C A Kaiser, C L Myers, B J Andrews, and C Boone. The Genetic Landscape of a Cell. *Science*, 327(5964):425–431, 2010.

[181] William G. Kaelin. Genetic Interactions in Cancer Progression and Treatment. *Nature Reviews Cancer*, 5(9):689–98, 2005.

[182] E Szczurek and N Beerenwinkel. Modeling Mutual Exclusivity of Cancer Mutations. *Plos Computational Biology*, 10(3), 2014.

[183] R Kelley and T Ideker. Systematic interpretation of genetic interactions using protein networks. *Nature Biotechnology*, 23(5):561–566, 2005.

[184] S.W. James, Carolyn D Silflow, M.D. Thompson, L.P.W. Ranum, and P.A. Lefebvre. Extragenic suppression and synthetic lethality among Chlamydomonas reinhardtii mutants resistant to anti-microtubule drugs. *Genetics*, 122(3):567, 1989.

[185] Michael L Nonet and Richard A Young. Intragenic and extragenic suppressors of mutations in the heptapeptide repeat domain of Saccharomyces cerevisiae RNA polymerase II. *Genetics*, 123(4):715–24, dec 1989.

[186] Adilson E Motter, Natali Gulbahce, Eivind Almaas, and Albert-László Barabási. Predicting synthetic rescues in metabolic networks. *Molecular systems biology*, 4(168):168, 2008.

[187] Amal Aly and Shridar Ganesan. Review BRCA 1 , PARP , and 53 BP 1 : conditional synthetic lethality and synthetic viability. *Journal of Molecular Cell Biology*, (3):66–74, 2011.

[188] Sebastian M B Nijman. Synthetic lethality: General principles, utility and detection using genetic screens in human cells. *FEBS Letters*, 585(1):1–6, 2011.

[189] Bert Vogelstein, Nickolas Papadopoulos, Victor E Velculescu, Shibin Zhou, Luis a Diaz, and Kenneth W Kinzler. Cancer genome landscapes. *Science (New York, N.Y.)*, 339(6127):1546–58, 2013.

[190] N Conde-Pueyo, A Munteanu, R V Sole, and C Rodriguez-Caso. Human synthetic lethal inference as potential anti-cancer target gene detection. *Bmc Systems Biology*, 3, 2009.

[191] Nigel J. O'Neil, Derek M. van Pel, and Philip Hieter. Synthetic lethality and cancer: Cohesin and PARP at the replication fork. *Trends in Genetics*, 29(5):290–297, 2013.

[192] O Folger, L Jerby, C Frezza, E Gottlieb, E Ruppin, and T Shlomi. Predicting selective drug targets in cancer through metabolic networks (vol 7, pg 501, 2011). *Molecular Systems Biology*, 7, 2011.

[193] X W Lu, P R Kensche, M A Huynen, and R A Notebaart. Genome evolution predicts genetic interactions in protein complexes and reveals cancer drug targets. *Nature Communications*, 4, 2013.

[194] C Frezza, P J Pollard, and E Gottlieb. Inborn and acquired metabolic defects in cancer. *Journal of Molecular Medicine-Jmm*, 89(3):213–220, 2011.

[195] Gregory Prelich. Suppression mechanisms: themes from variations. *Trends in Genetics*, 15(7):261–266, 1999.

[196] D G Moerman, S Plurad, R H Waterston, and D L Baillie. Mutations in the unc-54 myosin heavy chain gene of Caenorhabditis elegans that alter contractility but not muscle structure. *Cell*, 29(3):773–81, 1982.

[197] K Zhang and H Wang. [Cancer Genome Atlas Pan-cancer Analysis Project]. *Zhongguo Fei Ai Za Zhi*, 18(4):219–223, 2015.

[198] Christina Curtis, Sohrab P. Shah, Suet-Feung Chin, Gulisa Turashvili, Oscar M. Rueda, Mark J. Dunning, Doug Speed, Andy G. Lynch, Shamith Samarajiwa, Yinyin Yuan, Stefan Gräf, Gavin Ha, Gholamreza Haffari, Ali Bashashati, Roslin Russell, Steven McKinney, Carlos Caldas, Samuel Aparicio,

Christina Curtis, Sohrab P. Shah, Carlos Caldas, Samuel Aparicio, James D. Brenton, Ian Ellis, David Huntsman, Sarah Pinder, Arnie Purushotham, Leigh Murphy, Carlos Caldas, Samuel Aparicio, Carlos Caldas, Helen Bardwell, Suet-Feung Chin, Christina Curtis, Zhihao Ding, Stefan Gräf, Linda Jones, Bin Liu, Andy G. Lynch, Irene Papatheodorou, Stephen J. Sammut, Gordon Wishart, Samuel Aparicio, Steven Chia, Karen Gelmon, David Huntsman, Steven McKinney, Caroline Speers, Gulisa Turashvili, Peter Watson, Ian Ellis, Roger Blamey, Andrew Green, Douglas Macmillan, Emad Rakha, Arnie Purushotham, Cheryl Gillett, Anita Grigoriadis, Sarah Pinder, Emanuele di Rinaldis, Andy Tutt, Leigh Murphy, Michelle Parisien, Sandra Troup, Carlos Caldas, Suet-Feung Chin, Derek Chan, Claire Fielding, Ana-Teresa Maia, Sarah McGuire, Michelle Osborne, Sara M. Sayalero, Inmaculada Spiteri, James Hadfield, Samuel Aparicio, Gulisa Turashvili, Lynda Bell, Katie Chow, Nadia Gale, David Huntsman, Maria Kovalik, Ying Ng, Leah Prentice, Carlos Caldas, Simon Tavaré, Christina Curtis, Mark J. Dunning, Stefan Gräf, Andy G. Lynch, Oscar M. Rueda, Roslin Russell, Shamith Samarajiwa, Doug Speed, Florian Markowetz, Yinyin Yuan, James D. Brenton, Samuel Aparicio, Sohrab P. Shah, Ali Bashashati, Gavin Ha, Gholamreza Haffari, Steven McKinney, Anita Langerø d, Andrew Green, Elena Provenzano, Gordon Wishart, Sarah Pinder, Peter Watson, Florian Markowetz, Leigh Murphy, Ian Ellis, Arnie Purushotham, Anne-Lise Bø rresen Dale, James D. Brenton, Simon Tavaré, Carlos Caldas, and Samuel Aparicio. The genomic and transcriptomic architecture of 2,000 breast tumours reveals novel subgroups. *Nature*, 2012.

[199] International Agency for Research on Cancer. International Agency for Research on Cancer Iarc Monographs on the Evaluation of Carcinogenic Risks To Humans. *Iarc Monographs On The Evaluation Of Carcinogenic Risks To Humans*, 96:i–ix+1–390, 2002.

[200] Michael Kuhn, Monica Campillos, Ivica Letunic, Lars Juhl Jensen, and Peer Bork. A side effect resource to capture phenotypic effects of drugs. *Molecular systems biology*, 6:343, 2010.

[201] W. H. Goodson, L. Lowe, D. O. Carpenter, M. Gilbertson, A. Manaf Ali, A. Lopez de Cerain Salsamendi, A. Lasfar, A. Carnero, A. Azqueta, A. Amedei, A. K. Charles, A. R. Collins, A. Ward, A. C. Salzberg, A. Colacci, A.-K. Olsen, A. Berg, B. J. Barclay, B. P. Zhou, C. Blanco-Aparicio, C. J. Baglole, C. Dong, C. Mondello, C.-W. Hsu, C. C. Naus, C. Yedjou, C. S. Curran, D. W. Laird, D. C. Koch, D. J. Carlin, D. W. Felsher, D. Roy, D. G. Brown, E. Ratovitski, E. P. Ryan, E. Corsini, E. Rojas, E.-Y. Moon, E. Laconi, F. Marongiu, F. Al-Mulla, F. Chiaradonna, F. Darroudi, F. L. Martin, F. J. Van Schooten, G. S. Goldberg, G. Wagemaker, G. Nangami, G. M. Calaf, G. Williams, G. T. Wolf, G. Koppen, G. Brunborg, H. Kim Lyerly, H. Krishnan, H. Ab Hamid, H. Yasaei, H. Sone, H. Kondoh, H. K. Salem, H.-Y. Hsu,

H. H. Park, I. Koturbash, I. R. Miousse, A. I. Scovassi, J. E. Klaunig, J. Vondracek, J. Raju, J. Roman, J. P. Wise, J. R. Whitfield, J. Woodrick, J. A. Christopher, J. Ochieng, J. F. Martinez-Leal, J. Weisz, J. Kravchenko, J. Sun, K. R. Prudhomme, K. B. Narayanan, K. A. Cohen-Solal, K. Moorwood, L. Gonzalez, L. Soucek, L. Jian, L. S. D'Abronzo, L.-T. Lin, L. Li, L. Gulliver, L. J. McCawley, L. Memeo, L. Vermeulen, L. Leyns, L. Zhang, M. Valverde, M. Khatami, M. F. Romano, M. Chapellier, M. A. Williams, M. Wade, M. H. Manjili, M. Lleonart, M. Xia, M. J. Gonzalez, M. V. Karamouzis, M. Kirsch-Volders, M. Vaccari, N. B. Kuemmerle, N. Singh, N. Cruickshanks, N. Kleinstreuer, N. van Larebeke, N. Ahmed, O. Ogunkua, P. K. Krishnakumar, P. Vadgama, P. A. Marignani, P. M. Ghosh, P. Ostrosky-Wegman, P. Thompson, P. Dent, P. Heneberg, P. Darbre, P. Sing Leung, P. Nangia-Makker, Q. Cheng, R. B. Robey, R. Al-Temaimi, R. Roy, R. Andrade-Vieira, R. K. Sinha, R. Mehta, R. Vento, R. Di Fiore, R. Ponce-Cusi, R. Dornetshuber-Fleiss, R. Nahta, R. C. Castellino, R. Palorini, R. Abd Hamid, S. A. S. Langie, S. Eltom, S. A. Brooks, S. Ryeom, S. S. Wise, S. N. Bay, S. A. Harris, S. Papagerakis, S. Romano, S. Pavanello, S. Eriksson, S. Forte, S. C. Casey, S. Luanpitpong, T.-J. Lee, T. Otsuki, T. Chen, T. Massfelder, T. Sanderson, T. Guarnieri, T. Hultman, V. Dormoy, V. Odero-Marah, V. Sabbisetti, V. Maguer-Satta, W. K. Rathmell, W. Engstrom, W. K. Decker, W. H. Bisson, Y. Rojanasakul, Y. Luqmani, Z. Chen, and Z. Hu. Assessing the carcinogenic potential of low-dose exposures to chemical mixtures in the environment: the challenge ahead. *Carcinogenesis*, 36(Suppl 1):S254–S296, 2015.

[202] Elisabeth Corcelle, Marielle Nebout, Soumeya Bekri, Nils Gauthier, Paul Hofman, Philippe Poujeol, Patrick Fénichel, and Baharia Mograbi. Disruption of autophagy at the maturation step by the carcinogen lindane is associated with the sustained mitogen-activated protein kinase/extracellular signal-regulated kinase activity. *Cancer Research*, 66(13):6861–6870, 2006.

[203] Jer-Yen Yang, Cong S Zong, Weiya Xia, Hirohito Yamaguchi, Qingqing Ding, Xiaoming Xie, Jing-Yu Lang, Chien-Chen Lai, Chun-Ju Chang, Wei-Chien Huang, Hsin Huang, Hsu-Ping Kuo, Dung-Fang Lee, Long-Yuan Li, Huang-Chun Lien, Xiaoyun Cheng, King-Jen Chang, Chwan-Deng Hsiao, Fuu-Jen Tsai, Chang-Hai Tsai, Aysegul a Sahin, William J Muller, Gordon B Mills, Dihua Yu, Gabriel N Hortobagyi, and Mien-Chie Hung. ERK promotes tumorigenesis by inhibiting FOXO3a via MDM2-mediated degradation. *Nature cell biology*, 10(2):138–148, 2008.

[204] S Ries, C Biederer, D Woods, O Shifman, S Shirasawa, T Sasazuki, M McMahon, M Oren, and F McCormick. Opposing effects of Ras on p53: transcriptional activation of mdm2 and induction of p19ARF. *Cell*, 103(2):321–330, 2000.

[205] Amy J. Burke, Francis J. Sullivan, Francis J. Giles, and Sharon a. Glynn. The yin and yang of nitric oxide in cancer progression. *Carcinogenesis*, 34(3):503–512, 2013.

[206] Ramiro Iglesias-Bartolome, Daniel Martin, and J. Silvio Gutkind. Exploiting the head and neck cancer oncogenome: Widespread PI3K-mTOR pathway alterations and novel molecular targets. *Cancer Discovery*, 3(July):722–725, 2013.

[207] Panomwat Amornphimoltham, Vyomesh Patel, Kantima Leelahavanichkul, Robert T Abraham, and J Silvio Gutkind. A retroinhibition approach reveals a tumor cell-autonomous response to rapamycin in head and neck cancer. *Cancer Research*, 68(4):1144–1153, 2008.

[208] E. Eisenberg and E.Y. Levanon. Human housekeeping genes are compact. *TRENDS in Genetics*, 19(7):362–365, 2003.

[209] Leroy Hood and Stephen H Friend. Predictive, personalized, preventive, participatory (P4) cancer medicine. *Nature reviews. Clinical oncology*, 8(3):184–187, 2011.

[210] V Law, C Knox, Y Djoumbou, T Jewison, A C Guo, Y F Liu, A Maciejewski, D Arndt, M Wilson, V Neveu, A Tang, G Gabriel, C Ly, S Adamjee, Z T Dame, B S Han, Y Zhou, and D S Wishart. DrugBank 4.0: shedding new light on drug metabolism. *Nucleic Acids Research*, 42(D1):D1091–D1097, 2014.

[211] M M Gottesman, T Fojo, and S E Bates. Multidrug resistance in cancer: role of ATP-dependent transporters. *Nat Rev Cancer*, 2(1):48–58, 2002.

[212] Allon Wagner, Noa Cohen, Thomas Kelder, Uri Amit, Elad Liebman, David M Steinberg, Marijana Radonjic, and Eytan Ruppin. Drugs that reverse disease transcriptomic signatures are more effective in a mouse model of dyslipidemia. *Molecular systems biology*, 11(1):791, 2015.

[213] Prerna Malaney, Santo V Nicosia, and Vrushank Davé. One mouse, one patient paradigm: new avatars of personalized cancer therapy. *Cancer letters*, 344(1):1–12, 2014.

[214] Adrian FM Smith and Gareth O Roberts. Bayesian computation via the gibbs sampler and related markov chain monte carlo methods. *Journal of the Royal Statistical Society. Series B (Methodological)*, pages 3–23, 1993.

[215] William Valdar, Jeremy Sabourin, Andrew Nobel, and Christopher C Holmes. Reprioritizing genetic associations in hit regions using lasso-based resample model averaging. *Genetic epidemiology*, 36(5):451–462, 2012.

[216] Verena Zuber, A Pedro Duarte Silva, and Korbinian Strimmer. A novel algorithm for simultaneous snp selection in high-dimensional genome-wide association studies. *BMC bioinformatics*, 13(1):284, 2012.

[217] Martin Kircher, Daniela M Witten, Preti Jain, Brian J O'Roak, Gregory M Cooper, and Jay Shendure. A general framework for estimating the relative pathogenicity of human genetic variants. *Nature genetics*, 46(3):310–315, 2014.

[218] Gleb Kichaev, Wen-Yun Yang, Sara Lindstrom, Farhad Hormozdiari, Eleazar Eskin, Alkes L Price, Peter Kraft, and Bogdan Pasaniuc. Integrating functional data to prioritize causal variants in statistical fine-mapping studies. *PLoS genetics*, 10(10):e1004722, 2014.

[219] Joseph K. Pickrell. Joint analysis of functional genomic data and genome-wide association studies of 18 human traits. *American Journal of Human Genetics*, 94(4):559–573, 2014.

[220] Jack J Dongarra, James R Bunch, Cleve B Moler, and Gilbert W Stewart. *LINPACK users' guide*, volume 8. Siam, 1979.

[221] Bradley Efron and Robert Tibshirani. *An introduction to the bootstrap*. Number 57. Chapman & Hall, New York, 1993.

[222] G Bindea, B Mlecnik, H Hackl, P Charoentong, M Tosolini, A Kirilovsky, W H Fridman, F Pages, Z Trajanoski, and J Galon. ClueGO: a Cytoscape plug-in to decipher functionally grouped gene ontology and pathway annotation networks. *Bioinformatics*, 25(8):1091–1093, 2009.

[223] Damian Szklarczyk, Andrea Franceschini, Stefan Wyder, Kristoffer Forslund, Davide Heller, Jaime Huerta-Cepas, Milan Simonovic, Alexander Roth, Alberto Santos, Kalliopi P Tsafou, Michael Kuhn, Peer Bork, Lars J Jensen, and Christian von Mering. STRING v10: protein-protein interaction networks, integrated over the tree of life. *Nucleic acids research*, 43(Database issue):D447–52, 2015.

[224] National Toxicology Program (NTP). Report on Carcinogens. Technical report, 2014.

[225] J Zhang, J Baran, A Cros, J M Guberman, S Haider, J Hsu, Y Liang, E Rivkin, J Wang, B Whitty, M Wong-Erasmus, L Yao, and A Kasprzyk. International Cancer Genome Consortium Data Portal–a one-stop shop for cancer genomics data. *Database (Oxford)*, 2011:bar026, 2011.

[226] P J Marie, E Hay, D Modrowski, L Revollo, G Mbalaviele, and R Civitelli. Cadherin-mediated cell-cell adhesion and signaling in the skeleton. *Calcif Tissue Int*, 94(1):46–54, 2014.

[227] M Ciro, E Prosperini, M Quarto, U Grazini, J Walfridsson, F McBlane, P Nucifero, G Pacchiana, M Capra, J Christensen, and K Helin. ATAD2 Is a Novel Cofactor for MYC, Overexpressed and Amplified in Aggressive Tumors. *Cancer Research*, 69(21):8491–8498, 2009.

[228] J X Zou, Z J Duan, J J Wang, A Sokolov, J Z Xu, C Z Chen, J J Li, and H W Chen. Kinesin Family Deregulation Coordinated by Bromodomain Protein ANCCA and Histone Methyltransferase MLL for Breast Cancer Cell Growth, Survival, and Tamoxifen Resistance. *Molecular Cancer Research*, 12(4):539–549, 2014.

[229] Kun Zhang and Bernhard Sch. Multi-Source Domain Adaptation : A Causal View. 2008.

[230] Anne Mette Buhl, Jesper Jurlander, Flemming S Jørgensen, Anne Marie Ottesen, Jack B. Cowland, Lise Mette Gjerdrum, Brian V Hansen, and Henrik Leffers. Identification of a gene on chromosome 12q22 uniquely overexpressed in chronic lymphocytic leukemia. *Blood*, 107(7):2904–2911, 2006.

[231] Jun Suzuki, Daniel P Denning, Eiichi Imanishi, H Robert Horvitz, and Shigekazu Nagata. Xk-related protein 8 and CED-8 promote phosphatidylserine exposure in apoptotic cells. *Science (New York, N.Y.)*, 341(6144):403–6, 2013.

[232] Juan Sandoval, Jesus Mendez-Gonzalez, Ernest Nadal, Guoan Chen, F. Javier Carmona, Sergi Sayols, Sebastian Moran, Holger Heyn, Miguel Vizoso, Antonio Gomez, Montse Sanchez-Cespedes, Yassen Assenov, Fabian Müller, Christoph Bock, Miquel Taron, Josefina Mora, Lucia a. Muscarella, Triantafillos Liloglou, Michael Davies, Marina Pollan, Maria J. Pajares, Wenceslao Torre, Luis M. Montuenga, Elisabeth Brambilla, John K. Field, Luca Roz, Marco Lo Iacono, Giorgio V. Scagliotti, Rafael Rosell, David G. Beer, and Manel Esteller. A prognostic DNA methylation signature for stage I non-small-cell lung cancer. *Journal of clinical oncology : official journal of the American Society of Clinical Oncology*, 31(32):4140–4147, 2013.

[233] M Chanrion, V Negre, H Fontaine, N Salvetat, F Bibeau, G Mac Grogan, L Mauriac, D Katsaros, F Molina, C Theillet, and J M Darbon. A gene expression signature that can predict the recurrence of tamoxifen-treated primary breast cancer. *Clinical Cancer Research*, 14(6):1744–1752, 2008.

[234] J A Trendel. The hurdle of antiandrogen drug resistance: drug design strategies. *Expert Opinion on Drug Discovery*, 8(12):1491–1501, 2013.

[235] E Yague, A Arance, L Kubitza, M O'Hare, P Jat, C M Ogilvie, I R Hart, C F Higgins, and S Raguz. Ability to acquire drug resistance arises early during the tumorigenesis process. *Cancer Research*, 67(3):1130–1137, 2007.

[236] Guangchuang Yu, Fei Li, Yide Qin, Xiaochen Bo, Yibo Wu, and Shengqi Wang. GOSemSim: an R package for measuring semantic similarity among GO terms and gene products. *Bioinformatics (Oxford, England)*, 26(7):976–8, 2010.

[237] Mu-Shui Dai, Shelya X Zeng, Yetao Jin, Xiao-Xin Sun, Larry David, and Hua Lu. Ribosomal protein L23 activates p53 by inhibiting MDM2 function in response to ribosomal perturbation but not to translation inhibition. *Molecular and cellular biology*, 24(17):7654–7668, 2004.

[238] Michael Wanzel, Annika C Russ, Daniela Kleine-Kohlbrecher, Emanuela Colombo, Pier-Guiseppe Pelicci, and Martin Eilers. A ribosomal protein L23-nucleophosmin circuit coordinates Mizl function with cell growth. *Nature cell biology*, 10(9):1051–61, 2008.

[239] A E Pegg. Regulation of ornithine decarboxylase. *Journal of Biological Chemistry*, 281(21):14529–14532, 2006.

[240] Michael S. Lawrence, Petar Stojanov, Craig H. Mermel, James T. Robinson, Levi a. Garraway, Todd R. Golub, Matthew Meyerson, Stacey B. Gabriel, Eric S. Lander, and Gad Getz. Discovery and saturation analysis of cancer genes across 21 tumour types. *Nature*, 505(7484):495–501, 2014.

[241] Vivian G Cheung, Laura K Conlin, Teresa M Weber, Melissa Arcaro, Kuang-Yu Jen, Michael Morley, and Richard S Spielman. Natural variation in human gene expression assessed in lymphoblastoid cells. *Nature genetics*, 33(3):422–5, March 2003.

[242] J Wang, X X Zhou, J Zhu, Y Y Gu, W Y Zhao, J F Zou, and Z Guo. GO-function: deriving biologically relevant functions from statistically significant functions. *Briefings in Bioinformatics*, 13(2):216–227, 2012.

[243] Panomwat Amornphimoltham, Vyomesh Patel, Akrit Sodhi, Nikolaos G Nikitakis, John J Sauk, Edward A Sausville, Alfredo A Molinolo, and J Silvio Gutkind. Mammalian Target of Rapamycin , a Molecular Target in Squamous Cell Carcinomas of the Head and Neck. 1(21):9953–9962, 2005.